

Universidad Autónoma de
Madrid



Facultad de Ciencias
Departamento de Física Teórica

Consejo Superior de
Investigaciones Científicas



Instituto de Física Teórica
IFT UAM-CSIC

The High Energy Limit of QCD and $\mathcal{N} = 4$ SYM and the Effective Action Approach

Memoria de Tesis Doctoral presentada por
JOSÉ DANIEL MADRIGAL MARTÍNEZ
para optar al título de **Doctor en Física** por la
Universidad Autónoma de Madrid.

Tesis Doctoral dirigida por **Dr. D. Agustín Sabio Vera**,
profesor del Departamento de Física Teórica
de la Universidad Autónoma de Madrid.

May 26, 2013

Preface

The dynamics of the high energy limit of gauge theories —and in particular Quantum Chromodynamics (QCD), the theory of strong interactions— still offers, forty years after the discovery of asymptotic freedom, a major challenge. This regime, where scattering processes are characterized by a center-of-mass energy s much bigger than the momentum transfer $|t|$, is not only vital for an accurate description of forward and diffractive scattering in modern hadron colliders, and perhaps most importantly for the study of high density parton systems, but also displays a number of intriguing deep properties.

When all momentum scales in the problem are high enough, the coupling α_s becomes small and one can rely on perturbation theory for its study. Significant simplifications in scattering amplitudes occur in this limit, allowing to resum all the contributions enhanced by factors $(\alpha_s \ln s)^n$ using the self-consistent BFKL ansatz based on Regge theory (which claims that high-energy scattering proceeds via the exchange of an effective particle, the reggeon). It should be possible to reproduce in the framework of QCD the appealing features of this phenomenological theory, rooted on the combination of general properties of the S-matrix and the analytical continuation of angular momentum to complex values. In particular, there is (motivated) hope that some smooth transition occurs between the perturbative and non-perturbative regions of Regge asymptotics, allowing to access fundamental data of hadron dynamics from the perturbative high-energy limit.

According to Regge theory, QCD can be recast in this limit as a 2+1-dimensional field theory where the fundamental degree of freedom is the reggeon. An important step towards the understanding of high-energy QCD is the derivation of the effective reggeon vertices from QCD. In the leading $\ln s$ approximation, known elements of reggeon field theory exhibit remarkable properties, such as transverse coordinate conformal invariance of the 2–4 and 2–6 reggeon transitions and the integrability in the large- N_c limit of states of arbitrary many reggeons. It is widely believed that these properties are inherited from

$\mathcal{N} = 4$ Super-Yang-Mills (SYM) theory, which is equivalent to QCD to leading $\ln s$ order.

In fact, the recent impressive discoveries on the structure of scattering amplitudes in $\mathcal{N} = 4$ SYM, and its major role in the AdS/CFT correspondence, have led to consider this supersymmetric version of QCD, which is presumably exactly solvable, as a perfect model to extract—at least qualitatively—important physics of the strong interactions. The parallel between QCD and $\mathcal{N} = 4$ SYM is expected to be closer in the Regge limit. Important questions such as the origin of conformal invariance and integrability in high-energy QCD and the existence of a gravity dual to reggeon field theory remain to be answered.

A promising tool in the study of these questions is the high-energy effective action proposed by Lipatov. Derived by requiring gauge invariance and agreement with perturbative computations in the so-called quasi-multi-Regge kinematics, this action encompasses by construction the unitarity corrections needed in dense partonic systems, and should lead to 2+1 reggeon field theory after integrating over quark and gluon degrees of freedom. In the spirit of effective theories, computation of amplitudes in the high-energy limit is greatly simplified as well.

Lipatov's action is unusual, however, in the sense that rather than integrating out degrees of freedom à la Wilson, new reggeon fields are added to the QCD Lagrangian with the understanding that locality in rapidity is to be imposed. Enforcing this requirement in loop computations is not a trivial task. New spurious divergences appear as well, calling for a consistent regularization.

The comparison of QCD and $\mathcal{N} = 4$ SYM behaviors for relevant observables in the Regge limit and the consistent application of Lipatov's action beyond tree level constitute the main topics of the present thesis. Before discussing them, we introduce in the first chapter important concepts of high-energy scattering in QCD, with the emphasis on the BFKL formalism. While trying to cover all the relevant concepts that will be used in the following chapters, this introduction is not aimed at a detailed derivation of results or a comprehensive description of this vast field. We have preferred in this respect to refer to the literature and emphasize the main ideas and the connections among them. A large number of interesting out-of-mainstream remarks have been included, usually in footnotes, that can be skipped without losing the central ideas. Some remarks on the issue of unitarity corrections and nonlinear evolution are also given in the last section to put our work also in the context of

this rapidly developing field.

The second chapter is devoted to a comparative study of QCD and $\mathcal{N} = 4$ SYM in high-energy scattering. After a concise introduction to the key properties of $\mathcal{N} = 4$ SYM and the features shared by the two theories, we go on to compute in both models several observables chosen specifically so that they do not depend on the nonperturbative properties of the colliding hadrons: the azimuthal decorrelation in dijets widely separated in rapidity, and the diffusion pattern and multiplicities associated to the BFKL Green's function.

In Chapter III we turn to applications of the Lipatov's action approach in loop computations. After a brief summary of the ideas underlying this action we describe how to account for the apparent overcounting and light-cone divergences. We then exemplify this procedure with the computation of the one-loop forward jet vertex and the two-loop gluon Regge trajectory. We explain how one can consider loop corrections as reggeon wavefunction and vertex renormalization. Finally, we have provided several appendices with details on color algebra and Feynman rules, multi-Regge kinematics, the Mellin-Barnes representation and the explicit evaluation of master integrals for the gluon trajectory at two loops.

Tomelloso, May 2013.

Prefacio

La dinámica de las teorías gauge en el límite de alta energía —y en particular de la Cromodinámica Cuántica (QCD), la teoría de las interacciones fuertes— presenta aún hoy, cuarenta años después del descubrimiento de la libertad asintótica, importantes desafíos. Este régimen cinemático, en el que los procesos de dispersión vienen caracterizados por energías de centro de masas s mucho mayores que el momento transferido $|t|$, no sólo es vital para describir de forma precisa los procesos difractivos y las dispersiones de bajo ángulo en los colisionadores de hadrones modernos —y quizá mas importante aún para entender la física de sistemas con alta densidad partónica— sino que también presenta un buen número de profundas propiedades de interés *per se*.

Cuando todas las escalas de momento en el problema son suficientemente grandes, el acoplo α_s se hace pequeño y permite la aplicación de la teoría de perturbaciones. Una simplificación notable de las amplitudes de dispersión ocurre en el límite de alta energía (o límite de Regge), posibilitando la resumación de todas las contribuciones dominantes de la forma $(\alpha_s \ln s)^n$ mediante el ansatz autoconsistente de BFKL basado en la teoría de Regge (según la cual la dispersión a alta energía ocurre mediante el intercambio de una partícula efectiva, el reggeón). Cabe esperar que QCD reproduzca las atractivas propiedades de esta teoría fenomenológica, cimentada en las propiedades generales de la matriz S y la continuación analítica del momento angular a valores complejos. En particular, hay ciertas indicaciones de que una transición suave ocurre entre las regiones perturbativa y no perturbativa del límite de Regge, permitiendo obtener importante información sobre la dinámica hadrónica desde el régimen perturbativo de alta energía.

De acuerdo con la teoría de Regge, QCD puede formularse en este límite como una teoría de campos en 2+1 dimensiones donde el grado de libertad fundamental es el reggeón. La derivación de los vértices efectivos de esta teoría en el marco de QCD es una cuestión relevante. En la aproximación dominante en $\ln s$, los elementos conocidos de la teoría de

campos reggeizados presentan notables propiedades, como la invariancia conforme en el plano transversal de los vértices describiendo las transiciones de 2 a 4 y de 2 a 6 reggeones, o la integrabilidad en el límite $N_c \rightarrow \infty$ de estados con un número arbitrario de reggeones. En general, se considera que estas propiedades vienen heredadas de las que posee la teoría $\mathcal{N} = 4$ Super Yang-Mills, equivalente a QCD en los términos dominantes en $\ln s$.

De hecho, los importantes descubrimientos sobre la estructura de las amplitudes de dispersión en $\mathcal{N} = 4$ SYM en los últimos años, y el papel protagonista que juega esta teoría en la correspondencia AdS/CFT, han llevado a considerar esta versión supersimétrica de QCD, que es probablemente exactamente resoluble, como un perfecto modelo simplificado para extraer —al menos de forma cualitativa— importantes intuiciones sobre la física de las interacciones fuertes. Se espera que este paralelismo entre QCD y $\mathcal{N} = 4$ SYM sea mayor en cierto sentido en el límite de Regge. Cuestiones importantes como el origen de la invariancia conforme y la integrabilidad que aparecen en QCD a alta energía, así como la existencia de un dual gravitacional a la teoría de campos reggeizados, siguen esperando respuesta.

Una herramienta prometedora para el estudio de estas cuestiones es la acción efectiva propuesta por Lipatov. Derivada mediante el requerimiento de consistencia entre invariancia gauge y la llamada cinemática de quasi-multi-Regge, esta acción incluye por construcción las correcciones de unitariedad necesarias en sistemas con gran densidad partónica, y debería dar lugar a la teoría de campos reggeizados tras integrar sobre los campos físicos de quarks y gluones. La acción efectiva también permite simplificar considerablemente el cálculo perturbativo de amplitudes en el límite de alta energía.

La acción de Lipatov es no obstante inusual en el sentido de que, en lugar de integrar grados de libertad à la Wilson, los campos que describen reggeones son añadidos al Lagrangiano completo de QCD, entendiendo, implícitamente, que se debe imponer que las interacciones sean locales en rapidez. Este último requerimiento es difícil de llevar a cabo cuando aparecen correcciones cuánticas. Un problema relacionado es la aparición de nuevas divergencias que han de ser consistentemente regularizadas.

La comparación de las dinámicas de QCD y $\mathcal{N} = 4$ SYM para observables relevantes en el límite de Regge, y la aplicación coherente de la acción de Lipatov más allá del nivel árbol, constituyen los principales temas de esta tesis. Antes de discutirlos en detalle, presentamos en el primer capítulo importantes conceptos de QCD a altas energías, centrándonos en el

formalismo de BFKL. Aunque tratamos de cubrir de forma lo más autocontenida posible todos los conceptos que aparecerán en los siguientes capítulos, no pretendemos ofrecer en esta introducción derivaciones detalladas de los resultados o una descripción en profundidad de todos los aspectos de este vasto campo de investigación. Hemos preferido referir al lector interesado a la literatura para estos detalles y poner el énfasis en las ideas principales y las conexiones entre ellas. Un buen número de ideas que consideramos interesantes pero que no forman parte de la discusión principal han sido relegadas a notas a pie de página, que pueden ser omitidas sin perder la continuidad de la discusión. Un breve resumen sobre restauración de la unitariedad y evolución no lineal se ha incluido en la última sección de la introducción para poner nuestro trabajo en el contexto de este campo en rápida evolución.

El segundo capítulo se dedica al estudio comparativo de QCD y $\mathcal{N} = 4$ SYM en la dispersión a altas energías. Tras una concisa introducción a $\mathcal{N} = 4$ SYM y los rasgos compartidos por las dos teorías, calculamos en ambas varios observables que han sido elegidos de forma que no dependen de la física no perturbativa de los hadrones que participan en la colisión: la decorrelación azimutal en dijets ampliamente separados en rapidez, y el patrón de difusión y las multiplicidades asociados a la función de Green de BFKL.

En el Capítulo III pasamos a estudiar las aplicaciones de la acción de Lipatov en cálculos de amplitudes con correcciones cuánticas. Comenzamos repasando las principales ideas que aparecen en la construcción de la acción, y explicamos cómo se pueden tratar consistentemente el aparente doble conteo y las divergencias en el cono de luz. Este procedimiento es puesto en práctica mediante el cálculo de las correcciones a un lazo del vértice de jet y a dos lazos de la trayectoria de Regge del gluón. Explicamos cómo se pueden considerar las correcciones perturbativas como una renormalización de los vértices y la función de onda del reggeón. Finalmente, hemos incluido varios apéndices con detalles sobre el álgebra de color, las reglas de Feynman, la cinemática de multi-Regge, las representaciones de Mellin-Barnes y algunos cálculos realizados en detalle.

Tomelloso, Mayo de 2013.

Conventions and Acronyms

Natural units ($\hbar = c = 1$) are used throughout the text. Our convention for Minkowski metric is $g_{\mu\nu} = g^{\mu\nu} = \text{diag}(+1, -1, -1, -1)$. The Levi-Civita density is defined with the convention $\epsilon^{0123} = +1$ (this implies $\epsilon_{0123} = -1$). Generic 4-vectors are written in Cartesian components as $A^\mu = (A^0, A^1, A^2, A^3) = (A^0, \mathbf{A}_\perp, A^3) = (A^0, \mathbf{A})$. Conventions for light-cone components and normalization of the Sudakov parametrization are given in APPENDIX B.

Greek indices ($\alpha, \beta, \dots, \mu, \nu, \dots$) are Lorentz tensor indices. Latin indices are used to label color: i, j, k are quark color indices ($i, j, k = 1, \dots, N_c$) and a, b, c are gluon indices ($a, b, c = 1, \dots, N_c^2 - 1$). Einstein summation convention is understood unless otherwise stated.

Conventions for the QCD Lagrangian and Feynman rules follow those of Peskin and Schröder [PS95]. Dirac spinors are normalized so as to satisfy $\bar{u}(p, s)\gamma^\mu u(p, s') = 2p^\mu \delta_{ss'}$. Momentum eigenstates are normalized as $\langle p|p' \rangle = (2\pi)^3 2E \delta(\mathbf{p} - \mathbf{p}') = (2\pi)^3 2p^+ \delta(p^+ - p'^+) \delta(\mathbf{p}_\perp - \mathbf{p}'_\perp)$.

e and g will be employed, respectively, for the electromagnetic and strong couplings, with $\alpha \equiv \frac{e^2}{4\pi}$ and $\alpha_s \equiv \frac{g^2}{4\pi}$. We will also introduce the shorthand notations $\bar{\alpha}_s \equiv \frac{\alpha_s N_c}{\pi}$ and $[dk] \equiv \frac{d^d k}{(2\pi)^d}$. The convention for dimensional regularization is $d = 4 + 2\epsilon$, $\epsilon \rightarrow 0$.

The convention for the Fourier transform is the symmetric one:

$$\mathcal{F}(\mathbf{k}) = \int \frac{d^n \mathbf{x}}{(2\pi)^{n/2}} \mathcal{F}(\mathbf{x}) e^{-i\mathbf{k}\cdot\mathbf{x}} \text{ (Euclidean); } \quad \mathcal{F}(k) = \int \frac{d^n x}{(2\pi)^{n/2}} \mathcal{F}(x) e^{ik\cdot x} \text{ (Minkowski)}. \quad (1)$$

Acronyms

BFKL Balitsky-Fadin-Kuraev-Lipatov

BK Balitsky-Kovchegov

BLM	Brodsky-Lepage-Mackenzie
CCFM	Ciafaloni-Catani-Fiorani-Marchesini
CGC	Color Glass Condensate
CM	Center-of-Mass
DGLAP	Dokshitzer-Gribov-Lipatov-Altarelli-Parisi
DIS	Deep Inelastic Scattering
EFT	Effective Field Theory
GGR	Gluon-Gluon-Reggeon
IR	InfraRed
JIMWLK	Jalilian-Marian-Iancu-McLerran-Weigert-Leonidov-Kovner
LHC	Large Hadron Collider
(N)LLA	(Next-to-) Leading Log Approximation
(N)LO	(Next-to-) Leading Order
MB	Mellin-Barnes
MOM	MOMentum (Subtraction Scheme)
$\overline{\text{MS}}/\text{MS}$	(Modified) Minimal Subtraction Scheme
(Q)MRK	(Quasi)-Multi-Regge Kinematics
PDF	Parton Distribution Function
(p)QCD	(Perturbative) Quantum ChromoDynamics
QFT	Quantum Field Theory
RFT	Reggeon Field Theory
RG/RS	Renormalization Group/Scheme
RRG	Reggeon-Reggeon-Gluon
(M)SYM	(Maximally) Supersymmetric Yang-Mills
UV	UltraViolet

Agradecimientos

Con gusto puedo decir que tengo mucho que agradecer a mucha gente, empezando por la familia (mis padres, mis hermanos Ana y Juanjo, y los más cercanos) por tantas manos que me han echado siempre y lo que me han animado, interesándose por lo que estudiaba (hasta el punto de regalarme una camiseta con su visión pictórica de los gluones...). Siempre me había hecho ilusión dedicar algo de este estilo a mis abuelos, por su espíritu de trabajo que tanto admiro, y aprovecho la ocasión aquí. Un agradecimiento especial es para Juanjo, de quien siempre he bromeado que había de sacarme media tesis adelante, por su paciencia explicándome matemáticas, con un estilo completamente original, y por su ofrecimiento para ayudar siempre a lo largo de esta tesis.

El agradecimiento más directo, evidentemente, es para mi director de tesis, Agustín Sabio Vera. Gracias no sólo por el mero hecho de que este trabajo, y mi iniciación a la investigación, hubieran sido imposibles sin su constante ayuda, sino también por su admirable trato más allá de lo académico. Gracias porque la segunda vez que fui a verlo no comenzó preguntándome qué había sacado en claro de los artículos que me había recomendado estudiar la primera vez, sino preguntándome qué tal me iba ahora en Madrid; por los ratos tan buenos que he pasado en su despacho, por no hacer caso a los correos del viernes por la tarde, y no haberme matado en alguna ocasión que él bien sabe... Gracias por su optimismo en los momentos más difíciles y, en definitiva, por ser un magnífico tutor y amigo.

También en mi trabajo he tenido la oportunidad de colaborar con varias personas a las que estoy muy agradecido por haber estado siempre disponibles. Mucho le debo a Martin Hentschinski, que tantas veces ha debido soportar estoicamente mis preguntas y me ha enseñado mucho a lo largo de estos años. Y a Greg Chachamis, que también ha tenido su paciencia conmigo, y confió que las cosas saldrían bien cuando no estaba claro. A Michele Angioni, Francesco Caporale y Beatrice Murdaca les agradezco su colaboración en algunos de los artículos. Dentro del grupo, un lugar especial lo tienen Clara Salas y Edu Serna, al

igual que yo doctorandos de Agustín, con los que he pasado muy buenos ratos.

Un recuerdo especial es para todos mis amigos, a quienes tanto debo —más de lo que piensan—, en especial los que hemos estado juntos estos años en Santa María y Alejandro Ferrant (¡qué grandes sois, y lo que os voy a echar de menos!). Somos muchos y me gustaría poner a todos: pongo aquí como representante a Ramón, ¡qué grande ha sido tener otro compañero de fatigas escribiendo la tesis a destajo! Y para los colegas de Miguel Esteban: Clemente, Huertas, Chema...: cada semana traía siempre algo nuevo. Gracias también a otro gran amigo, Pere Talavera, que me introdujo en este mundo de la física que tanto he disfrutado, y me ha ayudado a ir más allá, en la física y fuera de ella.

Por último (y, como se suele decir, no por ello menos importante) quiero agradecer a todos sus miembros el buen ambiente que he encontrado en el IFT. Mikel, Luis Fer, Yago, Rodrigo, Antonio, Fermín, Luis, David, Alfonso... son muchos los que han hecho más fácil el trabajo cotidiano. Se merecen también un buen reconocimiento Andrés por sus ayudas informáticas e Isabel, Chabely y Roxanna que tantas manos me han echado con el papeleo. Gracias, finalmente, a los profesores del Máster de Física Teórica, por su competencia y su apertura, que me han hecho posible aprender muchas cosas. En especial he de dar las gracias a Margarita García-Pérez, Carlos Pena, Pepe Barbón, Ángel Uranga, Esperanza López y Karl Landsteiner, por lo que aprendí en sus clases, y por las horas extra que han dedicado a mis dudas con una paciencia increíble y un trato personal admirable.

A todos vosotros, muchas gracias.

Table of Contents

Preface	i
Prefacio	v
Conventions and Acronyms	ix
Agradecimientos	xi
<hr/>	
I Introduction	1
<hr/>	
I High Energy Scattering in QCD	3
1 QCD and the Renormalization Group	3
Building Blocks of the QCD Lagrangian □ The Renormalization Group and Effective Field Theories □ From Confinement to Asymptotic Freedom □ Changing the Renormalization Scheme	
2 A Tale of Two Limits	17
The Paradigm of Deep Inelastic Scattering: Factorization and DGLAP Evolution □ Semihard Processes and the Small- x Regime □ Insights from Regge Theory	
3 Reggeization and the BFKL Pomeron	42
Parton-Parton Scattering in the Leading $\ln s$ Approximation □ Gluon Reggeization and the Bootstrap □ The BFKL Equation □ Going Beyond the Leading Approximation □ Small- x Phenomenology and k_T Factorization	
4 Properties of the BFKL Equation	69
Unitarity and Diffusion Issues □ The Appearance of Conformal Invariance and Integrability	
5 Unitarity Corrections and Nonlinear Evolution	75
Saturation and Restoration of Unitarity □ High Parton Density QCD	

II QCD, $\mathcal{N} = 4$ SYM and the High-Energy Effective Action 81

II Comparing QCD and $\mathcal{N} = 4$ SYM in the Regge Limit 83

1 $\mathcal{N} = 4$ SYM as a Testing Ground for QCD 83

The Maximally Supersymmetric Yang-Mills Theory \square $\mathcal{N} = 4$ SYM as the Harmonic Oscillator of Quantum Field Theory \square Connections Between QCD and $\mathcal{N} = 4$ SYM and the Role of Conformal Invariance \square Pomeron in $\mathcal{N} = 4$ SYM

2 High Energy Dijets in $\mathcal{N} = 4$ SYM [ACMS11] 90

Mueller-Navelet Jets and Dijet Azimuthal Decorrelation \square The Role of Higher Conformal Spins \square The BLM Procedure \square Azimuthal Angle Correlations in QCD and $\mathcal{N} = 4$ SYM

3 The Diffusion Pattern in $\mathcal{N} = 4$ SYM at High Energies [CCM⁺13] 103

The Gluon Green's Function in $\mathcal{N} = 4$ SYM \square Monte Carlo Approach to the BFKL Equation \square Analysis of Diffusion and Multiplicities

III Lipatov Effective Action Approach to High Energy QCD 111

1 Lipatov's Effective Action 112

Virtual Modes in Multi-Regge Kinematics \square Quasielastic and Central Production Vertices in QMRK \square Gauge Invariance and Lipatov's Effective Action \square Connection with Reggeon Field Theory and Other Formalisms

2 Loop Computations and Lipatov's Action [CHMS12a] 122

Overcounting and Spurious Divergences \square Light-Cone Regularization and Pole Prescription \square Gauge Invariant Subtraction

3 Two-Loop Gluon Regge Trajectory [CHMS12c, CHMS13] 126

Subtraction and Renormalization \square Computation of the Reggeon Self-Energy

4 Forward Jet Production [CHMS12b] 139

Real Corrections \square One-Loop Gluon-Gluon-Reggeon Vertex

IV Conclusions and Outlook 149

V Conclusiones 153

III Appendices

157

A Miscellaneous Formulæ

159

SU(3) Matrices, Color Algebra and Color Projectors □ Feynman Rules for QCD and the High-Energy Effective Action □ S -Matrix Elements, Cross Sections and the Optical Theorem

B Kinematics of Scattering Processes

167

Mandelstam Variables □ Elastic Scattering in the Center-of-Mass System □ Light-Cone Components, Sudakov Parametrization and Rapidity □ Multi-Regge Kinematics

C Feynman Integrals and Mellin-Barnes Representation

175

The Mellin Transform □ Mellin-Barnes Representation and Evaluation of Master Integrals for the Two-Loop Gluon Trajectory

D Details of Some Computations

179

References

204

Part I

Introduction



High Energy Scattering in QCD

1 QCD AND THE RENORMALIZATION GROUP

Quantum Chromodynamics (QCD), the field theory of quarks and gluons, has stood the passing of time since its original formulation in 1973 [FGML73, GW73, Wei73] to become the generally accepted theory describing strong interactions. Detailed treatments of the basics of QCD, focusing on the perturbative regime, can be found in [DKS08, Mut10, ESW03, Col11].

QCD is a non-abelian gauge theory with color gauge group $SU(3)$ ¹. In spite of the apparent

¹ The correct clues towards QCD (see [Mut10, DKS08, Man99] for a review) came from the discovery of a new degree of freedom, color —experimentally supported by the spin-statistics Δ^{++} paradox [Gre64] in the flavor $SU(3)$ pattern of the quark model [GM64, Zwe64], and the factors necessary to account, for instance, for the observed $e^+e^- \rightarrow \text{hadrons}$ or $\pi^0 \rightarrow \gamma\gamma$ cross sections—; and the Bjorken scaling [Bjo69] discovered in DIS experiments at SLAC [Fri91], which pointed towards the quark-parton model and, eventually, to asymptotic freedom. Gauge invariance is the only known way to construct a sensible quantum field theory with interactions mediated by spin-1 massless bosons [Wei95]. Furthermore, as shown by Coleman and Gross [CG73], asymptotic freedom only appears in non-abelian gauge theories, and then the guess to identify the color symmetry $SU(N_c)$ with the one to be gauged appeared natural. The gauge group is essentially fixed by the requirement that all hadron states in the asymptotic spectrum and physical observables are color singlets (see [Mut10], pp. 14-15).

The history of the discovery of QCD is extremely interesting [Cao97, Cao10]. For a long while Yang-Mills theory [YM54] was thought incompatible with the short-range of nuclear forces. This difficulty was overcome, first in the early 60s, with the discovery of spontaneous symmetry breakdown [NJL61a, NJL61b, Gol61], and

I. High Energy Scattering in QCD

simplicity of its Lagrangian, the theory is outstandingly rich and currently an exact analytic determination of its correlation functions is out of reach. Indeed, while the problem of confinement still waits for a satisfactory explanation [JW00, Gre11], asymptotic freedom, the other conceptual pillar of QCD, took long time to be conveniently understood [Gro98, tH98], due in particular to a misunderstanding of the renormalization group [LP55, Lan60, Wei09]. It is asymptotic freedom that allows us to make sense of a perturbative treatment of short-distance phenomena. On the other hand, nonperturbative effects associated to energy scales where the theory becomes strongly coupled, will be ubiquitous in the analysis of most processes. Lattice field theories, QCD sum rules and phenomenological approaches like Regge theory are the only tools here. Hence the property of factorization —justified by Wilson’s operator product expansion (OPE) [Wil69]—, allowing us to extract from a given process the purely perturbative part, will be extremely useful.

1.1 Building Blocks of the QCD Lagrangian

The QCD (classical) Lagrangian, describing the interaction between quark fields ψ and gluon fields A_μ^a is²

$$\mathcal{L}_{\text{class}} = -\frac{1}{4}F_{\mu\nu}^a F^{\mu\nu,a} + \sum_{\text{flavors}}^{N_f} \bar{\psi}_i (i\not{D} - m_f)_{ij} \psi_j. \quad (\text{I.1})$$

Here $F_{\mu\nu}^a$ is the field strength tensor

$$F_{\mu\nu}^a = \partial_\mu A_\nu^a - \partial_\nu A_\mu^a + g f^{abc} A_\mu^b A_\nu^c, \quad (\text{I.2})$$

where f^{abc} ($a, b, c = 1, \dots, 8$) are the structure constants of the SU(3) color group. The covariant derivative D has the form

$$(D_\mu)_{ij} = \partial_\mu \delta_{ij} - ig(t^a A_\mu^a)_{ij}; \quad (D_\mu)_{ab} = \partial_\mu \delta_{ab} - ig(T^c A_\mu^c)_{ab}, \quad (\text{I.3})$$

when acting on quark and gluon fields, respectively. t^a and T^a are the generators in the fundamental and adjoint representations, respectively, of SU(3)³.

then in 1972-73 with the discovery of asymptotic freedom in non-abelian Yang-Mills theories [tH72, GW73, Pol73], and the proof [tHV72] of the renormalizability of non-Abelian gauge theories.

²We have omitted the so-called Θ -term $\mathcal{L}_\Theta = \Theta \frac{g^2}{32\pi^2} F_{\mu\nu}^a \tilde{F}^{a,\mu\nu}$. \mathcal{L}_Θ can be expressed as the total divergence of a gauge dependent current, contributing only a surface term to the action which naïvely may be neglected. However, the surface integral is related to a topological invariant, the Pontryagin index, and the non-trivial topological structure of the vacuum of QCD is such that \mathcal{L}_Θ gives a non-perturbative contribution. Θ turns out to be very small, giving rise to the strong CP problem. So we adopt the pragmatic view of simply setting $\Theta = 0$; in any case the Θ -term does not give rise to any perturbative physics.

³Important relations of color algebra are collected in APPENDIX A.

Path integral quantization of QCD —and, in general, non-abelian gauge theories— involves the Faddeev-Popov procedure [DeW64, DeW67, FP67] to isolate a single contribution to the partition function, corresponding to the configuration $f(A^\vartheta) = 0$, from the infinitely many equivalent of the gauge orbit (parametrized by ϑ)

$$\begin{aligned} Z &= \int \mathcal{D}\bar{\psi}\mathcal{D}\psi\mathcal{D}A e^{i\int d^4x\mathcal{L}_{\text{class}}} \times \int \mathcal{D}\vartheta \det \left| \frac{\delta f(A^\vartheta)}{\delta \vartheta} \right| \delta(f(A^\vartheta)) \\ &\rightarrow \int \mathcal{D}\bar{\psi}\mathcal{D}\psi\mathcal{D}A\mathcal{D}\eta^\dagger\mathcal{D}\eta e^{i\int d^4x \left[\mathcal{L}_{\text{class}} - \frac{1}{2\xi} f(A)^2 + \eta^\dagger \frac{\delta f(A^\vartheta)}{\delta \vartheta} \eta \right]}. \end{aligned} \quad (\text{I.4})$$

This results in the addition of two more terms to the effective Lagrangian:⁴

$$\mathcal{L}_{\text{gauge-fixing}} = -\frac{1}{2\xi}(\partial_\mu A_a^\mu)^2, \quad \mathcal{L}_{\text{ghost}} = \partial_\mu \eta^{a\dagger} (\partial^\mu \delta^{ab} + g f_{abc} A^{c\mu}) \eta^b. \quad (\text{I.6})$$

The ghost fields η^a , resulting from the determinant of the Jacobian matrix, are unphysical, complex valued, Lorentz scalars which obey Fermi-Dirac statistics. We observe that the bracketed term in $\mathcal{L}_{\text{ghost}}$ is the covariant derivative for the adjoint representation $T_{bc}^a = -if_{abc}$. It provides a kinetic term for the ghost fields and in this covariant gauge a ghost-gluon coupling. The Feynman rules for QCD are presented in APPENDIX A.

1.2 The Renormalization Group and Effective Field Theories⁵

The bare charge g and mass m entering the QCD Lagrangian (I.1) are not physical values. Transition from bare parameters to physical quantities, i.e. to the quantities that can be (at least in principle) experimentally measured, is called renormalization.

⁴We choose to work in covariant gauges, what implies the need to incorporate ghosts. Two typical choices of gauge parameter are $\xi = 1$ (Feynman gauge) and $\xi = 0$ (Landau gauge). The form of the gauge-fixing term is different for other choices: for instance, for axial gauges, which do not require ghosts (at the price of having a much more involved expression for the gluon propagator, which explicitly forbids non-physical polarizations), $\mathcal{L}_{\text{g.f.}} = -\frac{1}{2\xi}(n_\mu A_a^\mu)^2$. A particularly important choice here is $\xi = 1, n^2 = 0$, the light-cone gauges, which we will have occasion to use. Polarization sums in this case are evaluated through

$$\sum_\lambda \epsilon_\lambda^\mu(p) \epsilon_\lambda^{\nu*}(p) = - \left(g^{\mu\nu} - \frac{p^\mu n^\nu + p^\nu n^\mu}{p \cdot n} \right). \quad (\text{I.5})$$

Global subtleties in the gauge-fixing from Gribov copies (see e.g. [IFL10]) will not concern us here.

⁵In this section we provide a detailed conceptual view of renormalization. Our interest lies in showing the physical meaning of renormalization schemes —which will be important in discussing the BLM procedure (SEC. II.2.3)—; discussing the notion of universality, which motivates in many cases the approximation of QCD by simpler theories; and reviewing the Wilsonian notion of effective theories, which helps understand the subtleties of Lipatov’s action (CHAP. III).

I. High Energy Scattering in QCD

The word renormalization was attached for many years to the mechanism of sweeping infinities under the rug. In quantum field theory, the Lorentz-invariant generalization of the uncertainty principle allows for quantum fluctuations of arbitrarily high energies. When computing how much interactions of real particles are modified by their interaction with very energetic virtual particles, one often gets divergent answers. In renormalizable theories, for which all couplings have non-negative dimensions, a procedure was devised to render these answers meaningful, being possible to absorb all divergences in the transition from bare to renormalized quantities. This involves as a first step regularization: suppressing the high-energy modes of virtual particles introducing a cutoff Λ , in order to get well-defined (non-divergent) quantities in the integrals over the momenta of virtual particles⁶. Then a key observation is that, when the above mentioned requisite for renormalizability is satisfied, the potentially divergent terms in n -point functions are of the form of the most general terms in the Lagrangian compatible with the original field content and renormalizability⁷, with couplings depending on Λ . Hence, redefining the fields in the Lagrangian, $\phi \rightarrow Z_\phi(\Lambda)\phi$, and the couplings (which amounts to add counterterms) we can get rid of the divergences. This usually requires that the bare couplings diverge as $\Lambda \rightarrow \infty$. The procedure can be shown to be consistent when applied order by order in perturbation theory, in spite of technical issues like overlapping divergences (see, e.g. [Wei95]).

Getting rid of UV divergences is not enough⁸. When regularizing the theory we break the unitarity essential to quantum mechanics, as we have arbitrarily removed part of the phase space to which there was associated a non-zero amplitude. Moreover, we have a spurious dependence on Λ , and the ambiguity on choosing the counterterms to adjust the finite part of renormalization. If we can make all physical observables at an energy scale $\mu \ll \Lambda$

⁶As emphasized by Zee [Zee10], the cutoff must not be seen as just an artifact, but it parametrizes our ignorance of the physics at even higher energies. Usually, a brute force momentum cutoff, breaking any underlying symmetry, is not a good choice from the computational point of view. Many other methods exist to suppress the high-energy modes in a more suitable fashion. Among them, dimensional regularization [tHV72, BG72], based on the observation that divergencies are milder when lowering the dimension of spacetime d , and everything appearing in Feynman integrals —but for, possibly, $\epsilon^{\mu_1 \dots \mu_d}$ (and, therefore, γ^5)—, is an analytical function of d , is usually the most convenient. Some integrals are evaluated through dimensional regularization in APPENDIX C.

⁷Actually, this is also true for a non-renormalizable theory if one considers in the Lagrangian all terms allowed by symmetries. Therefore these theories can be considered perfectly consistent effective theories up to some energy scale [Wei95, Dun12, Don95].

⁸Renormalization would make sense even if ultraviolet divergences were absent. Although in this case that renormalization would be finite, so that physical quantities could be expressed through bare parameters, it would be more convenient to express the former in terms of experimentally measured ones. In the actual case of existence of UV divergences, renormalization is not only convenient but mandatory.

independent of Λ then we can safely take $\Lambda \rightarrow \infty$. The procedure that allows removing the cutoff leaving something that makes sense is the renormalization group (RG) flow⁹ pioneered by Wilson [Wil71a, Wil71b, Wil79]. The RG picture formalizes two important observations: 1) the low energy (long distance) behavior of many systems is largely independent of the details of what goes on at higher energy scales; and 2) couplings and masses are not constant at all, but depend on the scale at which we are looking [GML54, LAK54].

In the RG approach, the finite renormalization is fixed by *defining* the physical (renormalized) values of n -point functions at some scale μ (R stands for renormalized, $_0$ for bare quantities)

$$\Gamma_R(p_i; g_R, \mu) = Z^{-n/2} (g_0(\Lambda), \Lambda/\mu) \Gamma_0(p_i; g_0(\Lambda), \Lambda). \quad (\text{I.7})$$

Requiring that physics at scale μ does not depend on Λ ($\Lambda \frac{d\Gamma_R}{d\Lambda} = 0$) leads to the RG equation

$$[\Lambda \partial_\Lambda + \beta(g_0) \partial_{g_0} - n\eta(g_0)] \Gamma_0(p_i; g_0, \Lambda) = 0, \quad \beta(g_0) \equiv \Lambda \frac{dg_0}{d\Lambda}, \quad \eta(g_0) \equiv \frac{1}{2} \Lambda \frac{d}{d\Lambda} \ln Z. \quad (\text{I.8})$$

In this way, starting from a theory defined at the cutoff Λ with (a set of) bare coupling(s), we can get *the same low energy physics* at $\mu \ll \Lambda$ when integrating out a momentum shell $(\Lambda - \delta\Lambda, \Lambda)$ provided the couplings change with the floating cutoff according to the beta function $\beta(g_0)$ in (I.8). Equivalently, we can demand that Γ_0 , taken from the fields in the Lagrangian, is independent of the scale μ at which we define our physical quantities:¹⁰

$$0 = [\mu \partial_\mu + \beta(g_R) \partial_{g_R} + n\gamma(g_R)] \Gamma_R(p_i; g_R, \mu), \quad \beta(g_R) = \frac{dg_R}{d \ln \mu}, \quad \gamma(g_R) = \frac{1}{2} \frac{d \ln Z}{d \ln \mu}. \quad (\text{I.9})$$

This is the Callan-Symanzik equation [Cal70, Sym70, Sym71]. Its solution can be written (see, e.g. [Mag05]) making explicit the notion of running coupling as

$$\Gamma_R(up_i; g_R, \mu) = u^{d_\Gamma} \exp \left\{ n \int_0^{\ln u} \gamma(g_{\text{eff}})(u') d \ln u' \right\} \Gamma_R(p_i; g_{\text{eff}}(u), \mu), \quad (\text{I.10})$$

where d_Γ is the mass dimension of Γ_R and $u \rightarrow 0$ in the continuum limit¹¹. From (I.10) we see that the rescaling of energies, in the limit when masses can be neglected, is summarized

⁹A very good account on some of these issues can be found in [Sho07, Ban08, AGVM12, Hol13].

¹⁰The functional form of the β -functions appearing in (I.8) and (I.9) is intimately related. In fact, from the relation between bare and renormalized couplings, $g_R(\mu) = Z \left(\frac{\mu}{\Lambda}\right) g_0(\Lambda)$, it is easy to see that $\frac{d \ln g_R}{d \ln \mu} = \frac{d \ln g_0}{d \ln \Lambda}$, i.e. $\beta(g_0) = \frac{g_0}{g_R} \beta(g_R)$. In particular, both β -functions have the same zeros.

¹¹Solution of equation (I.8) is identical to that of (I.9) with the evident substitutions $\Lambda \leftrightarrow \mu, g_0 \leftrightarrow g_R$, and $\eta(g_0) \leftrightarrow -\gamma(g_R)$. The effective (floating) cutoff is then Λ/u , which goes to infinity as $u \rightarrow 0$.

I. High Energy Scattering in QCD

by two effects: 1) naive dimensional analysis breaks¹², and instead of a simple overall factor u^{d_T} we get also a modification determined by the γ function, called the anomalous dimension; 2) the coupling g_R at the scale μ is replaced by $g_{\text{eff}}(u)$, or $g_{\text{eff}}(E)$ with $E = \mu/u$, which is called the running coupling and plays the role of an effective renormalized coupling.

Removing the cutoff (sending $u \rightarrow 0$) means that $g_{\text{eff}}(u \rightarrow 0)$ approaches a zero of the beta function, as can be seen from the formula $\int_{g_0}^{g_{\text{eff}}(u)} \frac{dg'}{\beta(g')} = \ln u$ ¹³. In order not to end with a trivial (with all couplings being infinity) or scale-invariant theory (in which all relevant couplings are zero) at the scale μ when $\Lambda \rightarrow \infty$, we must take a *double scaling limit*: we send the high energy cutoff $\Lambda \rightarrow \infty$, simultaneously sending the bare relevant coupling constant¹⁴ closer and closer to the critical surface (the surface of null relevant couplings), in such a way that the limit gives a theory with a finite relevant coupling at the scale μ (FIG. I.1). The way in which this limit is taken defines the renormalization scheme.

In most cases of interest, just a small number of relevant parameters exist that encode all the physics at the scale μ . Measuring these couplings we can make unique predictions of the physics at the scale μ while remaining ignorant about the information encoded in (potentially infinitely many) irrelevant couplings. This explains why physics at some scale is shielded off from the effects of physics at much shorter distances. On the other hand, in nonrenormalizable theories, where some of the irrelevant couplings have non-zero value at the scale μ , we cannot consistently remove the cutoff: when $\Lambda \rightarrow \infty$ those couplings need to grow without bound (FIG. I.1)¹⁵. So nonrenormalizable QFTs are not consistent theories for all energy scales, in this sense they cannot be fundamental. However, they are perfectly

¹²This is a consequence of dimensional transmutation: UV divergences force us to introduce a new dimensional scale, the cutoff Λ , which is eventually traded for the renormalization point μ .

¹³This is a general property of RG flow when it occurs in multi-dimensional coupling (or theory) space, and is based upon the fact that the asymptotic behavior of gradient flows is dominated by fixed points [Pol84]. Fixed points, corresponding to scale-invariant (usually conformal) theories, are relatively few in the space of theories. This leads to the phenomenon of *universality*: since points on the same RG trajectory describe the same macroscopic physics, all the points on the critical surface that lie in the basin of attraction of the same fixed point correspond to equivalent theories. In this way, the space of possible renormalized QFTs is split into a few equivalence classes—the universality classes—in one-to-one correspondence with the fixed points on the critical surface. This also expresses the idea that, though in principle one can take the continuum limit in any point of the critical surface, most of the choices are equivalent. These are different *renormalization schemes* which are just different ways of parameterizing the relevant and marginal couplings (see below). The notion of universality appears naturally in the application of RG methods to statistical systems, where systems apparently very different microscopically—but with the same dimensionality and symmetries—share the same critical exponents.

¹⁴We distinguish between relevant (renormalizable) and irrelevant (non-renormalizable) operators, according to their respective couplings flowing away or towards their fixed point values, respectively.

¹⁵This is the case for instance of QED, where one finds the Landau pole problem. In the same way triviality in the Higgs sector is related to the Higgs coupling λ being marginally irrelevant.

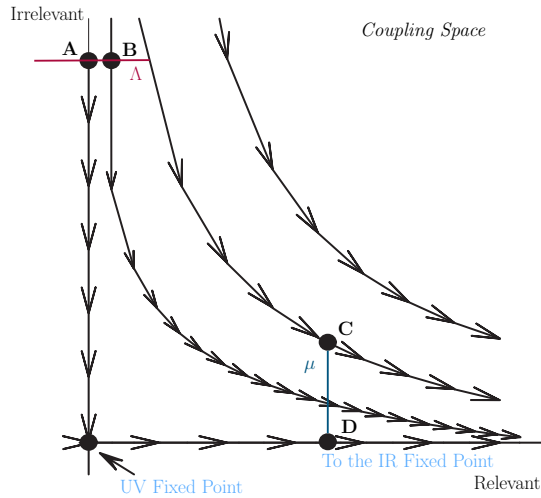


Figure I.1: Flow of coupling constants in the vicinity of a fixed point with one relevant and one irrelevant coupling. Arrows go in the direction of decreasing values of u (asymptotically $u \rightarrow 0$). While point **A** represents a theory (defined at Λ) where the relevant coupling has been tuned to the critical surface (the vertical axis where relevant couplings are zero), the theory represented by **B** will never hit the fixed point. Point **D** corresponds to a renormalizable QFT describing the physics at an energy scale μ : a UV fixed point (e.g. $\mathcal{L} = \frac{1}{2}(\partial\phi)^2$) is perturbed by a relevant operator (e.g. $\frac{1}{2}m^2\phi^2$). Flowing further to lower energies we eventually hit an IR fixed point (in the scalar field example, the trivial $m = \infty$). On the other hand, point **C** corresponds to a nonrenormalizable QFT. Adding a non-zero coupling to an irrelevant operator shoots us away from the UV fixed point we naively thought we were perturbing when tracking backwards the RG flow. Adapted from [Sho07].

fine as effective field theories valid below a certain finite cutoff Λ usually identified with the scale of new physics¹⁶. Certainly, renormalizable theories (such as the extremely successful Standard Model) keep a distinguished role as we expect that at sufficiently low energies all non-renormalizable interactions are highly suppressed by powers of the cutoff. Nevertheless, irrelevant operators, though suppressed, may have observable effects, especially when they

¹⁶One could think that the need to fix an infinite number of quantities by comparison with experiment, makes non-renormalizable theories to lose their predictive power beyond tree level. However, this is only an apparent disaster. The point is that non-renormalizable terms are damped by powers of the cutoff. Thus, taking for definiteness a coupling with mass dimension -2 , $\lambda \equiv 1/M^2$, and having just one typical energy scale μ , the renormalized perturbative expansion of an N -point amplitude A_N to order n reads

$$A_N(\mu) = A_N^0(\mu) \left[1 + c_1 \frac{\mu^2}{M^2} + c_2 \left(\frac{\mu^2}{M^2} \right)^2 + \cdots + c_n \left(\frac{\mu^2}{M^2} \right)^n \right] \quad (\text{I.11})$$

While c_1, \dots, c_{n-1} are finite and calculable, once renormalized the amplitudes A_I , $I > N$, because of the genuinely new divergence at order n , the coefficient c_n must instead be fixed by comparison with experiment, and this is the source of the lack of predictivity. However, at low energy $\mu \ll M$, lack of predictivity in c_n becomes irrelevant as it is multiplied by the very small quantity $(\mu/M)^{2n}$. So, to any given accuracy, only a finite number of parameters must be determined experimentally. Of course, we see from (I.11) that non-renormalizable theories break completely at energies $\mu \sim M$ (it is remarkable, by the way, that the theory predicts its own range of validity; considering the Standard Model as an effective theory, it is expected to break as a good description at most at energies $\Lambda_{\text{SM}} \sim M_{\text{Planck}} = 1.2 \cdot 10^{18}$ GeV). The program we have just outlined has been applied to computation of quantum corrections in gravity [Don95].

I. High Energy Scattering in QCD

induce phenomena that cannot be produced by renormalizable terms (e.g. baryon number non-conservation). Indeed, our best current way to add neutrino masses to the Standard Model Lagrangian is through a dimension-five (non-renormalizable) operator [Wei79a].¹⁷

Reformulation of QFTs as effective field theories that include the relevant degrees of freedom at some energy scale [Pol92, Man96, Pic98] is as well a very powerful method for the analysis of multi-scale problems. It simplifies practical calculations and allows to derive results which are only very hard or even impossible to be obtained from the parent QFT. In the case of QCD, popular examples of such effective theories are Chiral Perturbation Theory (χ PT) [Wei79b], Soft-Collinear Effective Theory (SCET) [BFPS01, BCDF02], Heavy Quark Effective Theory (HQET) [Geo90] or Non-Relativistic QCD (NRQCD) [CL86].

According to Wilson's RG picture, to obtain an effective field theory valid up to some energy scale M , one divides the fields in the parent theory in high and low frequency modes separated by some cutoff $\Lambda < M$: $\phi = \phi_L(\omega < \Lambda) + \phi_H(\omega > \Lambda)$, and obtains the Wilsonian effective action for cutoff Λ by making the path integral over (*integrating out*) the hard modes¹⁸

$$Z[J_L] = \int \mathcal{D}\phi_L \mathcal{D}\phi_H e^{iS(\phi_L, \phi_H) + i \int d^d x J_L(x) \phi_L(x)} \equiv \int \mathcal{D}\phi_L e^{iS_\Lambda(\phi_L) + i \int d^d x J_L(x) \phi_L(x)} \quad (\text{I.12})$$

The effective Lagrangian is nonlocal on scales $\Delta x^\mu \sim 1/\Lambda$, and can be written in terms of local fields using Wilson's OPE [Wil69], $\mathcal{L}_\Lambda^{\text{eff}}(x) = \sum_i g_i \mathcal{O}_i(x)$. The Wilson coefficients g_i are determined by matching with the original theory. Only a small number of local operators $\mathcal{O}_i(x)$ is actually relevant, as can be seen from power-counting arguments¹⁹ [Neu05, Ynd06].

In CHAP. III we will focus on the formulation of an effective action for high-energy QCD. We will see how this program is difficult to apply in this kinematic region, which problems arise and how can one make sense of the non-Wilsonian Lipatov's action.

¹⁷It is somewhat ironical that this scaling with the cutoff faces us with very difficult questions when applied to the *well-behaved* renormalizable terms. Their couplings should be of order a certain non-negative power of Λ_{SM} . If they turn out to be much lower, this must be seen as a fine tuning. This is the basis of the Strong CP Problem (why $\Theta \ll \Lambda_{\text{SM}}^0$), the Hierarchy Problem (why $m_{\text{Higgs}} \ll \Lambda_{\text{SM}}^2$), and the Cosmological Constant Problem (why $\Lambda \ll \Lambda_{\text{SM}}^4$, where Λ here denotes the cosmological constant). This last puzzle entails a fine tuning of more than 120 orders of magnitude [Wei89, Bou07].

¹⁸When this integral is gaussian, it is equivalent to substitute ϕ_H by their equations of motion.

¹⁹The idea is the same as before: at low energy ($E \ll \Lambda < M$), the contribution of a given operator \mathcal{O}_i in the effective Lagrangian to an observable (which for simplicity we assume to be dimensionless) is expected to scale on the basis of naturalness as $C_i(M/E)^{\gamma_i}$, with $C_i \sim \mathcal{O}(1)$ and γ_i the mass dimension of g_i . Only those operators whose couplings have $\gamma_i \geq 0$ are relevant at low energies. Usually one can construct with the low-energy fields few operators compatible with symmetry satisfying this condition.

1.3 From Confinement to Asymptotic Freedom

Returning to equation (I.9), we can see that the qualitative behavior of a theory in the IR and UV is controlled by the sign of the β -function near the RG fixed points (FIG. I.2). Defining the perturbative series for the β -function as

$$\beta(g) = -g \left(\beta_0 \frac{\alpha_s}{4\pi} + \beta_1 \left(\frac{\alpha_s}{4\pi} \right)^2 + \dots \right), \quad \alpha_s \equiv \frac{g^2}{4\pi}, \quad (\text{I.13})$$

the result found by Gross, Wilczek and Politzer for β_0 is²⁰ [GW73, Pol73]

$$\beta_0 = \frac{11}{3}N_c - \frac{2}{3}N_f. \quad (\text{I.14})$$

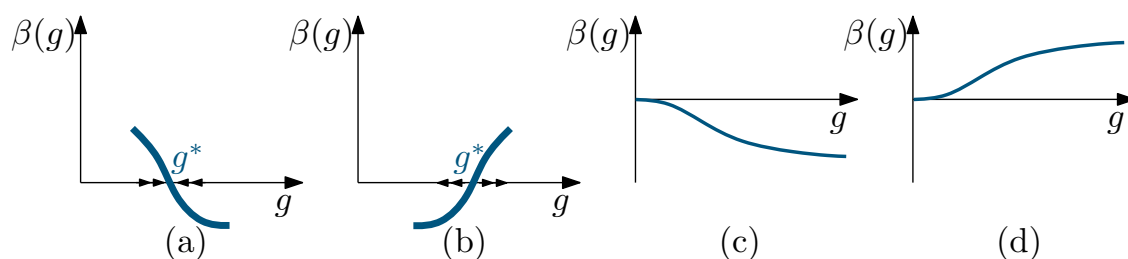


Figure I.2: (a) Ultraviolet stable fixed point; (b) Infrared stable fixed point; (c) Asymptotically free theory; (d) Infrared fixed point. Arrows denote evolution to the UV.

The computation of this result is worked out in detail, for instance in [GSS02, Sre07, IFL10]. It shows that in QCD ($N_c = 3, N_f < 33/2$) $\beta_0 > 0$ and the theory is asymptotically free. To arrive at this result, one renormalizes the bare couplings and fields appearing in (I.1) and (I.6), denoted with $_0$

$$A_{0,\mu}^a = Z_A^{\frac{1}{2}} A_\mu^a, \quad \psi_0 = Z_\psi^{\frac{1}{2}} \psi, \quad \eta_0^a = Z_\eta \eta^a, \quad \eta_0^{\dagger a} = \eta^{\dagger a}, \quad g_0 = Z_g g, \quad m_0 = Z_m m, \quad \xi_0 = Z_\xi \xi, \quad (\text{I.15})$$

giving rise to a Lagrangian in which we explicitly show the addition of counterterms (that produce new vertices so to speak) by defining $\delta Z_i = 1 - Z_i$ ²¹

²⁰The story of the discovery of asymptotic freedom is quite curious. For many years, a folklore theorem based on Lehmann positivity [Käl52, Leh54] ruled out the possibility of asymptotic freedom [Hos74]. The wavefunction renormalization unitarity bound does not apply, however, in non-abelian gauge theories, due to the existence of states of negative norm in the Hilbert space, viz. ghosts. G. 't Hooft had computed correctly (at least the sign of) the beta function before 1973 [tH72], but decided not to publish it for the moment. Asymptotic freedom could have been discovered even before [Shi01].

²¹We have directly assumed some relations between the couplings of the possible counterterms that preserve the gauge invariance of the renormalized Lagrangian. These relations follow from the Slavnov-Taylor identities [Tay71, Sla72], which are a generalization of the Ward identities in QED. While in QED fixing a

I. High Energy Scattering in QCD

$$\begin{aligned}
\mathcal{L}_{\text{QCD}} = & -\frac{1}{4}(\partial_\mu A_\nu^a - \partial_\nu A_\mu^a + g f^{abc} A_\mu^b A_\nu^c)^2 - \frac{1}{2\xi}(\partial_\mu A_\mu^a)^2 + \bar{\psi}(i\not{\partial} - m)\psi + g A_\mu^a \bar{\psi} \gamma^\mu t^a \psi \\
& - \eta^{a\dagger} \partial^\mu (\delta^{ab} \partial_\mu - g f^{abc} A_\mu^c) \eta^b + \delta Z_\psi \bar{\psi} i\not{\partial} \psi - (Z_\psi Z_m - 1) \bar{\psi} m \psi - \frac{1}{4} Z_A (\partial_\mu A_\nu^a - \partial_\nu A_\mu^a)^2 \\
& - (Z_g Z_A^{3/2} - 1) g \partial_\mu A_\nu^a f^{abc} A^{b,\mu} A^{c,\nu} + (Z_g Z_A^{1/2} Z_\psi - 1) g A_\mu^a \bar{\psi} \gamma^\mu t^a \psi - \delta Z_\eta \eta^{a\dagger} \square \eta^a \\
& - \frac{1}{4} (Z_g^2 Z_A - 1) g^2 f^{abc} A_\mu^b A_\nu^c f^{ade} A^{d,\mu} A^{e,\nu} - (Z_g Z_A^{1/2} Z_\eta - 1) g \eta^{a\dagger} f^{abc} \partial_\mu A_\mu^c \eta^b.
\end{aligned} \tag{I.16}$$

Notice that Z_g appears always together with other renormalization constants in (I.16). Hence, in order to determine it, one has to work out the radiative corrections coming from several diagrams, unlike in QED, where the vacuum polarization diagram completely determines charge renormalization. In particular, one needs to compute the radiative corrections to the quark propagator, the quark-quark-gluon vertex and the gluon propagator.

Nowadays, the QCD β -function is known to four loops [Cas74, Jon74, TVZ80, vRVL97]. For these higher order corrections, one must specify the renormalization prescription²². Usually it is most convenient to use dimensional regularization [tH73a], where renormalization constants Z_i are needed in order to cancel the poles in $\epsilon \equiv d/2 - 2$ that appear²³. The computed Z_g , in $\overline{\text{MS}}$ scheme, will have the form $Z_g = 1 + \sum_{n=1}^{\infty} \frac{Z_g^{(n)}}{\epsilon^n}$, $Z_g^{(n)} = \sum_{k=n}^{\infty} c_{kn} g^{2k}$. From the independence of the bare coupling with respect to μ , it follows that $\beta(g) = g^2 \frac{dZ_g^{(1)}(g)}{dg}$.

From (I.14), we get the running of the coupling at one loop

$$\alpha_s(\mu) = \frac{\alpha_s(\mu_0)}{1 + \frac{\alpha_s(\mu_0)}{4\pi} \beta_0 \ln\left(\frac{\mu^2}{\mu_0^2}\right)}. \tag{I.17}$$

gauge does not break conservation of the electromagnetic current, from which the Ward identities providing relations between Green functions that ensure gauge independence of observables follow (though there are some subtleties, see [LP11]), in non-abelian gauge theories fixing the gauge implies breakdown of current conservation. So simple Ward identities do not hold.

²²The first two coefficients of the β -function, β_0 and β_1 can be shown to be independent of the renormalization scheme (see, for instance, [Ynd06]), while the rest β_i , $i \geq 2$ is not. We notice, however, that this assertion is only valid in the limit of negligible masses, or for mass independent schemes like $\overline{\text{MS}}$ ones. In the MOM schemes (SEC. II.2.3) even the first coefficients depend on masses. This, which usually is a drawback of MOM as compared to $\overline{\text{MS}}$, is sometimes useful. In particular, in $\overline{\text{MS}}$ schemes β and γ functions are mass independent, while it is quite unnatural that they contain contributions from all quarks independently of their masses (for energies below their mass, quarks will not be excited in loops). This is in contradiction with the Appelquist-Carazzone decoupling theorem [AC75]. What one usually does is to introduce by hand the notion of *active flavors*: in Eq. (I.14) N_f only stands for the number of quark flavors with a mass $m \lesssim \mu$.

²³In the $\overline{\text{MS}}$ scheme one removes the combination $\frac{1}{\epsilon} \equiv \frac{1}{\epsilon} - \gamma_E + \ln 4\pi$, where γ_E is Euler's constant. The renormalization scale μ enters by giving correct dimensions to the coupling: $g_0 = Z_g \mu^{-\epsilon} g$.

I. High Energy Scattering in QCD

Gluon virtual loops also give rise to a diamagnetic effect, but at the same time produce an antiscreening dipole contribution larger by a factor of 12 (see [PS95] for a simple discussion of the SU(2) case). A qualitative explanation of this is shown in FIG. I.3: if, for instance, a red quark emits a red-antigreen gluon²⁵ that gives rise to a sequence of splittings, the quark becomes surrounded by a multitude of virtual gluons that bear *its* color, thereby magnifying it. This intuitive interpretation of $\beta_0 > 0$ is justified by a method designed by Hughes [Hug81] and Nielsen [Nie81], in which one views the vacuum state as a magnetic medium, and finds β_0 through the response to an external magnetic field. The method is applicable to any field theory and brings out the interesting view that asymptotic freedom is the outcome of a competition between Landau diamagnetism and Pauli paramagnetism, and depends crucially on the spins of the fields in the theory.

Asymptotic freedom is very useful because it tells us that perturbative calculations are trustable at high momentum transfers. As measured at energies of the order of the mass of the Z boson, the strong coupling is $\alpha_s(M_Z) = 0.1184(7)$ ²⁶ [Par10]. However, at low energies, following (I.17) α_s becomes bigger. Eventually, for μ sufficiently small, the strong coupling must become large enough to invalidate perturbation in α_s . Putting in the numbers, and remembering to remove the contribution of each quark flavor as μ falls below its mass

²⁵To see how color charge “flows” in quark-gluon-quark interactions, consider the SU(3) generators, in the usual Gell-Mann parametrization, forming the following linear combinations between them, while leaving untouched the diagonal ones ($t_3 = \frac{1}{2}\text{diag}(1, -1, 0)$ and $t_8 = \frac{1}{2\sqrt{3}}\text{diag}(1, 1, -2)$):

$$\tau_{12} = t_1 + it_2 = \begin{bmatrix} 0 & 1 & 0 \\ 0 & 0 & 0 \\ 0 & 0 & 0 \end{bmatrix}; \quad \tau_{13} = t_4 + it_5 = \begin{bmatrix} 0 & 0 & 1 \\ 0 & 0 & 0 \\ 0 & 0 & 0 \end{bmatrix}; \quad \tau_{23} = t_6 + it_7 = \begin{bmatrix} 0 & 0 & 0 \\ 0 & 0 & 1 \\ 0 & 0 & 0 \end{bmatrix}. \quad (\text{I.22})$$

The matrix τ_{ij} is a “color raising” matrix, which changes a quark of color j into one of color i . The hermitian conjugate $\tau_{ij}^\dagger = \tau_{ji}$ does the reverse. Now, defining the fields

$$\mathcal{A}^\mu \equiv A_3^\mu; \quad \mathcal{B}^\mu = A_8^\mu; \quad X^\mu = 2^{-1/2}(A_1^\mu + iA_2^\mu); \quad Y^\mu \equiv 2^{-1/2}(A_4^\mu + iA_5^\mu); \quad Z^\mu \equiv 2^{-1/2}(A_6^\mu + iA_7^\mu), \quad (\text{I.23})$$

we can rewrite the term in the Lagrangian having to do with quark interactions as

$$\mathcal{L}_{\text{quark int}} = g\bar{\psi}\mathcal{A}_a t^a \psi = g\bar{\psi}(t_3\mathcal{A} + t_8\mathcal{B})\psi + \frac{g}{\sqrt{2}}[\bar{\psi}(\tau_{21}\mathcal{X} + \tau_{31}\mathcal{Y} + \tau_{32}\mathcal{Z})\psi + \text{c.c.}]. \quad (\text{I.24})$$

From this we see that quarks carry two charges, denominated color isospin and color hypercharge, corresponding to eigenvalues of t_3 and t_8 , and they change color by emitting or absorbing the gluons X, Y, Z (which also carry charge in this way). So we can speak of having six color-anticolor gluons (e.g. red-antigreen) and two kind of ‘white’ gluons. For an analysis of color flow in gluon-gluon interactions see [Hua92].

²⁶The coupling in itself is not a physical observable, but rather a quantity defined in the context of perturbation theory, which enters predictions for experimentally measurable observables. Therefore, it depends on the renormalization scheme. The values given here are in $\overline{\text{MS}}$ scheme.

threshold, one finds using (I.17)

$$\alpha_s(M_Z) \simeq 0.12, \quad \alpha_s(m_b) \simeq 0.20, \quad \alpha_s(m_c) \simeq 0.30, \quad \alpha_s(m_s) \simeq 1.7, \quad (\text{I.25})$$

where m_b, m_c and m_s are the masses of the bottom, charm and strange quarks, respectively²⁷. Since the combination $\alpha_s/4\pi$ is the typical factor accompanying a loop correction, we may estimate that, although perturbation theory works well for $m_b \sim 5$ GeV, and is marginally acceptable for $m_c \sim 1.4$ GeV, it is expected to fail around $\mu \sim m_s \sim 200$ MeV. This is the scale corresponding to Λ_{QCD} . Below this threshold we should expect a dominant role of non-perturbative effects. The one-loop result (I.17) is not trustable.

So we see that asymptotic freedom at high energies indirectly points to *infrared slavery*. This allows us to expect that QCD explains confinement dynamically. Indeed, confinement is necessary for the consistency of asymptotic freedom. Because of antiscreening, the cloud of virtual particles surrounding an isolated charge would grow to infinity in a self-reinforcing, runaway process. The formation of this cloud would cost infinite energy. So an isolated quark would have infinite energy, and could not exist by itself. It is necessary that it is bounded, for instance, with an antiquark —whose cloud of charge would cancel the primitive one when overlapping— to form a meson. A hadron is built in an energetic compromise between Pauli principle forbidding its constituents to get too close and the energy associated to the non-canceled contributions to the charge cloud.

1.4 Changing the Renormalization Scheme

To conclude this crash introduction to renormalization, we will study in this section the ambiguities in perturbative computations derived from the freedom to choose the renormalization prescription. To be concrete, we consider the perturbative expansion of an observable R which, for simplicity, we choose to be dimensionless and only dependent on one energy scale Q :

$$R(Q) = a^N(\mu) \left(1 + r_1 \left(\frac{Q}{\mu} \right) a(\mu) + r_2 \left(\frac{Q}{\mu} \right) a^2(\mu) + \dots \right), \quad a = \frac{\alpha_s}{4\pi} = \frac{g^2}{(4\pi)^2}, \quad N > 0. \quad (\text{I.26})$$

As we saw before, renormalizability of the theory ensures that the perturbative predictions for physical observables R do not depend on the choice of renormalization scheme (RS), if we calculate them to all orders. In practice, of course, we have an n^{th} order calculation $R^{(n)}$

²⁷Due to confinement, the definition of quark masses is not an easy issue, see [Par10], Sec. 9.1.2.

I. High Energy Scattering in QCD

and all we can say is, formally,

$$\partial R^{(n)}/\partial(\text{RS}) = \mathcal{O}(a^{N+n}). \quad (\text{I.27})$$

While, in principle, any choice of scheme and scale is admissible, a wrong choice leads to a bad convergence of the series (I.26) and therefore a large deviation of $R^{(n)}$ from $R(Q)$. Since it is unlikely, in general, that the most suitable RS for comparing to data is also the most suitable for calculation, we must know how to transform our result to a new scheme. Changing from a scheme RS to a new one $\overline{\text{RS}}$ amounts to give a set of quantities $\{\mu, v_i\}$ relating its couplings by

$$\bar{a}(\bar{\mu}) = a(\mu) \left[1 + \sum_{k=1}^{\infty} v_k \left(\frac{\bar{\mu}}{\mu} \right) a^k(\mu) \right]. \quad (\text{I.28})$$

To be more precise, we will consider results to second order in the coupling

$$R^{(2)}(Q, \mu) = a^N(\mu) \left(1 + r_1 \left(\frac{Q}{\mu} \right) a(\mu) \right). \quad (\text{I.29})$$

Here a is really $a^{(2)}$, the solution of the truncated RG equation

$$\frac{1}{2} \frac{d \ln a}{d \ln \mu} = -\beta_0 a - \beta_1 a^2. \quad (\text{I.30})$$

One can check that (I.30) is invariant, to order $\mathcal{O}(a^3)$, under the simultaneous rescalings

$$\mu \rightarrow \bar{\mu} = \xi \mu; \quad a \rightarrow \bar{a} = a(1 + v_1 a), \quad \text{with } v_1 = -2\beta_0 \ln \xi. \quad (\text{I.31})$$

So we conclude that, to second order, a change of scheme is basically implemented by a rescaling of the scale μ , which is exactly the opposite of that for the Landau pole Λ ²⁸:

$$\bar{\Lambda} = \Lambda \exp(v_1(1)/2\beta_0). \quad (\text{I.32})$$

²⁸With the generalized definition (I.19), one can use the fact that as an integration constant Λ does not depend on μ to show that by virtue of asymptotic freedom the relation (I.32) holds to all orders in perturbation theory [CG79b].

2 A TALE OF TWO LIMITS

2.1 The Paradigm of Deep Inelastic Scattering: Factorization and DGLAP Evolution

Hadronic scattering, due to the intrinsically non-perturbative scale corresponding to the binding of quarks and gluons into hadrons, is very difficult to study. When the center-of-mass energy is large ($s > (\text{few GeV})^2$), the problem becomes tractable to some extent, because the large value of s sets a scale in the problem where the interactions are weak²⁹. This means that some quantities are computable or, to be more precise, one can derive relations between what will be measured in different experiments.

The simplest example of hadronic scattering at high energies is provided by electron-proton deep inelastic scattering (DIS): $e^-p \rightarrow e^-X$, where X means the multi-hadron final state. It is convenient to express the kinematics of the process in terms of the following standard Lorentz invariants (FIG. I.4)

$$\begin{aligned}
 s &\equiv (p + k)^2 && \text{center-of-mass energy squared;} \\
 Q^2 &\equiv -q^2 = -(k - k')^2 && \text{virtuality of the photon;} \\
 W^2 &\equiv (p + q)^2 = m_p^2 + 2\nu - Q^2 && \text{invariant mass of hadronic state } X; \\
 \nu &\equiv p \cdot q / m_p && e^- \text{ energy loss in proton } (p) \text{ rest frame;} \\
 x &\equiv Q^2 / 2p \cdot q = Q^2 / 2m_p \nu && \text{Bjorken variable;} \\
 y &\equiv p \cdot q / p \cdot k && \text{fractional energy transferred in } p \text{ rest frame.}
 \end{aligned}
 \tag{I.33}$$

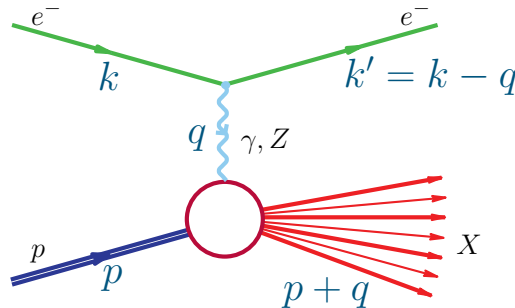


Figure I.4: Kinematics of DIS. k and p are known from the experimental setup, and k' is obtained by measuring the deflected lepton.

²⁹Low energy scatterings (e.g. e^-p^+ scattering) when there is no energy to probe the structure of the proton, and scattering involving pions and kaons at slightly higher energies, where chiral perturbation theory applies, are two other regimes susceptible of good quantitative analysis.

I. High Energy Scattering in QCD

When $Q^2 \gg m_p^2$, the virtual photon is a well known probe to study the hadron not involving the strong interactions³⁰. The fact that $W^2 \geq m_p^2$ implies according to (I.33) that $0 \leq x \leq 1$, with $x = 1$ when the proton is scattered elastically. Neglecting the electron mass we also have the important relation

$$xy = \frac{Q^2}{s - m_p^2} \simeq \frac{Q^2}{s} \quad (0 \leq y \leq 1). \quad (\text{I.34})$$

The simplest cross-section we can compute is the total inclusive one in which we sum over all possible hadronic final states:

$$E' \frac{d\sigma_{ep}}{d^3\mathbf{k}'} = \sum_{\{X\}} \int \frac{d\Pi_X}{32\pi^3(s - m_p^2)} (2\pi)^4 \delta(p + k - k' - p_X) \langle |\mathcal{A}_X|^2 \rangle, \quad (\text{I.35})$$

where we have used (A.25)-(A.27) (approximating Källén's λ to first order in m_p/s) and $\langle \rangle$ indicates average over all spin polarizations of the initial state and sum over those in the final state. The amplitude is decomposed into an electromagnetic part and a hadronic matrix element

$$\mathcal{A}_X = \frac{ie}{q^2} [\bar{u}(\mathbf{k}') \gamma^\mu u(\mathbf{k})] \langle X | J_\mu(0) | P(p) \rangle, \quad (\text{I.36})$$

where J_μ is the hadron electromagnetic current coupling to the photon and $|P(p)\rangle$ denotes the state of a proton with momentum p . Squaring the amplitude we have

$$E' \frac{d\sigma}{d^3\mathbf{k}'} = \frac{1}{32\pi^3(s - m_p^2)} \frac{e^2}{q^4} 4\pi L^{\mu\nu} W_{\mu\nu}, \quad (\text{I.37})$$

where the leptonic tensor (neglecting the electron mass) is

$$L^{\mu\nu} \equiv \langle \bar{u}(\mathbf{k}') \gamma^\mu u(\mathbf{k}) \bar{u}(\mathbf{k}) \gamma^\nu u(\mathbf{k}') \rangle = 2(k^\mu k'^\nu + k^\nu k'^\mu - g^{\mu\nu} k \cdot k'), \quad (\text{I.38})$$

and $W_{\mu\nu}$, the hadronic tensor, is defined by

$$\begin{aligned} 4\pi W_{\mu\nu} &\equiv \sum_{\{X\}} \int d\Pi_X (2\pi)^4 \delta(p + q - p_X) \langle \langle P(p) | J_\nu^\dagger(0) | X \rangle \langle X | J_\mu(0) | P(p) \rangle \rangle \\ &= \int d^4y e^{iq \cdot y} \langle \langle P(p) | J_\nu^\dagger(y) J_\mu(0) | P(p) \rangle \rangle. \end{aligned} \quad (\text{I.39})$$

$W_{\mu\nu}$ cannot be calculated by perturbative methods. It can only depend on the vectors q, p and the invariants which can be formed from them, Q^2 and x . Based only on its

³⁰This is not true in the photoproduction regime. When the virtuality of the photon is small it can fluctuate e.g. into a ρ meson.

tensorial structure, parity and time-reversal symmetry ($W^{\mu\nu} = W^{\nu\mu}$) and the Ward identity $q_\mu W^{\mu\nu} = 0$ ³¹, we can express W in terms of two scalar *structure functions* $F_{1,2}(x, Q^2)$ ³²:

$$W^{\mu\nu}(x, Q^2) = \left(-g^{\mu\nu} + \frac{q^\mu q^\nu}{q^2}\right) F_1(x, Q^2) + \frac{\hat{p}^\mu \hat{p}^\nu}{p \cdot q} F_2(x, Q^2); \quad \hat{p}_\mu \equiv p_\mu - \frac{q_\mu}{2x}. \quad (\text{I.40})$$

F_1 and F_2 turn out to be positive. Contracting (I.38) and (I.39) one eventually finds

$$\frac{d\sigma}{dx dy} = \frac{4\pi\alpha^2 s}{Q^4} \left(xy^2 F_1(x, Q^2) + \left[1 - y - \frac{xy m_p^2}{s} \right] F_2(x, Q^2) \right). \quad (\text{I.41})$$

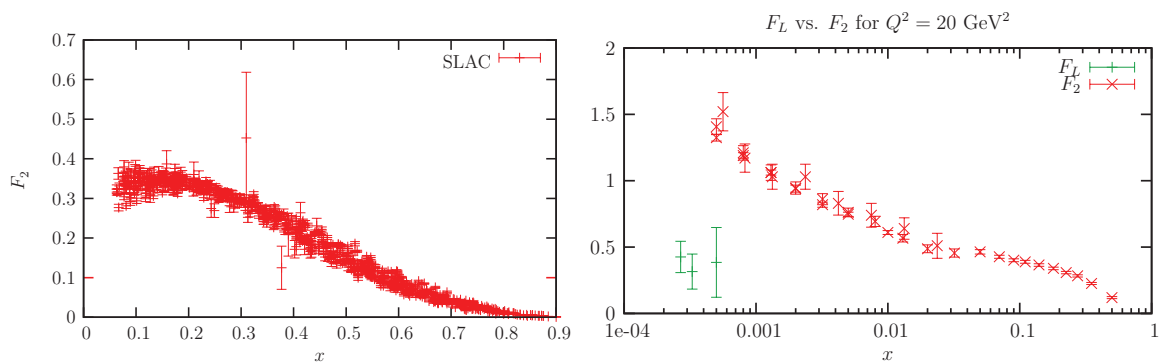


Figure I.5: SLAC results on DIS for structure functions F_2 and F_L . Adapted from [GLV07].

Having presented the basic aspects of DIS (see [Rob90, DCS09] for further details), we will illustrate with this process two main features of QCD: factorization and evolution. Of course, discussing these questions in any depth is beyond the aim of this text, and we refer the reader to [GSS02, Mut10, IFL10] for extensive discussion, and to [GLV07] and [Man99] for good crash introductions to factorization and evolution respectively. In our approach, we will discuss the parton model as a motivation for scaling and factorization, and will show how corrections arise perturbatively in this picture when considering interactions. We will also be interested in showing that DGLAP evolution is equivalent to a resummation of a tower of diagrams enhanced by collinear logarithms.

³¹A brief reminder of the consequences of Ward identities in the polarization structure of amplitudes: in QED, when considering an amplitude involving M incoming photons with momenta $k_i^{\mu_i}$, $i = 1, \dots, M$, and N outgoing photons with momenta $\kappa_j^{\nu_j}$, $j = 1, \dots, N$, it has the form $\mathcal{A} = \epsilon_{\nu_1}^*(\kappa_1) \cdots \epsilon_{\nu_N}^*(\kappa_N) M_{\mu_1 \dots \mu_M}^{\nu_1 \dots \nu_N} e^{\mu_1}(k_1) \cdots e^{\mu_M}(k_M)$. Then Ward identities imply that $\kappa_{j,\nu_j} M_{\mu_1 \dots \mu_M}^{\nu_1 \dots \nu_N} = M_{\mu_1 \dots \mu_M}^{\nu_1 \dots \nu_N} k_j^{\mu_j} = 0$ for any i, j , irrespectively of the value of κ_j^2 or k_i^2 (not necessarily on shell), while all the other momenta are put on shell. This is the result we apply when demanding $q_\mu W^{\mu\nu} = 0$. In QCD, the analogous restriction for an amplitude with several external gluons is not that constraining: one gets zero for \mathcal{A} if replacing one or several polarization vectors by its corresponding momenta, provided that all of these k_j 's and κ_i 's, with the exception of at most one of them, satisfy $k_j^2 = 0$ and $\kappa_i^2 = 0$ [LP11].

³²A term $i\epsilon^{\mu\nu\alpha\beta} \frac{q_\alpha p_\beta}{2p \cdot q} F_3(x, Q^2)$ is to be added to $W_{\mu\nu}$ when considering neutrino-initiated DIS, since weak interactions violate parity. Five additional structure functions dependent on the spin vector s are necessary when not performing the spin average.

I. High Energy Scattering in QCD

The parton model proposed by Bjorken and Feynman [BP69, Fey70] was born to explain the result of the DIS experiments at SLAC (FIG. I.5). It was found that electrons were scattered with large transfers of momentum more frequently than anticipated [Pan68], what suggested that the proton contained discrete scattering centers within. Furthermore, the distribution of scattered electrons in energy and angle exhibited the phenomenon of Bjorken scaling in the deep inelastic regime (formally $Q^2 \rightarrow \infty$ with ν/Q^2 fixed), which basically states that the structure functions $F_{1,2}$ defined in (I.40) (\simeq the DIS cross section once removed the kinematical dependence of the QED cross section) only depend on the dimensionless invariant x and not on Q^2 . This suggested that scattering centers had no internal structure, and hence were *pointlike*, since there is no dimensionful scale we could relate with the size of the target.

The main assumption of the parton model, which considers hadrons as consisting of pointlike constituents called partons (to be later identified with quarks, antiquarks and gluons) is that we can neglect parton interactions —so that their number and momenta is conserved— during the time τ_{int} they are probed, the same way we assume atoms to be instantaneously at rest when describing X-ray diffraction (*impulse approximation*). In this picture the variable x can be given a suggestive interpretation. If ξ is the hadronic momentum fraction carried by a parton, then neglecting the hadron mass and taking the final parton to be on shell

$$0 \simeq (\xi p + q)^2 \simeq 2\xi p \cdot q - Q^2 \implies \xi = x, \quad (\text{I.42})$$

i.e. the Bjorken variable is the momentum fraction carried by the interacting parton. Remarkably it can be measured in DIS by detecting only the scattered lepton.

For the naive parton interpretation to be valid one must work in a reference frame in which the initial hadron is highly boosted, so that $p^\mu \simeq \left(p + \frac{m^2}{2p}, 0, 0, p\right)$, $p \rightarrow \infty$.³³ In this frame the transverse momentum of partons can be neglected and no interaction with vacuum fluctuations arises because their lifetime is considerably smaller than that of partons [GLR83]; moreover the photon has a very small energy that prevents it from developing its own parton showers. Such simplicity is lost in the target rest frame, say (FIG. I.6).

³³There are infinite choices of such frames that respect the invariants x and Q^2 , according to the form of q . One such choice is the Breit frame $q = (0, 0, 0, \sqrt{Q^2})$, $p = \sqrt{Q^2}/2x$. Another choice is $q \simeq \left(\frac{Q^2}{2px}, \mathbf{q}_\perp, 0\right)$, with $Q^2 = \mathbf{q}_\perp^2$.

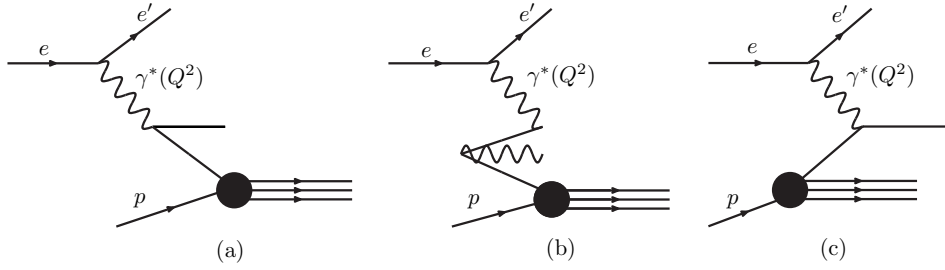


Figure I.6: *Simplicity of the parton model description of DIS space-time structure is lost in the target rest frame, since in general one must consider time-ordered processes [Gri00] where the virtual photon creates pairs (a) or scatters in vacuum fluctuations (b), in addition to the scattering on parton constituents present in the target wavefunction (c). In the limit of large photon energy process (a) is dominant [DKMT91].*

Using the infinite momentum frame we can make the impulse approximation $\tau_{\text{free}} \gg \tau_{\text{int}}$ more quantitative. τ_{free} is the lifetime of a certain partonic configuration inside a nucleus, and can be estimated as the inverse of the binding energy, which is expected to be at most the proton mass: $\tau_{\text{free}} \gtrsim m_p^{-1}$. On the other hand, a high energy nucleon as viewed from the incident electron looks like a flat pancake due to Lorentz contraction by a factor $1/\gamma \simeq m_p/E$, with E the energy of the nucleon. τ_{int} is roughly the time that the electron takes to pass through the nucleon. Since the nucleon has size $\sim m_p^{-1}$ in its rest frame, $\tau_{\text{int}} \simeq 1/E$ and, for $E \gg m_p$, as is the case in the infinite momentum frame, $\tau_{\text{int}} \ll \tau_{\text{free}}$.³⁴

The parton picture is of course only consistent in an asymptotically free theory, where interactions are switched off (logarithmically in the case of QCD) at asymptotically high momenta. It tells us that, because of the hierarchy of scales involved, the DIS cross section is the incoherent sum of cross sections for scattering off the individual components of the target.

³⁴There is still another condition to be fulfilled in order for the parton picture to apply, namely $\tau_{\text{ph}} \ll \tau_{\text{free}}$, where τ_{ph} is the duration of the interaction between the virtual photon and one parton

$$\frac{1}{\tau_{\text{ph}}} \sim q^0 \sim \sqrt{p^2 + W^2} - \sqrt{p^2 + m_p^2} \sim \frac{W^2 - m_p^2}{2p} = \frac{2m_p\nu - Q^2}{2p} = \frac{Q^2}{2p} \left(\frac{1}{x} - 1 \right). \quad (\text{I.43})$$

From the parton point of view a finer estimate than m_p^{-1} for τ_{int} can be obtained as the energy difference between the nucleon state and the sum of free partons

$$\frac{1}{\tau_{\text{free}}} \sim \Delta E = \sqrt{p^2 + m_p^2} - \sum_i \sqrt{(x_i p_{i\parallel})^2 + p_{i\perp}^2 + m_i^2} \sim \frac{1}{2p} \left[m_p^2 - \sum_i \left(\frac{m_i^2 + p_{i\perp}^2}{2x_i} \right) \right], \quad (\text{I.44})$$

where we used that $\sum_i x_i = 1$. τ_{ph} will be much shorter than τ_{free} if $Q^2 \gg m_p^2$ and $1 \gg x_i \gg \mu_i/p, p_{i\perp}/p$. Summing up, the condition for the impulse approximation to hold is being in the Bjorken asymptotic limit

$$E, Q^2, 2m_p\nu \gg m_p^2, \quad \text{i.e. } Q^2, \nu \rightarrow \infty \text{ with } x \text{ fixed.} \quad (\text{I.45})$$

I. High Energy Scattering in QCD

Thus, if we introduce the parton distribution functions $f_i(\xi)$, ($i = q, \bar{q}, g$) as the probability to find a parton (quark/antiquark/gluon) carrying a fraction ξ of the longitudinal momentum of the target, we can write the DIS differential cross section $d\sigma$ (I.41) in the factorized form

$$d\sigma = \sum_i \int d\xi f_i(\xi) d\hat{\sigma}_{ei \rightarrow ei} \left(\frac{x}{\xi} \right), \quad \frac{d\hat{\sigma}}{dy} = \frac{1}{16\pi(\xi s)^2} \frac{1}{4} \sum_{\lambda\lambda'\eta\eta'} \mathcal{A}_{\lambda\eta\lambda'\eta'}^{(ei \rightarrow ei)} \mathcal{A}_{\lambda\eta\lambda'\eta'}^{*(ei \rightarrow ei)}, \quad (\text{I.46})$$

where $\mathcal{A}^{ei \rightarrow ei}$ is the amplitude for electron-parton scattering via photon exchange. The only nonvanishing amplitudes are

$$\mathcal{A}_{++++} = \mathcal{A}_{----} = 2ie^2 e_i / y, \quad \mathcal{A}_{+--+} = \mathcal{A}_{-+-+} = 2ie^2 e_i (1 - y) / y. \quad (\text{I.47})$$

e_i are the electric charges of partons. Substituting these expressions in (I.46) and comparing with (I.41) we find that, within the parton model³⁵

$$F_1(x) = -\frac{x}{2} g^{\mu\nu} W_{\mu\nu} = \sum_i e_i^2 x f_i(x) \delta(x - x'_i); \quad F_L \equiv F_2 - 2xF_1 = 0. \quad (\text{I.48})$$

The relation $F_L = 0$ (FIG. I.5) is the Callan-Gross relation [CG69], first derived in the framework of current algebra [TJZW85, Cao10], and is a consequence of having assumed partons to be pointlike fermions with spin $1/2$ ³⁶. The verification of the Callan-Gross relation at SLAC pointed to an identification of partons and quarks. Things are, however, not so simple. Even supplementing the quark contribution of the valence quarks of the proton with contributions from the sea of virtual quark-antiquark pairs, the observed cross section was found to be uncomfortably small [BP69]. Data clearly indicated that there must be also electrically neutral partons: this is the contribution from gluons.

For all its success, the parton model cannot be the last word, however. No matter how large Q^2 may be making the interaction time smaller, in a quantum field theory fermions interact by exchanging virtual particles, which can have arbitrarily high momenta, thus having fluctuations associated to arbitrarily short time scales. Even in an asymptotically free theory, at any finite value of Q^2 the coupling will not be zero. So one expects that QCD calculations reveal violation of Bjorken scaling (FIG. I.7). In order to see how they arise, consider the first order corrections to γ^*q scattering, depicted in FIG. I.8.

³⁵ F_L , the longitudinal structure function describes the inclusive cross-section between the proton and a longitudinally polarized proton. F_1 and F_2 can also be related, via the optical theorem (APP. A), to the total cross section of virtual photoabsorption [BP02].

³⁶Had we taken scalar partons, we would have found $F_1(x) = 0$ [Chý04] (such a result can be shown to follow from angular momentum conservation in the Breit frame, see [CL82]).

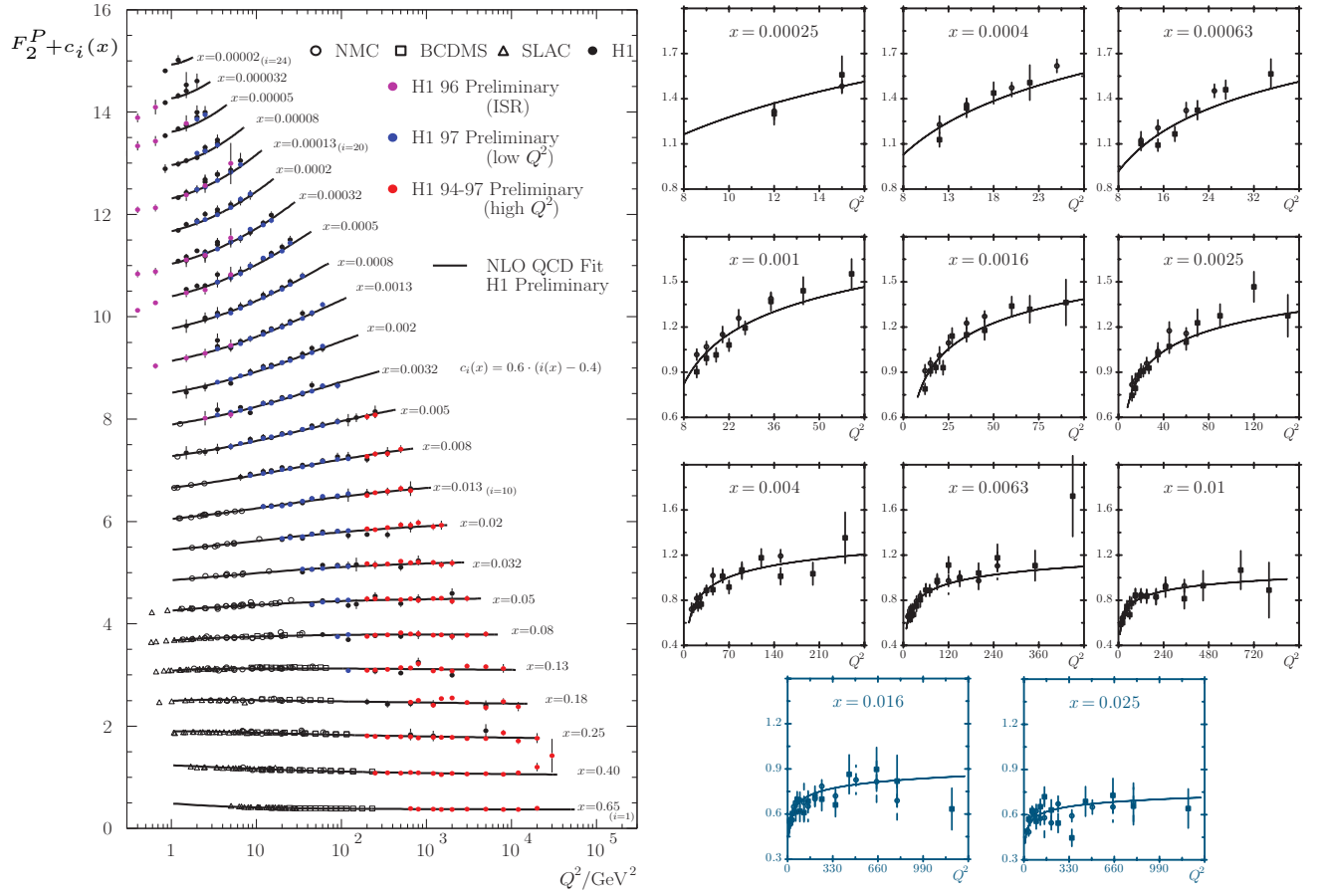


Figure I.7: The proton structure function $F_2(x, Q^2)$ vs Q^2 for diverse values of x [Par10]. The line is the next-to-leading order DGLAP fit. For display purposes $c(x) = 0.6(i(x) - 0.4)$, $i(x) = 1, \dots, 24$ is added to F_2 each time the value of x is increased. In the frames to the right, showing combined data from H1 and ZEUS, the asymptotic approach to exact scaling as $Q^2 \rightarrow \infty$ is clearly seen.

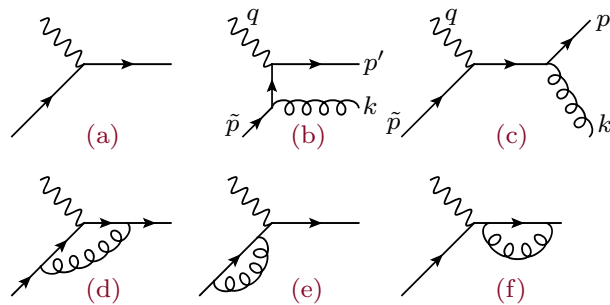


Figure I.8: Processes contributing to $\gamma^* q$ scattering to order $\mathcal{O}(\alpha \alpha_s)$. Diagram (a) is the leading (Born level) process.

Diagrams (b) and (c) are the real emission corrections to the Born level process. They develop two types of singularities: *i*) a collinear singularity, arising from the t -channel diagram (b) in the limit $t \rightarrow 0$ (note that it is proportional to $1/(\tilde{p} - k)^2 \simeq 1/(2\tilde{p} \cdot k)$, which diverges

I. High Energy Scattering in QCD

when k is emitted parallel to \tilde{p} , since $\tilde{p} \cdot k = \tilde{p}^0 k^0 (1 - \cos \theta) \xrightarrow{\cos \theta \rightarrow 1} 0$, where θ is the scattering angle in the CM frame); *ii*) a singularity due to soft gluon emission (when $k \rightarrow 0$ in case (b)).

Diagram (c) is also divergent, if k is emitted parallel to p' . This second divergence turns out to be harmless, since we are summing over all possible final states. Whether the final-state quark keeps all of its energy, or whether it decides to share it with a gluon emitted collinearly, an inclusive final-state measurement will not care. The collinear divergence can then be canceled by a similar divergence appearing in the final-state quark self-energy corrections. It turns out that soft divergences also cancel out in summing the contributions of real gluon and virtual gluon diagrams. This is an instance of a general result on the behavior of infrared singularities in QCD, the Kinoshita-Lee-Nauenberg (KLN) theorem [Kin62, LN64]³⁷.

The first divergence is more serious, since from the point of view of the incoming photon (which only sees the quark, not the gluon) it *does* make a difference whether the momentum is all carried by the quark or is shared between the quark and the gluon. This means that no cancellation between collinear singularities in the real emission and virtual emission is possible. To learn how to deal with these singularities, we have to compute the leading singularity contribution of diagrams (b) and (c) in FIG. I.8. The computation is performed in detail in [Man99]. A clever choice of gauge avoids having to compute the interference of both diagrams making it nonsingular in the collinear limit $k \parallel \tilde{p}$ (so that actually only diagram (b) is to be calculated). The correct answer is a light-cone gauge (see eq. (I.5))

$$k \cdot \varepsilon(k) = p' \cdot \varepsilon(k) = 0; \quad \sum \varepsilon_\mu(k) \varepsilon_\nu^*(k) = -g_{\mu\nu} + \frac{k^\mu p'^\nu + k^\nu p'^\mu}{k \cdot p'}. \quad (\text{I.49})$$

The following Sudakov expansion (APP. B) is carried out to isolate the collinear piece

$$k_\mu = (1 - z)\tilde{p}_\mu + \beta p'_\mu + (k_\perp)_\mu; \quad k^2 = 0 \implies \beta = \frac{\mathbf{k}^2}{2(1 - z)\tilde{p} \cdot p'}. \quad (\text{I.50})$$

³⁷The KLN theorem roughly asserts that, as a consequence of unitarity, transition amplitudes in a theory with massless fields do not exhibit IR divergences (of collinear or soft origin) when one sums over all initial and final degenerate states. This theorem ensures that one gets finite answers for completely inclusive processes, i.e. those in which one does not register the momenta of partons in the initial or final state, like the total cross section for e^+e^- annihilation, the jet cross section with fixed resolution in angle and energy, the transverse energy flux, etc.

When one or several partons are identified by measuring their momenta, the KLN theorem no longer applies, and the perturbative calculation presents large logarithms due to the collinear singularities. However, these logarithms can be resummed, as we shall see. In this kind of processes, soft singularities coming from virtual corrections and real emissions still cancel. This last class of processes includes DIS (where the active parton momenta is known from the measurement of the lepton), or the cross section for jets with fixed invariant mass of the observed particles. If one or more hadrons are observed, non-perturbative effects have a stronger importance and these processes require another kind of treatment.

After some algebra, the important result is that the amplitude squared for diagram (b), in the collinear limit, summed over colors and polarizations, reads

$$\sum_{a,\lambda} |\mathcal{A}_{(b)}|^2 = 2g^2 \frac{N_c^2 - 1}{2N_c} \frac{1-z}{\mathbf{k}_\perp^2} \left(\frac{1+z^2}{1-z} \right) \underbrace{N_c \text{Tr}[\not{p}' \Gamma \not{p} \Gamma^\dagger]}_{=\overline{\sum} |\mathcal{A}_{(a)}|^2}. \quad (\text{I.51})$$

The last term corresponds to the (averaged) Born amplitude (FIG. I.8, (a)) squared. So the one-gluon emission process factorizes in the collinear limit into the Born process times a factor which is independent of the beam's nature. This is the basis of collinear factorization³⁸

If we add the gluon phase space (APP. A) $d\Pi_g \equiv \frac{d^3\mathbf{k}}{(2\pi)^3 2k^0} = \frac{dz}{(1-z)} \frac{1}{16\pi^2} d\mathbf{k}_\perp^2$, we get³⁹

$$\sum_{a,\lambda} |\mathcal{A}_{(b)}|^2 d\Pi_g = \frac{d\mathbf{k}_\perp^2}{\mathbf{k}_\perp^2} dz \left(\frac{\alpha_s}{2\pi} \right) P_{qq}(z) \overline{\sum} |\mathcal{A}_{(a)}|^2, \quad P_{qq}(z) = C_F \frac{1+z^2}{1-z}. \quad (\text{I.53})$$

$P_{qq}(z)$ is the so-called Altarelli-Parisi splitting function [AP77] for the $q \rightarrow q$ transition. z is the momentum fraction of the original quark taken away by the quark after gluon emission.

Now we are ready to study the corrections to the parton model cross-section. In the naive parton picture, the cross section (e.g. for a DIS process) is given by (see also (I.46))

$$\begin{aligned} \sigma_0 &= \int_0^1 d\xi \sum_i e_i^2 f_i(\xi) \hat{\sigma}_0(\gamma^* q_i \rightarrow q'_i, \xi); \\ \hat{\sigma}_0(\gamma^* q_i \rightarrow q'_i) &= \frac{1}{\Phi} \overline{\sum} |\mathcal{A}_{(a)}|^2 \frac{d^3\mathbf{p}'}{(2\pi)^3 2p'_0} (2\pi)^4 \delta^4(p' - q - \tilde{p}) = \frac{1}{\Phi} \overline{\sum} |\mathcal{A}_{(a)}|^2 2\pi \delta(p'^2), \end{aligned} \quad (\text{I.54})$$

where Φ is the flux factor. Using that $p' = \xi p + q$, where p is the proton momentum, $p'^2 = 2\xi p \cdot q - Q^2$ and

$$\hat{\sigma}_0(\gamma^* q \rightarrow q') = \frac{2\pi}{\Phi} \overline{\sum} |\mathcal{A}_{(a)}|^2 \frac{1}{2p \cdot q} \delta(\xi - x). \quad (\text{I.55})$$

x is here the Bjorken variable. Inserting the last result in (I.54) we get

³⁸For a general parton scattering process with n external legs, by making collinear legs i and j we have

$$\lim_{\theta_{ij} \rightarrow 0} |\mathcal{A}^{(n)}|^2 = \frac{\alpha_s}{\pi p_k^2} P_{k \rightarrow ij}(z) |\mathcal{A}^{(n-1)}|^2, \quad p_k = p_i + p_j \sim (1-z)p_k + zp_k, \quad (\text{I.52})$$

where $P_{k \rightarrow ij}$ is the splitting function [AP77, MP91]. Collinear factorization and its breakdown at the level of the amplitude and the cross section is discussed in [CdR12].

³⁹Further corrections have to be incorporated from the evaluation of the virtual corrections in FIG. I.8 (diagrams (d), (e) and (f)). This gives the final result shown in the caption of FIG I.9 [ESW03].

I. High Energy Scattering in QCD

$$\sigma_0 = \frac{2\pi}{\Phi} \frac{\overline{\sum} |\mathcal{A}_{(a)}|^2}{Q^2} \sum_i x f_i(x) e_i^2 = \frac{2\pi}{\Phi} \frac{\overline{\sum} |\mathcal{A}_{(a)}|^2}{Q^2} F_2(x). \quad (\text{I.56})$$

Now, the contributions coming from the one-loop corrections give

$$\sigma_1 = \int d\xi f(\xi) \frac{1}{\Phi} \iint dz \frac{d\mathbf{k}_\perp^2}{\mathbf{k}_\perp^2} \left(\frac{\alpha_s}{2\pi} \right) P_{qq}(z) \overline{\sum} |\mathcal{A}_{(a)}|^2 2\pi \delta(p'^2). \quad (\text{I.57})$$

Using that $(p')^2 = (\tilde{p} - k + q)^2 \sim (z\tilde{p} + q)^2 = (\xi z p + q)^2$ and $\delta(p'^2) = \frac{1}{2p \cdot q} \frac{1}{z} \delta\left(\xi - \frac{x}{z}\right) = \frac{x}{z} \delta\left(\xi - \frac{x}{z}\right)$, one gets

$$\sigma_1 = \frac{2\pi}{\Phi} \left(\frac{\overline{\sum} |\mathcal{A}_{(a)}|^2}{Q^2} \right) \sum_i e_i^2 x \frac{\alpha_s}{2\pi} \int \frac{d\mathbf{k}_\perp^2}{\mathbf{k}_\perp^2} \int_x^1 \frac{dz}{z} P_{qq}(z) f_i\left(\frac{x}{z}\right). \quad (\text{I.58})$$

We then find a very important result: the inclusion of the $\mathcal{O}(\alpha_s)$ correction is equivalent to a contribution to the parton distribution function:

$$f_i(x) \rightarrow f_i(x) + \frac{\alpha_s}{2\pi} \int \frac{d\mathbf{k}_\perp^2}{\mathbf{k}_\perp^2} \int_x^1 \frac{dz}{z} P_{qq}(z) f\left(\frac{x}{z}\right). \quad (\text{I.59})$$

So we see that, thanks to collinear factorization, we can keep the cross section expressed as a convolution of a short distance cross section⁴⁰ with (effective, scale-dependent) parton distributions, like in (I.54). The parton densities redefinition does not depend upon the hard process in question: it is universal. For instance, if we consider the cross section for a hadronic collision, it can be expressed as⁴¹

$$\sigma = \sum_{a,b} \int_{\zeta_A}^1 dx_A \int_{\zeta_B}^1 dx_B f_{a/A}(x_A, \mu^2) f_{b/B}(x_B, \mu^2) \hat{\sigma}_{ab} \left(\frac{\zeta_A}{x_A}, \frac{\zeta_B}{x_B}, \alpha_s(\mu^2), \frac{Q^2}{\mu^2} \right), \quad (\text{I.60})$$

where $f_{a/A}$ is the probability that parton a is found in hadron A . The upper limit in the

⁴⁰Notice that this is not actually a cross section at the partonic level. In particular, it depends on the momentum scale Q^2 . The point is that it is computable within perturbation theory.

⁴¹A rigorous proof of collinear factorization is much harder than the arguments given here. The natural framework in which factorization is formulated is the OPE (see, e.g. [Pok00, Mut10]). In the case of DIS, one applies the OPE to the nonlocal product of currents appearing in (I.39). The expansion is organized in powers of the twist $t = d - s$ where d and s are the dimension and spin of an operator. The collinear factorization theorem is valid up to higher twist ($\mathcal{O}(1/Q^2)$) corrections (notice that we have taken the collinear limit when computing the amplitude).

The OPE approach was generalized by diagrammatic techniques in which the leading regions in a process are identified. Factorization is possible only for processes with a limited set of momentum regions of the space of loop and final state phase space momenta contributing to the leading power. In this way, collinear factorization was proved for several processes like DIS, e^+e^- annihilation, Drell-Yan, and jet and heavy quark inclusive production (see [CSS89] for a detailed review). Generalizations of the factorization theorems in other kinematic configurations is currently a very active research field [Col11].

integral $\int d\mathbf{k}_\perp^2/\mathbf{k}_\perp^2$ in (I.59) is basically Q^2 ⁴². The lower limit is in principle 0. Had we included a quark mass m , the propagator would have effectively cut off the integral at that value of m . However, the quark is bound inside a hadron and we do not know for sure what this value is. We tentatively cut off the integral at a scale Q_0 , and see what happens. The effective parton density becomes

$$f(x, Q^2) = f(x) + \ln\left(\frac{Q^2}{Q_0^2}\right) \frac{\alpha_s}{2\pi} \int_x^1 \frac{dz}{z} P_{qq}(z) f\left(\frac{x}{z}\right). \quad (\text{I.61})$$

We can relate the parton densities for different choices of the *factorization scale*⁴³, and this allows us to remove the dependence on the non-perturbative scale Q_0 by defining $f(x, Q^2)$ in terms of the parton density *measured* at a large, perturbative scale μ^2 :

$$f(x, Q^2) = f(x, \mu^2) + \ln\left(\frac{Q^2}{\mu^2}\right) \frac{\alpha_s}{2\pi} \int_x^1 \frac{dz}{z} P_{qq}(z) f\left(\frac{x}{z}\right). \quad (\text{I.62})$$

The physical interpretation of the effective PDFs $f_j(x, \mu^2)$ is that it gives (in the infinite momentum frame) the number of partons of type j carrying a fraction x of the longitudinal momentum of the incoming hadron and having a transverse dimension $r > 1/\mu$. As we increase the factorization scale μ , the number of partons will increase. Viewed on a smaller scale of transverse dimension r' , such that $r' \ll 1/\mu$, a single parton of dimension $1/\mu$ is resolved into a greater number of partons. The same way, $P_{ij}(z)$ gives the probability of finding a parton i in a parton of type j with a fraction z of the longitudinal momentum of the parent hadron and transverse size less than $1/\mu$. This probabilistic interpretation implies that the following sum rules must hold:

$$\begin{aligned} \int_0^1 dx \sum_i (P_{q_i q_j}(x) - P_{\bar{q}_i q_j}(x)) &= \int_0^1 dx x \left(\sum_i [P_{q_i q_j}(x) + P_{\bar{q}_i q_j}(x)] + P_{g q_j}(x) \right) \\ &= \int_0^1 dx x \left(\sum_i [P_{q_i g}(x) + P_{\bar{q}_i g}(x)] + P_{g g}(x) \right) = 0. \end{aligned} \quad (\text{I.63})$$

The scale μ in (I.62) is arbitrary, so $f(x, Q^2)$ should not depend on it. Imposing this requirement we get, in the same way we obtained the renormalization group equations

⁴² Q^2 is much greater than any transverse momentum associated to partons entering the hard interaction (that are almost collinear to the parent proton), because of the strong ordering in the DGLAP ladder.

⁴³The factorization scale separates grosso modo the perturbative and non-perturbative regimes. The same way it happened with renormalization, the factorization scale dependence of the PDFs should cancel exactly with that of the coupling, as it is not a physical scale. However, without having computed corrections to all orders, it is necessary to take an specific choice for Q_0 . To avoid the appearance of large logarithms it is usual to set both the factorization and renormalization scales to $Q_0^2 = \mu = Q^2$, though one should remember that the two scales are not conceptually the same.

I. High Energy Scattering in QCD

$$\frac{df(x, Q^2)}{d \ln \mu^2} = 0 \implies \mu^2 \frac{df(x, \mu^2)}{d\mu^2} = \frac{\alpha_s}{2\pi} \int_x^1 \frac{dz}{z} P_{qq}(z) f\left(\frac{x}{z}, \mu^2\right). \quad (\text{I.64})$$

This is the famous DGLAP (Dokshitzer-Gribov-Lipatov-Altarelli-Parisi) equation giving the scale dependence of the PDFs [GL72, Lip75, AP77, Dok77]. The DGLAP equation shows that, although perturbation theory cannot be used to calculate the PDF at any particular value $\mu^2 = Q_0^2$, it can be used to predict how the distribution evolves as μ^2 varies. Recall that $q_i(x, Q_0^2)$ can be obtained experimentally via $q_i(x, Q_0^2) = 2F_1(x, Q^2 = Q_0^2)/e_i^2$. Replacing μ^2 by Q^2 then tells us how the structure function evolves with Q^2 .

The DGLAP equations effectively resum a full tower of ladder diagrams giving leading logarithms of Q^2 . To see this, define $t = \ln(Q^2/\mu^2)$. Expanding $f(x, t)$ in powers of t , we have $f(x, t) = f(x, 0) + t \frac{df}{dt}(x, 0) + \frac{t^2}{2!} \frac{d^2 f}{dt^2}(x, 0) + \dots$. The first derivative is given by (I.64), while higher derivatives can be obtained by differentiating it:

$$\begin{aligned} f''(x, t) &= \frac{\alpha_s}{2\pi} \int_x^1 \frac{dz}{z} P_{qq}(z) \frac{df}{dt}\left(\frac{x}{z}, t\right) = \frac{\alpha_s}{2\pi} \int_x^1 \frac{dz}{z} P_{qq}(z) \frac{\alpha_s}{2\pi} \int_{\frac{x}{z}}^1 \frac{dz'}{z'} P_{qq}(z') f\left(\frac{x}{zz'}, t\right); \\ &\vdots \\ f^{(n)}(x, t) &= \frac{\alpha_s}{2\pi} \int_x^1 \dots \frac{\alpha_s}{2\pi} \int_{x/zz' \dots z^{(n-1)}}^1 \frac{dz^{(n)}}{z^{(n)}} P_{qq}(z^{(n)}) f\left(\frac{x}{zz' \dots z^{(n-1)}}, t\right). \end{aligned} \quad (\text{I.65})$$

We see that the n -th term in this expansion, proportional to $(\alpha_s t)^n$, corresponds to the emission of n gluons. It is just the n -fold iteration of the one-gluon emission case. Indeed, DGLAP equations can be obtained as a resummation of ladder diagrams with the emission of n collinear gluons (FIG. I.10). In the same way that we have computed the

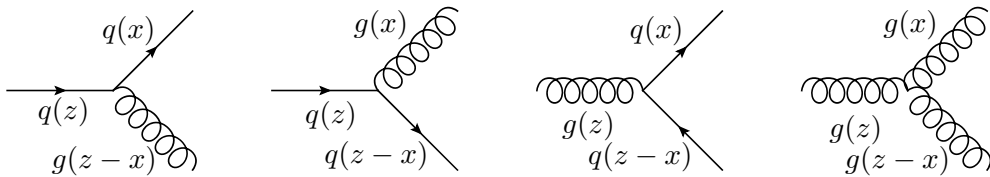


Figure I.9: The Altarelli-Parisi splitting functions. To leading order, their expressions are [ESW03]: $P_{qq}(z) = \frac{N_c^2 - 1}{2N_c} \left[\frac{1+z^2}{(1+z)_+} + \frac{3}{2} \delta(1-z) \right]$; $P_{qg}(z) = \frac{1}{2} [z^2 + (1-z)^2]$; $P_{gq}(z) = \frac{N_c^2 - 1}{2N_c} \frac{1+(1-z)^2}{z}$; $P_{gg}(z) = 2N_c \left[\frac{z}{(1-z)_+} + \frac{1-z}{z} + z(1-z) \right] + \left(\frac{11N_c - 2N_f}{6} \right) \delta(1-z)$, where A_+ is defined through $\int_0^1 dz A_+(z) f(z) = \int_0^1 dz A(z) [f(z) - f(1)]$.

qq splitting function, three more splitting functions have to be considered (FIG. I.9)⁴⁴. The DGLAP equations then become a set of coupled integro-differential equations (see, for

⁴⁴Because of charge conjugation one has $P_{q\bar{q}} = P_{\bar{q}q}$ and $P_{gq} = P_{g\bar{q}}$. At lowest order $P_{\bar{q}q} = P_{q_i q_j} = 0$ ($i \neq j$).

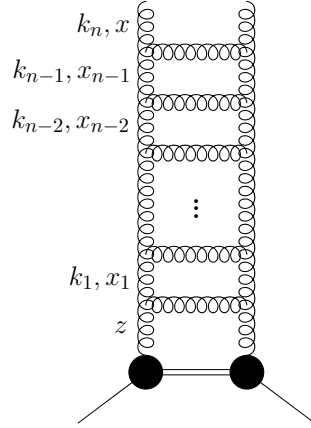


Figure I.10: *Gluon ladder diagram.*

instance, [ESW03])

$$\frac{d}{dt} \begin{pmatrix} q(x, t) \\ g(x, t) \end{pmatrix} = \frac{\alpha_s(t)}{2\pi} \int_x^1 \frac{d\xi}{\xi} \begin{pmatrix} P_{qq} \left(\frac{x}{\xi}, \alpha_s(t) \right) & P_{qg} \left(\frac{x}{\xi}, \alpha_s(t) \right) \\ P_{gq} \left(\frac{x}{\xi}, \alpha_s(t) \right) & P_{gg} \left(\frac{x}{\xi}, \alpha_s(t) \right) \end{pmatrix} \begin{pmatrix} q(\xi, t) \\ g(\xi, t) \end{pmatrix}. \quad (\text{I.66})$$

We will not consider its general solution, which usually is given in terms of the Mellin moments of the distribution functions. However, we find useful to end this section with an analytic estimate of the behavior of PDFs in the low x limit, which we will consider in next section. In the small- x regime the dominant PDF is the gluonic one, $g(x, Q^2)$ (notice the divergence of $P_{gg}(x)$ and $P_{gq}(x)$ as $x \rightarrow 0$, in the caption of FIG. I.9, while $P_{qq}(x)$ is constant at small x), as one can see in FIG. I.11. The enhanced contribution to P_{gg} at small x tells us that in the small x regime, gluon ladders with repeated iterations of P_{gg} dominate in the region $x \ll 1$, i.e. we have strong ordering in x . Indeed, the evaluation of a ladder diagram with n rungs (FIG. I.10) requires integrations over the internal momenta exchanged between rungs of the form

$$\alpha_s \int \frac{d\mathbf{k}_{\perp i}^2}{\mathbf{k}_{\perp i}^2} \cdots \int \frac{dx_i}{x_i} \cdots \quad (\text{I.67})$$

The dominant contribution to this kind of integrals comes from the region (see the arguments in SECTION I.3.2) of strongly ordered transverse and longitudinal momenta⁴⁵

$$Q^2 \gg \mathbf{k}_{\perp n}^2 \gg \cdots \gg \mathbf{k}_{\perp 1}^2 \gg Q_0^2; \quad x \ll x_{n-1} \ll \cdots \ll z. \quad (\text{I.68})$$

One has

⁴⁵The DGLAP equation resums the leading logarithms in Q^2 , corresponding to ladders strongly ordered in transverse momenta. The requirement of ordering in the longitudinal momenta comes from the DLL approximation.

I. High Energy Scattering in QCD

$$\int_{Q_0^2}^{Q^2} \frac{d\mathbf{k}_{\perp n}^2}{\mathbf{k}_{\perp n}^2} \int_{Q_0^2}^{k_{\perp n}^2} \frac{d\mathbf{k}_{\perp n-1}^2}{\mathbf{k}_{\perp n-1}^2} \dots \int_{Q_0^2}^{k_{\perp 2}^2} \frac{d\mathbf{k}_{\perp 1}^2}{\mathbf{k}_{\perp 1}^2} = \frac{1}{n!} \ln^n \frac{Q^2}{Q_0^2};$$

$$\int_x^1 \frac{dx_{n-1}}{x_{n-1}} \dots \int_{x_2}^1 \frac{dx_1}{x_1} \int_{x_1}^1 \frac{dz}{z} z g(z) \simeq \frac{1}{n!} \left(\ln \frac{1}{x} \right)^n \mathcal{F}^{(0)},$$
(I.69)

where we have used the results $\int_a^b \frac{\ln^n(x/a) dx}{x} = \frac{\ln^{n+1}(b/a)}{n+1}$ and $\int_a^1 \frac{\ln^n x}{x} dx = -\frac{\ln^{n+1} a}{n+1}$, and taken $\mathcal{F}^{(0)}(z, Q^2) \equiv z g(z, Q_0^2)$, the so-called input unintegrated gluon distribution, to be roughly independent of z . For definiteness we shall use the (somewhat unphysical) ansatz

$$Q^2 \mathcal{F}^{(0)}(x, Q^2) = \Theta(1-x) \Theta(Q^2/Q_0^2 - 1),$$
(I.70)

where the factor Q^2 is introduced on dimensional grounds. That the integration over transverse momenta gives a factor $\frac{1}{n!} \ln^n \frac{Q^2}{Q_0^2}$ was seen when displaying iteratively the DGLAP equation in (I.65). Now we also want to evaluate $g^{(n)}(x, t)$ in (I.65) within the small- x approximation. Rewriting this equation in terms of $\mathcal{F}(x, Q^2) = x g(x, Q^2)$,

$$\mathcal{F}^{(n)}(x, t) = \alpha_s^n \int_x^1 dz \dots \int_{\frac{x}{zz' \dots z^{(n+1)}}}^1 dz^{(n)} \frac{P_{gg}(z^{(n)})}{2\pi} \mathcal{F}^{(0)}\left(\frac{x}{zz' \dots z^{(n+1)}}, t\right),$$
(I.71)

taking into account that for $z \rightarrow 0$ (the dominant contribution in the studied regime), $\frac{P_{gg}(z)}{2\pi} \sim \frac{N_c}{\pi} \frac{1}{z}$, and inserting the ansatz (I.70) for $\mathcal{F}^{(0)}$, one can readily use (I.69) to get

$$Q^2 \mathcal{F}^{(n)}(x, Q^2) = \frac{1}{(n!)^2} \left(\bar{\alpha}_s \ln \frac{1}{x} \ln \frac{Q^2}{Q_0^2} \right)^n \Theta(Q^2 - Q_0^2); \quad \bar{\alpha}_s \equiv \frac{\alpha_s N_c}{\pi}.$$
(I.72)

Now one can sum the contribution from all rungs using the result $\sum_n \left(\frac{1}{n!}\right)^2 \left(\frac{y^2}{4}\right)^n = I_0(y) \sim \frac{e^y}{\sqrt{2\pi y}}$, $|y| \gg 1$, where I_0 is the modified Bessel function, thus getting

$$Q^2 \mathcal{F}(x, Q^2) \sim \exp \left[2 \sqrt{\bar{\alpha}_s \ln \frac{1}{x} \ln \frac{Q^2}{Q_0^2}} \right].$$
(I.73)

This result [dRGP⁺74] shows that the gluon distribution rises steeply at small x , with an effective power $\sqrt{\frac{\bar{\alpha}_s \ln(1/x)}{\ln(Q^2/Q_0^2)}}$ ⁴⁶ (FIGS. I.11 and I.12). This is a very important result, to which we will constantly refer in following sections. Note that although the rise is always weaker than a power of $1/x$, such a growth can be mimicked over a small region of x .

⁴⁶If one includes running of α_s the result of the integrations over transverse momenta is modified and the exponent is found to decrease slightly. This reduction of the scaling violation is not unexpected: since α_s decreases at larger scales, the evolution in Q^2 is slowed down.

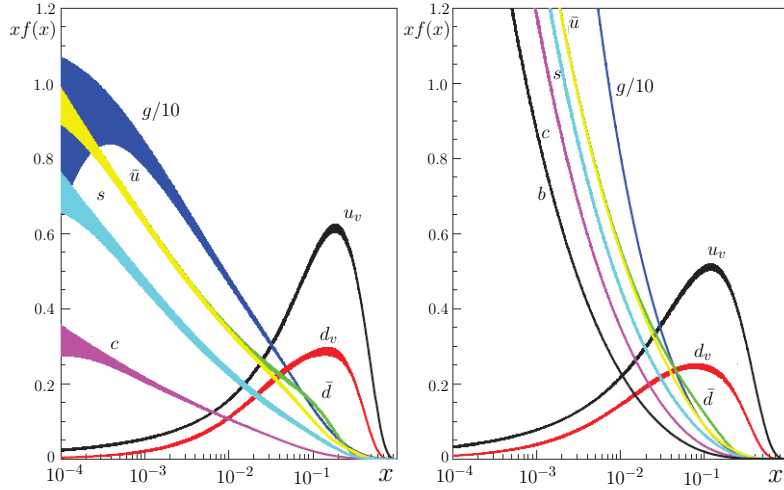


Figure I.11: Momentum distributions (x times the unpolarized parton distributions $f(x)$, where $f = u_v, d_v, \bar{u}, \bar{d}, s, c, b, g$) and their associated uncertainties using the NNLO MSTW2008 parametrization at a scale $\mu^2 = 10 \text{ GeV}^2$ (to the left) and $\mu^2 = 10,000 \text{ GeV}^2$ (to the right). Adapted from [Par10].

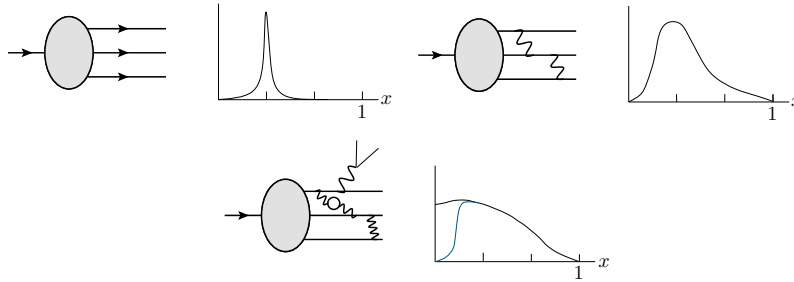


Figure I.12: The shape of structure functions can be qualitatively understood as follows: in the naive parton model the PDF is essentially a δ -function peaked in a certain value of x , say $1/3$. When we turn on the interactions of quarks with gluons this distribution becomes smeared. Finally, gluons are emitted with a probability $\sim dx/x$. Such a factor gives a tail of sea quarks at small x . Adapted from [CL82].

2.2 Semihard Processes and the Small- x Regime

Up to now, in our study of perturbative QCD features, exemplified by DIS, we have considered the existence of a unique hard (perturbative) scale set by the virtuality Q^2 . When moving to a kinematic region characterized by a hierarchy of two different large scales, typically large logarithms of the ratio of scales appear in the amplitudes [Wei95], that can compensate for the smallness of the coupling invalidating a fixed order perturbative calculation.

In so-called semihard processes, the center-of-mass energy squared s (APP. B) is much larger than the momentum transfer $|t|$, and amplitudes enhanced by logarithms of the type

I. High Energy Scattering in QCD

$[\alpha_s \ln(s/|t|)]^n$ have to be resummed to all orders in order for perturbative computations to be reliable. According to (I.34), this high-energy limit correspond in DIS to the small- x limit, and the dominant logarithms are of the form $[\alpha_s \ln(1/x)]^n$. In last section we took the small- x limit of the DGLAP evolution (sometimes called the double leading log approximation). When going to very small values of x , we need an all-orders resummation (FIG. I.13). The small- x resummation is carried out through the BFKL program, which we will treat in detail in SEC. I.3.

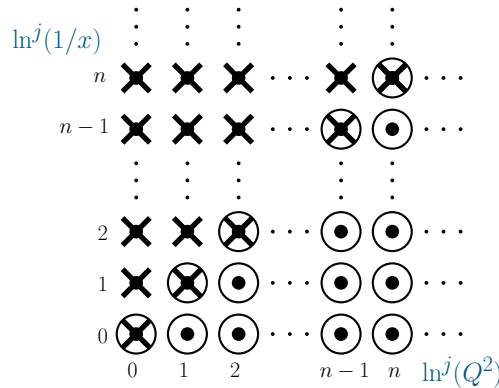


Figure I.13: The powers of $\ln Q^2$ and $\ln(1/x)$ resummed, up to the n -th perturbative order by DGLAP LL (circles), BFKL LL (crosses) and the double leading logarithmic approximation (DLLA, circles and crosses). Adapted from [BP02].

Interest in small- x physics was revived in the early 90's with the discovery at HERA, DESY, of the dramatic rise of DIS structure functions as $x \rightarrow 0$ [H1 93]. The need for an small- x resummation has been questioned in view that NLO DGLAP fits provide very good agreement to experimental determination of PDFs up to rather small values of x [MSTW09, N⁺08]. In SEC. I.3.5 we will make a brief review of the observables best suited for disentangling DGLAP and BFKL dynamics. For some of them, indications have been found in recent years of slight deviations from DGLAP predictions [ZEU06, H1 08, CFR10].

A simple kinematic estimate shows that in typical HERA kinematics the DGLAP approximation is still reliable. The rapidity span (APP. B) at HERA is approximately [Lev97, FSW05] $\ln(Q/xm_p) \sim 10$ for $x = 10^{-4}$ and $Q = 2.5$ GeV. In order for $\ln(x/x_0)$ to be large, where $x_0 \sim 0.1$ is a reference scale determined by the typical momentum fraction in the initial PDFs, the distance in rapidity between adjacent partons in the ladder (SEC. I.3.2) should be $\gg 2$. Therefore, the number of radiated gluons in multi-Regge kinematics at HERA is $\ll (10 - 4)/2 - 1 = 2$, taking into account that each of the fragmentation regions occupies at least 2 units of rapidity. Because one (two) logs of x are effectively taken

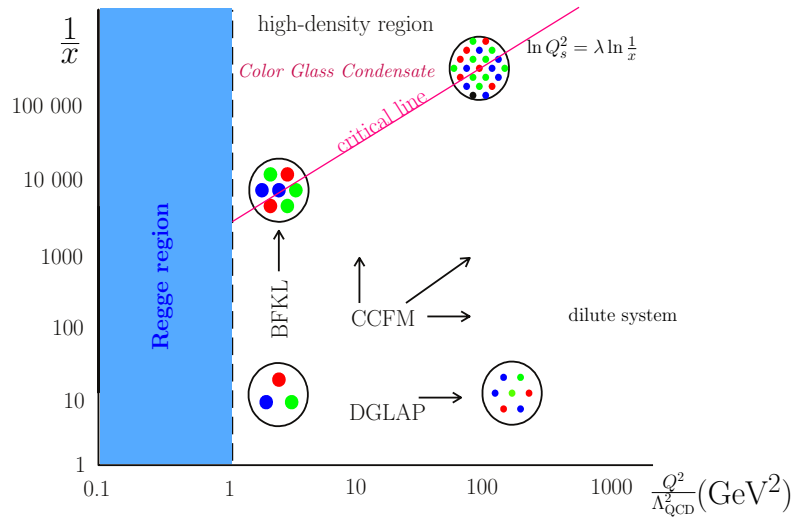


Figure I.14: Schematic of the different regimes in the $\ln 1/x - \ln Q^2$ plane and the evolution equations expected to hold therein. The critical line marks the appearance of saturation effects. The ‘size’ of the partons is also indicated in different regions. Adapted from [Fos01].

into account by the NLO (NNLO) DGLAP approximation (FIG. I.13), there is no need for a special treatment of $\ln(x_0/x)$ effects at HERA kinematics. A similar estimate shows that at LHC kinematics the radiation of 5-6 gluons is permitted. Thus, at LHC energies and above the resummation of $\ln(x_0/x)$ terms becomes a practical issue.

Apart from providing a correct framework for forward physics at hadron colliders, a thorough understanding of the small- x region (i.e., the high energy limit of QCD) will shed light on a number of very interesting phenomena⁴⁷. Among them we find: 1) it allows to establish the connection with Regge theory (SEC. I.2.3), thus providing a handle on nonperturbative hadron dynamics; 2) the growing of parton densities at small- x (I.73) due to the probability for gluon bremsstrahlung being proportional to $1/x$ ($dP_{\text{Brems}} \sim \frac{\alpha_s \{C_A, C_F\}}{\pi^2} \frac{dk^2}{k^2} \frac{dx}{x}$) has to stop at some point when the hadron is so populated that partons overlap (FIG. I.14): this leads to the interesting physics of saturation (SEC. I.5); 3) high-energy scattering exhibits remarkable simplifications, often rooted on hidden symmetry (SEC. I.4.2).

2.3 Insights from Regge Theory

Two basic properties of QFT are locality and unitarity. Locality of quantum fields is necessary for the theory to be causal, while unitarity is required for a meaningful probabilistic

⁴⁷In the words of A. H. Mueller [Mue90], *the small- x problem in QCD is, except for the understanding of confinement, the most interesting problem in QCD*. We want to emphasize here that knowing in detail the microscopic dynamics of a theory—in our case, the QCD Lagrangian—is a long way from understanding the emergent phenomena that it can account for *a priori* [And72].

I. High Energy Scattering in QCD

interpretation. The requirement of causality, expressed in the commutativity of local operators at spacelike separations, leads to analyticity properties of the scattering amplitudes⁴⁸.

Analyticity of the S -matrix amplitudes (on the kinematic variables it depends on, e.g. the Mandelstam invariants, considered to be complex) is so stringent a constraint that it was at one time⁴⁹ believed to provide (in conjunction with Lorentz invariance, unitarity, and the crossing symmetry property of amplitudes) an adequate basis for a complete theory of strong interactions, with no need for the explicit introduction of local fields [Man58, CM60, Che61]. This *bootstrap* program incorporated with time further assumptions to the original postulates; its logic can be found described in [Che61, Fra63, Str07, Cus90]. In the Regge limit,

$$s \gg -t, \tag{I.74}$$

a number of relevant results can be extracted in a more economic way. Next we give a crash introduction to Regge theory; for a detailed introduction see [Col77, BP02].

We have postulated that the only singularities of scattering amplitudes are those dictated by unitarity⁵⁰ (FIG. I.15). Another postulate (proved perturbatively in QFT) is that of crossing symmetry: the same amplitude describes the three different processes (B.1) and (B.3) (and the CPT related amplitudes), being obtained one from the other by crossing⁵¹

$$A_{1\bar{3}\rightarrow\bar{2}4}(s, t, u) = A_{12\rightarrow 34}(t, s, u); \quad A_{1\bar{4}\rightarrow\bar{2}3}(s, t, u) = A_{12\rightarrow 34}(u, t, s). \tag{I.75}$$

The crossing postulate (I.75) is magnified by analyticity. The fact that the kinematic domains of the three channels are non-overlapping (FIG. B.2) means that in fact *the same*

⁴⁸See [Dun12], Sec. 6.6., for a comprehensive discussion of the relation between microcausality and analyticity.

⁴⁹The so-called S -matrix approach [Hei43, Che61, ELOP66] was born out of the failures of QFT in describing strong interactions in the fifties. For all its ambitious views, it had limited success and was practically abandoned when QCD emerged. However, it has left a lot of interesting ideas. For us, the most important is Regge theory, from which the important concept of pomeron emerges. In the framework of the bootstrap, Veneziano [Ven68] found a Regge-behaved crossing symmetric amplitude that eventually gave rise to dual resonance models, the germ of string theory (see [CCCd12, GSW87] for an account). Some other features of the S -matrix program are being revived today [Zee10]: in words of A. M. Polyakov, *the garbage of the past often becomes the treasure of the present (and viceversa)* [Pol87].

⁵⁰One can see that, whenever one reaches a threshold for production of new intermediate states, a sudden new contribution to the sum in the r.h.s. of the unitarity equation (A.30) is added, in such a way that keeping (A.30) true for all values of the kinematic variables requires singularities of the transition amplitudes at those threshold values.

⁵¹For scattering of identical bosons these conditions lead to very powerful constraints, e.g. $A(s, t) = A(u, t) \xrightarrow{s/|t|\rightarrow\infty} A(-s, t)$. Everything becomes much more complex when dealing with particles with several quantum numbers [BP02].

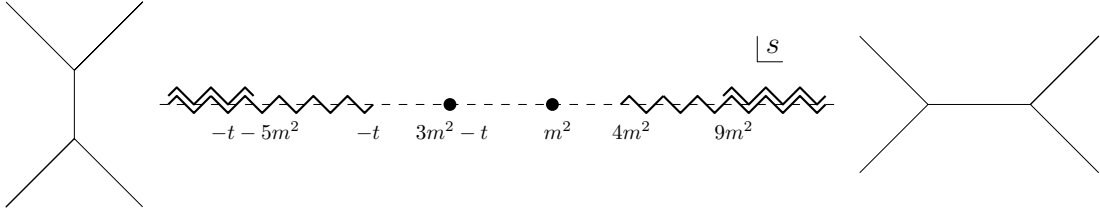


Figure I.15: Singularities of the scattering amplitude in the s plane. Broken lines mean branch-cuts. Singularities in the right part come from the s -channel propagator (diagram to the right). Singularities in the l.h.s. come, by crossing, from the t -channel propagator (diagram to the left).

function of s, t and u describes all the amplitudes in (I.75). So, if we know the scattering amplitude in a given channel, we can in principle analytically continue it to the other channels. This allows us to extract the full singularity structure of an amplitude. The following step is to exploit analyticity to derive dispersion relations.

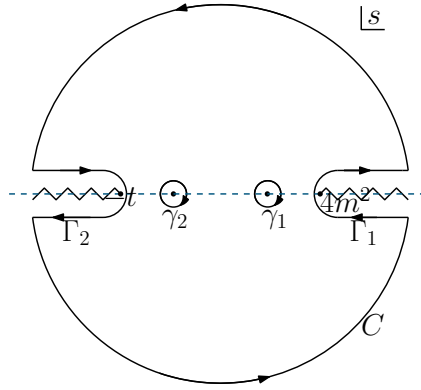


Figure I.16: The Cauchy contour to derive dispersion relations.

Using the contour in FIG. I.16, we have the following Cauchy's integral representation for $A(s, t)$ at fixed t :

$$A(s, t) = \frac{1}{2\pi i} \oint_{\Gamma} \frac{A(s', t)}{s' - s} ds' = \frac{1}{2\pi i} \left(\oint_{\gamma_1} + \oint_{\gamma_2} + \oint_{\Gamma_1} + \oint_{\Gamma_2} + \int_C \right) \frac{A(s', t)}{s' - s} ds'. \quad (\text{I.76})$$

The first two terms in (I.76) are pole contributions, $\frac{1}{2\pi i} (\oint_{\gamma_1} + \oint_{\gamma_2}) \frac{A(s', t)}{s' - s} ds' = \frac{f_1(t)}{s - m^2} + \frac{f_2(t)}{u - m^2}$, where the residues f_1 and f_2 are unspecified functions of t . If we assume that the amplitude vanishes uniformly when $|s|$ goes to infinity, $A(s, t) \xrightarrow{|s| \rightarrow \infty} 0$, we get the (single-variable) dispersion relation for the scattering amplitude at fixed t

$$A(s, t) = \frac{1}{\pi} \int_{4m^2}^{\infty} \frac{D_s(s', t)}{s' - s} ds' + \frac{1}{\pi} \int_{-\infty}^{-t} \frac{D_s(s', t)}{s' - s} ds' + \text{pole terms}, \quad (\text{I.77})$$

where

I. High Energy Scattering in QCD

$$D_s(s, t) \equiv \text{Disc}_s A(s, t) \equiv \frac{1}{2i} \lim_{\epsilon \rightarrow 0^+} [A(s + i\epsilon, t) - A(s - i\epsilon, t)] = \Im A_s(s, t), \quad (\text{I.78})$$

is the discontinuity along the s -channel threshold branchcut. Making in the second integral in (I.77) the change of variables $s' \rightarrow u' = 4m^2 - s' - t'$ we get the more symmetric expression

$$A(s, t) = \frac{1}{\pi} \int_{4m^2}^{\infty} \frac{D_s(s', t)}{s' - s} ds' + \frac{1}{\pi} \int_{4m^2}^{\infty} \frac{D_u(u', t)}{u' - u} du' + \text{pole terms}. \quad (\text{I.79})$$

If $A(s, t) \underset{s \rightarrow \infty}{\sim} s^\lambda$, $\lambda \in \mathbb{R}^+$, the contribution at infinity is nonvanishing, but still a dispersion relation can be written for the quantity $\frac{A(s, t)}{(s-s_1)(s-s_2)\cdots(s-s_N)}$, $N = [\lambda] + 1$, with s_1, \dots, s_N arbitrary constants. Proceeding as above one gets the N -times subtracted dispersion relation

$$\begin{aligned} A(s, t) &= \sum_{n=0}^{N-1} c_n(t) s^n + \frac{1}{\pi} (s - s_1) \cdots (s - s_N) \int_{4m^2}^{\infty} \frac{D_s(s', t)}{(s' - s_1) \cdots (s' - s_N)(s' - s)} ds' \\ &+ \frac{1}{\pi} (u - u_1) \cdots (u - u_N) \int_{4m^2}^{\infty} \frac{D_u(u', t)}{(u' - u_1) \cdots (u' - u_N)(u' - u)} du' + \text{pole terms}, \end{aligned} \quad (\text{I.80})$$

where $u_i = 4m^2 - s_i - t$ ⁵². A concrete realization of (I.80) we shall extensively use is

$$\Im (A(s, t)) = A s \ln^n s \implies A(s, t) = -\frac{A}{(n+1)\pi} \ln^{n+1} s. \quad (\text{I.81})$$

In Regge theory [Reg59], the amount of information to be extracted from dispersion relations is optimized by separating the components of definite angular momentum. For $2 \rightarrow 2$ scattering, we can write the following partial wave expansion⁵³

⁵²Notice that (I.80) contains an undetermined polynomial of degree $N-1$. In particular, if $\sigma_{\text{tot}} \underset{s \rightarrow \infty}{\sim} \text{const.}$, as one expects in Regge theory, $\Im A_{\text{el}}(s, 0) \underset{s \rightarrow \infty}{\sim} s$ because of the optical theorem and the forward elastic amplitude can be fully reconstructed in terms of the total cross section and two unknowns $c_0(0)$ and $c_1(0)$.

⁵³In non-relativistic quantum mechanics plane wave momentum eigenstates $|\mathbf{p}\rangle \equiv |p, \vartheta, \phi\rangle$ are given in terms of (orbital) angular momentum eigenstates $|p\ell m\rangle$ by $|\mathbf{p}\rangle = \sum_{\ell=0}^{\infty} \sum_{m=-\ell}^{\ell} Y_{\ell m}^*(\hat{\mathbf{p}}) |p\ell m\rangle$. The spherical harmonics $Y_{\ell m}$, which play the role of Clebsch-Gordan coefficients, are given by $Y_{\ell m}(\vartheta, \phi) = (-1)^{\frac{m+|m|}{2}} \left[\frac{2\ell+1}{4\pi} \frac{(\ell-|m|)!}{(\ell+|m|)!} \right]^{\frac{1}{2}} P_{\ell}^{|m|}(\cos \vartheta) e^{im\phi}$, where $P_{\ell}^m(\cos \vartheta)$ are the associated Legendre polynomials and ℓ is the orbital angular momentum quantum number. In the case of scattering by a central potential this expansion reduces to $A(\theta, \phi) = \sum_{\ell} (2\ell+1) a_{\ell}(p) P_{\ell}(\cos \theta)$.

The generalization to relativistic scattering of particles with spin is best carried out in the helicity formalism [JW59] (see [Dev02] for a pedagogical introduction). Using helicity eigenstates has the advantages of a good massless limit and no need to split the orbital and spin angular momentum contributions, among others. A generalized partial wave expansion of the form $A_{\lambda_3 \lambda_4; \lambda_1 \lambda_2}(\vartheta, \phi) = \sum_j (2j+1) D_{\lambda_i \lambda_f}^{j*}(\vartheta, \phi, 0) f_{\lambda_f \lambda_i}^j$, with $\lambda_i = \lambda_a - \lambda_b$, $\lambda_f = \lambda_c - \lambda_d$, holds. For the case of spinless particles the total angular momentum quantum number j reduces to ℓ , $\lambda_a, \lambda_b, \lambda_c, \lambda_d = 0$ and $D_{\lambda_i \lambda_f}^{j*}(\vartheta, \phi, 0) \rightarrow D_{00}^{\ell*}(\vartheta, \phi, 0) = P_{\ell}(\cos \phi)$ so that one ends with the nonrelativistic spinless partial wave expansion. It is within this generalized representation that j should be *interpreted* as the spin carried by the intermediate ‘particle’. The reggeization procedure described below must now be applied to each of the helicity amplitudes separately [DDLN02].

$$A_{1\bar{3}\rightarrow\bar{2}4}(s, t) = \sum_{\ell=0}^{\infty} (2\ell+1) a_{\ell}(s) P_{\ell}(1+2t/s), \quad a_{\ell}(s) = \frac{1}{2} \int_{-1}^1 d \cos \vartheta P_{\ell}(\cos \vartheta) A(s, \cos \vartheta). \quad (\text{I.82})$$

Using crossing symmetry (I.75) this expression can be analytically continued into the s -channel by interchanging s and t ($\cos \vartheta_t \equiv 1 + 2s/t \equiv z_t$)

$$A_{12\rightarrow 34}(s, t) = \sum_{\ell=0}^{\infty} (2\ell+1) a_{\ell}(t) P_{\ell}(1+2s/t), \quad a_{\ell}(t) = \frac{1}{2} \int_{-1}^1 d \cos \vartheta_t P_{\ell}(\cos \vartheta_t) A(s, \cos \vartheta_t). \quad (\text{I.83})$$

We can apply the machinery of dispersion relations to the partial wave expansion (I.83) by analytically continuing ℓ to complex values [Gri61]. The result (see [BP02] for a derivation) is the Sommerfeld-Watson transform [Wat18, Som49]

$$A(z_t, t) = - \sum_i \pi (2\alpha_i(t) + 1) \tilde{\beta}_i(t) \frac{P_{\alpha_i}(-z_t)}{\sin \pi \alpha_i} - \frac{1}{2i} \int_{c-i\infty}^{c+i\infty} (2\ell + 1) a(\ell, t) \frac{P_{\ell}(-z_t)}{\sin \pi \ell} d\ell, \quad (\text{I.84})$$

where $\alpha_i(t)$ is the location of the i -th pole of $a(\ell, t)$ in the complex angular momentum plane (a Regge pole) and $\tilde{\beta}_i(t)$ is its associated residue.

A subtle issue is posed by the analytical continuation $a_{\ell}(t) \rightarrow a(\ell, t)$. From (I.84) it appears not to be unique since in principle we can add to $a(\ell, t)$ any analytic function vanishing for $\ell \in \mathbb{Z}$ without affecting the above result. It turns out, however, that $a(\ell, t)$ is unique provided $a(\ell, t) < \exp(\pi|\ell|)$ as $|\ell| \rightarrow 0$ [Car18]. This is not the case since there are contributions to the partial wave amplitudes proportional to $(-1)^{\ell}$ and the required inequality is violated along the imaginary axis. This can be amended [Gri61, Fro61] introducing two different analytic continuations of the even and odd partial wave amplitudes. (I.84) is then generalized to

$$A(z_t, t) = - \sum_{\xi \pm 1} \sum_{i_{\xi}} \frac{1 + \xi e^{-i\pi \alpha_{i_{\xi}}(t)}}{2} \pi (2\alpha_{i_{\xi}}(t) + 1) \tilde{\beta}_{i_{\xi}}(t) \frac{P_{\alpha_{i_{\xi}}}(-z_t)}{\sin \pi \alpha_{i_{\xi}}(t)} - \frac{1}{2i} \sum_{\xi \pm 1} \int_{c-i\infty}^{c+i\infty} \frac{1 + \xi e^{-i\pi \ell}}{2} (2\ell + 1) a^{\xi}(\ell, t) \frac{P_{\ell}(-z_t)}{\sin \pi \ell} d\ell. \quad (\text{I.85})$$

The *quantum number* ξ is called the signature, a kind of parity under exchange of the s and u channels. The sum i_{ξ} is over poles of definite signature.

Our focus is the Regge or high-energy limit $s \rightarrow \infty$ (for fixed t), i.e. $|z_t| \rightarrow \infty$. The asymptotic behavior of Legendre polynomials [OLBC10] is $P_{\ell}(z) \underset{|z| \rightarrow \infty}{\sim} \frac{1}{\sqrt{\pi}} \frac{\Gamma(\ell + \frac{1}{2})}{\Gamma(\ell + 1)} (2z)^{\ell}$, $\Re \ell \geq -\frac{1}{2}$,

I. High Energy Scattering in QCD

forcing the contribution along the contour in (I.85) to be suppressed. We can go further and keep only the dominant (rightmost) pole, located at $\alpha(t)$ and with signature ξ . Redefining its residue to absorb some factors, $\beta(t) = \frac{\pi}{2}(2\alpha(t) + 1)\tilde{\beta}(t)2^{\alpha(t)}$, we have

$$A(s, t) \underset{\frac{s}{|t|} \rightarrow \infty}{\sim} -\beta(t) \frac{1 + \xi e^{-i\pi\alpha(t)}}{\sin \pi\alpha(t)} \left(\frac{s}{|t|}\right)^{\alpha(t)}. \quad (\text{I.86})$$

Analogously, from the s -channel partial wave expansion we get

$$A(s, t) \underset{\frac{|t|}{s} \rightarrow \infty}{\sim} -\beta(s) \frac{1 + \xi e^{-i\pi\alpha(s)}}{\sin \pi\alpha(s)} \left(\frac{|t|}{s}\right)^{\alpha(s)}. \quad (\text{I.87})$$

For partial wave amplitudes one can see [BP02] from (I.85) that in the Regge limit

$$a^\xi(\ell, t) = \int_1^\infty D_s^\xi(s, t) \left(\frac{s}{|t|}\right)^{-\ell-1} d\left(\frac{s}{|t|}\right), \quad D_s^\xi(s, t) \equiv D_s(s, t) + \xi D_u(s, t) \quad (\text{I.88})$$

i.e. $a^\xi(\ell, t)$ becomes the Mellin transform of the signaturized discontinuity $D_s^\xi(s, t)$ (APP. C). We have

$$\begin{aligned} D_s^\xi(s, t) \sim s^\alpha &\implies a(\ell, t) \sim \frac{1}{\ell - \alpha} \quad (\text{simple pole}); \\ D_s^\xi(s, t) \sim s^\alpha (\ln s)^{-1} &\implies a(\ell, t) \sim \ln(\ell - \alpha) \quad (\text{cut}). \end{aligned} \quad (\text{I.89})$$

Equations (I.86) and (I.87) tell us a fundamental result: the leading complex angular momentum singularity of the partial wave amplitude in a given channel determines the asymptotic behavior in the crossed channels. In particular, scattering in the Regge limit is governed by the rightmost complex angular momentum singularity in the t -channel.

To interpret what these singularities in the crossed channel mean, consider that for some t_0 we have $\alpha(t_0) = \ell + i\epsilon$, $\ell \in \mathbb{Z}$, $\epsilon \ll 1$. Then the partial wave amplitude reads for $t \rightarrow t_0$

$$a(\ell, t) \underset{\ell \rightarrow \alpha(t)}{\sim} \frac{1}{\ell - \alpha(t)} \underset{t \rightarrow t_0}{\sim} \frac{1}{t - t_0 + i\Gamma}, \quad \Gamma \equiv \frac{\epsilon}{\alpha'(t_0)}. \quad (\text{I.90})$$

Assuming that $\alpha'(t_0)$ is such that Γ is real, this is the typical Breit-Wigner pattern for a resonance of mass $M = \sqrt{t_0}$ [Wei95, BM07]. Thus, for real and positive (unphysical, see FIG. B.2) values of t , when t is a mass squared, Regge poles represent resonances and bound states with angular momentum (spin) ℓ . We say that $\alpha(t)$ is a Regge trajectory (or reggeon) interpolating between these resonances/bound states. Hence we can visualize the s -channel asymptotic behavior (I.86) as due to the exchange of a family of resonances in the crossed

channel. Notice that if $\alpha(t)$ has signature $\xi = +1(-1)$ not only the denominator but also the numerator in (I.86) vanishes when $\alpha(t)$ crosses an integer spin that is odd (even) respectively, so that a trajectory with $\xi = 1 (-1)$ interpolates between even (odd) spin resonances.

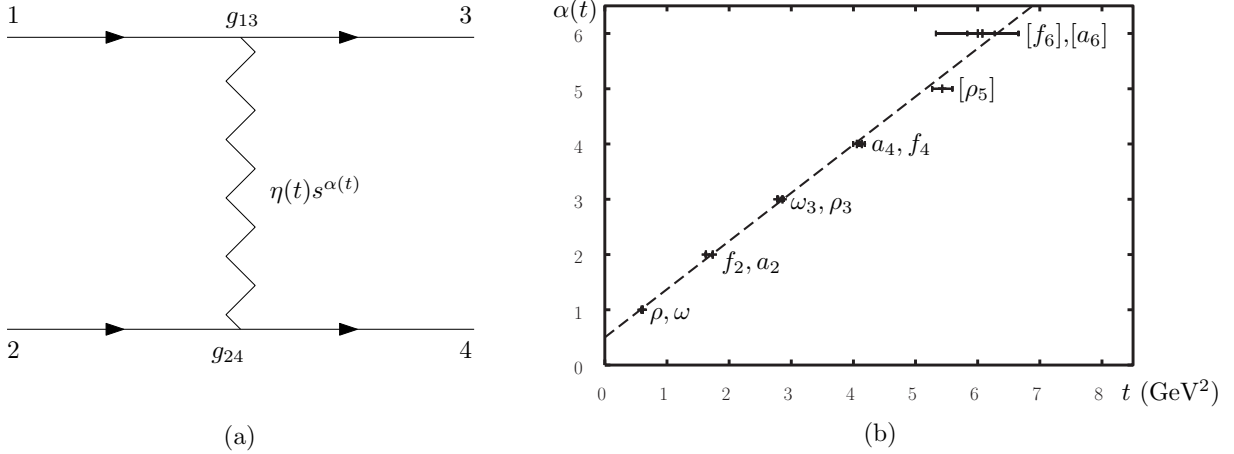


Figure I.17: (a) *Reggeon exchange*; (b) *Chew-Frautschi plot showing the four (almost degenerate) leading mesonic trajectories* [DDLN02]: the f_2 ($P = +1, C = +1, G = +1, I = 0, \xi = +1$), the ρ ($P = -1, C = -1, G = +1, I = 1, \xi = -1$), the ω ($P = -1, C = -1, G = -1, I = 0, \xi = -1$) and the a_2 ($P = +1, C = +1, G = -1, I = 1, \xi = +1$), where P, C, G , and I stand for parity, charge conjugation, G -parity (see e.g. [HKP98] for a discussion of this quantum number) and isospin. Particle spins are plotted against their squared masses t . The straight line is $\alpha(t) = 0.5 + 0.9 t$.

A striking feature of the spectrum of hadrons is that when their spin is plotted against their mass squared one finds that those mesons or baryons with the same quantum numbers fall on a straight line. In 1960 Chew and Frautschi conjectured from limited data that all strongly interacting particles fall into straight Regge trajectories of the form

$$\alpha(t) = \alpha(0) + \alpha' t, \quad (\text{I.91})$$

where the Regge slope α' is universal (though this is not exact, in fact one sees that approximately $\alpha' = 0.9 \text{ GeV}^{-2}$ for all trajectories). Such a relation was recognized to be the one expected from a model of mesons like rotating relativistic strings joining a quark and an antiquark⁵⁴ [Nam69, Nie70, Sus70, Got71]. $\alpha(0)$ is called the intercept and is equal to 0.5 for the leading mesonic trajectories.

A very rich hadronic phenomenology can be derived from Regge theory [IW77, Col77]. Here we will just consider two important aspects:

⁵⁴See [Gre11] for a toy model derivation. In QCD, such a spinning stick with constant energy per unit length is believed to be associated with chromoelectric flux tubes.

I. High Energy Scattering in QCD

Factorization When one pole clearly dominates over the others, a scattering amplitude is dominated by the exchange of a single reggeon (FIG. I.17). Then the residue in (I.86) factorizes and we get

$$A(s, t) = \eta(t)\gamma_{13}(t)\gamma_{24}(t)s^{\alpha(t)}, \quad \eta(t) = -\frac{1 + \xi e^{-i\pi\alpha(t)}}{\sin \pi\alpha(t)}. \quad (\text{I.92})$$

In some sense this is related to high-energy factorization (SEC. I.3.5).

Total Cross-Sections and the Pomeron From (I.86) it is immediate to obtain the total cross section via the optical theorem. When only the dominant pole $\alpha(t)$ contributes

$$\sigma_{\text{tot}} \underset{s \rightarrow \infty}{\simeq} \frac{1}{s} \Im m A(s, t=0) \underset{s \rightarrow \infty}{\sim} s^{\alpha(0)-1}. \quad (\text{I.93})$$

Though it is usually implicit, in this expression s should be normalized to some fixed value s_0 , which gives the scale where the asymptotic approximation (I.93) breaks down, usually of the order of 1 GeV^2 . If more than one pole contributes,

$$\sigma_{\text{tot}} \sim \sum_i A_i s^{\alpha_i(0)-1}. \quad (\text{I.94})$$

The Regge trajectories in FIG. I.17 have intercept lower than 1, so according to (I.93) they lead to cross sections that decrease with energy asymptotically. However, it is experimentally known that hadronic total cross sections, as a function of s , are rather flat around $\sqrt{s} \sim (10 - 20) \text{ GeV}^2$ and increase at higher energies (FIG. I.18).

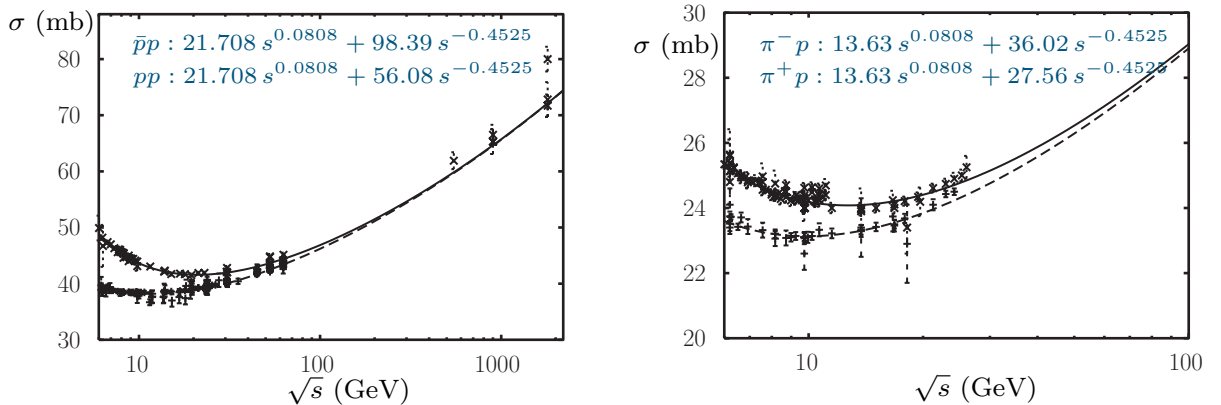


Figure I.18: *Donnachie-Landshoff fit. Adapted from [DDLN02].*

Donnachie and Landshoff [DL92] were able to fit quite well the available cross section data using the ansatz (I.94) with the dominant and subdominant trajectories. Total cross sections

for pp , $\bar{p}p$, $K^\pm p$, $\pi^\pm p$ and γp are fitted by

$$\sigma_{\text{tot}} = X s^{0.0808} + Y s^{-0.4525}. \quad (\text{I.95})$$

The dominant trajectory at high energies, causing the cross section to rise with s , has intercept $\alpha_{\mathbb{P}}(0) \simeq 1.08$ and, according to Pommeranchuk's theorem⁵⁵ [OP56, Pom56], must correspond to the exchange of vacuum quantum numbers ($P = +1, C = +1, G = +1, I = 0, \xi = +1$). It is called pomeron, after Pommeranchuk, and is denoted by \mathbb{P} . The pomeron trajectory does not correspond to any known particle, its recurrences are expected to be glueballs. From fitting elastic scattering data, one finds that the pomeron trajectory is much flatter than the others ($\alpha'_{\mathbb{P}} \simeq 0.25 \text{ GeV}^{-2}$).

A pomeron intercept greater than 1 conflicts with the Froissart bound⁵⁶. One could claim that at the presently achieved energies we are still far from the asymptotic regime, since other parameterizations are able to describe the data without such a power dependence up to the currently explored energies. In any case, this is a good place to point out that several assumptions have been made during our analysis. Most importantly, we disregarded contributions from cuts, considering only poles. In fact, the existence of poles automatically requires cuts via unitarity⁵⁷ [AFS62], since the exchange of several reggeons leads to branch points at the production thresholds of two or more reggeons in the crossing channel.

The whole picture of Regge theory becomes much more involved with the introduction of cuts. However, lot of information can still be extracted from the singularity structure of the

⁵⁵Pommeranchuk's theorem states that —under some very reasonable hypothesis— the total cross sections for particle-particle and particle-antiparticle scattering become equal at asymptotically high energies

$$\sigma_{\text{tot}}(ab) \underset{s \rightarrow \infty}{\simeq} \sigma_{\text{tot}}(a\bar{b}). \quad (\text{I.96})$$

This means that the cross section vanishes asymptotically for processes involving charge exchange. Foldy and Peierls [FP63] then noticed the converse, that if for a particular scattering process the cross-section does not fall as s increases then that process must be dominated by the exchange of vacuum quantum numbers (i.e. zero isospin and even under charge conjugation). In fact, if a particle is exchanged with vacuum quantum numbers it will couple equally to particles and antiparticles, giving rise to the equality of $\sigma_{\text{tot}}(ab)$ and $\sigma_{\text{tot}}(a\bar{b})$ up to subleading corrections decreasing with s that could be mediated by charge exchange processes.

⁵⁶The Froissart unitarity bound [Fro61, Mar63] puts a strict limit to the rate of growth with energy of *any* total cross section. It states that total cross sections cannot grow faster than $\ln^2 s$:

$$\sigma_{\text{tot}} \leq \frac{\pi}{m_\pi^2} \ln^2 s, \quad \text{as } s \rightarrow \infty. \quad (\text{I.97})$$

An intuitive derivation by Heisenberg [Hei52] is discussed in [DDLN02]. A rigorous derivation from the S -matrix postulates is offered in [BP02].

⁵⁷The breakdown of simple Regge factorization due to cuts has recently been proved in pQCD [CdR12].

I. High Energy Scattering in QCD

complex angular momentum plane, by interpreting reggeons as quasiparticles. The multi-Reggeon branch-points can be regarded as Reggeon production thresholds. In particular, Reggeon unitarity relations can be derived forcing the existence of vertices changing the number of reggeons. The result is a theory of interacting pomerons living in 2+1 dimensions, with rapidity playing the role of time [Gri68, ABSW75, Mos78]. The Lagrangian of this *reggeon field theory* (RFT) can be written as

$$\mathcal{L}_{\text{RFT}}(\mathbf{x}, y) = \frac{i}{2} \phi^\dagger \partial_y \phi - \frac{\alpha'_0}{2} \nabla \phi^\dagger \cdot \nabla \phi - \Delta_0 \phi^\dagger \phi - \frac{i\lambda}{2} \phi^\dagger \phi^\dagger \phi + \text{hermitian conjugate.} \quad (\text{I.98})$$

In this approach, no attempt is made to understand the spectrum of Regge trajectories: instead, one attempts to study their interactions given that they exist. In CH. III we will study an effective action derived from QCD aiming at deriving the elements of RFT.

3 REGGEIZATION AND THE BFKL POMERON

A natural question now is how the insights from Regge theory, specially the pomeron, emerge from QCD. Predating this theory, it was shown in the 60s [ELOP66] that Regge pole behavior could be obtained in field theory resumming leading $\ln s$ terms corresponding to diagrams with ladder exchange (FIG. I.19). The ϕ^3 model of the figure was improved by a more realistic model where the pomeron couples to quarks as a $C = +1$ photon [LP71]. Then Low and Nussinov [Low75, Nus75] proposed to picture the pomeron as a two-gluon exchange. Two is the minimal number of gluons needed to reproduce vacuum quantum numbers, as the gluon is a colored object. One can expect that the gluon, with the highest spin, will give a dominant exchange contribution according to (I.86) and that quark insertions in the gluon ladder will be subleading in the Regge limit. The picture of the pomeron as a gluon ladder exchange turns out to be essentially correct, as we will see⁵⁸.

\sim means $as \ s \rightarrow \infty$

$$A^{(1)} \sim \frac{g^2}{s}$$

$$A^{(2)} \sim \frac{g^2}{s} K(t) \ln s$$

$$A^{(n)} \sim \frac{g^2}{s} \frac{(K(t) \ln s)^{n-1}}{(n-1)!}$$

$$K(t) \sim g^2 \int \frac{d^2 \mathbf{k}_\perp}{(\mathbf{k}_\perp^2 + m^2)[(\mathbf{k}_\perp + \mathbf{q}_\perp)^2 + m^2]}$$

$$A(s, t) = \sum_{n=1}^{\infty} A^{(n)} \sim \sum_{n=1}^{\infty} \frac{g^2 (K(t) \ln s)^{n-1}}{(n-1)!} \simeq \frac{g^2}{s} e^{K(t) \ln s} \simeq g^2 s^{\alpha(t)}$$

Figure I.19: Resummation of ladder diagrams in ϕ^3 theory gives rise to Regge behavior.

⁵⁸The details of most of the computations given in this section can be found in [BP02]. See also Appendices A and B for details on the computation of color factors and Feynman rules for iA .

3.1 Parton-Parton Scattering in the Leading $\ln s$ Approximation

At lowest order in α_s , qq scattering proceeds via one-gluon exchange (FIG. I.20). We take quarks to have different flavors so that there is no u -channel contribution. Helicity indices are obviated as helicity is conserved at each vertex⁵⁹. The one-gluon exchange amplitude is

$$iA_{qq' \rightarrow qq'}^{(0)}(s, t) = ig^2 t_{ij}^a t_{kl}^a \bar{u}(p'_1) \gamma^\mu u(p_1) \frac{g_{\mu\nu}}{q^2} \bar{u}(p'_2) \gamma^\nu u(p_2). \quad (\text{I.99})$$

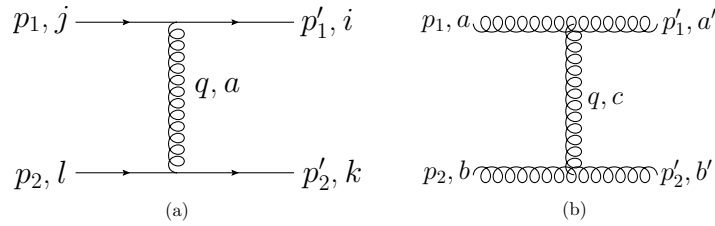


Figure I.20: (a) Quark-quark and (b) gluon-gluon scattering via one-gluon exchange.

Instead of working directly with the amplitude squared in the large- s limit, a more convenient procedure we will use henceforth is to take the large- s limit already at the level of the vertices, introducing the so-called eikonal approximation. Consider the upper vertex in FIG. I.20. When $s \gg |t|$ all q^μ components are very small compared to those of p_1^μ and p_2^μ (APP. B),

$$ig\bar{u}(p_1 + q)\gamma^\mu u(p_1) \simeq ig\bar{u}(p_1)\gamma^\mu u(p_1) = 2igp_1^\mu. \quad (\text{I.100})$$

(I.100) is the qqg eikonal vertex. Approximating the lower vertex in the same fashion, we get for large s

$$A_{qq' \rightarrow qq'}^{(0)} = g^2 t_{ij}^a t_{kl}^a \frac{4p_1 \cdot p_2}{q^2} = 8\pi\alpha_s t_{ij}^a t_{kl}^a \frac{s}{t} \implies |A_{qq' \rightarrow qq'}^{(0)}|^2 = \frac{8}{9} g^4 \frac{s^2}{t^2}. \quad (\text{I.101})$$

We get the ggg eikonal vertex in FIG. I.20 the same way⁶⁰

$$\begin{aligned} & -gf^{aa'c} [g_{\mu\mu'}(p_1 + p'_1)_\rho + g_{\rho\mu'}(p_1 + q)_\mu - g_{\mu\rho}(p_1 + q)_{\mu'}] \\ & \simeq -gf^{aa'c} [2g_{\mu\mu'}p_{1\rho} - g_{\rho\mu'}p_{1\mu} - g_{\mu\rho}p'_{1\mu'}] = -2gf^{aa'c} g_{\mu\mu'}p_{1\rho}. \end{aligned} \quad (\text{I.102})$$

⁵⁹This is strictly true within the eikonal approximation, in which one has $\bar{u}(p_1 + q, \lambda)\gamma^\mu u(p_1, \lambda') \rightarrow \bar{u}(p_1, \lambda)\gamma^\mu u(p_1, \lambda') = 2p_1^\mu \delta_{\lambda\lambda'}$.

⁶⁰In deriving the last equality in (I.102) we have used that, if external gluons have physical polarizations, the two last terms cancel when contracted with polarization vectors ($\varepsilon(p_1) \cdot p_1 = \varepsilon(p'_1) \cdot p'_1 = 0$). Notice that both eikonal vertices (I.100) and (I.102) are proportional to the momentum of the incoming particle, which has large components.

I. High Energy Scattering in QCD

Now the amplitude for FIG. I.20 in the high energy limit is

$$A_{gg \rightarrow gg}^{(0)} = -ig^2 f^{aa'c} f^{bb'c} g_{\mu\mu'} \frac{4p_1 \cdot p_2}{q^2} g_{\nu\nu'} \varepsilon_{\lambda_1}^\mu(p_1) \varepsilon_{\lambda_1'}^{*\mu'}(p_1') \varepsilon_{\lambda_2}^\nu(p_2) \varepsilon_{\lambda_2'}^{*\nu'}(p_2'). \quad (\text{I.103})$$

Squaring (I.103), the sum over the gluon polarizations is performed using (I.5) taking $n = p_2$ when summing over $\varepsilon_{\lambda_1}^\mu(p_1)$, $n = p_1$ when summing over $\varepsilon_{\lambda_2}^\nu(p_2)$, and so on⁶¹. We have

$$\overline{|A_{gg \rightarrow gg}^{(0)}|^2} = g^4 \frac{N_c^2}{N_c^2 - 1} 4 \frac{s^2}{t^2} = \frac{9}{2} g^4 \frac{s^2}{t^2} = \frac{C_A}{C_F} \overline{|A_{qg \rightarrow qg}^{(0)}|^2} = \left(\frac{C_A}{C_F} \right)^2 \overline{|A_{qq' \rightarrow qq'}^{(0)}|^2}. \quad (\text{I.104})$$

In deriving (I.104) only the t -channel contribution to gg scattering was considered, which is the relevant one in the Regge limit.

Now we want to study the radiative corrections to the $qq' \rightarrow qq'$ amplitude. At one loop, the relevant diagrams are shown in FIG. I.21. Self-energy insertions and vertex corrections are not considered as they are subleading in $\ln s$: these diagrams indeed have an extra factor of g^2 with respect to the leading graph (FIG. I.20), but no $\ln s$ enhancement, as the vertex or bubble subdiagram cannot depend on s , because the entering momenta when squared are zero (external legs on-shell) or are of the order of $\sqrt{-t}$ ⁶². The most economic way to compute the diagrams in FIG. I.21 is the application of Cutkosky rules [Cut60] based on unitarity⁶³. They allow to extract the imaginary piece of the amplitude

$$\Im A_{(a)}^{(1)} = 4\alpha_s^2 (t^a t^b)_{ij} (t^a t^b)_{kl} s \int \frac{d^2 \mathbf{k}_\perp}{\mathbf{k}_\perp^2 (\mathbf{k} - \mathbf{q})_\perp^2}, \quad (\text{I.105})$$

from which the full amplitude is reconstructed using (I.81)

$$A_{(a)}^{(1)}(s, t) = -\frac{16\pi\alpha_s}{N_c} (t^a t^b)_{ij} (t^a t^b)_{kl} \frac{s}{t} \ln \left(\frac{s}{t} \right) \omega(t); \quad \omega(t) \equiv \frac{N_c \alpha_s}{4\pi^2} \int d^2 \mathbf{k}_\perp \frac{-\mathbf{q}_\perp^2}{\mathbf{k}_\perp^2 (\mathbf{k} - \mathbf{q})_\perp^2}. \quad (\text{I.106})$$

⁶¹Equation (I.5) guarantees that only physical polarization states are taken into account, the crucial assumption for the legitimate use of the eikonal vertex (I.102). In fact, using (B.35) (with $p_A \rightarrow p_1, p_b \rightarrow p_2$) the sum (I.5) for the upper incoming gluon, with the choice $n = p_2$, becomes $\sum_{\lambda_1} \varepsilon_{\lambda_1}^\mu(p_1) \varepsilon_{\lambda_1'}^{*\mu'}(p_1) = -[g^{\mu\nu} - \frac{2}{s}(p_1^\mu p_2^\nu + p_1^\nu p_2^\mu)] = -g_\perp^{\mu\nu}$.

⁶²All components of the transverse momenta (k , say) are much lower than those of external particles, p_1 and $p_1 - k$ (APP. B), so $k \cdot p_1 \ll s$ too.

⁶³This is a close generalization of the optical theorem in APP. A, at the level of the amplitude. The recipe says that the physical discontinuity of any Feynman diagram ($2i$ times its imaginary part) is given by the following algorithm: 1) Cut through the diagram in all possible ways such that the cut propagators can simultaneously be put on shell; 2) For each cut, replace $\frac{1}{p^2 - m^2 + i0} \rightarrow -2\pi i \Theta(p^0) \delta(p^2 - m^2)$ in each cut propagator, then perform the loop integrals; 3) Sum the contributions of all cuts. An example of its use is given below when computing the leading log parton scattering amplitude at two loops.

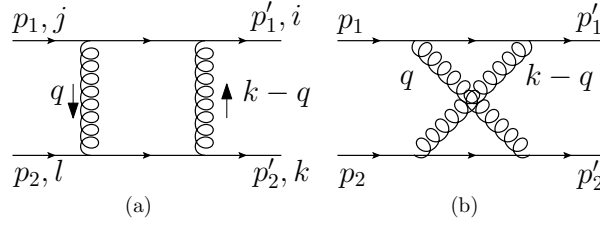


Figure I.21: qq scattering via two-gluon exchange: (a) the box diagram; (b) the crossed diagram.

The amplitude is essentially real in the Regge limit since $\ln(s/t) = \ln(s/|t|) - i\pi$. Notice that $\omega(t)$ is infrared divergent. The origin of the singularity is that we have put the external quarks on-shell. However, quarks are actually confined inside hadrons and their off-shellness provides an infrared cutoff μ^2 . Adding eventually the contribution of diagram (b) in FIG. I.21, which can be obtained through crossing and rearranging color factors, we get

$$A^{(1)} = A_{(a)}^{(1)} + A_{(b)}^{(1)} = -\frac{16\pi\alpha_s}{N_c} (t^a t^b)_{ij} \frac{s}{t} \left\{ [t^a, t^b]_{kl} \ln\left(\frac{s}{|t|}\right) - i\pi (t^a t^b)_{kl} \right\} \omega(t). \quad (\text{I.107})$$

Remember that our goal is to build the pomeron in pQCD. Therefore, we must isolate the color-singlet piece of this amplitude. The qq scattering amplitude A_{kl}^{ij} can be decomposed as a sum over the SU(3) representations in the t -channel⁶⁴ (APP. A)

$$A_{kl}^{ij}(s, t) = \sum_R \mathcal{P}_{lk}^{ji}(R) \mathcal{A}_R(s, t), \quad \mathcal{P}_{kl}^{ij}(R) \mathcal{P}_{mn}^{lk}(R') = \mathcal{P}_{mn}^{ij}(R) \delta_{RR'}. \quad (\text{I.108})$$

$\mathcal{P}_{lk}^{ji}(\mathbf{1})$ and $\mathcal{P}_{lk}^{ji}(\mathbf{8})$ are given in (A.20). The amplitudes for singlet and octet exchange are

$$\mathcal{A}_{\mathbf{1}}(s, t) = \mathcal{P}_{lk}^{ji}(\mathbf{1}) A_{ji}^{kl}(s, t), \quad \mathcal{A}_{\mathbf{8}}(s, t) = \frac{1}{N_c^2 - 1} \mathcal{P}_{lk}^{ji}(\mathbf{8}) A_{ji}^{kl}(s, t), \quad (\text{I.109})$$

where we have used (A.11). Computing the relevant color factors we get

$$A_{\mathbf{8}}^{(1)}(s, t) = 8\pi\alpha_s t_{ij}^a t_{kl}^a \frac{s}{t} \ln\left(\frac{s}{|t|}\right) \omega(t), \quad A_{\mathbf{1}}^{(1)}(s, t) = 4i\pi^2 \alpha_s \delta_{ij} \delta_{kl} \frac{N_c^2 - 1}{N_c^2} \frac{s}{t} \omega(t). \quad (\text{I.110})$$

Color-singlet gluon exchange is suppressed by a factor $\ln s$ with respect to the color-octet exchange at the same order in α_s and the amplitude is purely imaginary.

⁶⁴Notice the ordering of indices in the projector. $\mathcal{P}_{lk}^{ji} = \langle kl | \mathcal{P} | ij \rangle$ is the projector for the process $ij \rightarrow kl$. We have designed by A_{kl}^{ij} the amplitude for the process $jl \rightarrow ik$ (see FIG. I.21 for notation). This is because the projectors derived in APPENDIX A are not for the t -channel process $jl \rightarrow ik$ but for the s -channel associated one $ij \rightarrow kl$ (the meaning of projection is clearer in the s -channel). Therefore, when studying quark-quark scattering in the t -channel, it can be viewed as quark-antiquark scattering in the s -channel, and we have projections on the singlet and the octet ($\mathbf{3} \times \bar{\mathbf{3}} = \mathbf{1} + \mathbf{8}$).

I. High Energy Scattering in QCD

One can now try to go to two loops in the perturbative expansion. Many diagrams contribute here (FIG. I.22). Cutkosky rules come to the rescue by splitting the diagrams into simpler subamplitudes. Self-energy and vertex corrections are rejected in leading log approximation.

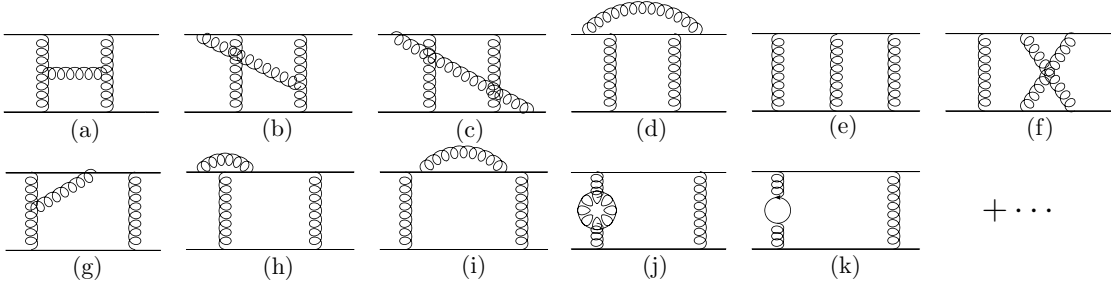


Figure I.22: Some diagrams contributing to qq scattering at two loops.

There are two different kinds of contributions: real emissions, in which the cut goes through one intermediate gluon (FIG. I.24) and virtual corrections (FIG. I.25). A clever insight of Lipatov is that real emissions may be cast as an effective vertex (FIG. I.23). Then all relevant real contributions are given by the diagram in FIG. I.24:

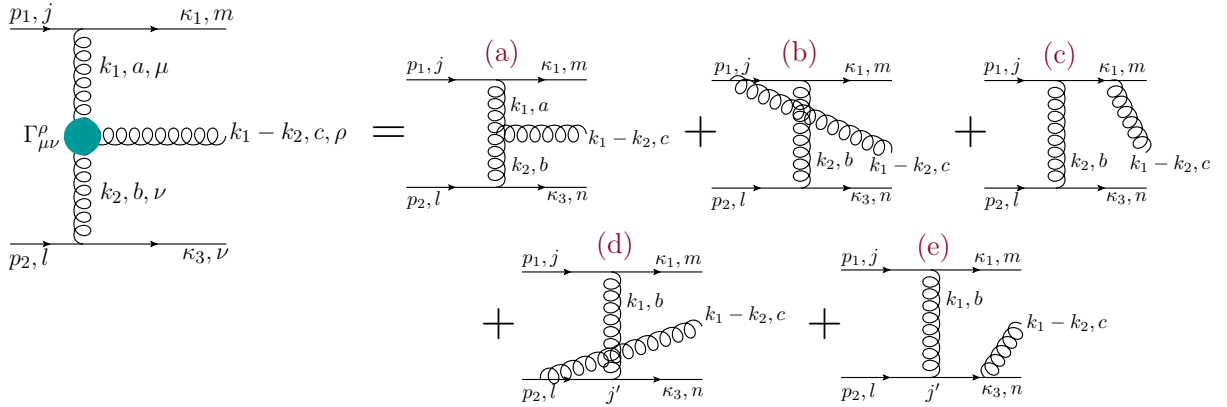


Figure I.23: The Lipatov effective vertex. The blob gives a factor $gf_{abc}\Gamma_{\mu\nu}^{\rho}(k_1, k_2)$.

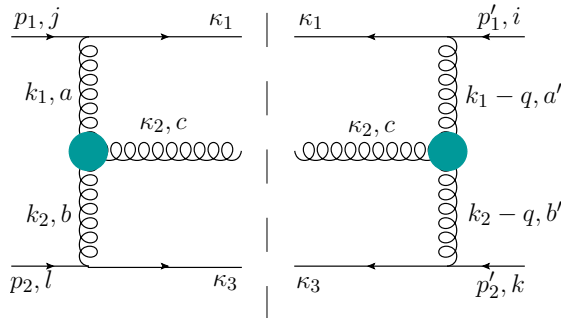


Figure I.24: The real-gluon contribution to qq scattering at order α_s^3 .

$$\Im m A_{\text{real}}^{(2)}(s, t) = -\frac{g_{\rho\sigma}}{2} \int d\Pi_3 A_{2 \rightarrow 3}^\rho(k_1, k_2) A_{2 \rightarrow 3}^{\sigma\dagger}(k_1 - q, k_2 - q). \quad (\text{I.111})$$

Introducing the Sudakov parametrization for the t -channel exchanged gluons⁶⁵

$$k_1 = \alpha_1 p_1 + \beta_1 p_2 + k_{1\perp}, \quad k_2 = \alpha_2 p_1 + \beta_2 p_2 + k_{2\perp}, \quad (\text{I.112})$$

the phase space in (I.111) reads

$$\begin{aligned} \int d\Pi_3 &= \frac{s^2}{4(2\pi)^5} \int d\alpha_1 d\beta_1 d^2\mathbf{k}_1 \int d\alpha_2 d\beta_2 d^2\mathbf{k}_2 \delta(-\beta_1(1-\alpha_1)s - \mathbf{k}_1^2) \\ &\times \delta(\alpha_2(1+\beta_2)s - \mathbf{k}_2^2) \delta((\alpha_1 - \alpha_2)(\beta_1 - \beta_2)s - (\mathbf{k}_1 - \mathbf{k}_2)^2). \end{aligned} \quad (\text{I.113})$$

The dominant piece in these integrals is given by multi-Regge kinematics (APP. B)

$$\mathbf{k}_1^2 \simeq \mathbf{k}_2^2 \simeq (\mathbf{k}_1 - \mathbf{k}_2)^2 \simeq \mathbf{q}^2 \ll s; \quad 1 \gg \alpha_1 \gg \alpha_2, \quad 1 \gg |\beta_2| \gg |\beta_1|. \quad (\text{I.114})$$

In this approximation⁶⁶

$$\int d\Pi_3 \sim \frac{1}{4(2\pi)^5} \int_{\alpha_2}^1 \frac{d\alpha_1}{\alpha_1} \int_0^1 d\alpha_2 \iint d^2\mathbf{k}_1 d^2\mathbf{k}_2 \delta(\alpha_2 s - \mathbf{k}_2^2) \sim \frac{1}{4(2\pi)^5 s} \int_{\frac{q^2}{s}}^1 \frac{d\alpha_1}{\alpha_1} \iint d^2\mathbf{k}_1 d^2\mathbf{k}_2. \quad (\text{I.116})$$

Now, the left subamplitude in FIG. I.24 equals

$$A_{2 \rightarrow 3}^\rho = 4ig^3 \frac{p_1^\mu p_2^\nu}{\mathbf{k}_1^2 \mathbf{k}_2^2} t_{mj}^a t_{nl}^b f_{abc} \Gamma_{\mu\nu}^\rho, \quad (\text{I.117})$$

where $\Gamma_{\mu\nu}^\rho$ is the Lipatov effective vertex, represented by a blue blob in FIG. I.23:

$$\Gamma_{\mu\nu}^\rho(k_1, k_2) = \frac{2p_{2\mu} p_{1\nu}}{s} C^\rho; \quad C^\rho = \left[\left(\alpha_1 + \frac{2\mathbf{k}_1^2}{\beta_2 s} \right) p_1^\rho + \left(\beta_2 + \frac{2\mathbf{k}_2^2}{\alpha_1 s} \right) p_2^\rho - (k_{1\perp}^\rho + k_{2\perp}^\rho) \right]. \quad (\text{I.118})$$

⁶⁵From now on, in order not to muddle notation, we will not keep the distinction between Sudakov components of t -channel exchanges —designated up to now and in APP. B with a bar— and of s -channel emissions, without bar. In the same way we will omit the subindex \perp for 2-dimensional transverse vectors.

⁶⁶From the last equality in (I.115) we can see that MRK (I.114) generates the leading $\ln s$ behavior. Introducing two parameters $\epsilon_{1,2}$ such that $1 \gg \epsilon_1, \epsilon_2 \gg \frac{q^2}{s}$, we can write the integral over α_1 in (I.116) as

$$\int_{\frac{q^2}{s}}^1 \frac{d\alpha_1}{\alpha_1} = \left[\int_{\frac{q^2}{s}}^{q^2/s\epsilon_1} + \int_{\frac{q^2}{s\epsilon_1}}^{1/\epsilon_2} + \int_{1/\epsilon_2}^1 \right] \frac{d\alpha_1}{\alpha_1} = -\ln \epsilon_1 + (\ln(\epsilon_1/\epsilon_2) + \ln(s/q^2)) + \ln \epsilon_2. \quad (\text{I.115})$$

Since $s/q^2 \gg 1/\epsilon_1, 1/\epsilon_2$ (at least for extremely large values of s) this is dominated for the middle part of the integral for which $1 \gg \alpha_1 \gg q^2/s (= \alpha_2)$, as required. Thus we have justified the assumption of strong ordering in the α 's which, together with the on-shell conditions for the cut lines, give a similar strong ordering (in the opposite direction) for the β 's.

I. High Energy Scattering in QCD

This non-local vertex has the important property of being gauge invariant

$$(k_{1\rho} - k_{2\rho})\Gamma_{\mu\nu}^\rho(k_1, k_2) = 0. \quad (\text{I.119})$$

Having computed all the pieces appearing in (I.111), we only need to add the u -channel contribution (which we get by replacing s by $u \simeq -s$ and tracking the modifications in the color factors) and make the color projection as before. For the octet projection the result is

$$\begin{aligned} \Im m A_{\mathbf{8},\text{real}}^{(2)}(s, t) &= \frac{\alpha_s^3 N_c^2}{\pi^2} \frac{1}{2} t_{ij}^a t_{kl}^a s \ln\left(\frac{s}{|t|}\right) \iint d^2\mathbf{k}_1 d^2\mathbf{k}_2 \left[\frac{\mathbf{q}^2}{\mathbf{k}_1^2 \mathbf{k}_2^2 (\mathbf{k}_1 - \mathbf{q})^2 (\mathbf{k}_2 - \mathbf{q})^2} \right. \\ &\quad \left. - \frac{1}{\mathbf{k}_2^2 (\mathbf{k}_1 - \mathbf{q})^2 (\mathbf{k}_1 - \mathbf{k}_2)^2} - \frac{1}{\mathbf{k}_1^2 (\mathbf{k}_2 - \mathbf{q})^2 (\mathbf{k}_1 - \mathbf{k}_2)^2} \right]. \end{aligned} \quad (\text{I.120})$$

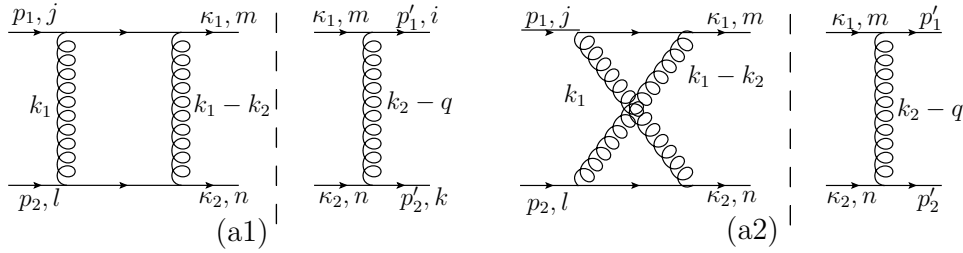


Figure I.25: Two-loop virtual corrections to qq scattering.

The computation of the virtual corrections (FIG. I.25) goes along the same lines:

$$\begin{aligned} \Im m A_{\mathbf{8},\text{virt}}^{(2)}(s, t) &= \frac{N_c^2 \alpha_s^3}{2\pi^2} t_{ij}^a t_{kl}^a s \ln\left(\frac{s}{|t|}\right) \iint d^2\mathbf{k}_1 d^2\mathbf{k}_2 \left[\frac{1}{\mathbf{k}_1^2 (\mathbf{k}_2 - \mathbf{q})^2 (\mathbf{k}_1 - \mathbf{k}_2)^2} \right. \\ &\quad \left. + \frac{1}{\mathbf{k}_2^2 (\mathbf{k}_1 - \mathbf{q})^2 (\mathbf{k}_1 - \mathbf{k}_2)^2} \right]. \end{aligned} \quad (\text{I.121})$$

And now we see that due to the particular form of the color-octet factors kind of miraculous cancellation occurs when summing (I.120) and (I.121):

$$\begin{aligned} \Im m A_{\mathbf{8}}^{(2)}(s, t) &= \Im m A_{\mathbf{8},\text{real}}^{(2)}(s, t) + \Im m A_{\mathbf{8},\text{virt}}^{(2)}(s, t) = \frac{N_c^2 \alpha_s^3}{2\pi^3} t_{ij}^a t_{kl}^a s \ln\left(\frac{s}{|t|}\right) \\ &\quad \times \iint d^2\mathbf{k}_1 d^2\mathbf{k}_2 \frac{1}{\mathbf{q}^2} \mathbf{k}_1^2 \mathbf{k}_2^2 (\mathbf{k}_1 - \mathbf{q})^2 (\mathbf{k}_2 - \mathbf{q})^2 = 8\pi^2 \alpha_s t_{ij}^a t_{kl}^a \frac{s}{|t|} \ln\left(\frac{s}{|t|}\right) \omega^2(t) \\ &\implies A_{\mathbf{8}}^{(2)}(s, t) = 4\pi \alpha_s t_{ij}^a t_{kl}^a \frac{s}{t} \ln^2\left(\frac{s}{|t|}\right) \omega^2(t). \end{aligned} \quad (\text{I.122})$$

No such cancellation arises for the singlet projection. There is a deep reason for this.

3.2 Gluon Reggeization and the Bootstrap

After having gone through the first three orders in perturbation theory, it is the moment to make some educated guesses. First of all, our experience suggests that the leading $\ln s$ approximation is given by ladder diagrams⁶⁷ where the gluons emitted in the *rungs* are subject to multi-Regge kinematics (see FIG. I.26, where only the cut subamplitude is shown). Then, real corrections are considered to all orders by promoting the vertices in the ladder to effective vertices⁶⁸. So the amplitude for gluon production is given in the factorized form

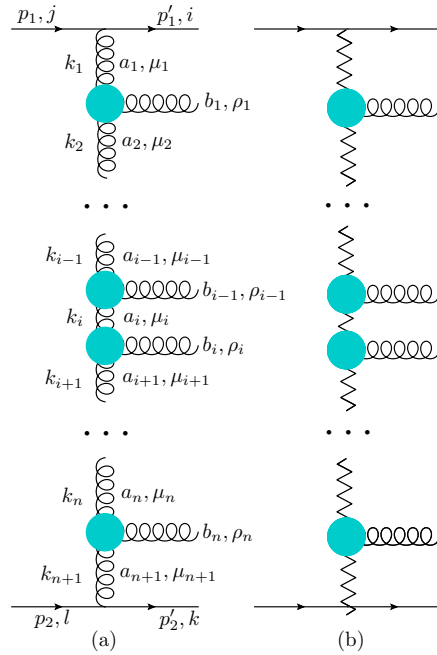


Figure I.26: Diagram for the process $qq \rightarrow qq+n$ gluons: at tree level (a) and with virtual radiative corrections (b). The blobs represent Lipatov vertices, and the wavy lines reggeized gluons.

$$\begin{aligned}
 A_{2 \rightarrow n+2}^{\rho_1 \dots \rho_n} &= 2isgt_{ij}^{a_1} \frac{i}{\mathbf{k}_1^2} \left[-gf_{a_1 a_2 b_1} C^{\rho_1}(k_1, k_2) \frac{i}{\mathbf{k}_2^2} \right] \left[-gf_{a_2 a_3 b_2} C^{\rho_2}(k_2, k_3) \frac{i}{\mathbf{k}_3^2} \right] \\
 &\dots \times \left[-gf_{a_n a_{n+1} b_n} C^{\rho_n}(k_n, k_{n+1}) \frac{i}{\mathbf{k}_{n+1}^2} \right] gt_{kl}^{a_{n+1}}.
 \end{aligned} \tag{I.123}$$

A rather elegant proof of (I.123) will be presented now [GLR83, FR97]⁶⁹. Consider the $2 \rightarrow n+2$ amplitude in FIG. I.26. If we cut the i th vertical gluon, with momentum k_i , the amplitude separates into an upper part $\mathcal{M}_\mu(p_1, k_1, \dots, k_i)$, and a lower part $\mathcal{N}_\nu(p_2, k_i, \dots, k_n)$. Since all but the cut gluon lines are on shell, these Green functions obey the Ward identities

⁶⁷Notice the analogy with DGLAP resummation (SEC. I.2.1).

⁶⁸The eikonal approximation, used in the derivation of Lipatov's vertex, is enforced here by MRK.

⁶⁹The basis of the proof consists in exploiting the gauge invariance of Lipatov's vertex to reduce the effective ladder in FIG. I.26 to a genuine ladder diagram.

I. High Energy Scattering in QCD

$$k_i^\mu \mathcal{M}_\mu(p_1, k_1, \dots, k_i) = 0; \quad k_i^\nu \mathcal{N}_\nu(p_2, k_i, \dots, k_n) = 0. \quad (\text{I.124})$$

The largest momentum in the amplitude \mathcal{M}_μ is p_1 , hence \mathcal{M}^μ will be proportional in the leading approximation to p_1^μ . In the same way, $\mathcal{N}^\nu \propto p_2^\nu$. Therefore, using the Sudakov parametrization $k_i = \alpha_i p_1 + \beta_i p_2 + k_{i\perp}$, and the fact that $p_1^2 = p_2^2 = 0$, (I.124) becomes

$$\begin{aligned} k_{i\perp}^\mu \mathcal{M}_\mu(p_1, k_1, \dots, k_i) &= -\beta_i p_2^\mu \mathcal{M}_\mu(p_1, k_1, \dots, k_i); \\ k_{i\perp}^\nu \mathcal{N}_\nu(p_2, k_i, \dots, k_n) &= -\alpha_i p_1^\nu \mathcal{N}_\nu(p_2, k_i, \dots, k_n). \end{aligned} \quad (\text{I.125})$$

Now we can use the Sudakov parametrization (B.23) (or, with our normalization, (B.35)) for the polarization tensor appearing in the propagator of the i th t -channel gluon. As we have to contract it with $p_1^\mu p_2^\nu$, we can neglect its transverse part and approximate it by

$$g_{\mu\nu} \simeq \frac{2}{s} p_{2\mu} p_{1\nu} \left(= \frac{(n^+)_\mu (n^-)_\nu}{2} \right), \quad (\text{I.126})$$

which gives an extra factor of s in the contraction. Then, using (I.124) we can go even further and say that we can replace the numerator of the cut gluon propagator by $g_{\mu\nu} \rightarrow \frac{2k_{i\perp}^\mu k_{i\perp}^\nu}{\alpha_i \beta_i s}$, since $g_{\mu\nu} \mathcal{M}_\mu \mathcal{N}_\nu \simeq \frac{2p_1^\mu p_2^\nu}{s} \mathcal{M}_\mu \mathcal{N}_\nu \simeq \frac{2k_{i\perp}^\mu k_{i\perp}^\nu}{\alpha_i \beta_i s} \mathcal{M}_\mu \mathcal{N}_\nu$. This reasoning can be applied to all t -channel gluons in the ladder, so we can associate a factor of $\sqrt{2/s} k_{i\perp}^\mu / \beta_i$ with the vertex at the top of the i th vertical gluon and a factor $\sqrt{2/s} k_{i\perp}^\nu / \alpha_i$ with the corresponding vertex at the bottom. The amplitude for the ladder then becomes

$$\begin{aligned} A_{2 \rightarrow n+2}^{\rho_1 \dots \rho_n} &= 2isg^2 t_{ij}^{a_1} t_{kl}^{a_{n+1}} \frac{i}{\mathbf{k}_1^2} \prod_{i=1}^n f_{a_i a_{i+1} b_i} \frac{(-ig)}{\mathbf{k}_{i+1}^2} \\ &\times \frac{2k_{i\perp}^{\mu_i} k_{i+1\perp}^{\nu_i}}{\alpha_i \beta_{i+1} s} \left[g_{\mu_i \nu_i} (-k_i - k_{i+1})^{\rho_i} + g_{\mu_i}^{\rho_i} (2k_i - k_{i+1})_{\nu_i} + g_{\nu_i}^{\rho_i} (2k_{i+1} - k_i)_{\mu_i} \right]. \end{aligned} \quad (\text{I.127})$$

Substituting k_i and k_{i+1} by its Sudakov decomposition in the last bracket representing the ordinary 3-gluon vertex, one can check that the second line in (I.127) is equal to $C^{\rho_i}(k_i, k_{i+1})$ up to terms proportional to the momenta of the emitted gluons $(k_i - k_{i+1})^\rho$, which vanish when contracted with the polarization vectors of these gluons, because they are on-shell and hence their polarization vectors must be transverse. This finishes our proof of (I.123).

It remains to incorporate virtual corrections. Putting together the results of the first three orders of perturbation theory (I.101), (I.110) and (I.122), we find that up to $\mathcal{O}(\alpha_s^3)$ the color-octet amplitude in LLA has the suggestive form $A_8(s, t) = 8\pi\alpha_s \frac{s}{t} t_{ij}^a t_{kl}^a \left[1 + \omega(t) \ln\left(\frac{s}{|t|}\right) + \frac{\omega^2(t)}{2} \ln^2\left(\frac{s}{|t|}\right) + \dots \right]$. It is then natural to conjecture that

these are the first three terms in the expansion of

$$A_{\mathbf{8}}(s, t) = 8\pi\alpha_s t_{ij}^a t_{kl}^a \frac{s}{t} \left(\frac{s}{|t|}\right)^{\omega(t)} = -8\pi\alpha_s t_{ij}^a t_{kl}^a \left(\frac{s}{|t|}\right)^{\alpha_g(t)}, \quad \alpha_g(t) = 1 + \omega(t), \quad (\text{I.128})$$

that would mean that the gluon *reggeizes* (see Eq. (I.92)). The reggeization hypothesis (I.128) is equivalent to modify the t -channel gluon propagator by

$$\frac{-i}{k_i^2} \rightarrow \frac{-i}{k_i^2} \left(-\frac{s_i}{k_i^2}\right)^{\omega(-k_i^2)} \simeq \frac{-i}{k_i^2} \left(\frac{\alpha_{i-1}}{\alpha_i}\right)^{\omega(-k_i^2)}, \quad (\text{I.129})$$

where $s_i = (k_{i-1} + k_i)^2 \simeq \frac{\alpha_{i-1}}{\alpha_i} \mathbf{k}_i^2$ (Eq. (B.41)). Indeed, (I.128) is obtained from (I.101) by performing the substitution (I.129).

As we have seen, Regge poles (reggeons) can be interpreted as bound states or resonances exchanged in the t -channel, not as elementary particles in the usual sense, since their effective spin $\alpha(t)$ is in general complex and depends on t . However, if there exist some physical particle of mass m and spin j with the same quantum numbers (apart from spin) of a given Regge trajectory, then it is often the case that $\alpha(m^2) = j$. The idea that elementary particles may reggeize dates back to the days of Chew's S -matrix program [Cao91]⁷⁰.

The contribution of an elementary particle with mass m and spin j to the partial wave amplitude is proportional $\delta_{\ell j}$ and therefore not analytically continuable in the ℓ -plane [Col77]. Gell-Mann, Goldberger and others [GMG62, GMGL⁺64a, GMGL⁺64b] then pointed out that in a vector field theory elementary particles could become reggeized as a consequence of radiative corrections, that in particular would generate terms canceling the non-analytic behavior. Conditions for such behavior to be possible were studied [Man65, AKT70, GST73] and perturbative calculations to several loops were carried in QED [FGL70, FGL71, CW69, CW70b, CW70a, MW76], QCD [Mas76, Tyb76, FS76, Lip76, CL77] and unification theories with general gauge groups (see, e.g. [GS79, Bar80b]). The general conclusion is that in gauge theories reggeization of gauge bosons is possible—and most probably takes place—only in non-abelian gauge theories with semi-simple gauge groups. Also fermions reggeize. So in QED the electron reggeizes while the photon does not; in the

⁷⁰In their aim to show that no particles are more elementary than others, Chew and Frautschi formulated the following criterion: composite particles lay on Regge trajectories, associated to poles in the ℓ -plane moving with s (for the process obtained by crossing symmetry in which the reggeon is exchanged in the s -channel), whereas elementary particle poles are associated with unique angular momenta, and do not admit continuation in ℓ . Since all particles involved in hadronic processes have been found to lie in Regge trajectories, this would question the existence of elementary particles.

I. High Energy Scattering in QCD

SU(2)×U(1) electroweak sector the W^\pm reggeize but the Z and the photon do not, being related with the original U(1); and in QCD both gluons and quarks reggeize.

Reggeization of any particle assumes the *signaturized*⁷¹ amplitude to acquire an asymptotic behavior like $s^{\alpha(t)}$ when exchanging this particle in the t -channel in the Regge limit $s \gg t$. If we assume from the form of the octet amplitude that radiative corrections build the reggeized gluon, then it is natural to assume that at the level of the production amplitude (I.123) the effect of incorporating virtual corrections is reggeizing any of the intermediate t -channel gluons of the ladder. Thus we have the following ansatz⁷² (FIG. I.26)

$$\begin{aligned}
A_{2 \rightarrow n+2}^{\rho_1 \dots \rho_n} &= 2i s g t_{ij}^{a_1} \left(\frac{i}{\mathbf{k}_1^2} \right) \left(\frac{1}{\alpha_1} \right)^{\omega(-\mathbf{k}_1^2)} \left[-g f_{a_1 a_2 b_1} C^{\rho_1}(k_1, k_2) \left(\frac{i}{\mathbf{k}_2^2} \right) \left(\frac{\alpha_1}{\alpha_2} \right)^{\omega(-\mathbf{k}_2^2)} \right] \\
&\times \left[-g f_{a_2 a_3 b_2} C^{\rho_2}(k_2, k_3) \left(\frac{i}{\mathbf{k}_3^2} \right) \left(\frac{\alpha_2}{\alpha_3} \right)^{\omega(-\mathbf{k}_3^2)} \right] \times \dots \\
&\times \left[-g f_{a_n a_{n+1} b_n} C^{\rho_n}(k_n, k_{n+1}) \left(\frac{i}{\mathbf{k}_{n+1}^2} \right) \left(\frac{\alpha_n}{\alpha_{n+1}} \right)^{\omega(-\mathbf{k}_{n+1}^2)} \right] g t_{kl}^{a_{n+1}} \\
&= 2i s g^2 t_{ij}^{a_1} t_{kl}^{a_{n+1}} \left(\frac{i}{\mathbf{k}_1^2} \right) \left[\frac{1}{\alpha_1} \right]^{\omega(-\mathbf{k}_1^2)} \prod_{i=1}^n \left\{ -g f_{a_i a_{i+1} b_i} C^{\rho_i}(k_i, k_{i+1}) \frac{i}{\mathbf{k}_{i+1}^2} \left[\frac{\alpha_i}{\alpha_{i+1}} \right]^{\omega(-\mathbf{k}_{i+1}^2)} \right\}.
\end{aligned} \tag{I.130}$$

The consistency of our reggeization picture requires that if we assume (I.130) to be correct we must find, after resumming all ladders and projecting onto the antisymmetric octet, that the amplitude is given by (I.128), corresponding to the exchange of one reggeized gluon⁷³. This is what we will find indeed when performing the BFKL resummation. Gluon reggeization can moreover be *proven* by checking the compatibility of the s -channel unitarity equations (A.30) in all the subchannels with the form of the amplitude (I.130), which is an infinity of non-trivial constraints to be satisfied [Bar80b, BFF03]⁷⁴. Bootstrap conditions have been proved to NLL order [FFKR06].

⁷¹When speaking of reggeization of the intermediate gluons in a ladder (see FIG. B.3), signature in the t_l -channel means the (anti)-symmetrization with respect to the substitution $s_{ij} \leftrightarrow -s_{ij}$, for $i < l \leq j$, where s_{ij} is defined in (B.33). This generalizes the concept of signature as parity under the interchange $s \rightarrow u \simeq -s$ for multiparticle production in the Regge limit. For the case of gluon reggeization the signature will be $\xi = -1$, corresponding to the antisymmetric octet, because we advanced that $\xi = 1(-1)$ corresponds to even (odd) spin resonances.

⁷²Often this amplitude is expressed in terms of rapidities using that $\frac{\alpha_i}{\alpha_{i+1}} = e^{y_i - y_{i+1}}$. We note that this is only the s -channel contribution. We will add later on the u -channel contribution in the same way we made for lower orders.

⁷³We note that the reggeized gluon is quite an unusual construction that is composed of ladders of reggeized gluons (and so on), so we are effectively resumming an infinity of diagrams with the most diverse topologies. Is what Forshaw and Ross [FR97] call *ladders within ladders*.

⁷⁴See [Whi76, Col77] for the necessary background on the general structure of inelastic production amplitudes in the multi-Regge limit.

3.3 The BFKL Equation

Once we have the structure of the production amplitude (I.130), we can use unitarity to extract (the imaginary part of) the elastic scattering amplitude in which we are interested

$$\begin{aligned}
 \Im m A(s, t) &= \frac{1}{2} (-1)^n g_{\rho_1 \sigma_1} \cdots g_{\rho_n \sigma_n} \int d\Pi_{n+2} A_{2 \rightarrow n+2}^{\rho_1 \cdots \rho_n}(k_1, \cdots, k_n) A_{2 \rightarrow n+2}^{\sigma_1 \cdots \sigma_n \dagger}(k_1 - q, \cdots, k_n - q); \\
 d\Pi_{n+2} &= \frac{s^{n+1}}{2^{n+1} (2\pi)^{3n+2}} \int \prod_{i=1}^{n+1} d\alpha_i d\beta_i d^2 \mathbf{k}_i \delta(-\beta_1 (1 - \alpha_1) s - \mathbf{k}_1^2) \delta(\alpha_{n+1} (1 + \beta_{n+1}) s - \mathbf{k}_{n+1}^2) \\
 &\quad \times \prod_{j=1}^n \delta((\alpha_j - \alpha_{j+1})(\beta_j - \beta_{j+1}) s - (\mathbf{k}_j - \mathbf{k}_{j+1})^2) \\
 &\stackrel{\text{MRK}}{\simeq} \frac{1}{2^{n+1} (2\pi)^{3n+2}} \prod_{i=1}^n \int_{\alpha_{i+1}}^1 \frac{d\alpha_i}{\alpha_i} \int_0^1 d\alpha_{n+1} \prod_{j=1}^{n+1} \int d^2 \mathbf{k}_j \delta(\alpha_{n+1} s - \mathbf{k}^2).
 \end{aligned} \tag{I.131}$$

From (I.131), it follows that

$$\begin{aligned}
 \Im m \mathcal{A}_R(s, t) &= \frac{1}{2} \sum_{n=0}^{\infty} 4s^2 g^4 \mathcal{G}_R \int d\Pi_{n+2} \frac{1}{\mathbf{k}_1^2 (\mathbf{k}_1 - \mathbf{q})^2} \left(\frac{1}{\alpha_1} \right)^{\omega(-\mathbf{k}_1^2) + \omega((\mathbf{k}_1 - \mathbf{q})^2)} \\
 &\quad \times \prod_{i=1}^n \left\{ \frac{g^2 (-2\eta_R)}{\mathbf{k}_{i+1}^2 (\mathbf{k}_{i+1} - \mathbf{q})^2} K(\mathbf{k}_i, \mathbf{k}_{i+1}) \left(\frac{\alpha_i}{\alpha_{i+1}} \right)^{\omega(-\mathbf{k}_{i+1}^2) + \omega((\mathbf{k}_{i+1} - \mathbf{q})^2)} \right\},
 \end{aligned} \tag{I.132}$$

where the *kernel* is given by the contraction of Lipatov vertices

$$-\frac{1}{2} C^{\rho_i}(k_i, k_{i+1}) C_{\rho_i}(-k_i + q, -k_{i+1} + q) = \left[\mathbf{q}^2 - \frac{\mathbf{k}_i^2 (\mathbf{k}_{i+1} - \mathbf{q})^2}{(\mathbf{k}_i - \mathbf{k}_{i+1})^2} - \frac{\mathbf{k}_{i+1}^2 (\mathbf{k}_i - \mathbf{q})^2}{(\mathbf{k}_i - \mathbf{k}_{i+1})^2} \right] \equiv K(\mathbf{k}_i, \mathbf{k}_{i+1}). \tag{I.133}$$

The color octet and singlet projections only differ in color factors

$$\mathcal{G}_1 = \frac{N_c^2 - 1}{4N_c}, \quad \mathcal{G}_8 = -\frac{N_c}{8}; \quad \eta_1 = N_c, \quad \eta_8 = \frac{N_c}{2}. \tag{I.134}$$

Rather than applying directly a dispersion relation to (I.132) in order to reconstruct the full amplitude, it is convenient to work in terms of partial wave amplitudes

$$f_R(\omega, t) = \int_1^{\infty} d\left(\frac{s}{|t|}\right) \left(\frac{s}{|t|}\right)^{-\omega-1} \frac{\Im m \mathcal{A}_R(s, t)}{s} \implies \frac{\Im m \mathcal{A}_R(s, t)}{s} = \frac{1}{2\pi i} \int_{c-i\infty}^{c+i\infty} d\omega \left(\frac{s}{|t|}\right)^{\omega} f_R(\omega, t). \tag{I.135}$$

The reason why we work in terms of the Mellin transform is the convolution property (C.6) that allows us to disentangle the nested integrations appearing in (I.131). Addition of the u -channel contribution, that we have omitted up to now, is automatic using crossing and the

I. High Energy Scattering in QCD

definition of signature (I.85)

$$\Im \mathcal{A}_R(s, t) = -\xi_R \Im \mathcal{A}_R(u, t) \simeq -\xi_R \Im \mathcal{A}_R(-s, t), \quad \xi_1 = +1, \quad \xi_8 = -1, \quad (\text{I.136})$$

which amounts to substitute $f_R(\omega, t) \rightarrow (1 - \xi_R e^{-i\pi\omega}) f_R(\omega, t)$ in the partial wave amplitude. Now we can finally apply a dispersion relation to (I.135) or use directly the Watson-Sommerfeld transform

$$\mathcal{A}_R(s, t) = -\frac{1}{4\pi i} \int_{c-i\infty}^{c+i\infty} d\omega \left(\frac{s}{|t|} \right)^{\omega+1} \frac{\xi_R - e^{-i\pi\omega}}{\sin \pi\omega} f_R(\omega, t), \quad (\text{I.137})$$

that can be obtained taking the asymptotic behavior of the Legendre polynomials in (I.85). We get, applying (C.3) and (C.6) to (I.132)

$$\begin{aligned} f_R(\omega, \mathbf{q}^2) &= (4\pi\alpha_s)^2 \mathcal{G}_R \sum_{n=0}^{\infty} \prod_{i=1}^{n+1} \int \frac{d^2 \mathbf{k}_i}{(2\pi)^2} \frac{1}{\mathbf{k}_i^2 (\mathbf{k}_i - \mathbf{q})^2} \frac{1}{\omega - \omega(\mathbf{k}_i^2) - \omega((\mathbf{k}_i - \mathbf{q})^2)} \\ &\times (-2\alpha_s \eta_R) K(\mathbf{k}_1, \mathbf{k}_2) \frac{1}{\mathbf{k}_2^2 (\mathbf{k}_2 - \mathbf{q})^2} \frac{1}{\omega - \omega(\mathbf{k}_2^2) - \omega((\mathbf{k}_2 - \mathbf{q})^2)} \times (\dots) \\ &\times (-2\alpha_s \eta_R) K(\mathbf{k}_n, \mathbf{k}_{n+1}) \frac{1}{\mathbf{k}_{n+1}^2 (\mathbf{k}_{n+1} - \mathbf{q})^2} \frac{1}{\omega - \omega(\mathbf{k}_{n+1}^2) - \omega((\mathbf{k}_{n+1} - \mathbf{q})^2)}. \end{aligned} \quad (\text{I.138})$$

The great observation is that (I.138) can be recast as a recursive relation

$$f_R(\omega, \mathbf{q}^2) = (4\pi\alpha_s)^2 \mathcal{G}_R \int \frac{d^2 \mathbf{k}}{(2\pi)^2} \frac{\mathcal{F}_R(\omega, \mathbf{k}, \mathbf{q})}{\mathbf{k}^2 (\mathbf{k} - \mathbf{q})^2}, \quad (\text{I.139})$$

where the function $\mathcal{F}_R(\omega, \mathbf{k}, \mathbf{q})$ satisfies the integral equation

$$[\omega - \omega(-\mathbf{k}^2) - \omega(-(\mathbf{k} - \mathbf{q})^2)] \mathcal{F}_R(\omega, \mathbf{k}, \mathbf{q}) = 1 - \frac{2\alpha_s \eta_R}{4\pi^2} \int d^2 \boldsymbol{\kappa} \frac{K(\mathbf{k}, \boldsymbol{\kappa})}{\boldsymbol{\kappa}^2 (\boldsymbol{\kappa} - \mathbf{q})^2} \mathcal{F}_R(\omega, \boldsymbol{\kappa}, \mathbf{q}). \quad (\text{I.140})$$

This can be seen by solving the equation iteratively, starting with $\mathcal{F}_R^{(0)}(\omega, \boldsymbol{\kappa}, \mathbf{q}) = 0$. (I.140) is the general form of the Balitsky-Fadin-Kuraev-Lipatov (BFKL) equation [FKL75, Lip76, FKL76, FKL77, BL78, BL79].

For the particular value of the color factor $\eta_8 = \frac{N_c}{2}$, corresponding to the octet projection, (I.140) simplifies dramatically

$$\omega \mathcal{F}_8(\omega, \mathbf{k}, \mathbf{q}) = 1 - \frac{N_c \alpha_s}{4\pi^2} \int d^2 \boldsymbol{\kappa} \frac{\mathbf{q}^2}{\boldsymbol{\kappa}^2 (\boldsymbol{\kappa} - \mathbf{q})^2} \mathcal{F}_8(\omega, \boldsymbol{\kappa}, \mathbf{q}). \quad (\text{I.141})$$

This equation admits the \mathbf{k} -independent solution

$$\mathcal{F}_8(\omega, \mathbf{q}) = \frac{1}{\omega - \omega(-\mathbf{q}^2)} \xrightarrow{(I.139)} f_8(\omega, \mathbf{q}^2) = 2\pi^2 \alpha_s \frac{\omega(-\mathbf{q}^2)}{\mathbf{q}^2} \frac{1}{\omega - \omega(-\mathbf{q}^2)}. \quad (I.142)$$

From (I.142) we see that $f_8(\ell, t)$ has a pole at $\ell = \alpha_g(t) = 1 + \omega(t)$, as required by bootstrap. Taking the inverse Mellin transform we get

$$\Im m \mathcal{A}_8(s, t) = 2\pi^2 \alpha_s \omega(t) \left(\frac{s}{|t|} \right)^{1+\omega(t)} \xrightarrow{(I.137)} \mathcal{A}_8(s, t) = -4\pi \alpha_s t_{ij}^a t_{kl}^a [1 - e^{-i\pi\alpha_g(t)}] \left(\frac{s}{|t|} \right)^{\alpha_g(t)}. \quad (I.143)$$

For the singlet projection ($\eta_1 = N_c$), (I.140) takes a less compact form

$$[\omega - \omega(-\mathbf{k}^2) - \omega(-(\mathbf{k} - \mathbf{q})^2)] \mathcal{F}_1(\omega, \mathbf{k}, \mathbf{q}) = 1 - \frac{N_c \alpha_s}{2\pi^2} \int d^2 \boldsymbol{\kappa} \frac{K(\mathbf{k}, \boldsymbol{\kappa})}{\boldsymbol{\kappa}^2 (\boldsymbol{\kappa} - \mathbf{q})^2} \mathcal{F}_1(\omega, \boldsymbol{\kappa}, \mathbf{q}), \quad (I.144)$$

or, in terms of the BFKL Green's function

$$\mathcal{F}_1(\omega, \mathbf{k}, \mathbf{q}) = \int \frac{d^2 \mathbf{k}'}{\mathbf{k}'^2} \mathbf{k}'^2 f(\omega, \mathbf{k}, \mathbf{k}', \mathbf{q}), \quad (I.145)$$

directly related to the 4-point amplitude for off-shell gluons [FR97]

$$[\omega - \omega(-\mathbf{k}^2) - \omega(-(\mathbf{k} - \mathbf{q})^2)] f(\omega, \mathbf{k}, \mathbf{k}', \mathbf{q}) = \delta^2(\mathbf{k} - \mathbf{k}') - \frac{N_c \alpha_s}{2\pi^2} \int d^2 \boldsymbol{\kappa} \frac{K(\mathbf{k}, \boldsymbol{\kappa})}{\boldsymbol{\kappa}^2 (\boldsymbol{\kappa} - \mathbf{q})^2} f(\omega, \boldsymbol{\kappa}, \mathbf{k}', \mathbf{q}). \quad (I.146)$$

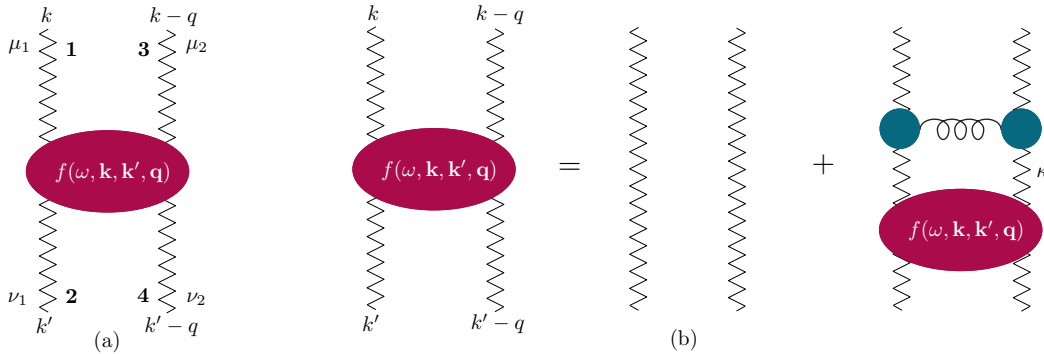


Figure I.27: (a) The four-gluon singlet Green function; (b) diagrammatic representation of the singlet BFKL equation in terms of the four-gluon Green function. Adapted from [FR97].

The singlet BFKL equation (I.146) is represented diagrammatically in FIG. II.3.1. It enjoys important properties. First of all, it is UV finite, as can be seen by taking the limits $\boldsymbol{\kappa}^2 \rightarrow \infty$ and $\mathbf{k}^2 \rightarrow \infty$ in the integrand of (I.146). As far as the IR behavior is concerned, (I.146) is regular for $\boldsymbol{\kappa}^2 \rightarrow 0$, and at $\mathbf{k} = \boldsymbol{\kappa}$. For $\mathbf{k}^2 \rightarrow 0$ infrared divergences arising from the virtual-gluon terms persist but one should recall that in the physical situation of colorless particle scattering, these divergences are regulated by the confinement of quarks

I. High Energy Scattering in QCD

and gluons [Lip86]⁷⁵. From (I.146), using (I.136) and (I.145), we have the imaginary part of the scattering amplitude via singlet exchange

$$\begin{aligned} \frac{\Im m \mathcal{A}_1(s, t)}{s} &= (8\pi^2 \alpha_s)^2 \frac{N_c^2 - 1}{4N_c} \int \frac{d^2 \mathbf{k}}{(2\pi)^2} \frac{d^2 \mathbf{k}'}{(2\pi)^2} \frac{f(s, \mathbf{k}, \mathbf{k}', \mathbf{q})}{\mathbf{k}'^2 (\mathbf{k} - \mathbf{q})^2}, \\ f(s, \mathbf{k}, \mathbf{k}', \mathbf{q}) &= \frac{1}{2\pi i} \int_{c-i\infty}^{c+i\infty} d\omega \left(\frac{s}{|t|} \right)^\omega f(\omega, \mathbf{k}, \mathbf{k}', \mathbf{q}). \end{aligned} \quad (\text{I.147})$$

In the case of elastic scattering ($t = 0$), the BFKL equation is greatly simplified⁷⁶

$$\begin{aligned} \omega f(\omega, \mathbf{k}, \mathbf{k}') &= \delta^2(\mathbf{k} - \mathbf{k}') + \int d^2 \boldsymbol{\kappa} \mathcal{K}(\mathbf{k}, \boldsymbol{\kappa}) f(\omega, \boldsymbol{\kappa}, \mathbf{k}') \equiv \mathbb{1} + \mathcal{K} \otimes f; \\ \mathcal{K}(\mathbf{k}, \boldsymbol{\kappa}) &= 2\omega(-\mathbf{k}^2) \delta^2(\mathbf{k} - \boldsymbol{\kappa}) + \frac{N_c \alpha_s}{\pi^2} \frac{1}{(\mathbf{k} - \boldsymbol{\kappa})^2}. \end{aligned} \quad (\text{I.149})$$

One can find an analytic solution of (I.149) by diagonalizing the kernel

$$\mathcal{K} \otimes \phi_\alpha = \omega_\alpha \phi_\alpha, \quad \sum_\alpha \phi_\alpha(\mathbf{k}) \phi_\alpha^*(\mathbf{k}') = \delta^2(\mathbf{k} - \mathbf{k}') \implies f(\omega, \mathbf{k}, \mathbf{k}') = \sum_\alpha \frac{\phi_\alpha(\mathbf{k}) \phi_\alpha^*(\mathbf{k}')}{\omega - \omega_\alpha}. \quad (\text{I.150})$$

Just with dimensional analysis arguments [BP02] one can realize that the eigenfunctions are

$$\phi_{n\nu}(|\mathbf{k}|, \vartheta) = \frac{1}{\pi\sqrt{2}} (\mathbf{k}^2)^{-\frac{1}{2}+i\nu} e^{in\vartheta}, \quad \nu \in \mathbb{R}; \quad \int d^2 \mathbf{k} \phi_{n\nu}(\mathbf{k}) \phi_{n'\nu'}^*(\mathbf{k}) = \delta_{nn'} \delta(\nu - \nu'). \quad (\text{I.151})$$

The labels n and $\gamma = \frac{1}{2} + i\nu$ are called conformal spin and anomalous dimension respectively (see [IFL10], Ch. 10.2, and SEC. I.4.2). Plugging in these eigenfunctions in (I.150), and making some algebra [dD95], we get the eigenvalues, expressed in terms of $\psi(z) = \Gamma'(z)/\Gamma(z)$

⁷⁵Using dimensional regularization, we can see that divergences of the integral with the kernel cancel with those of the trajectory (I.106) for the case of the singlet [IFL10]. This does not happen for other color projections in the t -channel. Within perturbation theory it is perfectly legitimate to consider projectiles which are not color singlets, even though the cross section of scattering of two nonsinglet objects is infrared divergent. In position space, the divergence appears as the result of integration over impact parameter, which is not bounded by confinement. When considering the non-perturbative effects leading to confinement, the projectiles must be color singlets, so that they can only exchange states that are overall color singlets. Amplitudes for other projections must then be considered unphysical. This is why the octet amplitude, though enhanced by a $\ln s$ factor with respect to the singlet one, is not usually paid much attention but for its role in gluon regeization.

⁷⁶From now on when talking about the BFKL equation we will refer to the singlet one unless explicitly stated. Notice that we can rephrase (I.149) as an integro-differential equation describing the evolution of the BFKL amplitude $f(s, \mathbf{k}, \mathbf{k}') \equiv f(s, \mathbf{k}, \mathbf{k}', 0)$ in $\ln s$. Using $\frac{\partial f(s, \mathbf{k}, \mathbf{k}')}{\partial \ln(s/\mathbf{k}^2)} = \frac{1}{2\pi i} \int_{c-i\infty}^{c+i\infty} d\omega \left(\frac{s}{\mathbf{k}^2} \right)^\omega \omega f(\omega, \mathbf{k}, \mathbf{k}')$, we get from (I.149)

$$\frac{\partial f(s, \mathbf{k}, \mathbf{k}')}{\partial \ln(s/\mathbf{k}^2)} = \frac{N_c \alpha_s}{\pi^2} \int \frac{d^2 \boldsymbol{\kappa}}{(\mathbf{k} - \boldsymbol{\kappa})^2} \left[f(s, \boldsymbol{\kappa}, \mathbf{k}') - \frac{\mathbf{k}^2}{\mathbf{k}^2 + (\mathbf{k} - \boldsymbol{\kappa})^2} f(s, \boldsymbol{\kappa}, \mathbf{k}') \right]. \quad (\text{I.148})$$

$$\omega(n, \nu) = -\frac{2\alpha_s N_c}{\pi} \Re e \left[\psi \left(\frac{|n| + 1}{2} + i\nu \right) - \psi(1) \right] \equiv \bar{\alpha}_s \chi_0(|n|, \nu), \quad \bar{\alpha}_s \equiv \frac{\alpha_s N_c}{\pi}, \quad (\text{I.152})$$

where $\psi(1) = -\gamma_E$ is the Euler-Mascheroni constant. Now, (I.150) becomes

$$\begin{aligned} f(\omega, \mathbf{k}, \mathbf{k}') &= \frac{1}{2\pi^2 (\mathbf{k}^2 \mathbf{k}'^2)^{1/2}} \sum_{n=-\infty}^{\infty} e^{in(\vartheta-\vartheta')} \int_{-\infty}^{\infty} d\nu \frac{e^{i\nu \ln\left(\frac{\mathbf{k}^2}{\mathbf{k}'^2}\right)}}{\omega - \omega(n, \nu)}; \\ f(y, \mathbf{k}, \mathbf{k}') &= \frac{1}{2\pi^2 (\mathbf{k}^2 \mathbf{k}'^2)^{1/2}} \sum_{n=-\infty}^{\infty} e^{in(\vartheta-\vartheta')} \int_{-\infty}^{\infty} d\nu e^{\omega(n, \nu)y} e^{i\nu \ln\left(\frac{\mathbf{k}^2}{\mathbf{k}'^2}\right)}, \end{aligned} \quad (\text{I.153})$$

with $y = \ln(s/\mathbf{k}^2)$ being the rapidity. The asymptotic behavior as $s \rightarrow \infty$ is controlled by the rightmost singularity of $f(\omega, \mathbf{k}, \mathbf{k}')$ on the real ω axis. Since $\omega(n, \nu)$ decreases with n (FIG. I.28), we can retain only the $n = 0$ term in (I.153). Furthermore, we can take the saddle point approximation around $\nu = 0$

$$\omega(0, \nu) = \bar{\alpha}_s (4 \ln 2 - 14\zeta(3)\nu^2 + \dots) \equiv \lambda - \frac{1}{2} \lambda' \nu^2 + \dots; \quad \lambda = 4 \ln 2 \bar{\alpha}_s, \quad \lambda' = 28\zeta(3)\bar{\alpha}_s, \quad (\text{I.154})$$

and then perform the Gaussian integral over ν to get the pomeron solution of the leading $\ln s$ BFKL equation

$$f(s, \mathbf{k}, \mathbf{k}') = \frac{1}{\sqrt{2\pi^3 \lambda' \mathbf{k}^2 \mathbf{k}'^2}} \frac{1}{\sqrt{\ln(s/\mathbf{k}^2)}} \left(\frac{s}{\mathbf{k}^2} \right)^\lambda \exp \left[-\frac{\ln^2(\mathbf{k}^2/\mathbf{k}'^2)}{2\lambda' \ln(s/\mathbf{k}^2)} \right]. \quad (\text{I.155})$$

The quantity

$$\alpha_{\mathbb{P}}(0) = 1 + \lambda = 1 + \frac{N_c \alpha_s}{\pi} 4 \ln 2, \quad (\text{I.156})$$

is the intercept of the perturbative QCD (or BFKL) pomeron. Inserting the solution (I.155) into (I.147) gives, via the optical theorem, the total cross section for quark-quark scattering

$$\sigma_{\text{tot}}^{qq} = \frac{1}{s} \Im m A_1(s, t=0) = 4\alpha_s^2 \left(\frac{N_c^2 - 1}{4N_c^2} \right) \int d^2 \mathbf{k} \int d^2 \mathbf{k}' \frac{f(s, \mathbf{k}, \mathbf{k}')}{\mathbf{k}^2 \mathbf{k}'^2}. \quad (\text{I.157})$$

The integral over \mathbf{k} diverges in the IR when substituting (I.155) in (I.157). In physical situations a natural cutoff \mathbf{k}_{\min} is provided by confinement. Then, defining $\bar{y} = \ln \frac{s}{\mathbf{k}_{\min}^2}$,

$$\sigma_{\text{tot}}^{qq} = \frac{\pi(N_c^2 - 1)}{N_c^2} \frac{\alpha_s^2}{\mathbf{k}_{\min}^2} \frac{e^{\lambda \bar{y}}}{\sqrt{\pi \lambda' \bar{y}/8}} \sim \frac{s^\lambda}{\ln s}. \quad (\text{I.158})$$

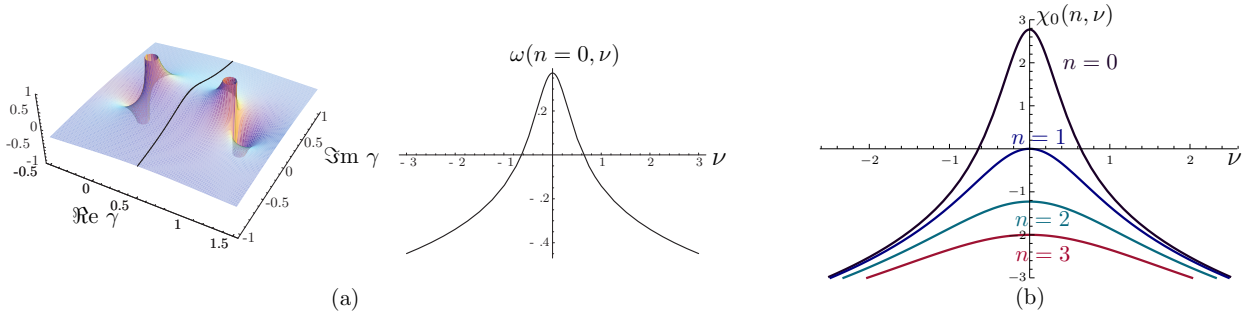


Figure I.28: (a) The leading order BFKL eigenvalue with $n = 0$ for $\alpha_s = 0.14$. (b) $\chi_0(n, \nu)$ decreases with n .

3.4 Going Beyond the Leading Approximation

There are a number of important limitations inherent to the BFKL leading log approximation (LL). LL BFKL predictions have restricted phenomenological applications because there are a longitudinal and transverse scale that are not fixed. The longitudinal one is the scale s_0 that scales s and determines the kinematic range of validity of BFKL through $\alpha_s \ln \frac{s}{s_0} \sim \mathcal{O}(1)$. The transverse one is the scale at which the coupling should be evaluated. The running of the coupling and the value of s_0 are not taken into account in LL BFKL because they give contributions that are formally subdominant.

Another problem is related to the lack of energy and longitudinal momentum conservation in the description of hadronic collisions. This is because the momentum fraction x of the incoming parton is reconstructed without the contribution to the total energy from the radiation of the BFKL ladder. Therefore, the analytic BFKL approach systematically underestimates the exact value of the x 's, and can thus grossly overestimate the parton luminosities⁷⁷. This problem, however, is not exclusive of the LL realm. Apart from computing the NLL corrections, which is extremely important, one often has to use some other criterion to select relevant contributions (see e.g. the discussion on collinear resummation below).

Looking back we find many places where we made approximations *only valid at the leading logarithmic level*: the strict multi-Regge kinematic regime, the strict eikonal approximation, the absence of fermion loops, the domination of ladders with reggeized gluons in their vertical lines, etc. We can then understand that the computation of NLL ($\alpha_s(\alpha_s \ln s)^n$) corrections to the BFKL singlet equation is a formidable program. In fact, ten years of hard

⁷⁷To see this in detail consider (B.31). The contribution in the r.h.s. coming from the radiation of n gluons cannot be accounted for, since the BFKL equation is solved by summing over any number of gluons radiated and integrating over the full allowed rapidity-ordered gluon phase space.

work by many authors were needed to complete the task since Fadin and Lipatov initiated the program computing the vertex for two gluon production [FL89] until all the pieces of the NLL BFKL kernel for $t = 0$ were put together and the corresponding eigenvalues computed by the same authors in 1998 [FL98] (see also [CC98]). A summary of the computations is given in [IFL10], where more recent developments on the field are also discussed.

With reggeization proved to hold at NLL order [FFKR06], the BFKL equation takes the same form as for LL order, the kernel having a similar structure:

$$\mathcal{K}(\mathbf{k}, \boldsymbol{\kappa}) = 2\omega(-\mathbf{k}^2)\delta^2(\mathbf{k} - \boldsymbol{\kappa}) + \mathcal{K}_{\text{real}}(\mathbf{k}, \boldsymbol{\kappa}). \quad (\text{I.159})$$

But now the reggeized gluon trajectory $\omega(-\mathbf{k}^2)$ needs to be computed in the two-loop approximation [FFK95, FFK96a, FFQ96, BRvN98, dDG01], and $\mathcal{K}_{\text{real}}$ gets contributions from gluon production at one-loop level [FL93, FFQ94, FFK96b, dDS99] and from two-gluon and $q\bar{q}$ production [FL89, CCH91, FL96, dD96b, dD96a, FKL97, FFFK98] (FIG. I.29). In the subleading approximation we have to include contributions where multi-Regge kinematics (MRK) is relaxed so that we lose one $\ln s$ factor. This is what we call quasi-multi-Regge kinematics (QMRK), where we allow two of the emitted gluons, or the components of an emitted quark-antiquark pair, to have similar rapidities. A generalized notion of QMRK will be needed for the use of the effective action (CH. III).

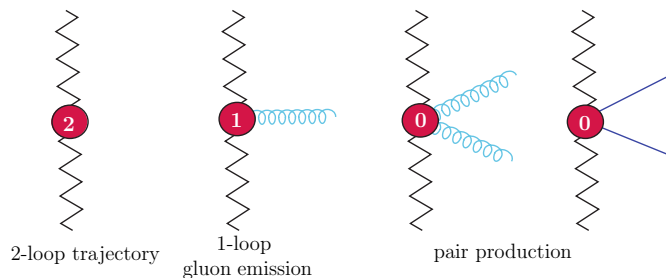


Figure I.29: Schematic representation of the corrections included at next-to-leading order. The number in the blob is the number of loops. Taken from [Cha06].

The action of the NLL kernel and its eigenvalues, are more conveniently expressed in bra-ket formalism [IP06, Sab06], defined by

$$\hat{q}|\mathbf{q}_i\rangle = \mathbf{q}_i|\mathbf{q}_i\rangle; \quad \langle \mathbf{q}_1|\hat{\mathbf{1}}|\mathbf{q}_2\rangle = \delta^{(2)}(\mathbf{q}_1 - \mathbf{q}_2); \quad \langle n', \nu'|n, \nu\rangle = \delta(\nu - \nu')\delta_{nn'}. \quad (\text{I.160})$$

The basis of LL eigenfunctions reads in this formalism $\langle \mathbf{q}|n, \nu\rangle = \frac{1}{\pi\sqrt{2}}(\mathbf{q}^2)^{i\nu-\frac{1}{2}}e^{in\vartheta}$. In the NLL case, these are no longer eigenfunctions of the kernel due to the running of the coupling

I. High Energy Scattering in QCD

(I.17), $\bar{\alpha}_s(\mathbf{q}^2) \simeq \bar{\alpha}_s(\mu^2) - \bar{\alpha}_s^2(\mu^2) \frac{\beta_0}{4N_c} \ln \frac{\mathbf{q}^2}{\mu^2}$, which breaks scale invariance (see also SEC. I.4.2)⁷⁸. The action of the NLL kernel —given in the $\overline{\text{MS}}$ scheme— on the basis $|n, \nu\rangle$ reads [KL00]

$$\begin{aligned} \langle n, \nu | \mathcal{K} | \nu', n' \rangle \equiv \omega(n, \nu) &= \bar{\alpha}_{s, \overline{\text{MS}}} \left[\chi_0 \left(|n'|, \frac{1}{2} + i\nu' \right) + \bar{\alpha}_{s, \overline{\text{MS}}} \chi_1 \left(|n'|, \frac{1}{2} + i\nu' \right) - \frac{\bar{\alpha}_{s, \overline{\text{MS}}} \beta_0}{8N_c} \right. \\ &\times \chi_0 \left(|n'|, \frac{1}{2} + i\nu' \right) \left. \left\{ -i\partial_{\nu'} + i\partial_{\nu} - 2 \ln \mu^2 \right\} + i \frac{\bar{\alpha}_{s, \overline{\text{MS}}} \beta_0}{8N_c} \partial_{\nu'} \chi_0 \left(|n'|, \frac{1}{2} + i\nu' \right) \right] \delta_{n, n'} \delta(\nu - \nu'), \end{aligned} \quad (\text{I.161})$$

where a symmetrized version in ν and ν' to express $\ln \mathbf{q}^2$ as a derivative with respect to either ν or ν' has been used [Sch07]. This is the natural choice when the two transverse scales \mathbf{q}_1^2 and \mathbf{q}_2^2 are similar, allowing us to discard the terms proportional to χ_0' in the NLL kernel for our analysis of SEC. II.2, without redefining the LL eigenfunctions⁷⁹ [FL98]. All the other functions in (I.161), with $\nu = i \left(\frac{1}{2} - \gamma \right)$, are

$$\begin{aligned} \chi_1(n, \gamma) &= \mathcal{S} \chi_0(n, \gamma) + \frac{3}{2} \zeta(3) - \frac{\beta_0}{8N_c} \chi_0^2(n, \gamma) + \Omega(n, \gamma) - \frac{\pi^2 \cos(\pi\gamma)}{4 \sin^2(\pi\gamma)(1-2\gamma)} \\ &\times \left\{ \left[3 + \left(1 + \frac{N_f}{N_c^3} \right) \frac{2 + 3\gamma(1-\gamma)}{(3-2\gamma)(1+2\gamma)} \right] \delta_{n0} \left(1 + \frac{N_f}{N_c^3} \right) \frac{\gamma(1-\gamma)}{2(3-2\gamma)(1+2\gamma)} \delta_{n2} \right\}; \end{aligned} \quad (\text{I.162})$$

$$\Omega(n, \gamma) \equiv \frac{1}{4} \left[\psi'' \left(\gamma + \frac{n}{2} \right) + \psi'' \left(1 - \gamma + \frac{n}{2} \right) - 2\phi(n, \gamma) - 2\phi(n, 1 - \gamma) \right]; \quad (\text{I.163})$$

$$\begin{aligned} \phi(n, \gamma) &= \sum_{k=0}^{\infty} \frac{(-1)^{k+1}}{k + \gamma + \frac{n}{2}} \left(\psi'(k + n + 1) - \psi'(k + 1) + (-1)^{k+1} (\beta'(k + n + 1) \right. \\ &\left. + \beta'(k + 1)) + \frac{\psi(k + 1) - \psi(k + n + 1)}{k + \gamma + \frac{n}{2}} \right); \quad 4\beta'(\gamma) = \psi' \left(\frac{1 + \gamma}{2} \right) - \psi' \left(\frac{\gamma}{2} \right). \end{aligned} \quad (\text{I.164})$$

In FIG. I.30 the $n = 0$ component of the LL and NLL kernels are compared, for a typical value of the coupling $\bar{\alpha}_s = 0.14$. The LL kernel has a single saddle point at $\gamma = \frac{1}{2}$. This property changes in the NLO case for $\bar{\alpha}_s$ above 0.05. If we examine the contour $\gamma = \frac{1}{2} + i\nu$ for real ν we find, instead of a maximum at $\nu = 0$, two maxima at $\nu \neq 0$ and a local minimum at $\nu = 0$. We have two saddle points off the real axis, at $\gamma = \frac{1}{2} + i\nu_0$ and $\gamma = \frac{1}{2} - i\nu_0^*$. These saddle points determine the high-energy behavior of the Green's function. From (I.153), considering only the $n = 0$ component, we can write

⁷⁸To see this, look at the action of the kernel on the LL eigenfunctions (I.161). The eigenvalues depend on \mathbf{q}^2 —and not only on n and ν — through factors $\sim \ln \frac{\mathbf{q}^2}{\mu^2}$ arising from the running of the coupling. So the LL eigenfunctions do no longer diagonalize the NLL kernel.

⁷⁹In general the kernel includes a piece not symmetric in $\gamma \rightarrow 1 - \gamma$. Though in our study we will be able to dispose of it because it cancels with the symmetric choice in ν, ν' when acting onto our impact factors, it can be avoided anyway by adding a factor $\sqrt{\frac{\bar{\alpha}_s(\mathbf{q}_1^2)}{\bar{\alpha}_s(\mathbf{q}_2^2)}}$ in the definition of the eigenfunctions. However, this redefined set is no longer orthonormal.

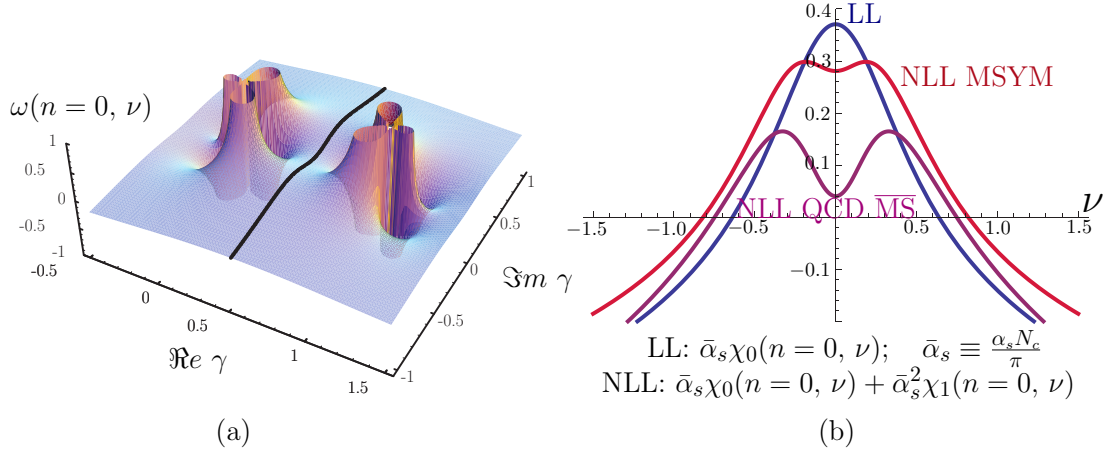


Figure I.30: (a) Structure in the complex γ plane of the $n = 0$ eigenvalue of the scale invariant part of the NLL kernel (for a scale $\mu = 30$ GeV), sometimes called itself the kernel by abuse of language; (b) Comparison of the LL and NLL kernels, for $\bar{\alpha}_s = 0.14$. We also show for comparison the NLL BFKL kernel of $\mathcal{N} = 4$ SYM (MSYM), which will be of importance in CH. II.

$$\pi |\mathbf{k}| |\mathbf{k}_0| f(y, \mathbf{k}, \mathbf{k}_0) = \int_{\mathcal{C}} \frac{d\gamma}{2\pi i} e^{y\omega(0, \nu)} \left(\frac{\mathbf{k}^2}{\mathbf{k}_0^2} \right)^{\gamma - \frac{1}{2}} \sim e^{y\omega(0, \frac{1}{2} + i\nu_0)} + e^{y\omega(0, \frac{1}{2} - i\nu_0^*)} \left(\frac{\mathbf{k}^2}{\mathbf{k}_0^2} \right)^{-i\nu_0^*}. \quad (\text{I.165})$$

where \mathcal{C} is the contour $\gamma = \frac{1}{2} + i\nu$, $\nu \in \mathbb{R}$. Since $\omega(0, \gamma) = \omega^*(0, \gamma^*)$ this gives

$$f(y, \mathbf{k}, \mathbf{k}_0) \sim \frac{e^{y\Re\omega(0, \frac{1}{2} + i\nu_0) - \Im m(\nu_0) \ln \frac{\mathbf{k}^2}{\mathbf{k}_0^2}}}{\pi |\mathbf{k}| |\mathbf{k}_0|} \cos \left\{ \Re(\nu_0) \ln \frac{\mathbf{k}^2}{\mathbf{k}_0^2} + y \Im m \left[\omega \left(0, \frac{1}{2} + i\nu_0 \right) \right] \right\}. \quad (\text{I.166})$$

We see that, though we can make $\omega(0, 1/2 + i\nu_0)$ real by getting rid of the term in the kernel not symmetric under $\gamma \leftrightarrow 1 - \gamma$, we run into problems when we have large collinear logarithms, i.e. $\mathbf{k}^2 \gg \mathbf{k}_0^2$. In this case the Green function presents an oscillatory behavior that is the source of many problems, to the point of leading to negative cross sections [Ros98].

An even more important problem with the NLL BFKL kernel concerns the size of the corrections. The size of corrections is estimated by the ratio $r(\gamma) = -\chi_1(0, \gamma)/\chi_0(0, \gamma)$. For $\gamma = \frac{1}{2}$, corresponding to the largest eigenvalue in LL, and hence to the pomeron intercept, one has [FL98]

$$r(1/2) \simeq 6.46 + 0.05 \frac{N_f}{N_c^3} + 2.66 \frac{N_f}{N_c^3} \implies \frac{\alpha_{\mathbb{P}}^{\text{NLL}}(0)}{\alpha_{\mathbb{P}}^{\text{LL}}(0)} = 1 - \bar{\alpha}_s r(1/2) \underset{N_f=0}{=} 0.0747. \quad (\text{I.167})$$

The value of the correction is very large, canceling the LL contribution practically. The prospects are not however that pessimistic and various proposals for the inclusion and resummation of higher-order terms with a view to stabilizing the perturbative series have

I. High Energy Scattering in QCD

been carried out through three basic strategies: 1) BLM resummation together with an appropriate scheme change (discussed in detail in SEC. II.2.3), a rapidity veto [Sch99, FRS99], and resummation of collinearly enhanced terms [Sal98, FRS01, CCSS03, AS03, AS04b].

Several studies showed that the origin of the bad behavior of the NLL kernel had its origin in the two-particle production in QMRK. Since we impose no restriction on the values of the transverse momenta for the emissions within the pair of particles close in rapidity, there can be final configurations where the transverse momenta of the pair of particles are strongly ordered. This leads to large logarithms of transverse momenta (collinear logarithms) that render the expansion in $\alpha_s \ln s$ unstable (remember the discussion after Eq. (I.166)). To account for these unphysical logarithms one can perform a complete DGLAP resummation of these large logarithms [CC99, CCS99].

The implementation of the program is based on the study of the pole structure of the kernels in the collinear (anticollinear) regions $\gamma = 0$ ($\gamma = 1$), that dominate the saddle point integration when two very different scales are present. From (I.152) and (I.162) we have

$$\begin{aligned} \chi_0(0, \gamma) &= \frac{1}{\gamma} + \{\gamma \rightarrow 1 - \gamma\} + \mathcal{O}(\gamma^0); & \chi_1(0, \gamma) &= -\frac{1}{2\gamma^3} + \frac{a}{\gamma^2} + \frac{b}{\gamma} + \{\gamma \rightarrow 1 - \gamma\} + \mathcal{O}(\gamma^0). \\ a &= \frac{5}{12} \frac{\beta_0}{N_c} - \frac{13}{36} \frac{N_f}{N_c^3} - \frac{55}{36}, & b &= -\frac{1}{8} \frac{\beta_0}{N_c} - \frac{N_f}{6N_c^3} - \frac{11}{12}. \end{aligned} \tag{I.168}$$

Now the BFKL equation should have the same collinear pole structure of the DGLAP equation for the case in which the ratio of transverse scales is large (or small, indeed the situation should be symmetric for the collinear and anticollinear regions [Sal99]). The Mellin transform of the DGLAP kernel $\frac{\alpha_s}{2\pi} \frac{xP_{gg}(x)}{Q^2} \Theta(Q^2 - \mathbf{k}^2) \underset{x \rightarrow 0}{\simeq} \frac{\bar{\alpha}_s}{Q^2} \Theta(Q^2 - \mathbf{k}^2)$ (analogous to the BFKL kernel $\bar{\alpha}_s \chi_0(0, \gamma)$), is $\frac{\bar{\alpha}_s}{\gamma} \left(+ \frac{\bar{\alpha}_s}{1-\gamma} \right)$. So the terms with collinear poles of higher order should be canceled from corrections of higher order in the $\ln s$ expansion. As said before, these contributions give by far the largest contribution to the NLL kernel. The origin of each piece is discussed in detail in [Sal99]. The $1/\gamma^2$ pole comes from running coupling and branching effects. The $1/\gamma^3$ pole, most interestingly, is related to the asymmetry in the two transverse scales. Indeed when passing from a symmetric choice of the scale $q_1 q_2 \equiv \sqrt{\mathbf{q}_1^2 \mathbf{q}_2^2}$ to a DIS-like situation with $Q^2 \equiv \mathbf{q}_1^2 \gg \mathbf{q}_2^2$, the NLL DGLAP contribution ($n = 2$ in (I.72)) changes by

$$\frac{1}{4} \left(\bar{\alpha}_s \ln \frac{s}{q_1 q_2} \ln \frac{\mathbf{q}_1^2}{\mathbf{q}_2^2} \right)^2 = \frac{1}{4} \left(\bar{\alpha}_s \ln \frac{1}{x} \ln \frac{\mathbf{q}_1^2}{\mathbf{q}_2^2} \right)^2 + \frac{1}{4} \bar{\alpha}_s^2 \ln \frac{1}{x} \ln^3 \frac{\mathbf{q}_1^2}{\mathbf{q}_2^2} + \text{NNLL}. \tag{I.169}$$

The Mellin transform of the \ln^3 term then gives a term proportional to $1/\gamma^3$. Instead of

decreasing that the terms not consistent with DGLAP in the NLL kernel should not be there (which would left uncanceled many collinear terms of presumable importance in higher orders) a hint on how to perform a full resummation canceling collinear logarithms to all orders comes from observing the effects of this change of scale to all orders. Using (I.147) and (I.153) we can write, for a symmetric choice of scale

$$\begin{aligned} f(s, \mathbf{q}_1, \mathbf{q}_2) &\sim \int \frac{d\omega}{2\pi i} \int \frac{d\gamma}{2\pi i} \left(\frac{s}{q_1 q_2}\right)^\omega \left(\frac{\mathbf{q}_1^2}{\mathbf{q}_2^2}\right)^{\gamma-1/2} \frac{1}{\omega - \bar{\alpha}_s \chi_0(\gamma)} \\ &= \int \frac{d\omega}{2\pi i} \int \frac{d\gamma}{2\pi i} \left(\frac{s}{\mathbf{q}_1^2}\right)^\omega \left(\frac{\mathbf{q}_1^2}{\mathbf{q}_2^2}\right)^{\gamma-\frac{1}{2}} \frac{1}{\omega - \bar{\alpha}_s \chi_0(\gamma - \omega/2)}, \end{aligned} \quad (\text{I.170})$$

where we have used for the second equality that $\left(\frac{s}{q_1 q_2}\right)^\omega \left(\frac{\mathbf{q}_1^2}{\mathbf{q}_2^2}\right)^\gamma = \left(\frac{s}{\mathbf{q}_1^2}\right)^\omega \left(\frac{\mathbf{q}_1^2}{\mathbf{q}_2^2}\right)^{\gamma+\omega/2}$. So the effect of the scale asymmetry is a shift in the position of the ω -pole. When exchanging \mathbf{q}_1^2 and \mathbf{q}_2^2 in (I.170) (anticollinear limit) the shift changes sign. In the collinear limit $\gamma \sim 0$, $\chi_0(\gamma) \sim \frac{1}{\gamma}$. Now the effect of the shift produced by the scale asymmetry is to introduce collinear poles of higher collinear order in the kernel⁸⁰

$$\omega \sim \frac{\bar{\alpha}_s}{\gamma - \omega/2} \rightarrow \omega \sim \frac{\bar{\alpha}_s}{\gamma} + \frac{\bar{\alpha}_s^2}{2\gamma^3} + \sum_{n=2}^{\infty} \frac{(2n)!}{2^n n! (n+1)!} \frac{\bar{\alpha}_s^{n+1}}{\gamma^{2n+1}}, \quad (\text{I.171})$$

that are not consistent with DGLAP RG evolution, because the powers of the collinear logarithms (taking the inverse Mellin transform) are higher than that of the coupling. To cancel these terms the obvious choice is to shift the collinear and anticollinear poles in the kernel in the other direction. So one should find the value of ω for which

$$\omega = \bar{\alpha}_s \left(2\psi(1) - \psi\left(\gamma + \frac{\omega}{2}\right) - \psi\left(1 - \gamma + \frac{\omega}{2}\right) \right). \quad (\text{I.172})$$

Salam [Sal99] was able to generalize the shift (I.172) to also include the running coupling and not-small- x branching effects to all orders [AGS96]

$$\begin{aligned} \omega &= \bar{\alpha}_s \left(1 + \left(a + \frac{\pi^2}{6} \right) \bar{\alpha}_s \right) \left(2\psi(1) - \psi\left(\gamma + \frac{\omega}{2} - b\bar{\alpha}_s\right) - \psi\left(1 - \gamma + \frac{\omega}{2} - b\bar{\alpha}_s\right) \right) \\ &+ \bar{\alpha}_s^2 \left(\chi_1(0, \gamma) + \left(\frac{1}{2} \chi_0(\gamma) - b \right) (\psi'(\gamma) + \psi'(1 - \gamma)) - \left(a + \frac{\pi^2}{6} \right) \chi_0(\gamma) \right), \end{aligned} \quad (\text{I.173})$$

⁸⁰When introducing firstly the approximation $\chi_0(\gamma - \omega/2) \simeq 1/(\gamma - \omega/2)$ the terms neglected are of higher order in α_s or γ than the powers appearing in (I.171). One could object that the solution ω of the iterative equation may not be small. However, the numerical value one obtains for ω goes to 0 as α_s and γ approach zero. To obtain the r.h.s. of (I.171) one finds $\alpha_s = \gamma \pm \sqrt{\gamma^2 - 2\bar{\alpha}_s} = \gamma(1 \pm \sqrt{1 - (2\bar{\alpha}_s/\gamma^2)})$ from the l.h.s. and uses the Taylor series $1 - \sqrt{1-x} = -\sum_{n=1}^{\infty} \frac{x^n (2n-3)!}{2^{2(n-1)} n! (n-2)!}$. For $\gamma > 0$ the result (I.171) is obtained.

I. High Energy Scattering in QCD

where a and b were defined in (I.168). A suitable implementation of the shifted kernel was found by Sabio Vera [Sab05], who showed that the shift (I.173) is equivalent to replace the term $-\frac{\bar{\alpha}_s^2}{4} \ln^2 \frac{q_1^2}{q_2^2}$ in the NLL kernel by

$$\left(\frac{q_1^2}{q_2^2}\right)^{-b\bar{\alpha}_s \frac{\|q_2\| - \|q_1\|}{|q_2| - |q_1|}} \sqrt{\frac{2(\bar{\alpha}_s + a\bar{\alpha}_s^2)}{\ln^2 \frac{q_1^2}{q_2^2}}} J_1 \left(\sqrt{2(\bar{\alpha}_s + a\bar{\alpha}_s^2)} \ln^2 \frac{q_1^2}{q_2^2} \right) - \bar{\alpha}_s - a\bar{\alpha}_s^2 + b\bar{\alpha}_s^2 \frac{\|q_2\| - \|q_1\|}{|q_2| - |q_1|} \ln \frac{q_1^2}{q_2^2}. \quad (\text{I.174})$$

The resummed kernel avoids the instabilities we previously encountered (FIG. I.31) and gives a reasonable value of the pomeron intercept.

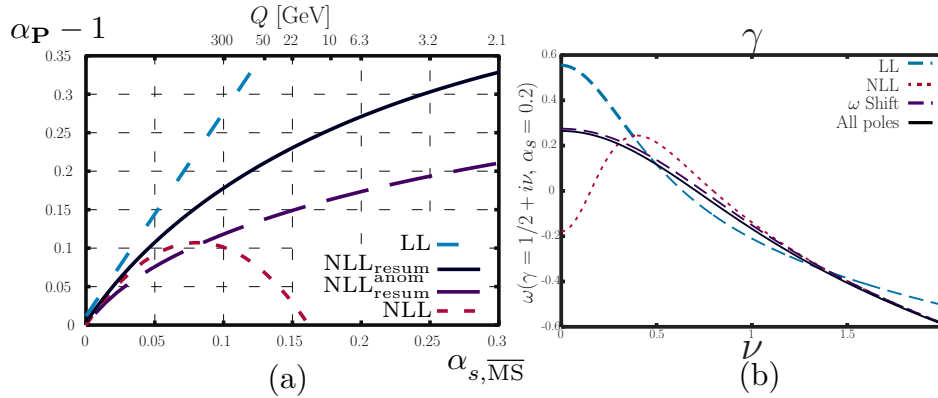


Figure I.31: (a) Value of the high energy exponent (pomeron intercept). The NLL resummed kernel gives results in agreement with data. $\text{NLL}_{\text{resum}}^{\text{anom}}$ indicates the high energy exponent that governs anomalous dimensions; (b) Suppression of the $\nu \neq 0$ saddle point causing oscillatory behavior in the resummed kernel. ‘All poles’ refers to the prescription (I.174), which reproduces very well the numerical results of the resummed kernel. Taken from [Sal99] (a) and [Sab05] (b).

3.5 Small- x Phenomenology and k_T Factorization

Before addressing in SEC. I.4 some properties of the BFKL pomeron solution, it is interesting to make a brief review of the phenomenological applications of BFKL physics. FIGS. I.32, I.33 and I.34 show some of the processes where BFKL signatures should arise more clearly.

So far we have worked at the partonic level, considering the interacting partons to be on shell. In order to compute the physical cross sections for these processes, involving hadrons in most cases in the initial or final states, we need some form of factorization. The kinematics here is quite different from that studied in SEC. I.2.1, and collinear factorization (I.60) does not apply.

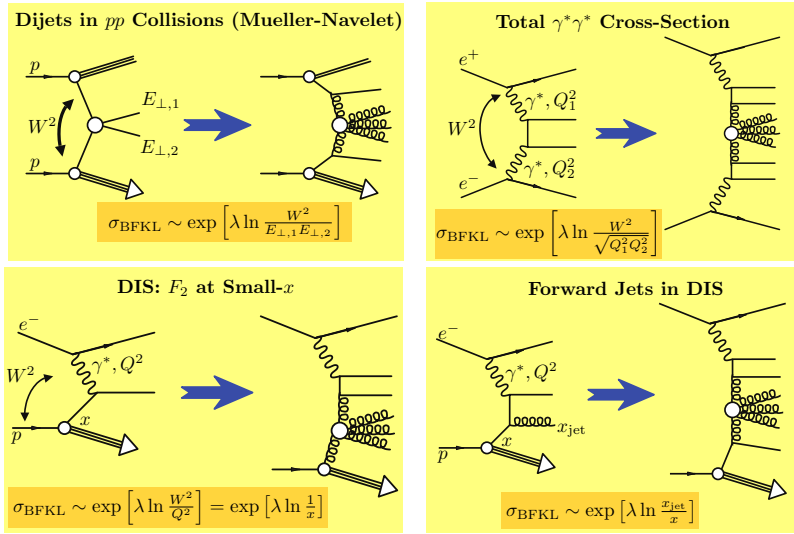


Figure I.32: Summary of some good observables to look for BFKL dynamics (from [Car01]).

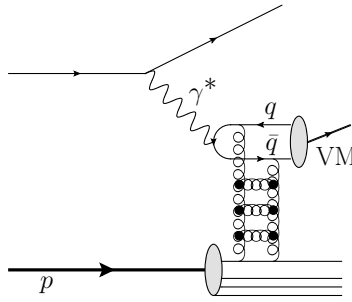


Figure I.33: Diffractive vector meson production.

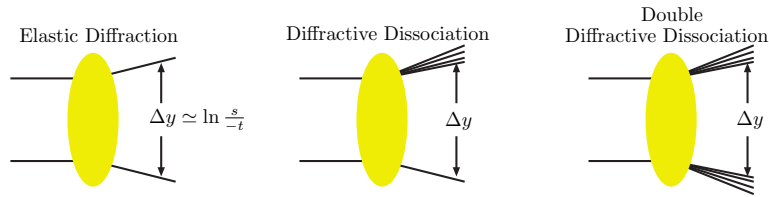


Figure I.34: Diffractive events are characterized by large rapidity gaps, associated to pomeron exchange.

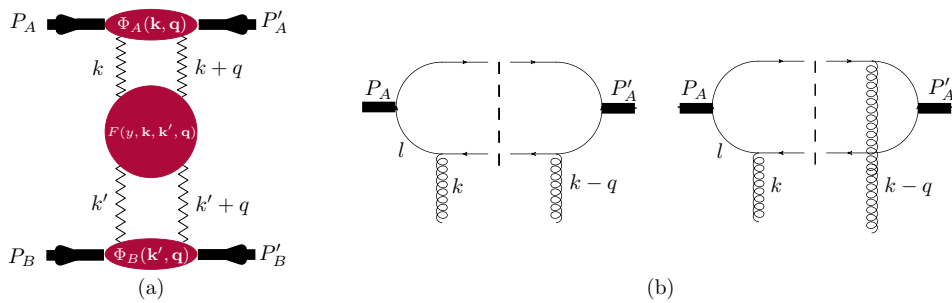


Figure I.35: (a) BFKL picture of hadron scattering; (b) Two of the four graphs used to compute the 1-loop photon impact factor.

I. High Energy Scattering in QCD

The amplitude for qq scattering via pomeron exchange, which we can get applying a dispersion relation to (I.147), reads

$$A_{\mathbf{1}}(s, t) = (8\pi^2\alpha_s)^2 \frac{N_c^2 - 1}{4N_c} \delta_{ij} \delta_{kl} i s \int \frac{d^2\mathbf{k}}{(2\pi)^2} \frac{d^2\mathbf{k}'}{(2\pi)^2} \frac{f(s, \mathbf{k}, \mathbf{k}', \mathbf{q})}{\mathbf{k}'^2 (\mathbf{k} - \mathbf{q})^2}. \quad (\text{I.175})$$

The amplitude for the elastic scattering of two hadrons A and B via pomeron exchange (FIG. I.35 (a)), in a generalization of (I.175), can be written as

$$A(s, t) = i s \mathcal{C} \int \frac{d^2\mathbf{k}}{(2\pi)^2} \int \frac{d^2\mathbf{k}'}{(2\pi)^2} \Phi_A(\mathbf{k}, \mathbf{q}) \Phi_B(\mathbf{k}', \mathbf{q}) \frac{F(y, \mathbf{k}, \mathbf{k}', \mathbf{q})}{\mathbf{k}'^2 (\mathbf{k} - \mathbf{q})^2}, \quad (\text{I.176})$$

where the impact factors Φ_i encode all intrinsically nonperturbative information from the initial and final states. The case of quark-quark scattering (I.175) is recovered for the color factor $\mathcal{C} = \frac{N_c^2 - 1}{4N_c}$ and the quark impact factor $\Phi_q = 8\pi^2\alpha_s$. Eq. (I.176), inspired in Regge factorization (I.92), is to be properly justified. Notice that the presence of two hard scales in the BFKL regime makes the transverse momenta of gluons not negligible as in collinear factorization. We are thus prompted to introduce the unintegrated gluon distribution⁸¹

$$\mathcal{F}(x, \mathbf{k}^2) = \frac{\partial[xg(x, \mathbf{k}^2)]}{\partial \ln \mathbf{k}^2}, \quad xg(x, Q^2) = \int^Q \frac{d\mathbf{k}^2}{\mathbf{k}^2} \mathcal{F}(x, \mathbf{k}^2). \quad (\text{I.178})$$

The new form of factorization that holds in the BFKL regime is the \mathbf{k}_\perp -factorization [CCH90, CCH91]. For the γ^*p cross section it reads

$$\sigma_\lambda^{\gamma^*p}(x, Q^2) = \int \frac{d\mathbf{k}^2}{\mathbf{k}^2} \mathcal{F}(x, \mathbf{k}^2) \int_x^1 \frac{dx'}{x'} \sigma_\lambda^{\gamma^*g}(x', \mathbf{k}^2, Q^2), \quad (\text{I.179})$$

where λ is the polarization of the virtual photon and $\sigma_\lambda^{\gamma^*g}$ the gluonic cross section. An intelligible proof of (I.179) is given in [BP02], Sec. 9.5.4. To make contact with the impact factor formalism we have from (I.176), using the optical theorem and reabsorbing the color factors in the definition of impact factors

$$\sigma_\lambda^{\gamma^*p}(x, Q^2) = \frac{1}{(2\pi)^4} \int \frac{d^2\mathbf{k}}{\mathbf{k}^2} \int \frac{d^2\mathbf{k}'}{\mathbf{k}'^2} \Phi_\lambda(\mathbf{k}^2, Q^2) \Phi_p(\mathbf{k}'^2) f(x, \mathbf{k}, \mathbf{k}'), \quad (\text{I.180})$$

⁸¹The BFKL equation (I.148) can be recast as an evolution equation for $\mathcal{F}(x, \mathbf{k}^2)$ (see [BP02], Sec. 9.6)

$$\frac{\partial \mathcal{F}(x, \gamma)}{\partial \ln(1/x)} = \mathcal{K}(\gamma) \mathcal{F}(x, \gamma), \quad \mathcal{F}(x, \gamma) = \int_1^\infty d\left(\frac{\mathbf{k}^2}{\mathbf{k}_0^2}\right) \left(\frac{\mathbf{k}^2}{\mathbf{k}_0^2}\right)^{-\gamma-1} \mathcal{F}(x, \mathbf{k}^2), \quad \mathcal{K}(\gamma) = \bar{\alpha}_s \chi_0(0, \gamma). \quad (\text{I.177})$$

Such an equation allows to relate rigorously predictions for amplitudes and cross sections and predictions for gluon densities. One finds in particular the famous result $\mathcal{F}(x, \mathbf{k}^2) \sim x^{-\lambda}$.

where Φ_λ is the photon impact factor and recall that $y = \ln(1/x)$. Defining the relation between the unintegrated gluon distribution and the BFKL amplitude by

$$\mathcal{F}(x, \mathbf{k}^2) = \frac{1}{(2\pi)^3} \int \frac{d^2\mathbf{k}'}{\mathbf{k}'^2} \Phi_p(\mathbf{k}'^2) \mathbf{k}^2 f(x, \mathbf{k}, \mathbf{k}'), \quad (\text{I.181})$$

leads to a definition of the photon impact factor

$$\sigma_\lambda^{\gamma^*p}(x, Q^2) = \frac{1}{2\pi} \int \frac{d^2\mathbf{k}}{\mathbf{k}^4} \mathcal{F}(x, \mathbf{k}^2) \Phi_\lambda(\mathbf{k}^2, Q^2); \quad \Phi_\lambda(\mathbf{k}^2, Q^2) = 2\mathbf{k}^2 \int_0^1 \frac{dx'}{x'} \sigma_\lambda^{\gamma^*g}(x', \mathbf{k}^2, Q^2). \quad (\text{I.182})$$

Of course we lack a fundamental knowledge of hadronic impact factors, that have to be modeled the same way we had to take an ansatz for the PDFs at some scale in the DGLAP evolution. The situation is much better when hadrons are replaced by virtual photons (FIG. I.35 (b)). Computation of the photon impact factor at LO is sketched in [FR97], Sec. 6.7. Since as we will see the total cross section of two photons with large and similar virtualities is the golden BFKL signature, lots of efforts have been directed to compute the NLO impact factor [BGK02, BCGK02, BK04], a task recently accomplished [BC11].

As advanced in SEC. I.2.2, it is difficult to have good probes of BFKL dynamics in the kinematic range explored up to now. Considerable effort was put at the HERA collider in this direction, in particular into the measurement of the F_2 proton structure function, shown in FIG. I.7 (see, e.g. [ZEU96]), for which a rise of the form $\sim x^{-\lambda}$ was expected for values of Q^2 ensuring the applicability of BFKL. Moreover, strong scaling violations (possibly reduced by the effects of the running of the coupling, as we remarked after Eq. (I.73)) should be observable from the dependence on \mathbf{k}^2 of $g(x, \mathbf{k}^2)$ as obtained from (I.177) [BP02]

$$g(x, \mathbf{k}^2) \sim (\mathbf{k}^2)^{1/2} \frac{x^{-(\alpha_P-1)}}{\sqrt{\ln(1/x)}} \exp\left(-\frac{\pi \ln^2(\mathbf{k}^2/\mathbf{k}_0^2)}{56\alpha_s N_c \zeta(3) \ln(1/x)}\right). \quad (\text{I.183})$$

Both qualitative features were indeed observed at HERA, but the data were shown to be also consistent with NLL DGLAP evolution [BF94, GRV95]. One can try with observables more directly sensitive to the gluon distribution than F_2 . For instance, the charm quark component of the structure function F_2^c is particularly sensitive because at leading order heavy quarks are only produced through gluon-boson fusion $\gamma^*g \rightarrow q\bar{q}$ [Wit76] (see also [DDT80, LRSvN93]). However, from the experimental point of view, the low efficiency in the tagging of charm mesons makes the measurement difficult [Lan96]. Something similar happens for the longitudinal structure function [CSDL91].

I. High Energy Scattering in QCD

Other properties of the hadronic final state have also been studied, such as transverse energy flows [GBKMS94, H1 95] or the distribution of jet multiplicities [KLM96]. In general one should expect from BFKL evolution larger multiplicities and transverse energy flow, because of the larger phase space available as we do not impose strong ordering in transverse momenta. However, the predictions of the parton-level calculation get smudged as we take into account the uncertainties in hadronization. As a general rule, the presence of a soft scale is bound to create problems.

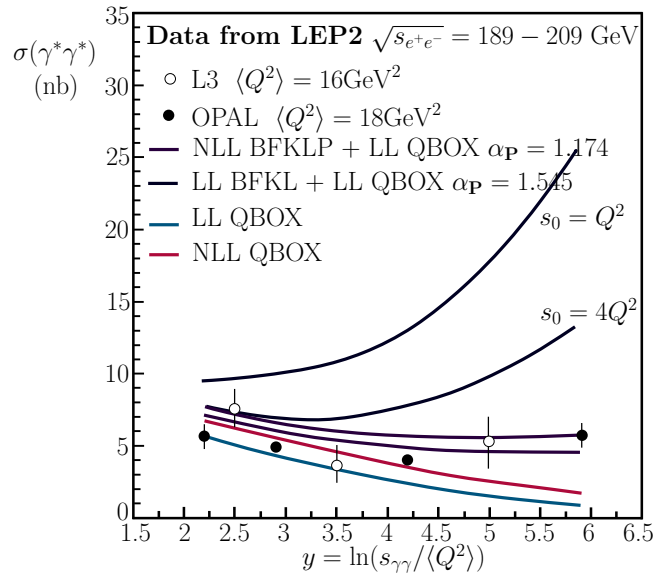


Figure I.36: The total $\gamma^*\gamma^*$ cross section as measured by the OPAL and L3 Collaborations at LEP, compared with BFKL and fixed order predictions. Adapted from [BFK⁺02].

The golden signature in which this kind of problems is absent (though one should take into account the intrinsic restrictions imposed by diffusion, see SEC. I.4.1) is the study of the $\gamma^*\gamma^*$ total cross-section for large values of Q^2 [BdRL96]. It can be measured at e^+e^- colliders by tagging both outgoing leptons close to the forward direction. The main practical limitation is that, because of the photon propagators, the event rate for the process falls off very rapidly with increasing photon virtualities, so that one cannot reach very large values of Q^2 . Such a measurement of $\sigma_{\text{tot}}^{\gamma^*\gamma^*}$ was performed by the L3 and OPAL Collaborations at LEP. The data are shown in FIG. I.36. While the LL BFKL prediction overestimates the cross section (as expected because of the higher value of the pomeron intercept), NLO fixed order predictions fail in the large rapidity region (also expected), while NLL BFKL with BLM scale setting (SEC. II.2.3) seems to improve the agreement with data [BFK⁺02]. The inclusion of the recently computed NLL impact factor [BC11] is to be done.

Perhaps a much better strategy is to consider less inclusive final states where DGLAP evolution is suppressed. A paradigmatic configuration is that of Mueller-Navelet jets, discussed in detail in SEC. II.3, in which the tagging of two jets is required to be well-separated in rapidity and with moderately large and similar transverse momenta, in such a way that the DGLAP evolution is suppressed and BFKL one is enhanced. Particularly convenient are diffractive events (FIGS. I.33 and I.34), characterized by a large rapidity gap where no emissions take place (see [BP02, Kep09, KL12] and references therein). It is not possible to review here all the advances in the field made in recent years. For up-to-date reviews, and prospects for the forward and diffractive physics program at the LHC, see [Sch09, dR12].

4 PROPERTIES OF THE BFKL EQUATION

In the last section we reviewed in detail the construction of the BFKL pomeron, which appeared as the solution to a Bethe-Salpeter-like equation describing the evolution in rapidity of a bound state of two reggeized gluons. Now we want to examine briefly some relevant aspects of this solution.

4.1 Unitarity and Diffusion Issues

We begin with two puzzling features of the BFKL equation: the violation of unitarity and the diffusion into the nonperturbative regime. Although we will consider here the leading log approximation, both two features persist at any order in the perturbative expansion.

Violation of the Froissart bound (I.97), and therefore, of unitarity, is apparent from the LL BFKL cross section (I.158). The pomeron intercept (I.156) is bigger than 1, in fact for a typical value of the coupling $\alpha_s \simeq 0.2$ it is quite large ($\alpha_P - 1 \simeq 0.5$). As shown in FIG. I.31, this value is lowered to approximately 0.3 using an all-orders collinear resummation, in agreement with the HERA data for the effective pomeron intercept $\lambda(Q^2)$ (FIG. I.37), defined by

$$\sigma(\gamma^* p) \sim F(Q^2)(W^2)^{\lambda(Q^2)} \implies f(Q^2)x^{-\lambda(Q^2)}. \quad (\text{I.184})$$

FIG. I.37 is actually very interesting. It shows that the effective intercept interpolates smoothly between the value for the NLL BFKL pomeron at big virtualities, and the Donnachie-Landshoff result (I.95), $\lambda \sim 0.1$, for the *soft* pomeron, which is nonperturbative in essence ($Q^2 < \Lambda_{\text{QCD}}$). The result points in the direction that only one pomeron exists,

I. High Energy Scattering in QCD

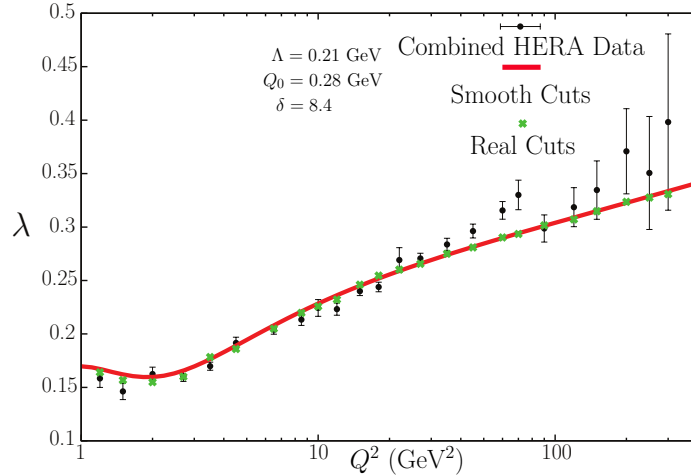


Figure I.37: Fit of the combined HERA data for the effective pomeron intercept [H1 10] using the collinear resummed BFKL kernel together with BLM renormalization prescription [HSS13].

with a smooth transition from hard to soft properties. The modification of the BFKL exponent at low Q^2 should be due to nonperturbative effects. An attempt to take them into account by modifying the gluon propagators according to properties of the QCD vacuum was undertaken by Landshoff and Nachtmann [LN87] (see also [DDLN02] for a wider exposition). Their analysis turns out to be equivalent to the insertion of an effective mass by hand in the gluon propagator [NZZ94]. The effect of this mass is indeed to decrease the pomeron intercept. However, a fully non-perturbative treatment implies much more than merely modifying the gluon propagators [KLRW10, KLR12]. A promising approach to address non-perturbative QCD and, in particular, the pomeron, is based on the AdS/CFT correspondence [PS02, BPST07].

The diffusion problem is also related to the appearance of non-perturbative phenomena. The solution (I.155) of the BFKL equation has the form of a Gaussian distribution in $\ln(\mathbf{k}^2/\mathbf{k}'^2)$, with a width growing with $y = \ln(s/\mathbf{k}^2)$ (FIG. I.38). This means that, as the energy increases, a wider range of transverse momenta is explored, and we finally enter the non-perturbative regime, invalidating the perturbative treatment. In fact, the BFKL equation (I.149) can be approximated (in the high energy limit) by a diffusion equation. To see this we write (I.149) as a recursion relation, where N is the iteration step. Using the equality $\left[\frac{1}{(k-q)^2} - \frac{1}{q^2+(k-q)^2}\right] = \frac{q^2}{(k-q)^2[q^2+(k-q)^2]}$ and neglecting the inhomogeneous δ -term, irrelevant for N high enough, we get

$$\omega f^{(N)}(\omega, \mathbf{k}_1) = \frac{N_c \alpha_s}{\pi^2} \int d^2 \mathbf{k}_2 \left\{ \frac{f^{(N-1)}(\omega, \mathbf{k}'_2) - (\mathbf{k}'_1/\mathbf{k}'_2) f^{(N-1)}(\omega, \mathbf{k}_1)}{(\mathbf{k}_1 - \mathbf{k}_2)^2} + \frac{\mathbf{k}_1^2 f^{(N-1)}(\omega, \mathbf{k}_1)}{\mathbf{k}_2^2 [\mathbf{k}_2^2 + (\mathbf{k}_1 - \mathbf{k}_2)^2]} \right\} \quad (\text{I.185})$$

We omitted the second argument in $f(\omega, \mathbf{k}_1, \mathbf{k}_2)$ since we will not consider the depen-

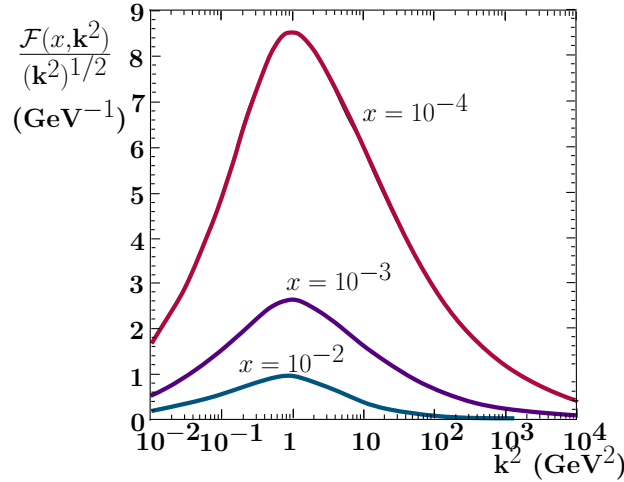


Figure I.38: BFKL evolution of $\mathcal{F}(x, \mathbf{k}^2)/(\mathbf{k}^2)^{1/2}$. The unintegrated gluon distribution $\mathcal{F}(x, \mathbf{k}^2)$ is defined in (I.178). An infrared cutoff \mathbf{k}_0^2 has been introduced by hand. Adapted from [AKMS94].

dence on it. From the form of the solution (I.153) we make the ansatz $f^{(N)}(\omega, \mathbf{k}_i^2) \sim (\mathbf{k}_i^2)^{-1/2} \psi_N(\xi_i)$, $\xi_i = \ln(\mathbf{k}_i^2/\mathbf{k}_0^2)$ for some reference scale \mathbf{k}_0^2 . In multi-Regge regime all transverse momenta are similar and we can approximate $\psi_{N-1}(\xi_2) \simeq \psi_{N-1}(\xi_1) + \frac{1}{2}(\xi_2 - \xi_1)^2 \frac{\partial^2 \psi_{N-1}(\xi_1)}{\partial \xi_1^2}$. Then (I.185) takes the form [dD95]

$$\begin{aligned} \omega \psi_N(\xi_1) = & \frac{N_c \alpha_s}{\pi} \int_0^\infty d\xi_2 \left\{ \left[\frac{e^{(\xi_2 - \xi_1)/2} - 1}{|1 - e^{\xi_2 - \xi_1}|} + \frac{1}{\sqrt{1 + 4e^{2(\xi_2 - \xi_1)}}} \right] \psi_{N-1}(\xi_1) \right. \\ & \left. + \frac{(\xi_2 - \xi_1)^2}{2} \frac{e^{(\xi_2 - \xi_1)/2}}{|1 - e^{\xi_2 - \xi_1}|} \frac{\partial^2 \psi_{N-1}(\xi_1)}{\partial \xi_1^2} \right\} = \lambda \psi_{N-1}(\xi_1) + \frac{\lambda'}{2} \frac{\partial^2 \psi_{N-1}(\xi_1)}{\partial \xi_1^2}, \end{aligned} \quad (\text{I.186})$$

with λ and λ' defined in (I.154). Taking now the continuum limit we find

$$\omega \frac{\partial \psi(N, \xi)}{\partial N} = (\lambda - \omega) \psi(N, \xi) + \frac{\lambda'}{2} \frac{\partial^2 \psi(N, \xi)}{\partial \xi^2}, \quad (\text{I.187})$$

and sitting in the minimum of the potential term $\lambda = \omega$ we find a diffusion equation with N playing the role of time. To get the physical meaning of N we match the solution of (I.187)

$$\psi(N, \xi) \sim \left(\frac{\lambda}{2\lambda'N} \right)^{\frac{1}{2}} \exp\left(-\frac{\lambda \xi^2}{2\lambda'N}\right) \quad \text{for an initial condition } \psi(0, \xi) = \frac{1}{(\pi\sigma^2)^{\frac{1}{4}}} \exp\left(-\frac{\xi^2}{2\sigma^2}\right) \quad (\text{I.188})$$

(note that we eventually neglected the initial width, $\lambda\sigma^2 \ll \lambda'N$) with (I.153) and find the correspondence $N/\lambda \leftrightarrow y = \ln(s/\mathbf{k}^2)$. So in the diffusive limit the BFKL equation can be recast in the form of a Schrödinger equation where, up to small redefinitions, angular momentum plays the role of energy and rapidity the role of time⁸².

⁸²It is interesting to reformulate the BFKL equation in Hamiltonian formalism. One can formally solve

The discussion of diffusion reminds us the importance of non-perturbative effects even if we study purely hard processes such as $\gamma^*\gamma^*$ collisions at very high Q^2 , for which no pomeron-hadron coupling has to be studied. In SEC. II.3, we will study in detail the diffusion pattern in QCD and $\mathcal{N} = 4$ SYM in the NLL approximation.

4.2 The Appearance of Conformal Invariance and Integrability

In 1986, Lipatov noticed [Lip86] that the LL BFKL equation (I.146) (for the general case $t \neq 0$) could be analytically solved using that it possesses a two-dimensional $SL(2, \mathbb{C})$ conformal symmetry, which is uncovered by taking the Fourier transform with respect to the transverse momenta, expressing the amplitude in impact parameter space

$$\delta(\mathbf{q}-\mathbf{q}')f(\omega, \mathbf{k}, \mathbf{k}', \mathbf{q}) = \int d^2\rho_1 d^2\rho_2 d^2\rho'_1 d^2\rho'_2 \exp\{i[\mathbf{k}\cdot\rho_1 + (\mathbf{q}-\mathbf{k})\cdot\rho_2 - \mathbf{k}'\cdot\rho'_1 - (\mathbf{q}'-\mathbf{k}')\cdot\rho'_2]\}. \quad (\text{I.192})$$

Then, introducing the holomorphic coordinates $\rho = \rho_x + i\rho_y$ (and their antiholomorphic complex conjugates $\bar{\rho} = \rho_x - i\rho_y$), and defining $\partial = \partial_\rho$ and $\bar{\partial} = \partial_{\bar{\rho}}$, the BFKL equation in impact parameter space reads schematically [Lip93a]

(I.149), with the kernel identified as the Hamiltonian, in the form

$$f(\omega) = \left[\omega - \frac{\alpha_s N_c}{\pi} \mathcal{H}_{\text{BFKL}} \right]^{-1} f^{(0)}(\omega). \quad (\text{I.189})$$

Here $f^{(0)}$ corresponds to the δ -factor accounting for the free exchange of two reggeized gluons. Now the singularities of the partial waves $f(\omega)$ are determined by the eigenvalues of the Hamiltonian

$$\mathcal{H}_{\text{BFKL}} \Psi_{n\nu} = E_{n\nu} \Psi_{n\nu}, \quad E_{n\nu} = -\frac{\pi\omega(n, \nu)}{\alpha_s N_c}. \quad (\text{I.190})$$

The high energy behavior of the scattering is dominated by the maximal eigenvalue, $(E_{n\nu})_{\text{max}} = E_{00}$, corresponding to the rightmost singularity of $f(\omega)$, for which $\omega = 1 + \omega_g$, with ω_g the trajectory. (I.190) has the interpretation of a 2d Schrödinger equation, $\Psi_{n\nu}$ being the pomeron wavefunction.

When rescaling the eigenfunctions by a factor $(\mathbf{k}^2)^{-1/2}$, $\tilde{\phi}_{n\nu}(\xi = \ln(\mathbf{k}^2/\mathbf{k}_0^2), \vartheta) = (\mathbf{k}^2)^{1/2} \phi_{n\nu}(\mathbf{k}^2, \vartheta)$, as we have made in the previous paragraph, the variables n and ν labelling the eigenvalues are dual to ϑ and $\xi = \ln(\mathbf{k}^2/\mathbf{k}_0^2)$ respectively (rescaling y it can be considered a rapidity). If considered as operators they can be represented as $n \rightarrow -i\frac{\partial}{\partial\vartheta}$ and $\nu \rightarrow -i\frac{\partial}{\partial\xi}$. This can be seen from the action of these operators on the eigenstates (I.151): $-i\partial_\vartheta \tilde{\phi}_{n\nu}(\xi, \vartheta) = n\tilde{\phi}_{n\nu}(\xi, \vartheta)$, $-i\partial_\xi \tilde{\phi}_{n\nu}(\xi, \vartheta) = \nu\tilde{\phi}_{n\nu}(\xi, \vartheta)$.

Now that we have operator representations of n and ν one can express the Hamiltonian (acting on the redefined eigenfunctions) by its eigenvalues with operator-valued arguments, according to (I.190). The eigenvalues, $E_{n\nu} = -\frac{\omega(n, \nu)}{\alpha_s}$, are approximated in the diffusion limit by (I.154), and we can write

$$\mathcal{H}_{\text{BFKL}}(\nu) = \mathcal{H}_{\text{BFKL}} \left(-i\frac{\partial}{\partial\xi} \right) \simeq -\frac{1}{\bar{\alpha}_s} \left(\lambda - \frac{1}{2}\lambda' \frac{\partial^2}{\partial\xi^2} \right). \quad (\text{I.191})$$

This is equivalent to the Schrödinger equation (I.187).

$$\omega f(\omega) = f(\omega)^{(0)} + \mathcal{H}_{\text{BFKL}} f(\omega), \quad \mathcal{H}_{\text{BFKL}} = \frac{\alpha_s N_c}{2\pi} (H + \bar{H}), \quad (\text{I.193})$$

where the holomorphic part of the Hamiltonian $\mathcal{H}_{\text{BFKL}}$ takes the form

$$H(\rho_1, \rho_2) = \ln[(\rho_1 - \rho_2)^2 \partial_1] + \ln[(\rho_1 - \rho_2)^2 \partial_2] - 2 \ln(\rho_1 - \rho_2) - 2\psi(1), \quad (\text{I.194})$$

with $\psi(z)$ the digamma function. The antiholomorphic part \bar{H} has the same functional form in terms of the coordinates $\bar{\rho}_1$ and $\bar{\rho}_2$. Written in the form (I.194) it is easy to check that $\mathcal{H}_{\text{BFKL}}$ is invariant under the $\text{SL}(2, \mathbb{C})$ group of Möbius transformations

$$\rho_i \rightarrow \frac{a\rho_i + b}{c\rho_i + d}, \quad a, b, c, d \in \mathbb{C} \quad ad - bc = 1. \quad (\text{I.195})$$

The generators of holomorphic $\text{SL}(2, \mathbb{C})$ transformations are

$$L_{k,-} = -\partial_{\rho_k}, \quad L_{k,0} = \rho_k \partial_{\rho_k}, \quad L_{k,+} = \rho_k^2 \partial_{\rho_k}, \quad k = 1, 2; \quad (\text{I.196})$$

with corresponding antiholomorphic generators. One can see that

$$[\mathcal{H}_{\text{BFKL}}, L_{1,a} + L_{2,a}] = [\mathcal{H}_{\text{BFKL}}, \bar{L}_{1,a} + \bar{L}_{2,a}] = 0; \quad a = +, -, 0. \quad (\text{I.197})$$

Therefore the BFKL Hamiltonian only depends on the two-particle Casimir operators of the $\text{SL}(2, \mathbb{C})$ group

$$H = H(L_{12}^2), \quad \bar{H} = \bar{H}(\bar{L}_{12}^2); \quad L_{12}^2 = -(\rho_1 - \rho_2)^2 \partial_1 \partial_2, \quad \bar{L}_{12}^2 = -(\bar{\rho}_1 - \bar{\rho}_2)^2 \partial_1 \partial_2, \quad (\text{I.198})$$

and the solutions of the BFKL equation have to be eigenstates of the Casimir operators

$$L_{12}^2 \Psi_{n,\nu} = h(h-1) \Psi_{n,\nu}, \quad \bar{L}_{12}^2 \Psi_{n,\nu} = \bar{h}(\bar{h}-1) \Psi_{n,\nu}; \quad \{h, \bar{h}\} = \frac{1 \pm n}{2} + i\nu. \quad (\text{I.199})$$

n and ν label the irreducible (principal series) representation of $\text{SL}(2, \mathbb{C})$ to which $\Psi_{n,\nu}$ belongs. The solutions to (I.198) are

$$\Psi_{n,\nu}(b_1, b_2) = \left(\frac{\rho_{12}}{\rho_{10}\rho_{20}} \right)^{(1+n)/2+i\nu} \left(\frac{\bar{\rho}_{12}}{\bar{\rho}_{10}\bar{\rho}_{20}} \right)^{(1-n)/2+i\nu}. \quad (\text{I.200})$$

They describe the pomeron wavefunction built from two reggeized gluons with coordinates $b_1 = (\rho_1, \bar{\rho}_1)$ and $b_2 = (\rho_2, \bar{\rho}_2)$. The integer n fixes the two-dimensional Lorentz spin of the state, while $\nu \in \mathbb{R}$ gives the scaling dimension $\ell = 1 + 2i\nu$. The coordinate $b_0 = (\rho_0, \bar{\rho}_0)$

I. High Energy Scattering in QCD

reflects the translational invariance of the system and can be understood as a center-of-mass coordinate. Finally, the BFKL eigenvalues turn out to coincide with those for the forward case (I.190).

Apart from conformal symmetry, another striking property of high energy QCD is integrability. Integrability is a very useful feature of selected physical models, that allows one to rely on certain algebraic properties to solve them exactly and to determine physical observables efficiently. Unfortunately, as a general rule, integrability is restricted to at most two-dimensional systems, like spin chains or σ -models [FS10]. Despite this severe restriction, integrability appears also in four-dimensional gauge theories. The crucial additional assumption which enables integrability here is the 't Hooft large- N_c or planar limit [tH73b], which effectively reduces the gauge group dynamics to two-dimensional surfaces on which the integrable structure lives.

Such an integrability in high-energy QCD was first discovered by considering the iteration of the BFKL Hamiltonian in the s -channel, describing multiple reggeon exchanges in the generalized leading logarithmic approximation [Bar80a, Bar80b, CDLO81] (FIG. I.39). In this approximation one includes all diagrams for which the number of reggeons exchanged in the t -channel is conserved, i.e., three-reggeon vertices are neglected. This turns out to be the minimal subset necessary to restore unitarity of the scattering amplitude in the direct (s - and t -) channels (though not in subchannels corresponding to different groups of particles in the final state). The amplitude $\mathcal{A}_N(s, t)$ corresponding to the exchange of N reggeized gluons satisfies the Bartels-Kwieciński-Praszałowicz equation [Bar80a, KP80, Jar80, Ewe03, BFLV13]. In the large N_c limit, the relevant Feynman diagrams have the topology of a cylinder [Lip94] and $\mathcal{H}_{\text{BKP}, N}$ reduces to the sum of terms corresponding to pairwise nearest-neighbor BFKL interactions

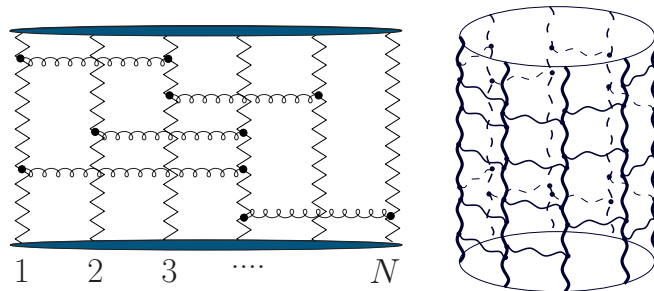


Figure I.39: Multiple reggeon exchange in the generalized leading log approximation. In the large N_c limit the relevant diagrams have a cylinder topology (to the right).

$$\mathcal{H}_{\text{BKP}, N} \xrightarrow{N_c \rightarrow \infty} \frac{1}{2} \sum_{r=1}^N H_{\text{BFKL}, r, r+1}; \quad \mathcal{H}_{N, N+1}^{\text{BFKL}} = \mathcal{H}_{N, 1}^{\text{BFKL}}. \quad (\text{I.201})$$

Lipatov [Lip93b, Lip94], and Faddeev and Korchemsky [FK95] showed that the Hamiltonian (I.201) is that of an integrable spin chain, that of the Heisenberg $\text{XXX}_{s=0}$ model. They were also able to map the problem of diagonalizing the XXX_0 chain into a diagonalization of the XXX_{-1} chain [Kor95], which admits a Bethe Ansatz [Bet31].

Another instance of integrability in large- N_c gauge theory is DIS where anomalous dimensions of local operators are responsible for scaling violations (SEC. I.2.1) in the OPE language. These anomalous dimensions are described by DGLAP evolution, but usually the corresponding Wilson operators, built from a number of quark and gluon fields together with covariant derivatives, are mixed under renormalization with other operators of the same spin and twist. Diagonalizing the mixing matrix for higher twist operators is a formidable problem already at one loop. Remarkably, the spectrum of anomalous dimensions can be found exactly in QCD in the sector of the so-called maximal-helicity Wilson operators, taking advantage of the fact that the one-loop mixing matrix can be mapped in the large- N_c limit into the Hamiltonian of the Heisenberg $\text{SL}(2, \mathbb{R})$ chain (see [Kor12, BKM03] and references therein).

There is indeed an interesting connection between the integrable structures appearing in the calculation of anomalous dimensions of gauge invariant twist-2 spin- M operators in $\mathcal{N} = 4$ SYM, and in MRK. As it was shown in [KLR⁺07], the link to the BFKL equation appears upon analytically continuing the anomalous dimension function to complex values of M . In particular, the pomeron corresponds to the first singularity at $M = \omega - 1$, for small ω .

5 UNITARITY CORRECTIONS AND NONLINEAR EVOLUTION

5.1 Saturation and Restoration of Unitarity

In the last section we saw how unitarity is violated by the BFKL equation. This is, as we will see, a consequence that it is a linear evolution equation. In order to see which is the mechanism behind the restoration of unitarity, let us have a look at FIG. I.14. The transverse size of the partons which can be resolved by a probe of

I. High Energy Scattering in QCD

virtuality Q^2 is proportional to $1/Q$, so that the area of partonic dots in FIG. I.14 falls as Q^2 rises. The figure also reflects that parton densities grow dramatically as x gets smaller.

But then, for particular combinations of parton size and density, the proton will eventually become ‘black’ to probes or, equivalently, the component gluons will become so dense that they cannot any longer be considered as free fields because their wavefunctions start to overlap (*shadowing*) and recombination effects must be taken into account. Naively, it can be assumed that the gluons inside the proton each occupy, on average, a transverse area of order πQ^{-2} , so that the total transverse area occupied by gluons is proportional to the number density multiplied by this area, i.e. $\pi Q^{-2} xg(x, Q^2)$ ⁸³. As x decreases this area becomes large, and we expect saturation to become important when

$$\frac{\alpha_s(\mu^2)}{\mu^2} xg(x, \mu^2) \gtrsim \pi R^2, \quad (\text{I.202})$$

where $R \sim 5 \text{ GeV}^{-1}$ is of the order of the proton radius. The additional factor of the coupling enters because the effective gluon-gluon cross section is $\sigma_{gg} \sim \alpha_s(\mu^2)/\mu^2$. The constraint (I.202) is essentially equivalent to demand that unitarity is not violated and the Froissart bound applies [Lev95].

Saturation corrections are indeed expected to end at some value of x with the steep rise of structure functions predicted by BFKL evolution. The main idea is that, in the same way that gluon splitting leads to a very high gluon density, recombination processes $gg \rightarrow g$, driven primarily by so-called *fan* diagrams (FIGURE I.40, (b)), must become important for large values of gluon densities. If the probability for the emission process in a cascade is of order $\alpha_s \rho$, where $\rho = \frac{xg(x, Q^2)}{\pi R^2}$ is shorthand for the parton density in the transverse plane, the probability for the recombination process will be, in first approximation, proportional to $\alpha_s \sigma_{gg} \rho^2$. The extra factor of α_s can be seen from the number of couplings taking part in the bifurcation in the fan diagram of FIG. I.40. The balance at which one arrives, including a non-linear recombination term, is called the Gribov-Levin-Ryskin (GLR) equation,

$$\frac{\partial^2 xg(x, Q^2)}{\partial \ln \frac{1}{x} \partial \ln Q^2} = \frac{\alpha_s N_c}{\pi} xg(x, Q^2) - \frac{\alpha_s^2 \gamma}{Q^2 R^2} (xg(x, Q^2))^2, \quad (\text{I.203})$$

after the authors that derived it by considering a full resummation of fan diagrams [GLR83]. The parameter γ was calculated order by order in perturbation theory by Mueller and Qiu

⁸³Recall that the gluon momentum distribution gives the number of gluons per unit of longitudinal phase space $dx/x = |d \ln(1/x)|$ with a transverse size greater than $1/\mu$, when probed at a scale $Q^2 = \mu^2$.

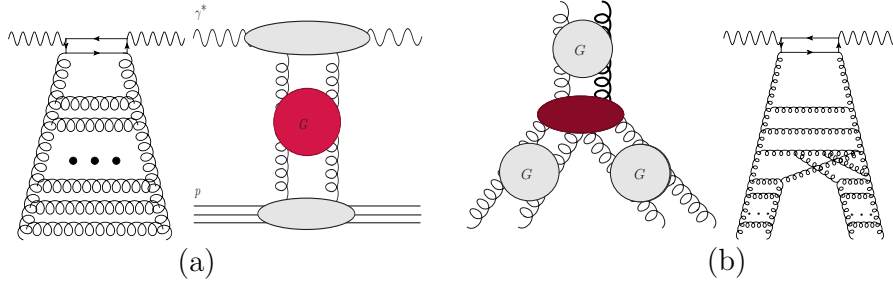


Figure I.40: Ladder diagrams characteristic of linear evolutions (a) and fan diagrams (b), giving rise to non-linear terms. We should keep in mind that evolution is usually depicted from below to above. The three-ladder vertex consists of a sum of several non-planar diagrams. An arbitrary number of branchings can take place in a fan diagram.

[MQ86] and it is equal to $\frac{81}{16}$ for $N_c = 3$. The GLR equation predicts saturation at the asymptotic value $xg(x, Q_s^2)_{\text{SAT}} = \frac{1}{27\pi\alpha_s} Q_s^2 R^2$ for which the second term exactly compensates the first one. However, in spite of this important prediction, the GLR equation only includes the first non-linear term. It considers no correlations between partons in the hadron, given by higher powers of ρ , and would be most important at even higher densities.

The appearance of a new dynamically-generated scale $Q_s \gg \Lambda_{\text{QCD}}$, the saturation momentum, ensures that saturation can be understood with perturbative methods. Balitsky and Kovchegov [Bal96, Kov99] showed systematically, from an effective Lagrangian and from Müller's dipole formulation⁸⁴ respectively, that in the large- N_c limit the important terms are fan diagrams⁸⁵ and obtained the correct kernel for the non-linear term. The BK evolution equation reads (in momentum space, so that we can see how it reduces to BFKL when discarding the nonlinear term)

$$\begin{aligned} \partial_y f(\mathbf{k}, \mathbf{q}) &= \frac{\bar{\alpha}_s}{\pi} \int \frac{d^2 \boldsymbol{\kappa}}{(\mathbf{k} - \boldsymbol{\kappa})^2} \left\{ f(\boldsymbol{\kappa}, \mathbf{q}) - \frac{1}{2} \left[\frac{\mathbf{k}^2}{\boldsymbol{\kappa}^2 + (\mathbf{k} - \boldsymbol{\kappa})^2} + \frac{(\mathbf{q} - \mathbf{k})^2}{(\mathbf{q} - \boldsymbol{\kappa})^2 + (\mathbf{k} - \boldsymbol{\kappa})^2} \right] f(\mathbf{k}, \mathbf{q}) \right. \\ &\quad \left. - \frac{\bar{\alpha}_s}{2\pi} \int d^2 \mathbf{k}' f(\mathbf{k}, \mathbf{k}') f(\mathbf{k}' - \boldsymbol{\kappa}, \mathbf{q} - \mathbf{k}) \right\}. \end{aligned} \quad (\text{I.204})$$

⁸⁴The color dipole approach to photon-hadron interactions [Mue94, MP94, NZZ94] can be seen to be equivalent to BFKL in momentum space and indeed it is maybe within this framework where a full derivation of the BFKL equation can be most simply obtained [KL12]. In this picture, low- x DIS is described in the proton rest frame. In this frame, when $x \rightarrow 0$, the virtual photon is *resolved* into a quark-antiquark pair (sometimes called *onium*) at very large distances upstream the target. Then, after quite a long time, the $q\bar{q}$ pair scatters off the proton. Since the interaction time is much shorter than the formation time of the pair, the transverse size of the $q\bar{q}$ dipole is approximately frozen during the scattering process. The emission of soft gluons by the initial $q\bar{q}$ pair gives rise to a cascade of secondary dipoles which build up the BFKL gluonic tower. One should notice that in this approach, however, the appearance of the important property of bootstrap is not clear.

⁸⁵In fact, the nonlinear term in the BK equation (I.204) can be obtained from the triple-pomeron vertex [BW95] in the large- N_c limit [Bra00].

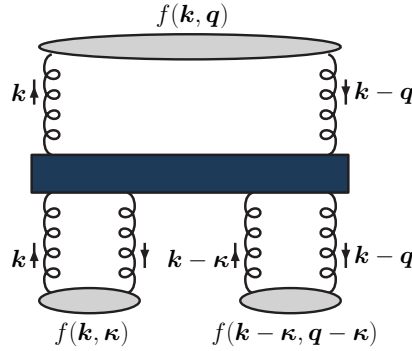


Figure I.41: Nonlinear contribution in the Balitsky-Kovchegov equation. Adapted from [KL12].

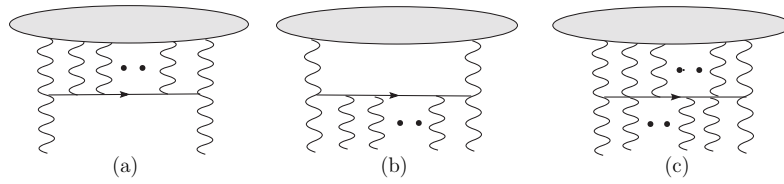


Figure I.42: (a) Recombination diagrams summed by the BK/JIMWLK equation. The upper blob represents the target; (b) Splitting diagrams; (c) Loop diagrams. Adapted from [HIM⁺06].

The BK equation is a central tool for understanding the initial conditions in hadronic collisions in situations where transverse gluon density approaches unitarity limits (see next section). Among its important properties is that it allows for traveling wave solutions [MP03, MP04] explicitly exhibiting geometric scaling [SGBK01], i.e. the property that in DIS collisions, $\sigma_{\gamma^*p}(x, Q^2) = 4\pi^2\alpha F_2(x, Q^2)/Q^2$ only depends on the two independent kinematic invariants Q^2 and W^2 through the specific combination $\tau = Q^2/Q_s^2(x)$, where $Q_s^2(x) \sim Q_0^2(x/x_0)^{-\lambda}$ [GBW99]. However, there are a number of contributions not considered in (I.204) that can be sizable, in particular running coupling [KL12] and pomeron loop contributions [Tri05] (FIG. I.42). In general, the scattering of two dilute systems remains still essentially an open problem.

5.2 High Parton Density QCD

The increase of the gluon distribution at small x leads to a major complication when applying QCD to compute processes in this regime. Perturbation theory is best suited for dilute systems, where a rather small number of diagrams contribute at each order. On the contrary, when parton densities increase, processes involving many parton become more and more important. The extreme situation arises when the gluon occupation is of order $1/\alpha_s$. Then, despite the coupling being weak, the problem becomes non-perturbative in the sense that there is an infinite number of graphs contributing at each order. Moreover, this

situation requires some knowledge of the two colliding projectiles, something which is not provided by the usual parton distributions (which only give the single-parton density).

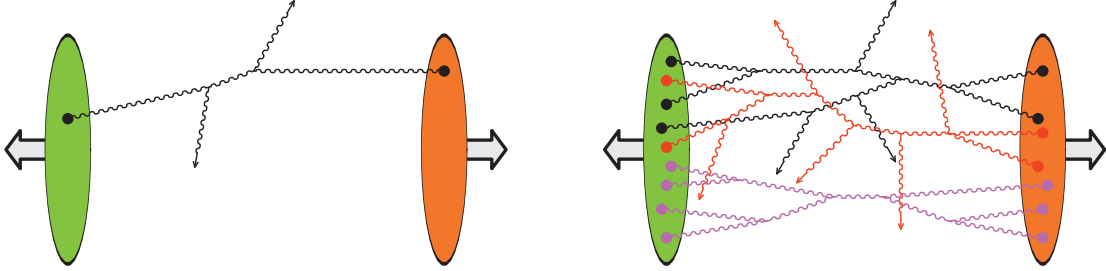


Figure I.43: Hadronic collisions in the dilute (left) and dense (right) regimes. From [Gel11].

A usual approach in this regime is the so-called color glass condensate (CGC) effective theory [ILM01b, ILM01a, FILM02] (for a review, see [Ian08, GIJMV10, KL12]). The main ideas of the CGC are two: 1) large occupation numbers or large charges give rise to classical fields (see, e.g. [Dun12], Sec. 8.2) —this is the origin of the term *condensate*; 2) there is a natural separation of scales in the problem (*glass*). To see this, recall from Eq. (I.43) that, for $x \ll 1$, the lifetime of a gluon is $\tau \sim 2xp/\mathbf{k}^2$. Hence, the smaller x , the shorter the lifetime. In an infinite momentum frame and considering light-cone gauge, for which the parton notion makes sense, gluons with $x' \ll x$ are *frozen* over the typical time scale for the dynamics τ at x ⁸⁶.

The idea now, first put forward by McLerran and Venugopalan [MV94], is the separation of the small- x degrees of freedom, treated as classical fields, from the fast color sources with $x' \gg x$ that give rise to these fields and are frozen (in some random configuration) during the collision. One can imagine the various field configurations at a given rapidity y as described by a wave functional $\Phi_y[A]$. Since the field does not change during the collision, the average over the field configurations will naturally involve the square of the wave function

$$\langle \cdots \rangle_y = \int \mathcal{D}A |\Phi_y[A]|^2 \langle A | \cdots | A \rangle. \quad (\text{I.205})$$

⁸⁶One can understand from this point of view the exponential increase of gluon density towards low x . In a gluon cascade with strongly ordered longitudinal momenta, all gluons below the final one (notice that we usually depict in figures the target, source of the cascade, in the bottom part) act as a frozen color charge distribution for the emission of the last gluon. Therefore the average color charge squared $\langle Q^a Q^a \rangle_\tau$, representing the source for the emission of a new gluon, is proportional to the number of preexisting gluons $N(\tau)$, which is of course the condition for an exponentially rising density.

I. High Energy Scattering in QCD

By taking the field A_μ as the solution of the classical Yang-Mills equations

$$[D_\mu, F^{\mu\nu}] = J^\nu, \quad (\text{I.206})$$

in the presence of a frozen color source, typically taken as $J^\mu(x^-, x_\perp) = \delta^{\mu+} \rho(x^-, x_\perp)$ for a hadron/nucleus moving at nearly the speed of light in the positive direction, the question of determining the distribution of field configurations $|\Phi_y[A]|^2$ is reduced to that of finding the distribution of color charges, denoted by $W_y[\rho]$.

In the final step, $W_y[\rho]$ is determined by a DGLAP-like renormalization group equation, the BK/JIMWLK equation [Bal96, Kov99, Kov00, JMKMW97a, JMKMW97b, JMKW98], which schematically reads

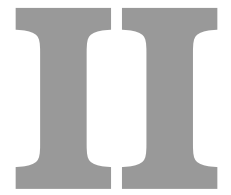
$$\partial_y W_y[\rho] = H_{\text{JIMWLK}} \left[\rho, \frac{\delta}{\delta \rho} \right] W_y[\rho]. \quad (\text{I.207})$$

For weak fields (or low density) H_{JIMWLK} reduces to the BFKL Hamiltonian. Moreover, the BK equation is recovered in this formalism in the large- N_c limit. However, it is not clear at all if this formalism can reproduce e.g. perturbative computations in the quasi-multi-Regge regime (Ch. III).

We should remark here that a thorough understanding of the physics of high parton density is key for the computation of the early-time dynamics in heavy ion collisions. A related problem is the rapid thermalization of the quark-gluon plasma (see e.g. [CSLM⁺11] and references therein). For a review of other open issues in high parton density physics see [KL12], Ch. 9.

Part II

QCD, $\mathcal{N} = 4$ SYM and the High-Energy Effective Action



Comparing QCD and $\mathcal{N} = 4$ SYM in the Regge Limit

1 $\mathcal{N} = 4$ SYM AS A TESTING GROUND FOR QCD

1.1 The Maximally Supersymmetric Yang-Mills Theory

We begin with a brief review of $\mathcal{N} = 4$ SYM¹ (or MSYM, Maximally Supersymmetric Yang-Mills) theory. It will necessarily consist of a sketchy set of statements that we will not analyze in depth and will not try to justify. A short course in supersymmetry with the material needed to introduce the present subject is given in [Ura07]. Good references to consult in more detail the formulation of supersymmetric Yang-Mills theories, including the superspace formalism, are [Soh85, FO01, Bin06, Sä09]. The exceptional properties of the theory are reviewed in [Kov98, Min11].

$\mathcal{N} = 4$ SYM in 4 dimensions was originally obtained by applying the method of di-

¹ \mathcal{N} denotes the number of Weyl spinor supercharges $Q_\alpha^I, \bar{Q}_{\dot{\alpha}I}$, with $I = 1, \dots, \mathcal{N}$. Since Weyl indices take two values, the number of supercharges for \mathcal{N} -extended supersymmetry is $4\mathcal{N}$.

II. Comparing QCD and $\mathcal{N} = 4$ SYM in the Regge Limit

mensional reduction à la Kaluza-Klein in a 6d torus to $\mathcal{N} = 1$ SYM in 10 dimensions [BSS77, GSO77]. The latter is the low energy effective theory coming from type I superstring theory and describes a $\mathcal{N} = 1$ vector multiplet in 10 dimensions consisting of one real vector and one Majorana-Weyl spinor. The trivial holonomy of the torus leads to a multiplet of fields in 4 dimensions inheriting an additional $SU(4) \sim SO(6)$ global symmetry².

The gauge multiplet of $\mathcal{N} = 4$ SYM consists of one vector field A_μ , four chiral spinors λ_I (and four antichiral ones $\bar{\lambda}^I$) and six real scalars X_M . The gauge multiplet transforms under the adjoint representation of the gauge group $SU(N_c)$. The Lagrangian of the theory reads³

$$\begin{aligned} \mathcal{L}_{\text{SYM}}^{\mathcal{N}=4} = \text{Tr} \left\{ -\frac{1}{4} F_{\mu\nu} F^{\mu\nu} + \frac{1}{2} D_\mu X_M D^\mu X_M + i \lambda_I \sigma^\mu D_\mu \bar{\lambda}^I - i g \lambda_I [\lambda_J, X^{IJ}] - i g \bar{\lambda}^I [\bar{\lambda}^J, X_{IJ}] \right. \\ \left. + \frac{1}{4} g^2 [X_M, X_N] [X_M, X_N] \right\}; \quad D_\mu \Phi = \partial_\mu \Phi - i g [A_\mu, \Phi] \quad (\Phi = X, \lambda). \end{aligned} \quad (\text{II.1})$$

$F_{\mu\nu}$ is defined in (I.2). In (II.1) we have omitted the Weyl indices $\alpha, \dot{\alpha}$ that label the two different $SU(2)$ components in which the Lorentz group is split, so that $\lambda \sigma^\mu \bar{\lambda}$ stands for $\lambda^\alpha \sigma_{\alpha\dot{\alpha}}^\mu \bar{\lambda}^{\dot{\alpha}}$. We have also introduced the notation $A_\mu = A_\mu^a T^a$. Indices I, J transform in a certain representation of the R -symmetry group $SU(4)_R$. X_M and X_{IJ} are related by the $SU(4)_R \sim SO(6)_R$ Σ symbols⁴

$$X_{IJ} = -\frac{1}{2} (\Sigma_M)_{IJ} X_M, \quad X^{IJ} = \frac{1}{2} (\Sigma_M^{-1})^{IJ} X_M; \quad \text{Tr}(\Sigma_M \Sigma_N^{-1}) = 4 \delta_{MN}, \quad X_M X_M = X_{IJ} X^{IJ}. \quad (\text{II.2})$$

Then we get

$$\begin{aligned} \mathcal{L}_{\text{SYM}}^{\mathcal{N}=4} = -\frac{1}{4} (\partial_\mu A_\nu^a - \partial_\nu A_\mu^a)^2 + \frac{1}{2} \partial_\mu X_M^a \partial^\mu X_M^a + i \bar{\lambda}_I^a \sigma^\mu \partial_\mu \bar{\lambda}^{Ia} - g f_{abc} \partial_\mu A_\nu^a A^{\mu b} A^{\nu c} \\ - \frac{1}{4} g^2 f_{abc} f_{cde} A_\mu^a A_\nu^b A^{\mu c} A^{\nu d} + g f_{abc} A^{\mu a} X_M^b \partial_\mu X_M^c + \frac{1}{2} g^2 f_{abc} f_{cde} A_\mu^a X_M^b A^{\mu c} X_M^d \\ - i g f_{abc} A_\mu^a \lambda_I^b \sigma^\mu \bar{\lambda}^{cI} - \frac{1}{4} g^2 f_{abc} f_{cde} X_M^a X_N^b X_M^c X_N^d + g f_{abc} X^{aIJ} \lambda_I^b \lambda_J^c + g f_{abc} X_{IJ}^a \bar{\lambda}^{bI} \bar{\lambda}^{cJ}. \end{aligned} \quad (\text{II.3})$$

²In general, in the dimensional reduction on a Riemannian manifold of dimension n the spin connection is a $SO(n)$ gauge field and consequently the spinors transform, upon parallel transport around a closed contractible curve, under a subgroup of $SO(n)$, which is the holonomy group. In the case at hand of \mathbb{T}^6 every spinor is covariantly constant, so that the whole $SO(6) \sim SU(4)$ becomes a global symmetry of the model. From the point of view of the $\mathcal{N} = 4$ theory this $SU(4)$ global symmetry is identified with the R -symmetry group of the $\mathcal{N} = 4$ supersymmetry algebra. This R -symmetry ($SU(\mathcal{N})$ for \mathcal{N} -extended SUSY) is a generalization of the $U(1)$ global symmetry of $\mathcal{N} = 1$ SUSY which does not commute with supersymmetry: $[Q_\alpha, R] = Q_\alpha$; $[\bar{Q}_{\dot{\alpha}}, R] = -\bar{Q}_{\dot{\alpha}}$.

³The Lagrangian can be also expressed in terms of $\mathcal{N} = 1$ superfields. This formulation is manifestly supersymmetric invariant. However, we are more interested in making contact with QCD.

⁴The scalars X_{IJ} transform in the $\mathbf{6}$ of $SU(4)$, while λ_I and $\bar{\lambda}^I$ transform in the $\mathbf{4}$ and $\bar{\mathbf{4}}$, and A in the singlet $\mathbf{1}$. $(\Sigma_M)_{IJ}$ are Clebsch-Gordan that couple two $\mathbf{4}$ s to a $\mathbf{6}$, being 6d generalizations of the 4d $\sigma_{\alpha\dot{\alpha}}^\mu$.

Since all the fields transform in the adjoint, color indices a, \dots, d go from 1 to $N_c^2 - 1$. Remember that the normalization of the generators in the adjoint is $\text{Tr}(T^a T^b) = N_c \delta^{ab}$. One can recognize in the Lagrangian (II.3) terms which are very similar to those of the QCD Lagrangian (I.16). Indeed the gluonic sector of both theories is identical. Note that the coupling appearing in each of the vertices is the same g^5 , which is a strong constraint coming from the requirement of supersymmetry.

1.2 $\mathcal{N} = 4$ SYM as the Harmonic Oscillator of Quantum Field Theory

$\mathcal{N} = 4$ SYM is an outstanding theory. It has the maximum possible amount of supersymmetry for a 4d gauge theory without gravity, i.e. including fields with spin equal or lower than 1: 16 real supercharges. Though its Lagrangian may seem at first sight quite complicated, we have reasons to consider it the simplest non-trivial quantum field theory [AHCK10]. It has been christened as *the harmonic oscillator of 21st century*, the same way that black holes are said to be the hydrogen atom of quantum gravity [Mal96].

Historically the interest in $\mathcal{N} = 4$ SYM arose from the vanishing of its β -function. For any $SU(N)$ gauge theory, the one-loop coefficient of the β -function (of which (I.14) is a particular case) is given by

$$\beta_0 = \frac{11}{3}N - \frac{1}{6} \sum_i C_i - \frac{1}{3} \sum_j \tilde{C}_j, \quad (\text{II.4})$$

where the first sum is over all real scalars with quadratic Casimir C_i and the second over all Weyl fermions with quadratic Casimir \tilde{C}_j . All fields in MSYM are in the adjoint, hence all Casimirs are N . Now we see that the theory has the exact matter content, six real scalars and eight Weyl fermions, to cancel β_0 . The non-renormalization of the coupling (and hence the finiteness of the theory) was then subsequently proven to two [Jon77, PP77] and three loops [VT80, GRS80] by direct computation. Eventually several proofs confirming the fact that $\beta(g) = 0$ to all orders in perturbation theory⁶ emerged, based on the computation of the axial anomaly, related to breaking of conformal invariance [SW81], or using the light-cone gauge [Man83, BLN83]. $\mathcal{N} = 4$ SYM is then UV-finite, and the conformal invariance of the Lagrangian at the classical level (deduced from the absence of any dimensionful parameter in it) is preserved at the quantum level.

⁵The $\mathcal{N} = 4$ SYM coupling is usually denoted g_{YM} in order not to mix up with the QCD coupling g . We will only use this notation when confusion could arise.

⁶There are also strong arguments to think that the superconformal symmetry of the theory is also preserved non-perturbatively.

II. Comparing QCD and $\mathcal{N} = 4$ SYM in the Regge Limit

The conformal symmetry, the supersymmetry and the R -symmetry of the $\mathcal{N} = 4$ SYM Lagrangian are in fact part of a larger symmetry group $\text{PSU}(2,2|4)$, called the $\mathcal{N} = 4$ superconformal group. This symmetry group is unbroken by quantum corrections and imposes strong constraints on the theory, in particular the form of the amplitudes. The last years have witnessed important developments that exhibit the amazing properties of scattering amplitudes in $\mathcal{N} = 4$ SYM⁷, starting from the strikingly compact Parke-Taylor formula [PT86, BG88] for MHV⁸ (n -gluon) amplitudes using the spinor helicity formalism. Recursion relations such as the BCFW [BCFW05] and CSW [CSW04] ones, inspired by Witten's ground-breaking connection with twistor theory [Wit04], were found that related tree-level amplitudes to amplitudes with fewer external legs, allowing to go beyond MHV amplitudes. With the help of a formalism that incorporates the constraints of supersymmetry [Nai88], all tree-level amplitudes in $\mathcal{N} = 4$ SYM could be eventually constructed [DH09]. To go beyond tree-level, unitarity methods have been employed (see, e.g. [BDDK94, DHKS08]). Again MHV amplitudes are simpler to deal with, being proportional to the tree-level amplitude, $A_n^{\text{MHV}} = A_n^{\text{MHV, tree}} M_n$. Moreover, the finite part of the loop correction M_n satisfies the BDS ansatz [BDS05]

$$F_n = \frac{1}{4} \gamma_K(g^2) F_n^{(1)}; \quad F_n \equiv \ln M_{n, \text{finite}} \quad (\text{II.5})$$

up to a remainder term [BLS09, GSVV10]. $F_n^{(1)}$ in (II.5) is a kinematic factor that can be obtained through a 1-loop computation and $\gamma_K(g^2)$ is the cusp anomalous dimension, given to all loops by an integral equation based on integrability [BES07]. Behind the BDS form of n -point amplitudes there is the constraint of a hidden dual conformal symmetry, that in addition to the original superconformal symmetry generates a so-called Yangian algebra [DHP09]⁹. This is an infinite dimensional symmetry algebra characteristic of integrable systems.

It is expected indeed that $\mathcal{N} = 4$ SYM in the planar limit¹⁰ becomes the first example of an

⁷Good reviews on (part of) the subject are [MP91, Dix96, AR08, Hen09a]. Further references can be found there. For more informal introductions to the subject see, for instance, [Zee10] and [Gun10].

⁸MHV (Maximally Helicity Violating) amplitudes are amplitudes with n external gluons, where two of them have an helicity opposite to the rest. At tree level they violate helicity conservation to the maximum extent possible. Tree amplitudes where all (or all but one) gluons have the same helicity vanish.

⁹This is a rapidly evolving field. An example of late development in this direction is a dual formulation of the S -matrix in which all-tree level amplitudes and the leading singularities of the amplitudes to all orders are determined from a surprisingly compact Grassmannian integral, whose integrand is essentially fixed by Yangian symmetry [AHCC10, AHCC10, AHBC⁺11].

¹⁰The planar or 't Hooft limit [tH73b] is the limit $N \rightarrow \infty$ (for a $\text{SU}(N)$ gauge theory) with the 't Hooft coupling $\lambda \equiv g^2 N$ fixed. Usually gauge theories are simplified in this limit. To first order in the $1/N$ expansion only planar diagrams (with the topology of a sphere) contribute, hence the name. Indeed, this expansion is a genus expansion like the one in string theory, the first order corresponding to the weak coupling limit.

integrable non-trivial quantum field theory in 4d [B⁺12]. This is surely related to the key role of this theory in the AdS/CFT correspondence [Mal98, GKP98, Wit98, AGM⁺00]¹¹. Maldacena’s conjecture states that there is a *dictionary* that maps string theory defined on a d -dimensional space —product of Anti-de Sitter (AdS) space and a closed manifold like a sphere, an orbifold or a noncommutative space—, and a QFT in $d - 1$ dimensions without gravity defined on the conformal boundary of this space. If the dimension d is 4, the conformal field theory (CFT) is $\mathcal{N} = 4$ SYM with $SU(N_c)$ gauge group and Yang-Mills coupling g_{YM} , and the dual string theory is type IIB string theory with string coupling g_s defined on an $\text{AdS}_5 \times S^5$ background. The metric of this space is

$$ds^2 = \frac{R^2}{z_0^2}(dz_0^2 + d\mathbf{x}^2) + R^2 d\Omega_5^2, \quad z_0 > 0, \quad \mathbf{x} = (x_1, \dots, x_4). \quad (\text{II.6})$$

The AdS/CFT conjecture says that the two theories are dual when

$$g_s = g_{\text{YM}}^2 \quad \text{and} \quad R^4 = l_s^4 g_s N_c = \alpha'^2 g_s N_c \quad \implies \quad \frac{\alpha'}{R^2} = \frac{1}{\lambda}. \quad (\text{II.7})$$

As many dualities, AdS/CFT maps the weak coupling regime of gauge theory to the strong coupling (tensionless, $\alpha'/R^2 \rightarrow \infty$) regime in string theory and vice versa¹². String theory on a general curved background is hardly tractable (it is not even known how to rigorously quantize it), but lots of tests of the AdS/CFT conjecture have been performed up to now in certain limits where the theory is much simpler. The first one is the aforementioned planar limit. The 't Hooft coupling $\lambda = g_{\text{YM}}^2 N_c$ is the relevant perturbative parameter in the planar limit, and if $\lambda \ll 1$, a perturbative treatment of $\mathcal{N} = 4$ SYM is possible, and we can compute with Feynman diagrams. The planar limit leads on the other hand to a weakly coupled string theory since $g_s = \lambda/N_c$. The type IIB string theory reduces to classical string theory on $\text{AdS}_5 \times S^5$ and string loops can be neglected.

An even weaker version of the correspondence is reached by taking a second limit, where the radius of AdS space goes to infinity $R/l_s \rightarrow \infty$, $l_s = \sqrt{\alpha'}$ ¹³, after having taken the planar limit. This is the strong coupling limit on the $\mathcal{N} = 4$ SYM side ($\lambda = (R/l_s)^4 \gg 1$), but the curvature of the string background is small and the massive string excitations decouple

¹¹For a very good introduction for pedestrians, see [Nas07].

¹²It is noteworthy that two different perturbative expansions occur in string theory. First there is the loop expansion in the string coupling constant g_s , which corresponds to the genus expansion summing over worldsheet topologies. Second, for any given worldsheet topology, the computation of the path integral over the (interacting) 2d field theory is done as a loop expansion in the 2d world, the α' expansion.

¹³We omit a conventional 2π factor in the definition of α' . l_s is the so-called string length.

II. Comparing QCD and $\mathcal{N} = 4$ SYM in the Regge Limit

from the low energy ones (we can make an α' expansion). The classical string theory can then be approximated by classical type IIB supergravity in 10d.

The correspondence is equipped with a full matching of symmetries, fields, operators and correlation functions in the two theories. The fact that it provides a connection between the weak and strong coupling regimes makes of AdS/CFT a unique tool to explore many systems, for instance the quark-gluon plasma, superconductivity or the structure of scattering amplitudes at strong coupling. Some recent review material on some of these subjects is given in [Pap11, CSLM⁺11, Har10, Ald08].

1.3 Connections Between QCD and $\mathcal{N} = 4$ SYM and the Role of Conformal Invariance

We end this review of properties of MSYM by studying its connection with QCD. $\mathcal{N} = 4$ SYM is not a realistic theory. That our world and the physical laws ruling its dynamics are not scale invariant was already pointed out by Galileo [Fey85]. In particular, $\mathcal{N} = 4$ SYM cannot exhibit phenomena like confinement. Supersymmetry, if having to do something with particle physics, must be a broken symmetry. Despite these important differences, $\mathcal{N} = 4$ SYM is very similar to QCD in some respects. Both theories are equivalent (considering QCD reduced to pure gluodynamics) at tree-level. Moreover, as we have seen, only gluons do play a role in the construction of the LL BFKL ladder, and hence $\mathcal{N} = 4$ SYM and QCD are also equivalent in the $\ln s$ approximation to all loops. Indeed, the computation of n -gluon MHV amplitudes that we wrote about before has its own importance for precision measurements at the LHC, where both signals and backgrounds are QCD processes.

Thus MSYM can be considered a theoretical laboratory to compare with observables computed in QCD [BDK04]. Calculations in $\mathcal{N} = 4$ SYM are much easier when done the right way through generalized unitarity relations. As an example, the amplitude at two loops for $gg \rightarrow gg$ in terms of loop integrals was finished in 1997 [BRY97], while the same computation in QCD took four more years [AGOTY01]. Another important issue is that the infrared behavior in both theories is very similar, paving the way to find well-defined observables in MSYM [Ste08, BKVZ09]. The last amazing connection is the so-called principle of maximal transcendentality [KL03, ES06, BES07, KL07]. The principle roughly asserts that $\mathcal{N} = 4$ SYM scattering amplitudes are pieces of the QCD amplitudes characterized by being the *simplest* ones, in terms of which types of loop

integrals appear, but the most *complicated* ones as they give the pieces with higher degree of transcendentality, where $\ln(x)$ and π are factors with transcendentality 1, and $\text{Li}_n(x)$ and $\zeta(n) = \text{Li}_n(1)$ have associated transcendentality n .

So, despite some crucial differences between the two theories, one can expect to learn important lessons for QCD—at least qualitatively—from computations with its supersymmetric version. This has inspired a whole program to describe collider physics from AdS/CFT [PS02, PS03, CCP07, HM08, HIM08]. The conclusions one can draw should help understand gauge theories at strong coupling. It is important in this respect to identify different types of observables and kinematic regions where QCD and MSYM can manifest similar behaviors. As remarked before, the connection should be closer in a sense in the high energy limit, where in the LLA both theories coincide and QCD inherits conformal invariance¹⁴.

1.4 Pomeron in $\mathcal{N} = 4$ SYM

The NLL BFKL kernel for $\mathcal{N} = 4$ SYM was found in [KL00, KL03]. In $\overline{\text{MS}}$ scheme it reads:

$$\begin{aligned} \langle n, \nu | \mathcal{K}_{\text{MSYM}} | \nu', n \rangle &= \lambda \left[\chi_0 \left(|n|, \frac{1}{2} + i\nu \right) + \lambda \chi_1^{\text{MSYM}} \left(|n|, \frac{1}{2} + i\nu \right) \right] \delta_{n,n'} \delta(\nu - \nu'); \\ \chi_1^{\text{MSYM}}(n, \gamma) &= \frac{1 - \zeta(2)}{12} \chi_0(|n|, \gamma) + \frac{3}{2} \zeta(3) + \Omega(|n|, \gamma), \quad \gamma = \frac{1}{2} + i\nu. \end{aligned} \quad (\text{II.8})$$

The functions $\chi_0(n, \gamma)$ and $\Omega(n, \gamma)$ are given in (I.152) and (I.163). λ is the 't Hooft coupling. Running coupling corrections are absent and, as compared to (I.161), the non-analytic terms proportional to δ_n^0 and δ_n^2 have disappeared. In FIG. I.30, the $n = 0$ eigenvalue of the NLL $\mathcal{N} = 4$ SYM kernel is plotted. One can see that the size of the NLL corrections is much smaller than in the QCD case.

Recently, high energy scattering in $\mathcal{N} = 4$ SYM has also been studied at strong coupling via AdS/CFT. It turned out that the exchange would be dominated by the graviton state with intercept $j_0 = 2$ [JP00, BPST07] ($j_0 = \alpha_{\mathbb{P}}$ in our notation in (I.156), giving the intercept at weak coupling). It is remarkable that the same diffusion pattern was found for the amplitude as in the weak coupling limit. This was interpreted as a diffusion in the radial coordinate of AdS space, corresponding to diffusion in the transverse momenta along the ladder on the

¹⁴The origin of the conformal invariance of the BFKL Hamiltonian is not clear. Notice that we have not taken any large- N_c during the derivation in SEC. I.3. Moreover, the $\text{SL}(2, \mathbb{C})$ generators in (I.196) correspond to a 2d field with conformal weights $h = \bar{h} = 0$. These quantum numbers correspond to a scalar field and are different from transverse components of a physical gluon field. Therefore the $\text{SL}(2, \mathbb{C})$ symmetry of $\mathcal{H}_{\text{BFKL}}$ does not follow directly from the conformal symmetry of the QCD Lagrangian [BKM03].

II. Comparing QCD and $\mathcal{N} = 4$ SYM in the Regge Limit

gauge theory side. The only difference is in the value of the intercept and the diffusion coefficient

$$\begin{aligned} j_0 &= 2 - \frac{2}{\sqrt{\lambda}}, & \mathcal{D} &= \frac{1}{2\sqrt{\lambda}}, & \lambda &= g^2 N_c \gg 1; \\ j_0 &= 1 + 4 \ln 2 \bar{\alpha}_s, & \mathcal{D} &= 7\zeta(3) \bar{\alpha}_s, & \lambda &\gg 1. \end{aligned} \quad (\text{II.9})$$

Recently [CGP12, KL13] higher order terms in the strong coupling expansion (II.9) have become available, allowing a smooth interpolation between weak and strong coupling regimes.

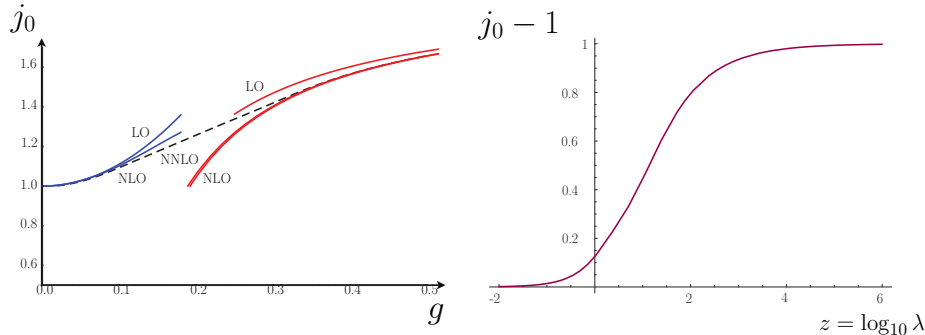


Figure II.1: (a) Weak and strong coupling expansions of the BFKL intercept [CGP12]; (b) Interpolation between both regimes showing the asymptotic behavior [KL13].

This analysis may shed light on the relation between the soft and hard pomeron [BPST07]. It can also be important to understand AdS/CFT correlation functions in the stringy regime of finite string tension (or finite 't Hooft coupling) beyond the supergravity approximation.

2 HIGH ENERGY DIJETS IN $\mathcal{N} = 4$ SYM [ACMS11]

In this section we study dijet production at large rapidity separation in QCD and $\mathcal{N} = 4$ SYM. In the process of identifying and computing the relevant well-behaved observables we will review many of the concepts introduced in CH. I. Special attention will be paid to the choice of renormalization scheme.

2.1 Mueller-Navelet Jets and Dijet Azimuthal Decorrelation

In 1987, Mueller and Navelet [MN87] proposed to study the energy dependence of the cross section for the production of two jets with similar transverse momenta $p_{1,2}^2$ at large rapidity separation y (and angular separation ϕ) as a decisive test of BFKL dynamics. We will now compute the cross-section for inclusive two-jet production in the configuration described above (FIG. II.2), discuss the main obstacles to obtain a conclusive BFKL signature, and

show how to extract this information in an optimal way through azimuthal angle decorrelations¹⁵.

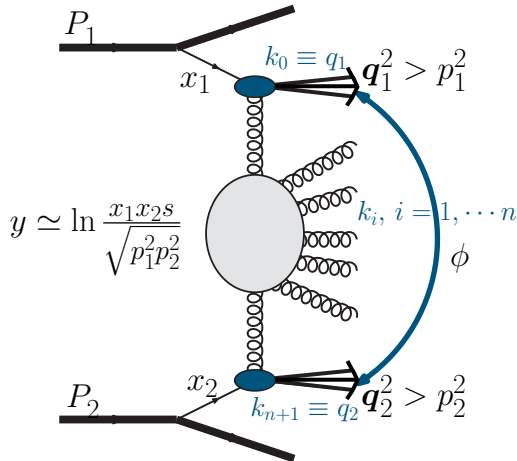


Figure II.2: Kinematic configuration for Mueller-Navelet jets.

If $x_{1,2}$ are the fractions of longitudinal momentum from the parent hadrons carried by the partons generating the jets then $y \simeq \ln(x_1x_2s/\sqrt{p_1^2p_2^2})$. When $x_{1,2}$ are big, collinear factorization (I.60) applies, and we have in terms of the jet rapidities $y_{1,2}$ ¹⁶

$$\frac{d\sigma}{d^2\mathbf{q}_1 d^2\mathbf{q}_2 dy_1 dy_2} = \sum_{ij} \int dx_1 \int dx_2 f_{i/1}(x_1, p^2) f_{j/2}(x_2, p^2) \frac{d\sigma^{ij}}{d^2\mathbf{q}_1 d^2\mathbf{q}_2 dy_1 dy_2}, \quad (\text{II.10})$$

where the sum \sum_{ij} runs over parton species/flavors and we have identified the factorization scale with $p^2 \simeq p_{1,2}^2$. x_1 and x_2 are obtained from momentum conservation (APP. B)

$$x_1 = \sum_{i=0}^{n+1} \frac{k_{i\perp}}{\sqrt{s}} e^{y_i} \stackrel{\text{MRK}}{\simeq} \frac{|\mathbf{q}_1|}{\sqrt{s}} e^{y_1}; \quad x_2 = \sum_{i=0}^{n+1} \frac{k_{i\perp}}{\sqrt{s}} e^{-y_i} \stackrel{\text{MRK}}{\simeq} \frac{|\mathbf{q}_2|}{\sqrt{s}} e^{-y_2}. \quad (\text{II.11})$$

The partonic cross section is given by (A.25)

¹⁵Although the configuration in which the two jets are produced with nearly balancing transverse momenta and a rapidity gap devoid of any other jets above a transverse momentum scale μ^2 is interesting [MT92], we will focus on the inclusive process, where distributions are affected by the hadronic activity in the rapidity interval y between the tagged jets, whether or not these hadrons (the so-called *minijets*) pass the jet-selection criteria (essentially having a transverse scale above some μ^2).

¹⁶Mueller-Navelet jets lie at the interface of collinear and k_T factorizations. Partons emitted from the hadrons carry large longitudinal momentum fractions. After scattering off each other, they produce the Mueller-Navelet jets. Because of the large transverse momentum of the jets, the partons are hard and obey the collinear factorization. In particular, its scale dependence is given by DGLAP evolution. Between the jets, on the other hand, we require a large rapidity gap which is described by BFKL dynamics. The hadronic cross section therefore factorizes into two collinear parton distribution function convoluted with the partonic cross section, described by BFKL. With respect to the cross section, the incoming partons are consequently considered on-shell and collinear to the parent hadrons.

II. Comparing QCD and $\mathcal{N} = 4$ SYM in the Regge Limit

$$d\sigma^{ij} = \frac{1}{2\hat{s}} \sum_{n=0} |A_{ij \rightarrow n+2}|^2 d\Pi_{n+2}, \quad s = x_1 x_2 \hat{s},$$

$$d\Pi_{n+2} = \int \frac{dy_1 d^2 \mathbf{q}_1}{4\pi(2\pi)^2} \int \frac{dy_2 d^2 \mathbf{q}_2}{4\pi(2\pi)^2} \prod_{i=1}^n \int \frac{dy_i d^2 \mathbf{k}_i}{4\pi(2\pi)^2} (2\pi)^4 \delta^4 \left(P_1 + P_2 - q_1 - q_2 - \sum_{i=1}^n \mathbf{k}_i \right). \quad (\text{II.12})$$

Now, using that $\frac{dx_i}{x_i} = dy_i$ and given that amplitudes at the partonic level are the same for qq , qg or gg scattering apart from the color factors (Eq. (I.104)), we can rewrite (II.10) in terms of an *effective parton distribution* $f_{\text{eff}}(x, \mu^2) = g(x, \mu^2) + \sum_f [q_f(x, \mu^2) + \bar{q}_f(x, \mu^2)]$:

$$\frac{d\sigma}{dx_1 dx_2 d^2 \mathbf{q}_1 d^2 \mathbf{q}_2} = f_{\text{eff}}(x_1, p^2) f_{\text{eff}}(x_2, p^2) \frac{d\sigma^{gg}}{d^2 \mathbf{q}_1 d^2 \mathbf{q}_2}. \quad (\text{II.13})$$

From (I.157) we have

$$\frac{d\sigma^{gg}}{d^2 \mathbf{q}_1 d^2 \mathbf{q}_2} = \left(\frac{2N_c^2}{N_c^2 - 1} \right)^2 \frac{d\sigma^{qq}}{d^2 \mathbf{q}_1 d^2 \mathbf{q}_2} = \frac{4N_c^2}{N_c^2 - 1} \frac{\alpha_s^2}{\mathbf{q}_1^2 \mathbf{q}_2^2} f(\hat{s}, \mathbf{q}_1, \mathbf{q}_2), \quad (\text{II.14})$$

that shows that the jet-production rate at fixed x 's can be directly related to the partonic cross section. Then, defining the *K-factor* as the quotient of the dijet cross-sections taking into account the BFKL corrections and not taking them (the Born level approximation (I.104), obtained replacing the BFKL Green function by a Dirac delta), the distribution functions cancel, and we should see a power rise with \hat{s} of the *K-factor*. The problem is that one usually does not dispose of a variable-energy collider in which a ramping run experiment could be performed (varying \hat{s} at fixed x 's implies varying s)¹⁷. One has to consider dijet production at fixed \sqrt{s} as a function of the jet rapidities, something like (II.13). Since at fixed \sqrt{s} and rapidities the x 's grow linearly with the transverse momenta (Eq. (II.11)) the integration over transverse momenta in the jet production rate will entail a varying unavoidable contribution from the parton densities. This convolution turns out to destroy the rising of the *K-factor*, that falls like $(1-y)$ as y decreases [dDS94a, Sti94, dD95].

As pointed by Mueller himself, the Mueller-Navelet proposal can also be modified for implementation in DIS, where the situation is milder [Mue90, Mue91]. Though the tagging of the forward jet is not an easy task, this signature has been widely pursued at HERA, both in H1 [H1 06, H1 08] and ZEUS experiments [ZEU99, ZEU06]. In general terms, it is shown the inadequacy of fixed order (NLO or NNLO) QCD computations, which in some

¹⁷Such a possibility was considered at Tevatron [D0 00], though their analysis was not conclusive. There are prospects for doing such a measurement using the runs with different energy at LHC.

cases predict cross sections for very small x that are a factor 10 lower than measured. DGLAP-based Monte Carlo simulations, like HERWIG [MWA⁺92], tend to fall below the data especially when DGLAP evolution is further suppressed by the requirement of an additional forward dijet [H1 08]. On the contrary, BFKL-like schemes seem to fit the data rather well.

In any case, rather than from the inclusive cross section, more conclusive information can be extracted from the study of the dijet azimuthal decorrelation. When no radiation takes place between the two jets, at Born level, we should expect to tag the jets back-to-back in azimuthal angle due to transverse momentum conservation. As first noted in [dDS94b], because the BFKL evolution is associated with the emission of gluons with transverse momenta of the same order (of the jet transverse momenta), it is to be expected that as we increase the rapidity difference between the two jets —thus increasing the phase space for gluon emission— a growing decorrelation in the directions of jets appears. A good measure of the decorrelation is given by the moments of the azimuthal angle ϕ between the jets

$$\langle \cos(n(\phi - \pi)) \rangle = \frac{\int_0^{2\pi} d\phi \cos(n(\phi - \pi)) (d\sigma/dy d\phi)}{\int_0^{2\pi} d\phi (d\sigma/dy d\phi)}. \quad (\text{II.15})$$

For a δ -function distribution at $\phi = \pi$, as occurs at the Born level, all of the moments will equal one, while for a flat distribution all of the moments will equal zero for $n \geq 1$. The decay of the moments from unity measures the decorrelation in ϕ .

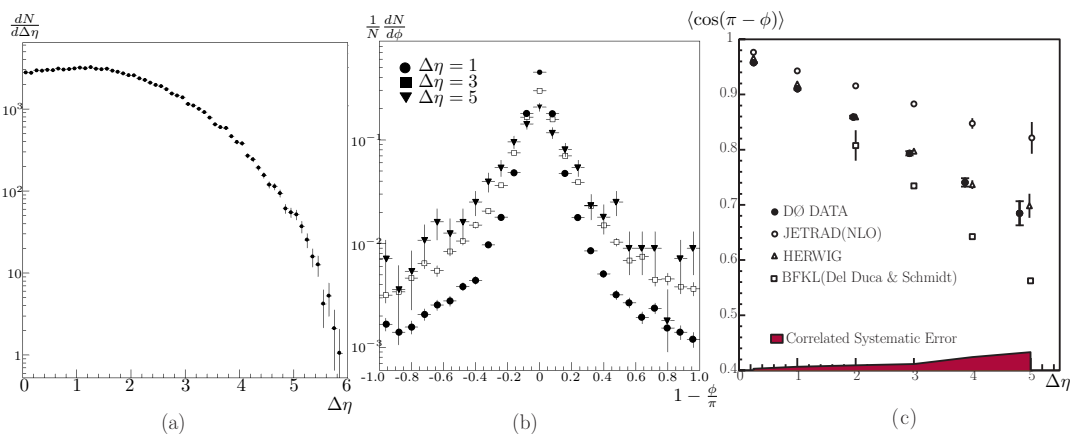


Figure II.3: Azimuthal decorrelation data from Tevatron at $\sqrt{s} = 1.8$ TeV: (a) distribution of events per pseudorapidity interval $\Delta\eta$; (b) distribution of events in the azimuthal angle difference between jets ϕ for three different rapidities, where one can see the decorrelating effect of higher rapidities; (c) fits to the data. Adapted from [DØ 96].

2.2 The Role of Higher Conformal Spins

The study of angular correlations gives us access to the information encoded by conformal spins $n > 0$, usually subdominant for $y \rightarrow \infty$ e.g. in total cross sections. Comparing the LL and NLL BFKL kernels for different values of the conformal spins (FIG. II.4), it turns out that in the region $\gamma = 1/2$ that gives the dominant contribution for asymptotically high energies the LL and (scale invariant) NLL kernels are very similar for conformal spins $n \geq 1$, but they differ notably for $n = 0$. This suggests that observables insensitive to the $n = 0$ conformal spin present a very good perturbative convergence.

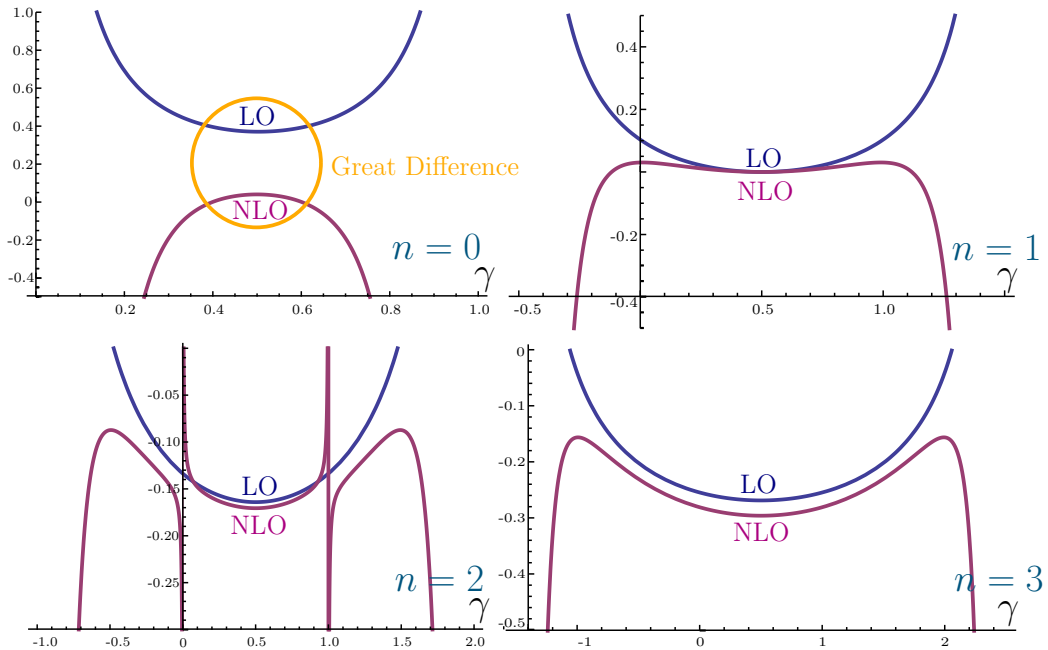


Figure II.4: Eigenvalues of the scale invariant sector of the BFKL kernel $\omega(n, \gamma) = \bar{\alpha}_s \chi_0(|n|, \gamma) + \bar{\alpha}_s^2 \chi_1(|n|, \gamma)$, for different values of the conformal spin n , as a function of γ .

In order to construct such an observable, we focus on the partonic cross section¹⁸, which is given according to k_T factorization (SEC. I.3.5) by the convolution of a differential partonic cross section with jet vertices $\Phi_{\text{jet}_{1,2}}$, playing the role of impact factors:

$$\sigma(\alpha_s, y, p_{1,2}^2) = \int d^2 \mathbf{q}_1 \int d^2 \mathbf{q}_2 \Phi_{\text{jet}_1}(\mathbf{q}_1, p_1^2) \frac{d\sigma}{d^2 \mathbf{q}_1 d^2 \mathbf{q}_2} \Phi_{\text{jet}_2}(\mathbf{q}_2, p_2^2), \quad (\text{II.16})$$

As the rapidity difference increases the azimuthal angle dependence is mainly driven by the

¹⁸This is an important point, so it deserves clarification. The observables we will define depend on ratios of cross sections, and then the dependence on the PDFs cancels. This is so because we are effectively taking y as a fixed parameter (something that is also useful to perform the analytical calculation of the necessary Mellin transforms, see below), say $y = \ln(x_1 x_2 s / s_0)$. The difference between considering s_0 fixed or $s_0 = \sqrt{\mathbf{q}_1^2 \mathbf{q}_2^2}$ can be understood as a NLL contribution to the vertices coupling the tagged jets to the external hadrons [SS07], which we are not considering.

kernel, so we will consider the jet vertices to leading order to avoid difficulties and keep the treatment analytical (this strategy was also followed e.g. in [MR09]; for the full incorporation of NLL jet vertices [BCV02, BCV03], see [CSSW10, CIM⁺12, CMSS13]):

$$\Phi_{\text{jet}_i}(\mathbf{q}, p_i^2) \simeq \Phi_{\text{jet}_i}^{(0)}(\mathbf{q}, p_i^2) = \Theta(\mathbf{q}^2 - p_i^2). \quad (\text{II.17})$$

Essentially, to leading order we identify a jet with a parton with a transverse momentum above some resolution scale p_i^2 . Using (II.14)

$$\sigma(\alpha_s, y, p_{1,2}^2) = \frac{4N_c^2}{N_c^2 - 1} \alpha_s^2 \int d^2 \mathbf{q}_1 \int d^2 \mathbf{q}_2 \frac{\Phi_{\text{jet}_1}^{(0)}(\mathbf{q}_1, p_1^2)}{\mathbf{q}_1^2} \frac{\Phi_{\text{jet}_2}^{(0)}(\mathbf{q}_2, p_2^2)}{\mathbf{q}_2^2} f(y, \mathbf{q}_1, \mathbf{q}_2). \quad (\text{II.18})$$

We will use the bra-ket notation (I.160) to find a suitable expression for the cross section. We can express the BFKL equation (I.149) in operator notation as

$$(\omega - \mathcal{K}) \hat{f}_\omega = \mathbb{1} \implies \hat{f}_\omega = (\omega - \bar{\alpha}_s \mathcal{K}_0)^{-1} + \bar{\alpha}_s^2 (\omega - \bar{\alpha}_s \mathcal{K}_0)^{-1} \mathcal{K}_1 (\omega - \bar{\alpha}_s \mathcal{K}_0)^{-1} + \text{NNLL terms}, \quad (\text{II.19})$$

where we have defined the expansion of the kernel as $\mathcal{K} = \bar{\alpha}_s \mathcal{K}_0 + \bar{\alpha}_s^2 \mathcal{K}_1 + \dots$. Now, we project the jet vertices on the basis $|n, \nu\rangle$, using (I.151)

$$\int d^2 \mathbf{q} \frac{\Phi_{\text{jet}_1}^{(0)}(\mathbf{q}, p_1^2)}{\mathbf{q}^2} \langle \mathbf{q} | \nu, n \rangle = \frac{1}{\sqrt{2}} \frac{1}{\left(\frac{1}{2} - i\nu\right)} \left(p_1^2\right)^{i\nu - \frac{1}{2}} \delta_{n,0} \equiv c_1(\nu) \delta_{n,0}. \quad (\text{II.20})$$

The $c_2(\nu)$ projection of $\Phi_{\text{jet}_2}^{(0)}$ on $\langle n, \nu | \mathbf{q} \rangle$ is the complex conjugate of (II.20) with p_1^2 being replaced by p_2^2 . The corresponding inverse relations, using (I.151), are

$$\frac{\Phi_{\text{jet}_1}^{(0)}(\mathbf{q}, p_1^2)}{\mathbf{q}^2} = \sum_{n=-\infty}^{\infty} \int_{-\infty}^{\infty} d\nu c_1(\nu) \delta_{n,0} \langle n, \nu | \mathbf{q} \rangle, \quad \frac{\Phi_{\text{jet}_2}^{(0)}(\mathbf{q}, p_2^2)}{\mathbf{q}^2} = \sum_{n=-\infty}^{\infty} \int_{-\infty}^{\infty} d\nu c_2(\nu) \delta_{n,0} \langle \mathbf{q} | \nu, n \rangle. \quad (\text{II.21})$$

The cross section can then be rewritten introducing completeness relations as

$$\sigma(\alpha_s, y, p_{1,2}^2) = \frac{4N_c^2}{N_c^2 - 1} \alpha_s^2 \sum_{n, n'=-\infty}^{\infty} \iint_{-\infty}^{\infty} d\nu d\nu' c_1(\nu) c_2(\nu') \delta_{n,0} \delta_{n',0} \int \frac{d\omega}{2\pi i} e^{\omega y} \langle n, \nu | \hat{f}_\omega | \nu', n' \rangle. \quad (\text{II.22})$$

Making use of (II.19), (I.161) and integration by parts, σ can be expressed as

$$\begin{aligned} \sigma(\alpha_s, y, p_{1,2}^2) &= \frac{4\pi^2 \bar{\alpha}_s^2}{N_c^2 - 1} \sum_{n=-\infty}^{\infty} \int_{-\infty}^{\infty} d\nu e^{\bar{\alpha}_s \chi_0(|n|, \nu) y} c_1(\nu) c_2(\nu) \delta_{n,0} \\ &\times \left\{ 1 + \bar{\alpha}_s^2 y \left[\chi_1(|n|, \nu) + \frac{\beta_0}{4N_c} \left(\ln(\mu^2) + \frac{i}{2} \frac{\partial}{\partial \nu} \ln \left(\frac{c_1(\nu)}{c_2(\nu)} \right) + \frac{i}{2} \frac{\partial}{\partial \nu} \right) \chi_0(|n|, \nu) \right] \right\}. \end{aligned} \quad (\text{II.23})$$

II. Comparing QCD and $\mathcal{N} = 4$ SYM in the Regge Limit

For the LL jet vertices the logarithmic derivative in (II.23) explicitly reads

$$-i \frac{\partial}{\partial \nu} \ln \left(\frac{c_1(\nu)}{c_2(\nu)} \right) = \ln(p_1^2 p_2^2) + \frac{1}{\frac{1}{4} + \nu^2}. \quad (\text{II.24})$$

Introducing the representation

$$c_1(\nu) c_2(\nu) \delta_{n,0} = \frac{1}{2\sqrt{p_1^2 p_2^2}} \frac{1}{\left(\frac{1}{4} + \nu^2\right)} \left(\frac{p_1^2}{p_2^2}\right)^{i\nu} \int_{-\pi}^{\pi} \frac{d\phi}{2\pi} e^{in\phi}, \quad (\text{II.25})$$

with $\phi = \vartheta_1 - \vartheta_2 - \pi$. and focussing on the case where the two resolution momenta are equal, $p_1^2 = p_2^2 \equiv p^2$, the angular differential cross section can be expressed as

$$\begin{aligned} \frac{d\sigma(\alpha_s, y, p^2)}{d\phi} &= \frac{2\pi^2}{N_c^2 - 1} \frac{\bar{\alpha}_s^2}{p^2} \sum_{n=-\infty}^{\infty} \frac{1}{2\pi} e^{in\phi} \int_{-\infty}^{\infty} d\nu e^{\bar{\alpha}_s \chi_0(|n|, \nu) y} \frac{1}{\left(\frac{1}{4} + \nu^2\right)} \\ &\times \left\{ 1 + \bar{\alpha}_s^2 y \left[\chi_1(|n|, \nu) - \frac{\beta_0}{8N_c} \chi_0(|n|, \nu) \left(2 \ln \left(\frac{p^2}{\mu^2} \right) + \frac{1}{\left(\frac{1}{4} + \nu^2\right)} \right) \right] \right\}. \end{aligned} \quad (\text{II.26})$$

The term proportional to $\frac{\partial \chi_0}{\partial \nu}$ in (II.23) gives no contribution after integration as it is an odd function in ν . Within NLL accuracy there is freedom to exponentiate the integrand of this result. In fact, due to the large and negative size of the NLL corrections it turns out that the exponentiated form is mandatory in order to reach convergent results [Sab06]. Within our accuracy we can also make the replacement $\bar{\alpha}_s - \bar{\alpha}_s^2 \frac{\beta_0}{4N_c} \ln \left(\frac{p^2}{\mu^2} \right) \rightarrow \bar{\alpha}_s(p^2)$, getting finally

$$\frac{d\sigma(\alpha_s, y, p^2)}{d\phi} = \frac{4\pi^3}{N_c^2 - 1} \frac{\bar{\alpha}_s^2}{p^2} \frac{1}{2\pi} \sum_{n=-\infty}^{\infty} e^{in\phi} \mathcal{C}_n(y), \quad (\text{II.27})$$

with

$$\mathcal{C}_n(y) = \int_{-\infty}^{\infty} \frac{d\nu}{2\pi} e^{\bar{\alpha}_s(p^2) y \left(\chi_0(|n|, \nu) + \bar{\alpha}_s(p^2) \left(\chi_1(|n|, \nu) - \frac{\beta_0}{8N_c} \frac{\chi_0(|n|, \nu)}{\left(\frac{1}{4} + \nu^2\right)} \right) \right)}. \quad (\text{II.28})$$

The Fourier coefficients \mathcal{C}_n in (II.28) are remarkably connected in a straightforward fashion with important observables. The first one is the total cross section:

$$\sigma(\alpha_s, Y, p_{1,2}^2) = \frac{4\pi^3 \bar{\alpha}_s^2}{(N_c^2 - 1) \sqrt{p_1^2 p_2^2}} \mathcal{C}_0(y); \quad \frac{\sigma(y)}{\sigma(0)} = \frac{\mathcal{C}_0(y)}{\mathcal{C}_0(0)}. \quad (\text{II.29})$$

The effect of higher conformal spins n , can be projected using ratios of azimuthal angle correlations [Sab06]

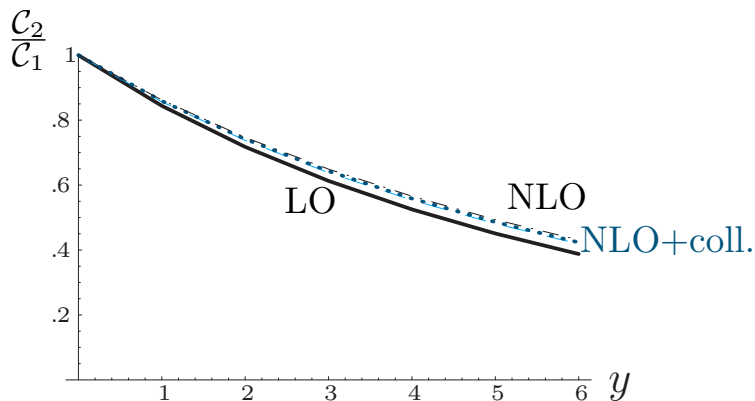


Figure II.5: The ratio C_2/C_1 as a function of rapidity. The LL, NLL, and all-orders collinearly resummed NLL predictions fall almost on top of each other. Adapted from [Sch07].

$$\langle \cos(m\phi) \rangle = \frac{C_m(y)}{C_0(y)}, \quad \mathcal{R}_{m,n} \equiv \frac{\langle \cos(m\phi) \rangle}{\langle \cos(n\phi) \rangle} = \frac{C_m(y)}{C_n(y)}. \quad (\text{II.30})$$

The ratios $\mathcal{R}_{m,n}$ are insensitive to the $n = 0$ component. In fact, they exhibit a remarkable perturbative convergence (FIG. II.5). Being insensitive to parton distributions, they are very well suited for a comparison between QCD and $\mathcal{N} = 4$ SYM.

2.3 The BLM Procedure

As remarked in SEC. I.1.4, there is an essential ambiguity in perturbative computations due to the choice of the renormalization prescription. We saw that at next-to-leading order the prescription was essentially fixed by a choice of the renormalization scale¹⁹. A clever choice of scale can in a sense resum higher order contributions. In fact, one can argue that, given an observable $R(Q)$, there is a scheme $\overline{\text{RS}}$ for which all coefficients $r_i, i \geq 1$ are zero, and we simply have $R(Q) = \bar{a}(Q) \equiv a(\mu_{\text{FAC}})$, where \bar{a} is the coupling in the $\overline{\text{RS}}$ scheme. This is the idea behind the FAC (fastest apparent convergence) renormalization prescription [Gru80, Gru84]. Another widely used strategy is the principle of minimal sensitivity (PMS) [Ste81a, Ste81b], in which the scheme and scale are chosen so as to minimize the sensitivity of the perturbative result $R^{(n)}$ under small variations of the parameters defining the scheme, $\frac{\partial R^{(n)}}{\partial(\overline{\text{RS}})} = 0$, replicating in this way the property $\frac{\partial R}{\partial(\overline{\text{RS}})} = 0$ of the exact result. A good review of these methods is provided in [IFL10], Sec. 1.11.

Both FAC and PMS approaches are designed, in the two-loop approximation, to absorb as much as possible the correction r_1 in (I.26) (r_1 is zero in FAC, and small and process-

¹⁹In this discussion for simplicity we assume the observable of interest to depend on a unique scale Q .

II. Comparing QCD and $\mathcal{N} = 4$ SYM in the Regge Limit

independent for PMS). As highlighted by Brodsky, Lepage and Mackenzie (BLM) [BLM83], a large r_1 can be a consequence of bad convergence of the perturbative expansion rather than a bad choice of expansion parameter. The BLM formalism proposes to absorb in the redefinition of the coupling only the piece of r_1 related to charge renormalization.

The idea of the BLM procedure is best visualized in the case of QED. The only true UV divergences in this theory are associated with vacuum polarization, because divergences in the vertex and fermion self-energy corrections cancel by the Ward identity (or are absent in Landau gauge). Moreover, being IR free, there is a natural initial condition for defining the running coupling $\alpha(Q^2)$ as $Q^2 \rightarrow 0$. The natural choice for the renormalization scale is then set by the momentum q of the photon propagator: $Q^2 = -q^2$. Including the running coupling before the loop integral in q is equivalent to resum all vacuum polarization corrections dressing the propagator.

No such natural criterion exist for QCD. The argument that in the limit $N_c \rightarrow 0$ one should recover the Abelian case leads us to the following prescription: determine the scale in such a way that only corrections coming from charge renormalization are absorbed in the redefined coupling. Therefore, the perturbative coefficients with the BLM prescription are identical to those of the conformal theory with $\beta_0 = 0$. The BLM prescription can be applied most straightforwardly to second order for processes that do not have gluon-gluon interactions in lowest order²⁰. For such processes, the dependence of the coefficient r_1 (Eq. (I.26)) on the number of flavors N_f comes only from the quark vacuum polarization. Since polarization is inseparably linked with charged renormalization, all terms proportional to N_f are absorbed into the scale. If $r_1(1) = AN_f + B$, we rescale μ to μ_{BLM} changing $a(\mu)$ according to (I.31)

$$a(\mu) \rightarrow a(\mu_{\text{BLM}}) = a(\mu)(1 - 2\beta_0 a(\mu) \ln(\mu_{\text{BLM}}/\mu) + \dots) \quad (\text{II.31})$$

and we get the observable $R^{(2)}$ in terms of $a(\mu_{\text{BLM}})$ as

$$\begin{aligned} R^{(2)} &= a(\mu)(1 + r_1 a(\mu)) = a(\mu_{\text{BLM}}) \left[1 + \left[AN_f + B + 2\beta_0 \ln \frac{\mu_{\text{BLM}}}{\mu} \right] a(\mu_{\text{BLM}}) \right] \\ &= a(\mu_{\text{BLM}})[1 + r_1^* a(\mu_{\text{BLM}})], \quad r_1^*(N_f) = AN_f + B + 2 \left(11 - \frac{2}{3} N_f \right) \ln \frac{\mu_{\text{BLM}}}{\mu}. \end{aligned} \quad (\text{II.32})$$

We now implement the BLM scheme by choosing μ_{BLM} such that r_1^* is independent of N_f :

²⁰For these processes no one-to-one correspondence between corrections coming from charge renormalization and terms proportional to N_f . This is precisely the case we will have in our BFKL calculation. One has to trace back and see what factors of N_f in the NLL kernel come from β_0 and which ones do not.

$$A = \frac{4}{3} \ln \frac{\mu_{\text{BLM}}}{\mu} \implies \mu_{\text{BLM}} = \mu \exp\left(\frac{3A}{4}\right). \quad (\text{II.33})$$

It is important to note that (II.32) now becomes

$$r_1^* = \frac{33}{2}A + B \implies r_1^*(\mu_{\text{BLM}}) = r_1\left(\mu, N_f = \frac{33}{2}\right) = r_1(\mu, \beta_0 = 0), \quad (\text{II.34})$$

as we had advanced. Summarizing, if we split the contributions to r_1 into those coming from the running of the coupling and those which we could call conformal ($\beta_0 = 0$)

$$r_1 = r_1^{\text{conf}} + r_1^\beta; \quad r_1^{\text{conf}} = \frac{33}{2}A + B, \quad r_1^\beta = -\frac{3}{2}A\beta_0, \quad (\text{II.35})$$

then we can express the BLM scale (II.33) as

$$\mu_{\text{BLM}} = \mu \exp\left(-r_1^\beta/2\beta_0\right). \quad (\text{II.36})$$

Obviously, the BLM criterion specifies the scale μ_{BLM} only with respect to some reference RS, something that is not needed in the FAC or PMS approaches. However, the BLM prediction turns out to be RS-independent (up to formally higher-order terms), as ensured by commensurate scale relations [BL95], i.e. the specific value of the renormalization scale is rescaled according to the choice of scheme so that the final result is scheme independent. The implementation of the BLM to higher orders in QCD is much more involved, but it can be pursued [BdG12, WBM13].

The BLM procedure was applied in [BFK⁺99] (see also the review [FKLP02]) taking as a physical observable the NLO BFKL intercept in $\gamma^*\gamma^*$ interactions to fix the scale. In order to enhance the effect of BLM in gluon dominated processes, it was argued that it is appropriate to use a physical scheme suitable for non-abelian interactions, such as MOM²¹, based on the 3-gluon vertex [CG79b, CG79a, PT80] or the Υ scheme based on $\Upsilon \rightarrow ggg$ decay. Though BLM setting does not completely solve the oscillatory behaviour of the Green function, certainly a much more sensible result for the pomeron intercept is achieved. Moreover, the NLL value for the pomeron intercept, improved by the BLM procedure, has a very weak dependence on the hard scale of the process, which is in agreement with Regge theory, guarantees a lower sensitivity to nonperturbative effects and leads to approximate scale invariance²².

²¹In MOM (momentum) schemes, the renormalization conditions for Green functions are specified at some off-shell values of momenta in the spacelike region.

²²The procedure was criticized in [Tho99] for the fact that, as remarked before, due to the running we

2.4 Azimuthal Angle Correlations in QCD and $\mathcal{N} = 4$ SYM

Following the example of [BFK⁺99], we will test several renormalization schemes ($\overline{\text{MS}}$, MOM and MOM+BLM²³) in the computation of azimuthal angle correlations in QCD and MSYM [ACMS11]. Transition between MOM to $\overline{\text{MS}}$ schemes is given by [CG79a, CG79b]

$$\begin{aligned} \alpha_{\text{MOM}} &= \alpha_{\overline{\text{MS}}} \left[1 + T_{\text{MOM}} \frac{\alpha_{\overline{\text{MS}}}}{\pi} \right]; \quad T_{\text{MOM}} = T_{\text{MOM}}^{\text{conf}} + T_{\text{MOM}}^{\beta}, \\ T_{\text{MOM}}^{\text{conf}} &= \frac{N_c}{8} \left[\frac{17}{2} I + \xi \frac{3}{2} (I - 1) + \xi^2 \left(1 - \frac{1}{3} I \right) - \xi^3 \frac{1}{6} \right], \quad T_{\text{MOM}}^{\beta} = -\frac{\beta_0}{2} \left[1 + \frac{2}{3} I \right], \end{aligned} \quad (\text{II.37})$$

where $I = -2 \int_0^1 dx \ln(x) / [x^2 - x + 1] \simeq 2.3439$.

To implement the BLM prescription we start by writing the BFKL kernel in the form

$$\omega_{\overline{\text{MS}}}(\mathbf{q}^2, n, \nu) = N_c \chi_0(n, \nu) \frac{\alpha_{\overline{\text{MS}}}(\mathbf{q}^2)}{\pi} \left[1 + r_{\overline{\text{MS}}}(n, \nu) \frac{\alpha_{\overline{\text{MS}}}(\mathbf{q}^2)}{\pi} \right], \quad (\text{II.38})$$

where, from (I.162), we have

$$\begin{aligned} r_{\overline{\text{MS}}}(n, \nu) &= r_{\overline{\text{MS}}}^{\beta}(n, \nu) + r_{\overline{\text{MS}}}^{\text{conf}}(n, \nu), \quad r_{\overline{\text{MS}}}^{\beta}(n, \nu) = -\frac{\beta_0}{4} \left[\frac{\chi_0(n, \nu)}{2} - \frac{5}{3} \right], \\ r_{\overline{\text{MS}}}^{\text{conf}}(n, \nu) &= -\frac{N_c}{4\chi_0(n, \nu)} \left[\frac{\pi^2 - 4}{3} \chi_0(n, \nu) - 6\zeta(3) - \left(\psi'' \left(\frac{n+1}{2} + i\nu \right) + \psi'' \left(\frac{n+1}{2} - i\nu \right) \right) \right. \\ &\quad \left. - 2\Phi \left(n, \frac{1}{2} + i\nu \right) - 2\Phi \left(n, \frac{1}{2} - i\nu \right) \right] + \frac{\pi^2}{2\nu} \text{sech}(\pi\nu) \tanh(\pi\nu) \\ &\quad \times \left\{ \left[3 + \left(1 + \frac{N_f}{N_c^3} \right) \left(\frac{3}{4} - \frac{1}{16(1+\nu^2)} \right) \right] \delta_{n0} - \left(1 + \frac{N_f}{N_c^3} \right) \left(\frac{1}{8} - \frac{3}{32(1+\nu^2)} \right) \delta_{n2} \right\}. \end{aligned} \quad (\text{II.39})$$

Now the NLL BFKL intercept in the MOM-scheme, evaluated at the optimal BLM scale, can be represented as follows:

$$\omega^{\text{MOM}}(\mathbf{q}_{\text{BLM}}^2, n, \nu) = N_c \chi_0(n, \nu) \frac{\alpha_{\overline{\text{MS}}}(\mathbf{q}_{\text{BLM}}^2)}{\pi} \left[1 + r^{\text{MOM}}(n, \nu) \frac{\alpha_{\overline{\text{MS}}}(\mathbf{q}_{\text{BLM}}^2)}{\pi} \right], \quad (\text{II.40})$$

have a dependence on \mathbf{q}^2 of the intercept, which is not now a real eigenvalue and lacks a direct physical interpretation.

²³We pointed below that the BLM prescription is RS-independent up to formally subleading terms. In [FKLP02] it is shown how, while BLM predictions for the NLL pomeron intercept are very similar within physical renormalization schemes, BLM scale setting did not modify substantially $\overline{\text{MS}}$ results. In a sense this is because $\overline{\text{MS}}$ scheme is less sensitive to gg interactions. In our computations in MOM scheme, we use the usual Yennie gauge $\xi = 3$.

with $r_{\text{MOM}}^{(\beta)}(n, \nu) = r_{\text{MS}}^{(\beta)}(n, \nu) + T_{\text{MOM}}$, and the BLM scale given by (II.36)

$$\mathbf{q}^2_{\text{BLM}}^{\text{MOM}}(n, \nu) = \mathbf{q}^2 \exp \left[-\frac{4r_{\text{MOM}}^{(\beta)}(n, \nu)}{\beta_0} \right] = \mathbf{q}^2 \exp \left[\frac{1}{2}\chi_0(n, \nu) + \frac{1}{3} + \frac{4}{3}I \right]. \quad (\text{II.41})$$

With this proviso, we can go on to show the results for the observables defined in SEC. II.2.2, which were computed numerically. In FIG. II.7 the intercept (II.40) for $n = 0$ computed in MOM scheme with BLM scale is confronted with the MSYM intercept and the results at LL and NLL with no BLM scale fixing. The coupling for MSYM is chosen in a range between $a = \bar{\alpha}_s(\mathbf{q}^2/4)$ [MSYM₋] and $\bar{\alpha}_s(4\mathbf{q}^2)$ [MSYM₊], which corresponds to the light yellow band. This intercept for the conformal invariant MSYM theory at NLO is very close to the LO one, already hinting towards a better convergence than QCD. It is important to note that the MOM-BLM scheme is the closest to MSYM theory of all renormalization schemes in QCD. This is natural since the BLM scheme collects the conformal contributions to the observable. In FIG. II.6 we have taken a typical scale $\mathbf{q}^2 = 15 \text{ GeV}^2$ to show the asymptotic intercepts for the first conformal spins n in the MOM-BLM scheme, which can be read from the value of the BFKL kernel at $\nu = 0$. We observe the well-known fact that the dominant component is $n = 0$ with all the other intercepts being negative. A similar behavior is found for other schemes and in the MSYM case.

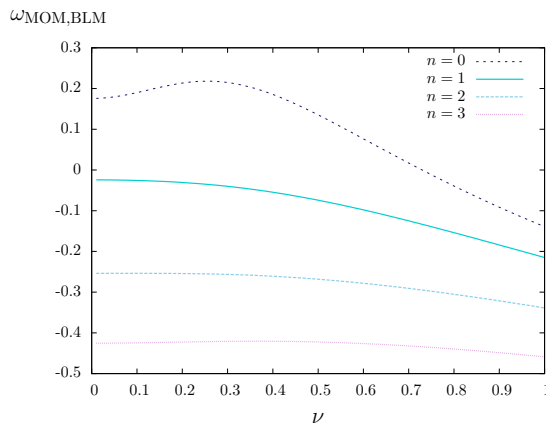


Figure II.6: Eigenvalues of the QCD BFKL kernel at NLL in MOM-BLM scheme, for different conformal spins n .

The $n = 0$ coefficient drives the cross section. The rise of C_0 (Eq. (II.29)) with y is shown in FIG. II.7 (right). There is a faster growth of the MSYM cross section showing that the NLO real emission in MSYM theory dominates over the virtual contributions in a much stronger fashion than in QCD, for any renormalization scheme. This also indicates that the effect of introducing the extra fields in the supersymmetric multiplet increases

II. Comparing QCD and $\mathcal{N} = 4$ SYM in the Regge Limit

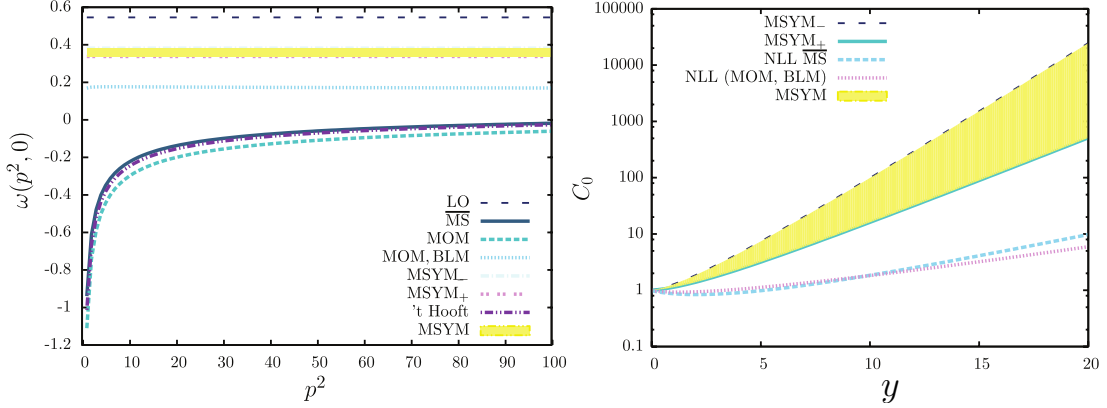


Figure II.7: (Left) Intercept vs jet resolution p^2 for different renormalization schemes in QCD and MSYM theory; (Right) Growth with dijet rapidity separation of the cross section in MSYM theory and QCD.

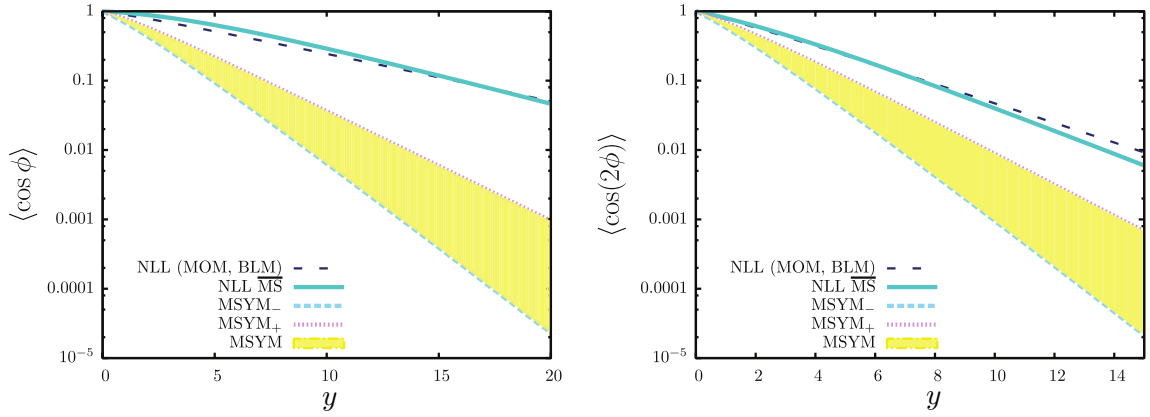


Figure II.8: Evolution of the average of $\cos \phi$ (left) and $\cos(2\phi)$ with jet rapidity separation in MSYM theory and QCD for different renormalization schemes.

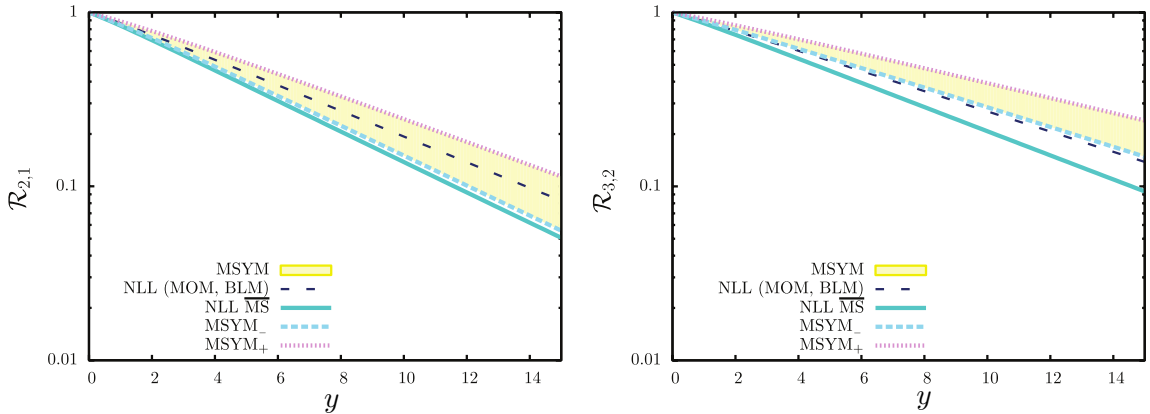


Figure II.9: Evolution of $\mathcal{R}_{2,1} = \frac{\langle \cos(2\phi) \rangle}{\langle \cos(\phi) \rangle}$ (left) and $\mathcal{R}_{3,2} = \frac{\langle \cos(3\phi) \rangle}{\langle \cos(2\phi) \rangle}$ with jet rapidity separation in MSYM theory and QCD for different renormalization schemes.

the minijet multiplicity in the final state (see next section). For small y the QCD result in the $\overline{\text{MS}}$ scheme is lower than in the MOM-BLM scheme, with the latter being closer to the $\mathcal{N} = 4$ SYM result. This is consistent with a renormalization scheme which resums conformal contributions. However, from $y \simeq 10$ the calculation in $\overline{\text{MS}}$ is now closer to the supersymmetric result. This hints at the collinear instability of the $n = 0$ component we discussed in SEC. II.2.2. It is natural to predict a similar crossing behavior at some y for any quantity sensitive to $n = 0$, like $\langle \cos(m\phi) \rangle$ (FIG. II.8). It is also interesting to note that dijets are less correlated in the azimuthal angle in $\mathcal{N} = 4$ SYM than in QCD, which corresponds to a higher multiplicity of parton radiation in the supersymmetric case.

The results in FIG. II.9 are more interesting. Here we plot a sample of the ratios of higher order correlations (II.30) as a function of rapidity. All low-order ratios show that QCD and MSYM predictions are extremely similar. Moreover, the agreement is systematically improved by the MOM-BLM scheme, independently of the separation in rapidity between the two tagged jets. Having removed the $n = 0$ dependence, the crossover does not take place any more.

These results are encouraging because they show that for well-chosen quantities, insensitive to the IR (in this case through the dependence on the PDFs) and with a good perturbative convergence, we can expect $\mathcal{N} = 4$ SYM computations to agree quantitatively with QCD. In the comparison, the selection of the renormalization prescription plays an important role. At least in the multi-Regge regime, where QCD is approximately conformal invariant, the choice of the BLM prescription seems to be the most natural choice.

3 THE DIFFUSION PATTERN IN $\mathcal{N} = 4$ SYM AT HIGH ENERGIES [CCM⁺13]

In this section we study in some detail the BFKL Green's function in QCD and $\mathcal{N} = 4$ SYM at next-to-leading order, where the evolution equations in both theories start being different. This is a topical subject in the context of studies of the pomeron at strong coupling (SEC. II.1.4). We separate the contributions of gluons from those of scalars and gluinos using a Monte Carlo implementation of the NLL BFKL equation, allowing us to give detailed information on the collinear behavior, the diffusion pattern and the multiplicity distributions of the Green's function.

3.1 The Gluon Green's Function in $\mathcal{N} = 4$ SYM

Consider the amplitude for off-shell reggeized gluons with transverse momenta $\mathbf{k}_{a,b}$, a relative azimuthal angle θ and a separation in rapidity y . The BFKL Green's function can be written, according to (I.153), as

$$f(\mathbf{k}_a, \mathbf{k}_b, y) = \sum_{n=-\infty}^{\infty} f_n(|\mathbf{k}_a|, |\mathbf{k}_b|, y) e^{in\theta};$$

$$f_n(|\mathbf{k}_a|, |\mathbf{k}_b|, y) = \int_0^{2\pi} \frac{d\theta}{2\pi} f(\mathbf{k}_a, \mathbf{k}_b, y) \cos(n\theta) = \frac{1}{\pi |\mathbf{k}_a| |\mathbf{k}_b|} \int \frac{d\gamma}{2\pi i} \left(\frac{\mathbf{k}_a^2}{\mathbf{k}_b^2} \right)^{\gamma - \frac{1}{2}} e^{\omega_n(a, \gamma)y}. \quad (\text{II.42})$$

The NLL BFKL eigenvalue $\omega_n(a, \gamma)$ (where a stands for the 't Hooft coupling in $\mathcal{N} = 4$ SYM and for $\bar{\alpha}_s$ in QCD), can be given by an expression unifying (I.161) and (II.8):

$$\begin{aligned} \omega_n(a, \gamma) = & \xi_{\Theta} \left(2\psi(1) - \psi\left(\gamma + \frac{n}{2}\right) - \psi\left(1 - \gamma + \frac{n}{2}\right) \right) + a^2 \frac{3}{2} \zeta(3) \\ & + \frac{a^2}{4} \left[\psi''\left(\gamma + \frac{n}{2}\right) + \psi''\left(1 - \gamma + \frac{n}{2}\right) - 2\Phi(n, \gamma) - 2\Phi(n, 1 - \gamma) \right] \\ & - \frac{\Theta a^2 \pi^2 \cos(\pi\gamma)}{4 \sin^2(\pi\gamma) (1 - 2\gamma)} \left\{ \left(3 + \frac{2 + 3\gamma(1 - \gamma)}{(3 - 2\gamma)(1 + 2\gamma)} \right) \delta_n^0 - \frac{\gamma(1 - \gamma) \delta_n^2}{2(3 - 2\gamma)(1 + 2\gamma)} \right\}. \end{aligned} \quad (\text{II.43})$$

The function of the coupling $\xi_{\Theta} = a + \frac{a^2}{4} \left(\frac{1}{3} - \frac{\pi^2}{3} + \Theta \right)$ has been introduced, where $\Theta = 1$ corresponds to diagrams with only gluons and $\Theta = 0$ to the full $\mathcal{N} = 4$ SYM result (there are cancellations due to the gluino and scalar contributions). We have not separated the scalars from the gluinos for simplicity since the expressions for the kernel, especially in k_T space, are rather complicated and do not add much information to our results. For this first, analytic, study we have not considered the contributions to the running of the coupling in the gluonic kernel since we wanted to work with true eigenfunctions also at NLO and keep all the terms in the kernel diagonal in γ space. But when working with a Monte Carlo code (SEC. II.3.2) we have included these running coupling terms (note that there are running contributions both in the gluon and gluino/scalars sectors independently, which cancel each other in the complete $N = 4$ SYM kernel).

Let us first scan the (anti)-collinear regions where one of the virtualities of the external reggeized gluons is much larger than the other. This is parameterized by the ratio k_a/k_b being away from one in the Green function values plotted in FIG. II.10 (we have fixed the coupling to 0.2, $y = 10$ and $k_b = 30$ GeV, but the features here discussed are generic). We have first focussed on the $n = 0$ component (azimuthal angle averaged kernel), which corresponds to pomeron exchange and is the relevant one when going to

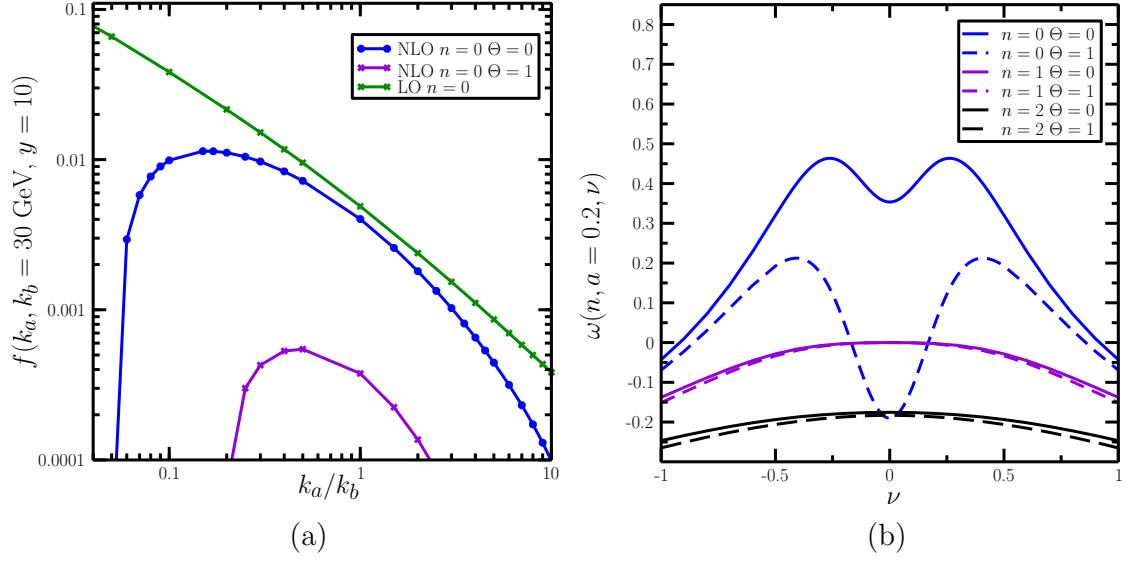


Figure II.10: (a) Collinear behavior of the gluon Green function for $n = 0$; (b) Eigenvalue of the BFKL kernel for different conformal spins, n .

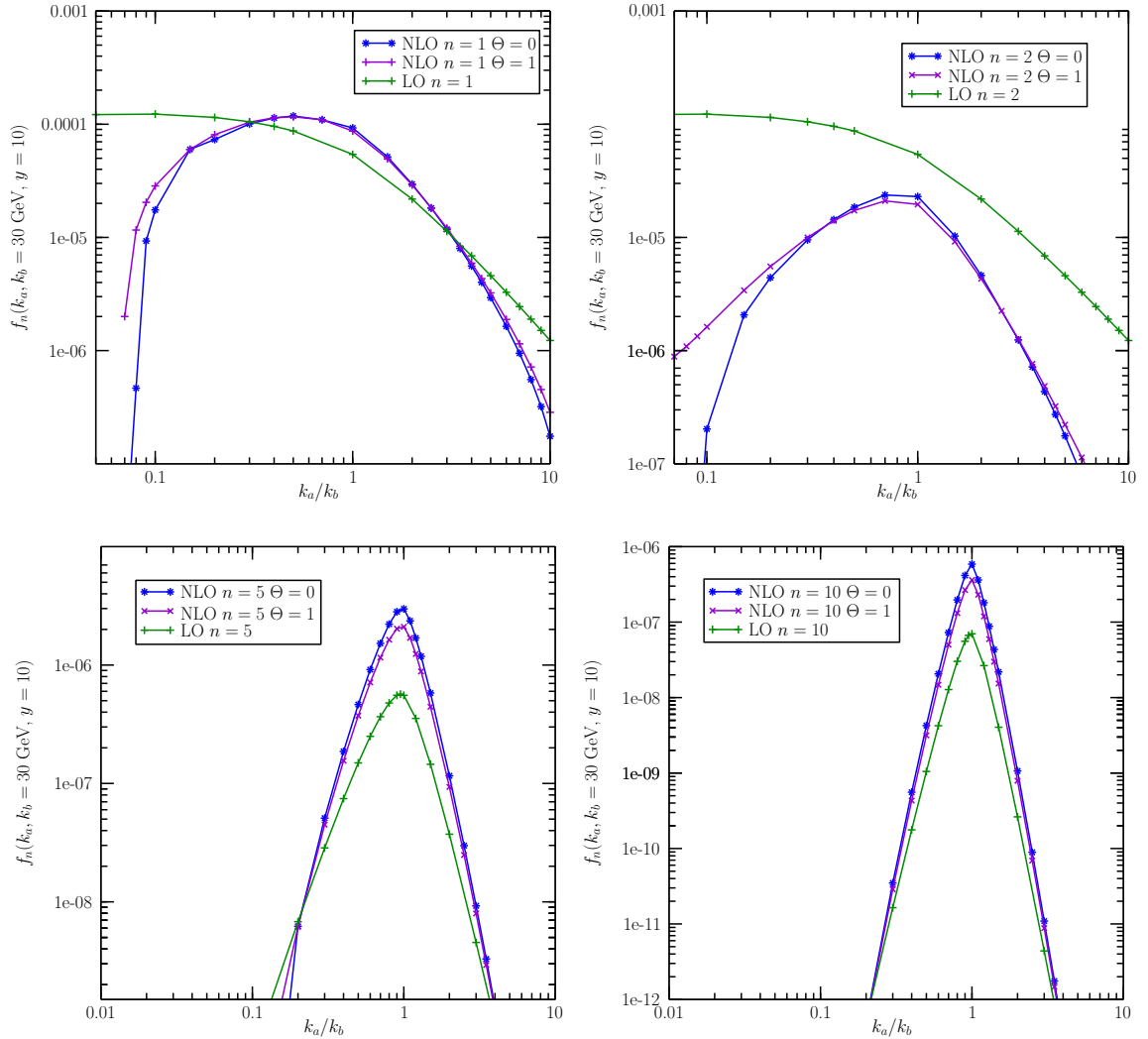


Figure II.11: Collinear behavior of the gluon Green function for different values of n .

II. Comparing QCD and $\mathcal{N} = 4$ SYM in the Regge Limit

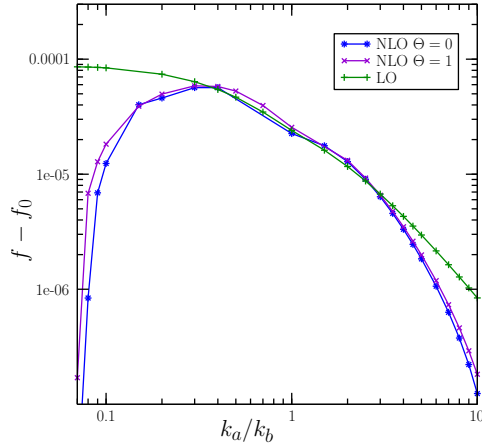


Figure II.12: Collinear behavior of the gluon Green function subtracting the $n = 0$ component.

the strong coupling limit [BPST07]. We observe that the LO Green function has good collinear behavior while the NLO lines go rapidly to zero when k_a is very different from k_b . This is a manifestation of the double maxima present in the eigenvalue of the kernel (FIG. II.10), as discussed in SEC. I.3.4. Since the eigenvalue is smaller, even negative at $\nu = 0$, for the purely gluonic case, it is in this case that the collinear behavior is worse (in the sense that the Green function hits negative values for values of k_a/k_b closer to one). The effect of the scalar and gluino pieces is to greatly improve the convergence, making the NLO corrections to the LO result not too large in a wide range of virtuality space.

In FIG. II.10 we also plot the $n = 1, 2$ eigenvalues and notice that the effect of the gluino and scalar contributions is very small. It is then natural to observe that, at the level of the gluon Green function, in FIG. II.11 the plots with $\Theta = 0, 1$ are very similar for all $n > 0$. We find it instructive to plot the full gluon Green function with all n components but subtracting the $n = 0$ term while showing the collinear shape in FIG. II.12. The perturbative convergence of the BFKL expansion for the $n \neq 0$ contributions is very good since the NLO corrections are very small in a very wide range of the plot.

We collect the full angular information in a single plot in FIG. II.13 (left). We have fixed $k_a = 20$ GeV, $k_b = 30$ GeV and $y = 3, 5$. The full NLO SUSY results are very similar in shape to the LO lines. An intriguing feature is that the Green function for the gluon contributions reaches a much smaller value at $\theta = \pi$ than when scalars and gluinos are included in the analysis ($\partial f / \partial \theta$ is much more negative in the $N = 4$ SYM case for $\theta > 1$).

To conclude this part of the analysis we can investigate the growth with energy of the gluon

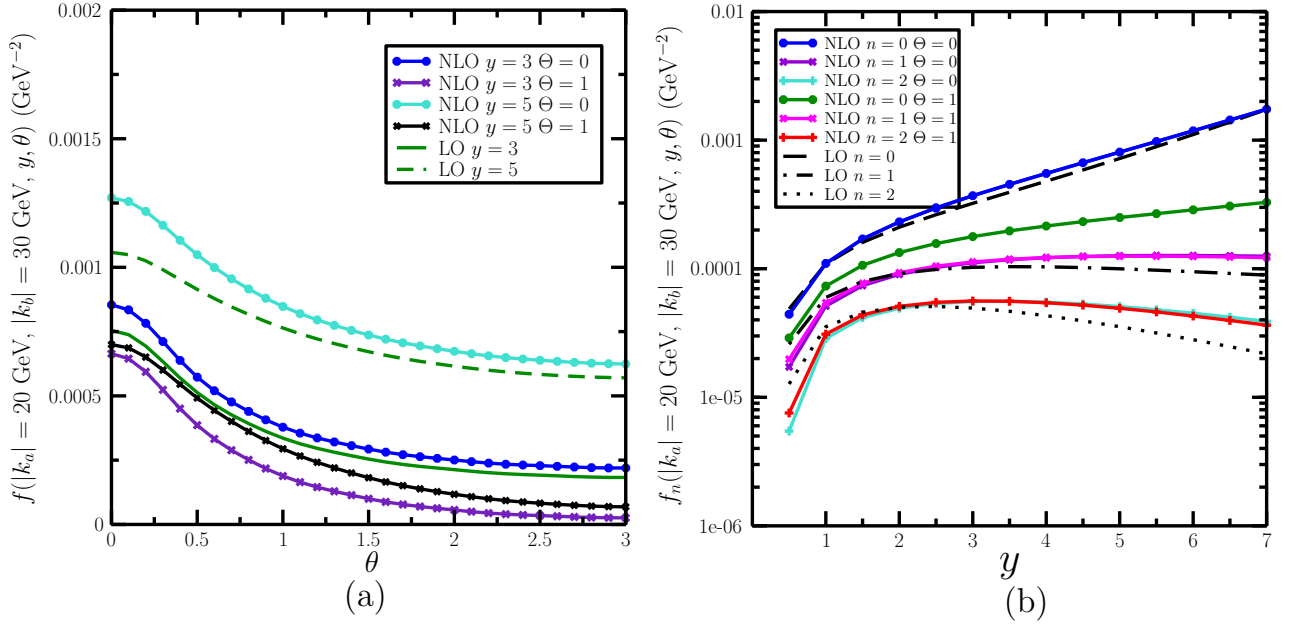


Figure II.13: (a) The gluon Green function versus θ ; (b) Growth with energy of the gluon Green function for different conformal spins n .

Green function for different conformal spins n . This is done in FIG. II.13 (right), where we can see that the LO and the full NLO SUSY results are surprisingly similar for the range of y we have chosen to plot (for $n = 0$). It is clear that the scalar and gluino contributions do push the Green function to higher values. This implies that they generate a larger amount of real emission and/or reduce the relative weight of the virtual diagrams, mainly via their contribution to the gluon Regge trajectory. For the coefficients associated to $n > 0$ the non-gluonic terms do not modify the gluonic ones, they give a very small contribution. As in QCD, only the $n = 0$ component, associated to the hard pomeron, grows with energy.

Let us highlight a very interesting property of the NLO eigenvalue, already pointed out in Ref. [Sab06] for the QCD case. When $n = 1$ the asymptotic intercept (at $\gamma = 1/2$) can be written as

$$\omega_{n=1} \left(a, \gamma = \frac{1}{2} \right) = a^2 \left(\frac{3}{2} \zeta(3) + \frac{1}{2} \psi''(1) - \Phi \left(1, \frac{1}{2} \right) \right) = 0. \quad (\text{II.44})$$

This result is independent of the scalar and gluino terms, i.e. it is an effect only associated to the gluon sector. A similar feature was found in QCD, where the quark contributions to this intercept were always multiplying the LO eigenvalue, which is also zero for $(\gamma, n) = (1/2, 1)$. The fact that this intercept is zero at LO and NLO seems to indicate that it is protected by some symmetry not broken by radiative corrections. It would be instructive to find out if it is present in the strong coupling limit and its connection to all-orders corrections to

II. Comparing QCD and $\mathcal{N} = 4$ SYM in the Regge Limit

odderon²⁴ exchange in QCD and SUSY theories (see [Kov12] for a related discussion).

3.2 Monte Carlo Approach to the BFKL Equation

In order to proceed further and obtain more exclusive information from the different pieces of the SUSY NLL BFKL kernel now we use a different, more numerical method, which generalizes the original work in [Sch97, OS97] (see [AS03, AS04b, AS04a, CDSS11, CS12a, CS12b] for related work). The starting point is the following representation for the BFKL equation in momentum space [AS03]

$$\begin{aligned} (\omega - \omega(\mathbf{k}_a^2, \lambda^2)) f_\omega(\mathbf{k}_a, \mathbf{k}_b) &= \delta^{(2)}(\mathbf{k}_a - \mathbf{k}_b) \\ &+ \int d^2\mathbf{k} \left(\frac{\xi_\Theta}{\pi\mathbf{k}^2} \Theta(\mathbf{k}^2 - \lambda^2) + \mathcal{K}(\mathbf{k}_a, \mathbf{k}_a + \mathbf{k}) \right) f_\omega(\mathbf{k}_a + \mathbf{k}, \mathbf{k}_b). \end{aligned} \quad (\text{II.45})$$

Here λ is a mass parameter used to regularize the infrared divergences. Results are λ -independent for small values of λ [AS03]. \mathcal{K} here is the ϵ -independent piece of the dimensionally regulated emission kernel

$$\begin{aligned} \mathcal{K}(\mathbf{q}, \mathbf{q}') &= \frac{a^2}{4\pi} \left\{ -\frac{1}{(\mathbf{q} - \mathbf{q}')^2} \ln^2 \frac{\mathbf{q}^2}{\mathbf{q}'^2} + \frac{2(\mathbf{q}^2 - \mathbf{q}'^2)}{(\mathbf{q} - \mathbf{q}')^2(\mathbf{q} + \mathbf{q}')^2} \right. \\ &\times \left(\frac{1}{2} \ln \frac{\mathbf{q}^2}{\mathbf{q}'^2} \ln \frac{\mathbf{q}^2 \mathbf{q}'^2 (\mathbf{q} - \mathbf{q}')^4}{(\mathbf{q}^2 + \mathbf{q}'^2)^4} + \left(\int_0^{-\frac{\mathbf{q}^2}{\mathbf{q}'^2}} - \int_0^{-\frac{\mathbf{q}'^2}{\mathbf{q}^2}} \right) dt \frac{\ln(1-t)}{t} \right) \\ &- \left(1 - \frac{(\mathbf{q}^2 - \mathbf{q}'^2)^2}{(\mathbf{q} - \mathbf{q}')^2(\mathbf{q} + \mathbf{q}')^2} \right) \left(\left(\int_0^1 - \int_1^\infty \right) dz \frac{1}{(\mathbf{q}' - z\mathbf{q})^2} \ln \frac{(z\mathbf{q})^2}{\mathbf{q}'^2} \right) \left. \right\} \\ &+ \Theta \frac{a^2}{4\pi} \left\{ \frac{(3(\mathbf{q} \cdot \mathbf{q}')^2 - 2\mathbf{q}^2 \mathbf{q}'^2)}{16\mathbf{q}^2 \mathbf{q}'^2} \left(\frac{2}{\mathbf{q}^2} + \frac{2}{\mathbf{q}'^2} + \left(\frac{1}{\mathbf{q}'^2} - \frac{1}{\mathbf{q}^2} \right) \ln \frac{\mathbf{q}^2}{\mathbf{q}'^2} \right) \right. \\ &- \left. \left(4 - \frac{(\mathbf{q}^2 + \mathbf{q}'^2)^2}{8\mathbf{q}^2 \mathbf{q}'^2} - \frac{(2\mathbf{q}^2 \mathbf{q}'^2 - 3\mathbf{q}^4 - 3\mathbf{q}'^4)}{16\mathbf{q}^4 \mathbf{q}'^4} (\mathbf{q} \cdot \mathbf{q}')^2 \right) \int_0^\infty \frac{dx}{\mathbf{q}^2 + x^2 \mathbf{q}'^2} \ln \left| \frac{1+x}{1-x} \right| \right\}. \end{aligned} \quad (\text{II.46})$$

and the NLL Regge gluon trajectory reads in this mass regularization

$$\omega(\mathbf{q}^2, \lambda^2) = -\xi_\Theta \ln \frac{\mathbf{q}^2}{\lambda^2} + a^2 \frac{3}{2} \zeta(3). \quad (\text{II.47})$$

²⁴The odderon is the leading exchange in hadronic scattering processes at high energies in which negative charge conjugation and parity quantum numbers are transferred in the t -channel. From the QCD perspective it is a bound state of three reggeized gluons [Ewe03]. An interesting property of the Bartels-Lipatov-Vacca odderon solution to the BKP equations [BLV00] is that its intercept is $\alpha_{\mathcal{O}} - 1 = \bar{\alpha}_s \chi_{\mathcal{O}}(n = \pm 1, \nu = 0) = 0$. This result seems to hold in the NLL approximation [Sab06, Kov12], possibly indicating that some underlying symmetry protects the value of the odderon intercept from perturbative corrections.

This mass regularization is much more convenient since it explicitly cancels the IR divergences of the kernel and the trajectory. Now it is possible to solve this equation iteratively and go back to rapidity space to obtain the following expression for the gluon Green function

$$\begin{aligned}
 f(\mathbf{k}_a, \mathbf{k}_b, y) = & \exp\left(\omega\left(\mathbf{k}_a^2, \lambda^2\right) y\right) \left\{ \delta^{(2)}(\mathbf{k}_a - \mathbf{k}_b) + \sum_{n=1}^{\infty} \prod_{i=1}^n \int d^2 \mathbf{k}_i \left[\frac{\Theta\left(\mathbf{k}_i^2 - \lambda^2\right)}{\pi \mathbf{k}_i^2} \xi_{\Theta} \right. \right. \\
 & + \mathcal{K}\left(\mathbf{k}_a + \sum_{l=0}^{i-1} \mathbf{k}_l, \mathbf{k}_a + \sum_{l=1}^i \mathbf{k}_l\right) \left. \int_0^{y_{i-1}} dy_i \exp\left[\omega\left(\left(\mathbf{k}_a + \sum_{l=1}^i \mathbf{k}_l\right)^2, \lambda^2\right)\right] \right. \\
 & \left. \left. - \omega\left(\left(\mathbf{k}_a + \sum_{l=1}^{i-1} \mathbf{k}_l\right)^2, \lambda^2\right)\right] y_i \delta^{(2)}\left(\sum_{l=1}^n \mathbf{k}_l + \mathbf{k}_a - \mathbf{k}_b\right) \right\}, \quad (\text{II.48})
 \end{aligned}$$

where $y_0 \equiv y$. We have obtained numerical results for this formula by performing a Monte Carlo integration of each of the terms in the sum [CS], which implies to solve a large amount of nested integrals in transverse momentum and rapidity space. This is a rather complicated procedure where the correct sampling of the integrands plays a very important role, but which allows for a complete handling of the exclusive information in the parton ladder since we know the statistical weight of the different final state configuration.

3.3 Analysis of Diffusion and Multiplicities

With the help of the Monte Carlo code, we can check that the distribution in the number of iterations of the kernel needed to construct the gluon Green function does not vary, qualitatively, when scalars and gluinos are added to the gluon terms, which drive the multiplicity distribution (see FIG. II.14, where the Green function corresponds to the area under the plots.). This statement is independent from introducing a running of the coupling in the gluon (QCD with no quarks) kernel (see last plot in FIG. II.14).

It is also possible to find out the typical transverse momentum scale running in the internal propagators of the BFKL ladder. This is conveniently shown in the Bartels' cigar plot²⁵ [Bar93, BLV96] in FIG. II.15 where the variable $\tau = \log \langle |\boldsymbol{\kappa}|_i \rangle / (\text{GeV}^2)$ is calculated (together with the lines of one standard deviation towards the IR and UV) as a function of the normalized rapidities of the corresponding emitted particles. The main lesson to be taken from these plots is that the region with diffusion in the IR is fully governed by the gluon

²⁵The Bartels' cigar measures the typical transverse momentum $\boldsymbol{\kappa}^2$ of a t -channel gluon in the BFKL ladder. Consider picking up a specific rung, dividing the ladder in two sub-ladders with corresponding Green's functions $f(\mathbf{k}, \boldsymbol{\kappa}, Y - y)$ and $f(\boldsymbol{\kappa}, \mathbf{k}', y)$, with Y the total rapidity difference in the original ladder. The $\boldsymbol{\kappa}$ -distribution is then given, for $\mathbf{k}^2 \sim \mathbf{k}'^2 \sim \boldsymbol{\kappa}^2$, by $\frac{dn}{d\boldsymbol{\kappa}^2} = \boldsymbol{\kappa}^2 f(\mathbf{k}, \boldsymbol{\kappa}, Y - y) f(\boldsymbol{\kappa}, \mathbf{k}', y) \sim \exp\left[-\frac{1}{56\zeta(3)\bar{\alpha}_s} \left(\frac{\ln^2(|\mathbf{k}|/|\boldsymbol{\kappa}|)}{Y-y} - \frac{\ln^2(|\boldsymbol{\kappa}|/|\mathbf{k}'|)}{y}\right)\right]$ (cf. (I.155)), in the diffusion approximation.

II. Comparing QCD and $\mathcal{N} = 4$ SYM in the Regge Limit

dynamics in the SUSY kernel (setting $\Theta = 0, 1$ does not modify the lower lines) while in the UV region the scalars and gluinos do squeeze the plot downwards, decreasing the diffusion probability towards large scales.

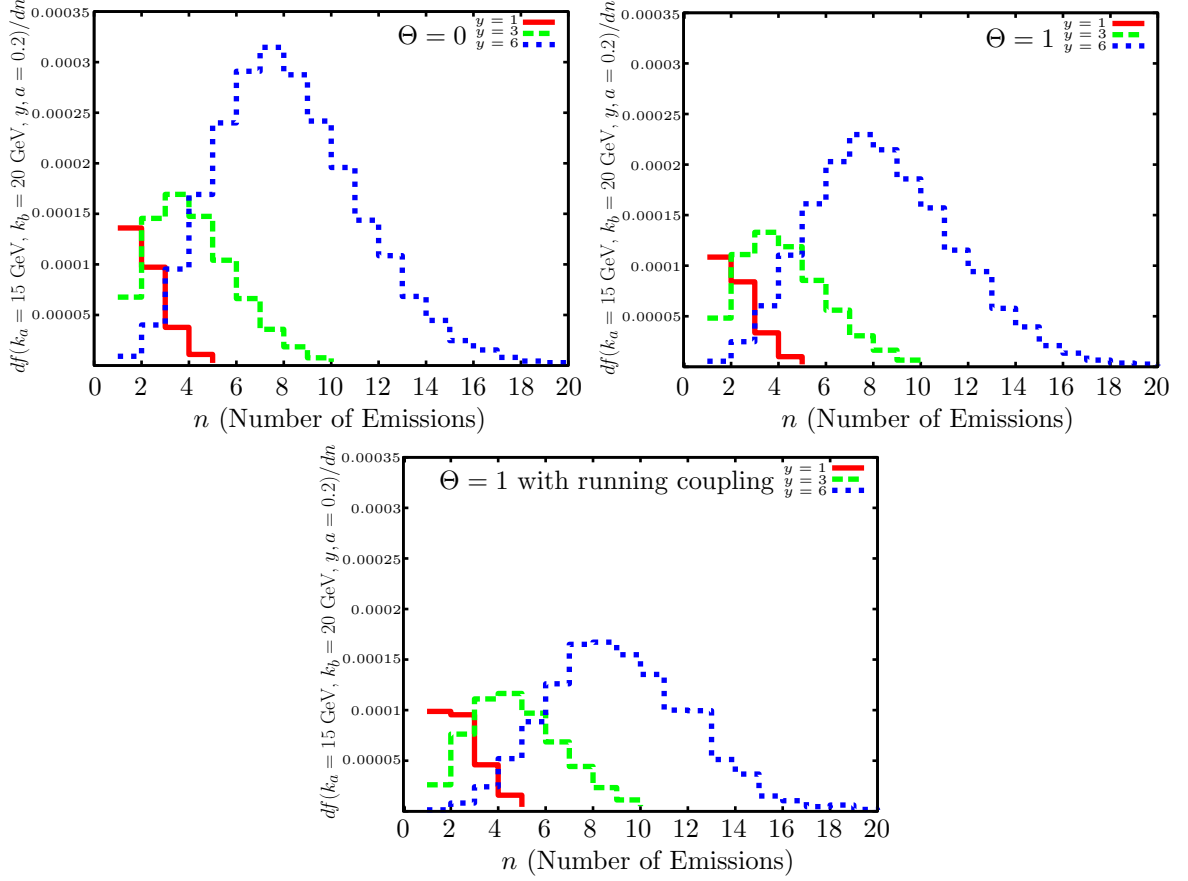


Figure II.14: Multiplicity distribution in the number of emissions contributing to the gluon Green function.

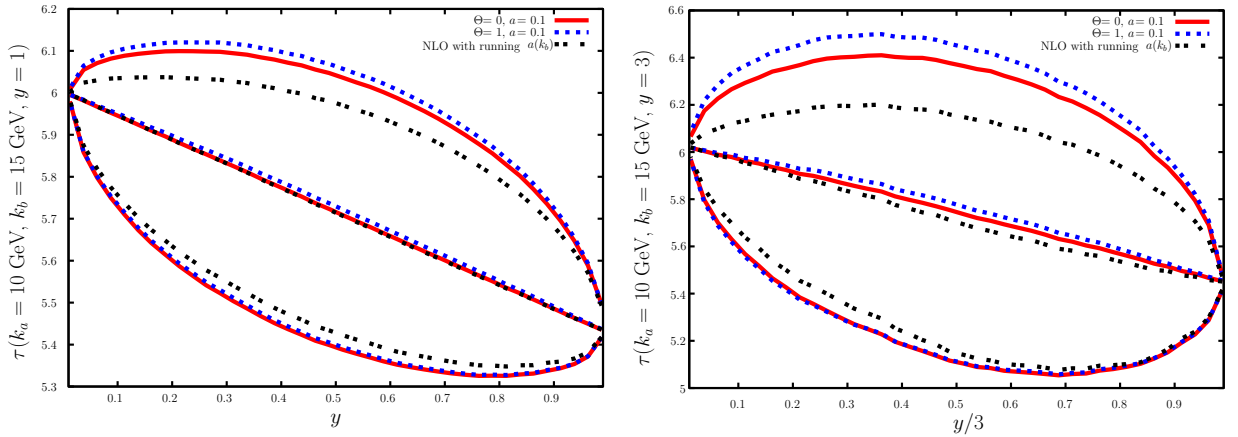
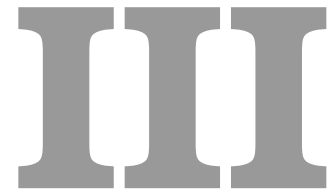


Figure II.15: Diffusion plots for the propagation of internal modes into IR and UV regions in transverse momenta when constructing the gluon Green function: $y = 1$ (left), $y = 3$ (right).



Lipatov Effective Action Approach to High Energy QCD

Effective field theories are powerful tools to deal with problems involving a hierarchy of characteristic scales. This is precisely the case in the high energy limit of gauge theories. As we have seen, it seems natural to reformulate in this region QCD in terms of reggeized gluon (reggeon)¹ interactions. In particular, one should expect to make contact with Gribov's reggeon field theory (SEC. I.2.3).

Another motivation for writing a high-energy effective action for QCD comes from the request of unitarity (SEC. I.4.1). A hermitian Lagrangian automatically incorporates all the requirements of unitarity in the simplest possible way. In particular it should include the ingredients to describe nonlinear evolution (SEC. I.5). In this chapter, we will discuss Lipatov's proposal for such an effective action. First of all, we review in some detail its original construction, which helps understand and interpret the subtleties of this action. Afterwards, we present a program to make sense of Lipatov's action beyond tree level, and illustrate the underlying philosophy with several perturbative computations.

¹In this chapter we will use the word reggeon in the sense of reggeized gluon state.

1 LIPATOV'S EFFECTIVE ACTION

1.1 Virtual Modes in Multi-Regge Kinematics

Gluon production amplitudes in MRK are given by the remarkably simple factorized expression (I.130)

$$A_{2 \rightarrow 2+n}^{\text{MRK}} = A_{2 \rightarrow 2+n}^{\text{tree}} \prod_{i=1}^{n+1} s_i^{\omega(t_i)}, \quad A_{2 \rightarrow 2+n}^{\text{tree}} = 2gs T_{A'A}^{c_1} \Gamma_1 \frac{1}{t_1} g T_{c_2 c_1}^{d_1} \Gamma_{2,1}^1 \frac{1}{t_2} \cdots g T_{c_{n+1} c_n}^{d_n} \Gamma_{n+1,n}^n \frac{1}{t_{n+1}} g T_{B'B}^{c_{n+1}} \Gamma_2, \quad (\text{III.1})$$

where A, B and $A', B', d_r (r = 1, \dots, n)$ are color indices for initial and final gluons correspondingly. We also have included the gluon-gluon-reggeon (GGR) and reggeon-reggeon-gluon (RRG) vertices

$$\begin{aligned} \Gamma_1 &= \frac{1}{2} \varepsilon_{\nu}^{\lambda A} \varepsilon_{\nu'}^{*\lambda A'} \Gamma^{\nu\nu'+}; & \Gamma_2 &= \frac{1}{2} \varepsilon_{\nu}^{\lambda B} \varepsilon_{\nu'}^{*\lambda B'} \Gamma^{\nu\nu'-}; & \Gamma_{r+1,r}^r &= -\frac{1}{2} \Gamma^{\mu+-}(q_r, q_{r+1}) \varepsilon_{\mu}^{*\lambda r}(k_r); \\ \Gamma^{\nu\nu'+}(p_A, p_{A'}) &= \gamma^{\nu\nu'+}(p_A, p_{A'}) - t(n^+)^{\nu} \frac{1}{p_A^+} (n^+)^{\nu'}; \\ \gamma^{\nu\nu'+}(p_A, p_{A'}) &= (p_a^+ + p_{A'}^+) g^{\nu\nu'} - 2p_{A'}^{\nu'} (n^+)^{\nu} - 2p_A^{\nu} (n^+)^{\nu'}; \\ \Gamma^{\mu+-}(q_1, q_2) &= -2C^{\mu}(q_1, q_2) = \gamma^{\mu+-} + \Delta^{\mu+-}, & \Delta^{\mu+-}(q_1, q_2) &= -2t_1 \frac{(n^-)^{\mu}}{k_1^-} + 2t_2 \frac{(n^+)^{\mu}}{k_1^+}. \end{aligned} \quad (\text{III.2})$$

We notice that both GGR and RRG vertices consist of the light-cone projection of the 3-gluon Yang-Mills vertex $\gamma^{\mu\nu\rho}$ and an additional induced term.

These effective vertices can be derived in the spirit of EFT directly from the QCD action [Lip91, KLS94, Szy94, KLS95], integrating out heavy modes. To do this, the gauge has to be fixed so that the identification of heavy modes is meaningful. Considering for the moment pure Yang-Mills theory², the action is simplified by choosing the light-cone gauge, $A_- = 0$ say ($\sigma = 1, 2$; $\square \equiv 4(\partial_+ \partial_- - \partial \partial^*)$, $\partial_{\pm} = \frac{1}{2}(\partial_0 \pm \partial_3)$, $\partial = \frac{1}{2}(\partial_1 - i\partial_2)$, $\partial^* = (\partial)^*$):

$$\begin{aligned} S_{\text{YM}} &= \int d^4x \left[\frac{1}{2} (A_{\sigma}^a \square A^{a\sigma} + (\partial_- A_+^a + \partial_{\sigma} A^{a\sigma})^2) \right. \\ &\quad \left. - g f^{abc} ((A_{\sigma}^a \partial_- A^{b\sigma}) A_+^c - A_{\sigma}^b A_{\sigma}^c \partial^{\sigma} A^{a\sigma}) - \frac{g^2}{4} f^{abc} f^{ab'c'} A_{\sigma}^b A_{\sigma}^c A^{b'\sigma} A^{c'\sigma} \right], \end{aligned} \quad (\text{III.3})$$

in such a way that A_+ only appears quadratically and one can perform a Gaussian integration in $A_+^a = A_+^a + \partial_-^{-1} \partial_{\sigma} A^{a\sigma}$, leaving a Lagrangian with three terms $\mathcal{L} = \mathcal{L}^{(2)} + \mathcal{L}^{(3)} + \mathcal{L}^{(4)}$:

²Terms involving quark fields can be reconstructed from pure gluodynamics using the supersymmetry of QCD action with a Majorana fermion in the adjoint representation (the $\mathcal{N} = 1$ SYM action) [KLS94, KLS95].

$$\begin{aligned}\mathcal{L}^{(2)} &= -\frac{1}{2}A^a\Box A^{a*}, \quad \mathcal{L}^{(4)} = -\frac{g^2}{8}[(AT^a\overleftrightarrow{\partial}_-A^*)\partial_-^{-2}(AT^a\overleftrightarrow{\partial}_-A^*) + (AT^aA^*)(AT^aA^*)], \\ \mathcal{L}^{(3)} &= -i\frac{g}{2}[(AT^a\overleftrightarrow{\partial}_-A^*)\partial_-^{-1}(\partial A^a + \partial^*A^{a*}) - (AT^aA^*)(\partial A - \partial^*A^*)] \equiv \mathcal{L}^{(3a)} + \mathcal{L}^{(3b)},\end{aligned}\tag{III.4}$$

where the notations $\overleftrightarrow{\partial} = \overrightarrow{\partial} - \overleftarrow{\partial}$ and $(\mathcal{A}_1T^a\mathcal{A}_2) = -if^{abc}\mathcal{A}_1^b\mathcal{A}_2^c$ have been used.

One can now integrate over heavy modes, i.e. those not appearing in the initial or final states, to get an effective action. Produced particles in the ladder will be close to their mass shell, $|k_+k_- - kk^*| \ll \mu^2$ (*scattering modes*), where $k = k_\perp^1 + ik_\perp^2$ and $k^* = k_\perp^1 - ik_\perp^2$; and t -channel exchanges are essentially transverse, $k_+k_- \ll kk^* \sim \mu^2$ (*exchange modes*), so heavy modes in MRK are to be identified with the strongly virtual contributions with $k_+k_- \gg kk^*$. Then we split our fields in heavy and moderately virtual modes respectively, $A_\rho \rightarrow A_\rho^H + A_\rho^M$, and substitute in (III.4). By definition, mixing of modes in propagators is small, therefore no interference appears in the kinetic Lagrangian: $\mathcal{L}^{(2)} \simeq 2A^{H\sigma}\partial_+\partial_-A^{H\sigma} + \frac{1}{2}A_\sigma^M\Box A^{M\sigma}$. For the piece of the interaction Lagrangian involving heavy modes we only keep the dominant components in MRK, i.e. those involving the operator ∂_-^{-1} acting on the field with smaller k_- component. With this in mind we get

$$\mathcal{L}_{\text{int}}^H \simeq 2A_\rho^H\partial_+\partial_-A^{H\rho} + ig[A_\sigma^MT^a\partial_-A^{H\sigma} + A_\sigma^HT^a\partial_-A^{M\sigma}](\partial_-^{-1}\partial_\rho A^{M\rho}).\tag{III.5}$$

The path integral over heavy modes can now be performed (e.g. using the equations of motion), giving a contribution

$$\Delta\mathcal{L} = \frac{g^2}{4}A_\rho^MT^a\partial_-A^{M\rho}\left(\frac{1}{\partial_+\partial_-}\partial_\sigma A^{M\sigma}\right)\partial_-^{-1}\partial_\eta A^{M\eta}\tag{III.6}$$

to the effective Lagrangian $\mathcal{L}^{\text{eff}} = \mathcal{L}_{A \rightarrow A^M}^{(\text{III.4})} + \Delta\mathcal{L}$. One should remember that due to MRK there is also a strong ordering in k_- among the A^M modes³. To make this manifest we split A^M in two contributions A and \tilde{A} indicating, respectively, scattering and exchange modes. In terms of these new fields $\Delta\mathcal{L}$ can be expressed as the product of more fundamental pieces: the triple vertex from $\mathcal{L}^{(3)}$ in (III.4)

$$\mathcal{L}^{\text{trv}} = -ig(\partial_-A_\sigma)T^aA^{M\sigma}\partial_-^{-1}(\partial_\rho\tilde{A}^{\rho}),\tag{III.7}$$

³For instance, in (III.6), the k_- component of the first two A^M fields is much bigger than the one for the last two fields.

III. Lipatov Effective Action Approach to High Energy QCD

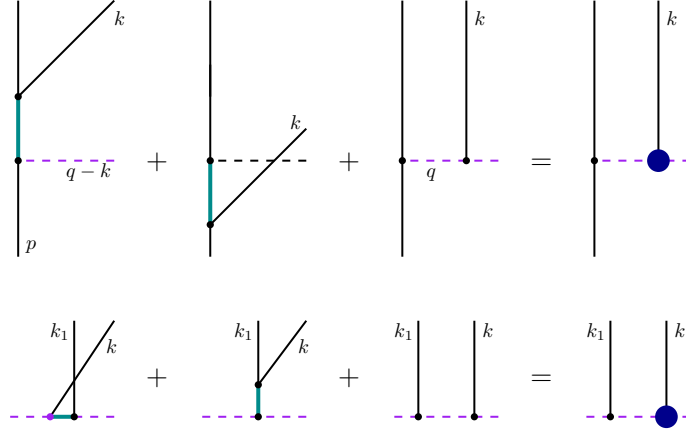


Figure III.1: The GGR (top) and RGG (bottom) vertices as a sum of induced and projection contributions. Black, dashed purple and fat cyan lines denote respectively scattering, exchange and heavy modes. The s -channel goes vertically and the t -channel horizontally. Lines going to the right carry smaller k_- . Each subdiagram represents a relevant contribution in MRK to $\mathcal{L}^{(3)}$. Effective vertices emerge from integrating out the heavy propagator, in the same way as the Fermi's coupling appears from collapsing a W propagator.

a transverse propagator $\frac{1}{2}\tilde{A}_q^a\partial_\sigma\partial^\sigma\tilde{A}^{ae}$, and an induced vertex whose associated Feynman rule can be identified to the induced contribution to the RGG vertex (FIG. III.1)

$$\Delta\mathcal{L}^{\text{ind}} = \frac{ig}{4}\partial_-\partial_-\tilde{A}^{ae}\left(\frac{1}{\partial_+\partial_-}\partial_\sigma A^{M\sigma}\right)T^a\partial_-^{-1}\partial_\eta A^{M\eta}. \quad (\text{III.8})$$

The terms not included in this vertex turn out to cancel against the original contributions coming from $\mathcal{L}^{(4)}$, so that collecting pieces we can write the effective Lagrangian as $\mathcal{L}^{\text{eff}} = (\mathcal{L}^{(2)} + \mathcal{L}^{(3b)})_{A\rightarrow A^M} + \mathcal{L}^{\text{trv}} + \Delta\mathcal{L}^{\text{ind}}$. Introducing the notation [Lip91, KLS94]⁴

$$\begin{aligned} A &= i\partial^*\phi, \quad A^* = -i\partial\phi^*; & A_+ &= -\frac{1}{\partial_-}\partial_\sigma\tilde{A}^\sigma = -\frac{2}{\partial_-}\partial\tilde{A}, \\ A_- &= -2\frac{\partial_-\partial_\sigma}{\partial_-\partial^e}\tilde{A}^\sigma = \frac{1}{2}\partial_-(\partial\partial^*)^{-1}(\partial\tilde{A} + \partial^*\tilde{A}^*). \end{aligned} \quad (\text{III.9})$$

The effective Lagrangian can be written compactly as a sum of three pieces⁵

$$\begin{aligned} \mathcal{L}^{\text{eff}} &= \mathcal{L}^{\text{kin}} + \mathcal{L}^s + \mathcal{L}^p, & \mathcal{L}^{\text{kin}} &= \frac{1}{2}(\partial_+\partial\phi^a)(\partial_-\partial^*\phi^{*a}) + 2(\partial A_+^a)(\partial^*A_-^a), \\ \mathcal{L}^s &= j_+^a A_-^a + j_-^a A_+^a, & \mathcal{L}^p &= j^a\phi^{*a} + j^{*a}\phi^a, \end{aligned} \quad (\text{III.10})$$

⁴ A_+ and A_- are defined to match the original field components A_+ and A_- , which are found applying the equations of motion to the QCD action. MRK imposes $\partial_\mp A_\pm = 0$ (see below). A_+ and A_- can then be considered as the fields creating and annihilating reggeized gluons. In what respects the complex scalar field ϕ , it was introduced in [Lip91] as the field describing the gauge transformations of A .

⁵Using the constraint $\partial_\mp A_\pm = 0$, derivatives can also act on the fields ϕ^* through integration by parts.

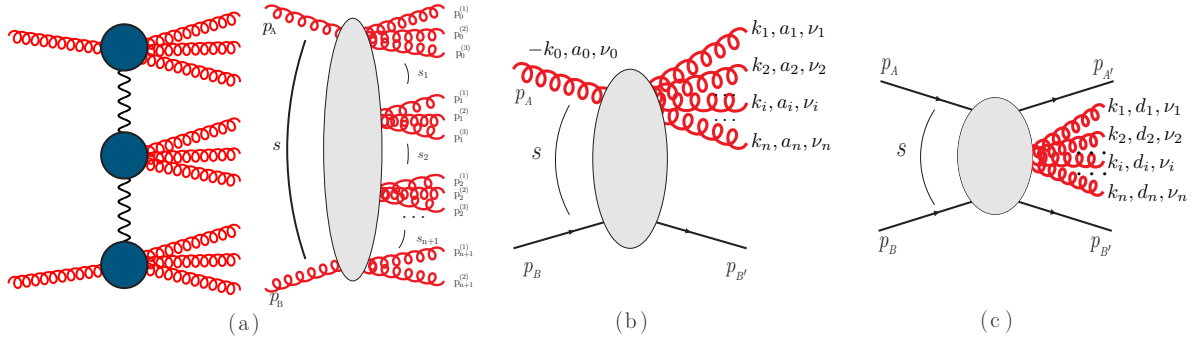


Figure III.2: (a) *Quasi-Multi-Regge Kinematics*; (b) *Quasielastic scattering of quark B on gluon A, where the gluon fragments into a cluster of gluons nearby in rapidity*; (c) *Central production*.

where \mathcal{L}^s and \mathcal{L}^p describe, respectively, the physical gluon scattering caused by the emission or absorption of a reggeized gluon (\sim GGR vertex) and the gluon production in the collision of two reggeized gluons (\sim RRG vertex), in terms of the currents

$$\begin{aligned} j_+^a &= ig(\partial^* \phi^*) T^a \partial_+ \partial \phi, & j_-^a &= ig(\partial \phi^*) T^a \partial_- \partial^* \phi, \\ j^a &= g(\partial^* A_-) T^a \partial A_+, & j^{*a} &= g(\partial^* A_+) T^a \partial A_-. \end{aligned} \quad (\text{III.11})$$

Notice that despite having integrated out heavy modes we still have two different kinds of fields with different momentum ranges suitable for them. One should not allow A_{\pm} to have momenta with $|k_+ k_-| \geq |\mathbf{k}^2|$, because this would violate the conditions of MRK. In the same way, one should not allow the field ϕ to have momenta with $|k_+ k_-| \ll |\mathbf{k}^2|$, because this would double a contribution already accounted for by the Coulomb fields. This reflects the fact that usual effective theory techniques are difficult to apply when a whole hierarchy of scales appear as in MRK (see [Don09, DW10] for a related discussion).

The Feynman rules obtained from the action (III.10) can be seen [KLS94] to generate the effective vertices (III.2) on the mass-shell. However, for virtual gluons these vertices are different, leading to inconsistencies in the theory. This drawback is absent in a more general setup that we describe in the remainder of this section.

1.2 Quasielastic and Central Production Vertices in QMRK

In SEC. 1.3.4 we pointed out that each time we allowed two gluons to be emitted close in rapidity along the BFKL ladder, we lost one $\ln s$ factor, or alternatively, we went to consider $\alpha_s (\alpha_s \ln s)^n$ terms (NLL approximation). This situation can be generalized to quasi-multi-Regge kinematics (QMRK), in which an arbitrary number of particles are

III. Lipatov Effective Action Approach to High Energy QCD

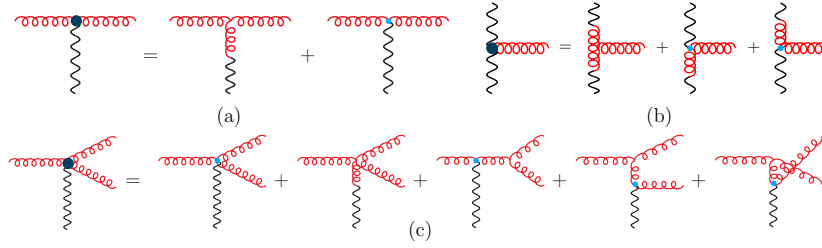


Figure III.3: (a) *GGR* vertex; (b) *RRG* vertex; (c) *Quasielastic two-gluon production*. Effective vertices consist of light-cone projections of usual QCD vertices and induced vertices (denoted by blue points).

allowed to be produced close to each other in rapidity in clusters well separated in rapidity among themselves (FIG. III.2). An effective action valid in this generalized kinematics was built by Lipatov [Lip95, Lip97] exploiting the requirement of gauge invariance. In the following we describe the main steps in the derivation, following closely [Lip95].

Consider first a quasielastic production process (FIG. III.2 (right)). With the notation as in the figure we can write, omitting polarization vectors of outgoing gluons $\varepsilon_{\nu_i}^*(k_i)$, the production amplitude as

$$A_{a_0 a_1 \dots a_n B' B}^{\nu_0 \nu_1 \dots \nu_n} = -\phi_{a_0 a_1 \dots a_n c}^{\nu_0 \nu_1 \dots \nu_n +}(k_0, k_1, \dots, k_n) \frac{1}{t} g p_B^- T_{B' B}^c \delta_{\lambda_{B'} \lambda_B}, \quad \sum_{i=0}^n k_i^+ = 0. \quad (\text{III.12})$$

For the simplest case in which one extra gluon is produced, one has at tree level [FL89]

$$\begin{aligned} \phi_{a_0 a_1 a_2 c}^{\nu_0 \nu_1 \nu_2 +} = g^2 \left\{ \Gamma_{a_0 a_1 a_2 c}^{\nu_0 \nu_1 \nu_2 +} - T_{a_1 a_0}^a T_{a_2 a}^c \frac{\gamma^{\nu_1 \nu_0 \sigma}(k_1, -k_0) \Gamma^{\nu_2 \sigma +}(k_2, k_2 + q)}{(k_0 + k_1)^2} - T_{a_2 a_0}^a T_{a_1 a}^c \right. \\ \left. \times \frac{\gamma^{\nu_2 \nu_0 \sigma}(k_2, -k_0) \Gamma^{\nu_1 \sigma +}(k_1, k_1 + q)}{(k_0 + k_2)^2} - T_{a_2 a_1}^a T_{a_0 a}^c \frac{\gamma^{\nu_2 \nu_1 \sigma}(k_2, -k_1) \Gamma^{\nu_0 \sigma +}(k_0, k_0 + q)}{(k_1 + k_2)^2} \right\}. \end{aligned} \quad (\text{III.13})$$

The last three terms in the brackets correspond to the last three diagrams in FIG. III.3 (c). The first term is $\Gamma_{a_0 a_1 a_2 c}^{\nu_0 \nu_1 \nu_2 +} = \gamma_{a_0 a_1 a_2 c}^{\nu_0 \nu_1 \nu_2 +} + \Delta_{a_0 a_1 a_2 c}^{\nu_0 \nu_1 \nu_2 +}$, with γ the light-cone projection of the 4-gluon QCD vertex (2nd diagram) and Δ a new induced contribution (1st diagram)

$$\Delta_{a_0 a_1 a_2 c}^{\nu_0 \nu_1 \nu_2 +}(k_0^+, k_1^+, k_2^+) = -t(n^+)^{\nu_0} (n^+)^{\nu_1} (n^+)^{\nu_2} \left(\frac{T_{a_2 a_0}^a T_{a_1 a}^c}{k_1^+ k_2^+} + \frac{T_{a_2 a_1}^a T_{a_0 a}^c}{k_0^+ k_2^+} \right). \quad (\text{III.14})$$

One can verify that the amplitude (III.12) is gauge invariant for $n = 2$: $(k_i)_{\nu_i} \phi^{\nu_0 \nu_1 \nu_2} = 0$, $i = 0, 1, 2$, where one has to use the Ward identities

$$(p_{A'})_{\mu} \gamma^{\mu \nu \sigma}(p_A, p_{A'}) = (t - p_A^2) g^{\nu \sigma} + p_{A'}^{\nu} q^{\sigma} + p_{a'}^{\sigma} p_{A'}^{\nu}; \quad (p_{A'})_{\mu} \gamma^{\mu \nu +}(p_A, p_{A'}) = -p_A^2 (n^+)^{\nu} + p_A^+ (p_A)^{\nu}. \quad (\text{III.15})$$

In order for ϕ to be gauge-invariant for $n \geq 3$, one has to add a new induced vertex $\Gamma_{a_0 a_1 \dots a_{r-1} c}^{\nu_0 \nu_1 \dots \nu_{r-1} +}(k_0^+, k_1^+, \dots, k_{r-1}^+) = \Delta_{a_0 a_1 \dots a_{r-1} c}^{\nu_0 \nu_1 \dots \nu_{r-1} +}(k_0^+, k_1^+, \dots, k_{r-1}^+)$ (no direct light-cone projection of a QCD vertex can appear now). Now one can consider the generalization of the last three terms in (III.13), built from induced vertices of lower order, gluon propagators and usual Yang-Mills vertices. Multiplying the corresponding sum of terms by (k_n^+) and using the Ward identity (III.15), one gets the nonvanishing sum $-\sum_{i=0}^{n-1} T_{a_n a_i}^a \Delta_{a_0 a_1 \dots a_{i-1} a_{i+1} \dots a_{n-1} c}^{\nu_0 \dots \nu_{n-1} +}(k_0^+, \dots, k_{i-1}^+, k_i^+ + k_n^+, \dots, k_{n-1}^+)$. This is to be compensated by the new n^{th} -order induced vertex, defining the recurrence relation

$$\Delta_{a_0 a_1 \dots a_n c}^{\nu_0 \nu_1 \dots \nu_n +}(k_0^+, k_1^+, \dots, k_n^+) = \frac{(n^+)^{\nu_n}}{k_n^+} \sum_{i=0}^{n-1} T_{a_n a_i}^a \Delta_{a_0 a_1 \dots a_{i-1} a_{i+1} \dots a_{n-1} c}^{\nu_0 \dots \nu_{n-1} +}(k_0^+, \dots, k_{i-1}^+, k_i^+ + k_n^+, \dots, k_{n-1}^+). \quad (\text{III.16})$$

The same treatment given to quasielastic gluon production can be applied to multigluon production at central rapidities (FIG. III.2 (c)). In this case the amplitude reads

$$A_{d_1 \nu_1 \nu_2 \dots \nu_n +}^{\nu_1 \nu_2 \dots \nu_n +} = -gp_A^+ T_{A'A}^{c_1} \Gamma_{AA'+} \frac{1}{t_1} \psi_{d_1 d_2 \dots d_n c_2 c_1}^{\nu_1 \nu_2 \dots \nu_n +} \frac{1}{t_2} gp_B^- T_{B'B}^{c_2} \Gamma_{B'B-}, \quad \sum_{i=0}^n k_i^+ = \sum_{i=0}^n k_i^- = 0. \quad (\text{III.17})$$

In the one-gluon production case we have Lipatov's vertex, $\psi_{d_1 c_2 c_1}^{\nu_1 +} = g \Gamma_{d_1 c_2 c_1}^{\nu_1 +}$. At the following order one has [FL89]

$$\psi_{d_1 d_2 c_2 c_1}^{\nu_1 \nu_2 +} = g^2 \left\{ \Gamma_{d_1 d_2 c_2 c_1}^{\nu_1 \nu_2 +} - \frac{T_{d_2 d_1}^d \gamma^{\nu_2 \nu_1 \sigma}(k_2, -k_1) \Gamma_{d_2 c_2 c_1}^{\sigma +}(q_1, q_2)}{(k_1 + k_2)^2} - \frac{\Gamma_{d_1 d_1}^{\nu_1 \sigma -}(k_1, k_1 - q_1) \Gamma_{d_2 d_2}^{\nu_2 \sigma +}(k_2, k_2 + q_2)}{(q_1 - k_1)^2} - \frac{\Gamma_{d_2 d_1}^{\nu_2 \sigma -}(k_2, k_2 - q_1) \Gamma_{d_1 d_2}^{\nu_1 \sigma +}(k_1, k_1 + q_2)}{(q_1 - k_2)^2} \right\}. \quad (\text{III.18})$$

The first term $\Gamma_{d_1 d_2 c_2 c_1}^{\nu_1 \nu_2 +} = \gamma_{d_1 d_2 c_2 c_1}^{\nu_1 \nu_2 +} + \Delta_{d_1 d_2 c_2 c_1}^{\nu_1 \nu_2 +}$ is again the sum of the light-cone projection of the 4-gluon vertex and a new induced term

$$\Delta_{d_1 d_2 c_2 c_1}^{\nu_1 \nu_2 +} = -2t_2 (n^+)^{\nu_1} (n^+)^{\nu_2} \left[\frac{T_{d_2 c_1}^d T_{d_1 d}^{c_2}}{k_1^+ k_2^+} - \frac{T_{d_2 d_1}^d T_{c_1 d}^{c_2}}{(k_1^+ + k_2^+) k_2^+} \right] - 2t_1 (n^-)^{\nu_1} (n^-)^{\nu_2} \left[\frac{T_{d_1 c_2}^d T_{d_2 d}^{c_1}}{k_2^- k_1^-} - \frac{T_{d_1 c_2}^d T_{c_2 d}^{c_1}}{(k_1^- + k_2^-) k_1^-} \right]. \quad (\text{III.19})$$

In this case as well, one should introduce induced vertices with an arbitrary number of external legs in order to ensure gauge invariance of the production amplitude for $n > 2$. Their form can be expressed in terms of light-cone projections of the quasielastic effective vertices (III.16)

$$\Gamma_{d_1 \dots d_n c_2 c_1}^{\nu_1 \dots \nu_n +} = \Delta_{c_1 d_1 \dots d_n c_2}^{+\nu_1 \dots \nu_n -}(k_0^+, k_1^+, \dots, k_n^+) + \Delta_{c_2 d_1 \dots d_n c_1}^{+\nu_1 \dots \nu_n -}(k_0^-, k_1^-, \dots, k_n^-); \quad k_0^\pm = -\sum_{i=0}^n k_i^\pm. \quad (\text{III.20})$$

1.3 Gauge Invariance and Lipatov's Effective Action

In [Lip95], Lipatov was able to build an action reproducing all the effective vertices we saw in last section. The key idea is the introduction of a reggeon field A_{\pm} (which we tentatively identified in SEC. III.1.1), in terms of which one can formulate the high-energy factorization of QMRK. These reggeon fields are identified with light-cone components of the vector potential v_{μ} ⁶ since, as we saw in (I.126), only the longitudinal part of the t -channel gluon propagator gives a large contribution proportional to s .

The effective vertices of SEC. III.1.2 describe interactions in a small rapidity range $(y_0 - \frac{\eta}{2}, y_0 + \frac{\eta}{2})$, $\eta \ll y \sim \ln s$. η acts as a UV cutoff in the relative longitudinal momenta of the particles inside each rapidity cluster. It also plays a complementary role as the minimum rapidity separation between clusters connected through reggeon exchange. As a factorization scale, any dependence on η must vanish in the computation of a physical amplitude. Taking into account that in QMRK the reggeon momenta are transverse (APP. B) and in the effective vertices one can consider A_{\pm} independent of the light-cone coordinate x_{\mp} (cf. (I.126)), up to power-suppressed (in s) contributions not relevant in QMRK

$$\partial_- A_+ = \partial_+ A_- = 0, \quad (\text{III.21})$$

then the reggeon field propagator is that of a $2d$ free field

$$\langle A_+^{y'}(x^{\pm}, \mathbf{x}) A_-^y(0, 0) \rangle \sim \Theta(y' - y - \eta) \delta(x^+) \delta(x^-) \ln |\mathbf{x}|. \quad (\text{III.22})$$

The reggeon field A_{\pm} is to be considered as a bare reggeon with fixed intercept equal to 1; the Regge trajectory is built through loop corrections to the effective action. In order to get an action local in rapidity reproducing the results of SEC. III.1.2, we naively decompose the gluon field into components V^y and A_{\pm}^y describing respectively gluons in the direct and crossing channels with rapidities inside of the interval η :

$$v = \sum_{y \in (y_0 - \frac{\eta}{2}, y_0 + \frac{\eta}{2})} V^y + A^y; \quad \{V_{\mu}, A_{\pm}, G_{\mu\nu}\} = -i \{V_{\mu}^a, A_{\pm}^a, G_{\mu\nu}^a\} t^a. \quad (\text{III.23})$$

Using the decomposition (III.23), the Yang-Mills action within a rapidity cluster can be written as [Lip95]

⁶In this section we use the notation v_{μ} for the gluon field, instead of A_{μ} , to avoid possible confusions.

$$\begin{aligned}
S_{\text{YM}} = & - \int d^4x \text{Tr} \left\{ \frac{1}{2} G_{\mu\nu}^2(V) - [D_\mu, G_{\mu-}]A_+ - [D_\nu, G_{\nu+}]A_- + [D_\mu, A_+][D_\mu, A_-] \right. \\
& - \frac{1}{2}[D_-, A_-][D_+, A_+] + \frac{g}{2}G_{+-}[A_-, A_+] - \frac{1}{4}[D_+, A_-]^2 - \frac{1}{4}[D_-, A_+]^2 \\
& \left. + \frac{g}{2}[D_+, A_-][A_-, A_+] + \frac{g}{2}[D_-, A_+][A_+, A_-] - \frac{g^2}{4}[A_+, A_-]^2 \right\}, \\
D_\mu = & \partial_\mu + gV_\mu, \quad G_{\mu\nu}(V) = \frac{1}{g}[D_\mu, D_\nu] = \partial_\mu V_\nu - \partial_\nu V_\mu + g[V_\mu, V_\nu].
\end{aligned} \tag{III.24}$$

As we discussed before, gauge invariance of local-in-rapidity amplitudes forces us to add new induced terms. Consider the quasielastic production amplitudes, linear in the reggeon fields. They correspond to a piece of the effective action of the form

$$S^{(1)} = - \int d^4x \text{Tr}[j_- A_+ + j_+ A_-]; \quad j_\pm = j_\pm^{\text{YM}} + j_\pm^{\text{ind}}. \tag{III.25}$$

The currents include the coefficients of the linear terms in A_\pm in the action (III.24), $j_\pm^{\text{YM}} = -[D_\mu, G_{\mu\pm}]$. These terms vanish classically so they cannot give any contribution to tree-level amplitudes. The current j_\pm^{ind} is built in order to reproduce the recurrence relations (III.16) order by order:

$$j_\pm^{\text{ind}}(V_\pm) = \partial_{\perp\sigma}^2 \left\{ V_\pm - gV_\pm \frac{1}{\partial_\pm} V_\pm + g^2 V_\pm \frac{1}{\partial_\pm} V_\pm \frac{1}{\partial_\pm} V_\pm - \dots \right\} = \partial_{\perp\sigma}^2 \partial_\pm \frac{1}{D_\pm} V_\pm. \tag{III.26}$$

In the same way one has for central rapidity production an action bilinear in A_\pm

$$S^{(2)} = - \int d^4x \text{Tr}[L_2^{\text{YM}} + L_2^{\text{ind}}], \quad L_2^{\text{YM}} = [D_\mu, A_{-+}][D_\mu, A_-] - \frac{1}{2}[D_-, A_-][D_+, A_+] + \frac{g}{2}G_{+-}[A_-, A_+]. \tag{III.27}$$

In order to reproduce (III.20), the induced term reads⁷

$$L_2^{\text{ind}} = A_- \frac{\partial}{\partial V_-} \text{Tr}[j_-^{\text{ind}}(V_-) - \partial_{\perp\sigma}^2 V_-] A_+ + \{+ \leftrightarrow -\}, \tag{III.28}$$

where it is implied that after differentiating j_\pm with respect to V_\pm , the fields A_\mp substitute the fields V_\mp at the corresponding empty positions.

The current j_\pm^{ind} in (III.26) can be resummed in terms of a Wilson line

$$\begin{aligned}
j_\pm^{\text{ind}}(V_\pm) = & -\frac{1}{g} \partial_{\perp\sigma}^2 \partial_\pm U(V_\pm); \\
U[V_\pm(x)] = & \mathcal{P} \exp \left\{ -\frac{g}{2} \int_{-\infty}^{x^\mp} dz^\pm V_\pm(z) \right\} = 1 - g \frac{1}{\partial_\pm} V_\pm + g^2 \left(\frac{1}{\partial_\pm} V_\pm \right)^2 - \dots = \frac{1}{D_\pm} \partial_\pm,
\end{aligned} \tag{III.29}$$

⁷Notice that the kinetic terms for reggeons have been subtracted since they already appeared in L_2^{YM} .

III. Lipatov Effective Action Approach to High Energy QCD

an expression from which can be checked that j_{\pm}^{ind} is gauge-invariant for gauge transformations vanishing as $x^{\pm} \rightarrow \infty$. This implies that the reggeon field must be gauge invariant in order for the effective action to be invariant as well⁸. However, the current j_{\pm}^{YM} transforms in the adjoint under a gauge transformation χ , $\delta j_{\pm}^{\text{YM}} = g[j_{\pm}^{\text{YM}}, \chi]$. One can still make $S^{(1)}$ in (III.25) invariant by modifying the current using the Wilson lines (III.29) transforming in the fundamental representation

$$j_{\pm}^{\text{YM}} \rightarrow j_{\pm}^{\text{YM},m} = U^{-1}(V_{\pm})j_{\pm}^{\text{YM}}U(V_{\pm}), \quad \delta j_{\pm}^{\text{YM},m} = 0. \quad (\text{III.30})$$

One has the freedom to perform such modification since both j^{YM} and j^m vanish classically and the modification does not alter tree-level production amplitudes. Actually, $j^{\text{YM},m}$ would have appeared directly multiplying the linear term in A_{\pm} had we chosen, instead of (III.23), the different decomposition for the gluon field

$$v_{\perp\mu} = \sum_y V_{\perp\mu}, \quad v_{\pm} = \sum_y [V_{\pm}^y + U(V_{\mp})A_{\pm}^yU^{-1}(V_{\mp})]. \quad (\text{III.31})$$

This is a much more natural decomposition for a gauge-invariant A_{\pm} , since now both terms in the sum transform in the same way under gauge transformations. It turns out that inserting the redefinition $A_{\pm} \rightarrow U(V_{\mp})A_{\pm}U^{-1}(V_{\mp})$ in (III.27) one can also render $S^{(2)}$ gauge-invariant, and one can finally recast all terms in the following action for local-in-rapidity interactions

$$\begin{aligned} S_{\text{eff}} &= \int d^4x (\mathcal{L}_{\text{QCD}}(v_{\mu}, \psi) + \mathcal{L}_{\text{ind}}(v_{\pm}, A_{\pm})); \\ \mathcal{L}_{\text{ind}}(v_{\pm}, A_{\pm}) &= -\text{Tr}[(A_{-}(v) - A_{-}]\partial_{\sigma}^2 A_{+}] - \text{Tr}[(A_{-}(v) - A_{-})\partial_{\sigma}^2 A_{+}], \\ A_{\pm}(v) &= -\frac{1}{g}\partial_{\pm}U(v_{\pm}) = v_{\pm} - gv_{\pm}(1/\partial_{\pm})v_{\pm} + g^2v_{\pm}(1/\partial_{\pm})v_{\pm}(1/\partial_{\pm})v_{\pm} - \dots \end{aligned} \quad (\text{III.32})$$

Notice that V has been traded by v everywhere. The Yang-Mills Lagrangian $-\frac{1}{2}\text{Tr}G_{\mu\nu}^2$, has been completed to the total QCD Lagrangian, including quark and ghost fields⁹. (III.32) is the final form of Lipatov's effective action. It enjoys a number of important properties: it is gauge invariant by construction, and hermitian (ensuring unitarity in all subchannels). It is also consistent with the analytical structure of QMRK amplitudes as expressed in Steinmann relations [Ste60]. The dependence on the regulator η can be formally seen to vanish [Lip97].

⁸The reggeon field transforms however under the adjoint for global $SU(N_c)$ transformations.

⁹In fact, one can obtain also the high-energy effective action for $\mathcal{N} = 4$ SYM by replacing \mathcal{L}_{QCD} in (III.32) by $\mathcal{L}_{\mathcal{N}=4 \text{ SYM}}$.

1.4 Connection with Reggeon Field Theory and Other Formalisms

In order to make contact with reggeon field theory, one has to integrate over the physical degrees of freedom v_μ . Because $A_\pm(v_\pm)$ has a linear term in v_\pm in the action (III.32), the classical extremum of S_{eff} takes place at a nonvanishing value $v = \tilde{v}$ given by the gauge invariant Euler-Lagrange equations

$$j_{\perp\sigma}^{\text{YM}}(\tilde{v}) = 0, \quad j_{\pm}^{\text{YM}}(\tilde{v}) = -\frac{\partial}{\partial v^\mp} \text{Tr} A_\mp(v_\mp) \partial_{\perp\sigma}^2 A_\pm \Big|_{v=\tilde{v}}. \quad (\text{III.33})$$

The solution to these equations can be found perturbatively

$$\begin{aligned} \tilde{v}_\pm &= A_\pm + g \partial_\mu^{-2} \{[(\partial_{\perp\sigma}^2 A_\pm), (\partial_-^{-1} A_\mp)] - \frac{1}{2} [A_\mp, \partial_\pm A_\pm]\} + \mathcal{O}(g^2), \\ \tilde{v}_{\perp\sigma} &= \frac{1}{2} g \partial_\mu^{-2} \{[A_+, \partial_{\perp\sigma} A_-] + [A_-, \partial_{\perp\sigma} A_+]\} + \mathcal{O}(g^2). \end{aligned} \quad (\text{III.34})$$

Let us remark that A_\pm can be interpreted as a classical field of v_\pm for very small couplings. The effective action calculated at the classical solution (III.34)

$$\begin{aligned} S_{\text{eff}}|_{v=\tilde{v}} &= - \int d^4x \text{Tr} \left[\frac{1}{2} (\partial_{\perp\sigma}^2 A_-) (\partial_{\perp\sigma}^2 A_+) - \frac{1}{2} g \left((\partial_{\perp\sigma}^2 A_-) [(\partial_+^{-1} A_+), A_+] \right. \right. \\ &\quad \left. \left. + (\partial_{\perp\sigma}^2 A_+) [(\partial_-^{-1} A_-), A_-] \right) \right] + \mathcal{O}(g^2) \end{aligned} \quad (\text{III.35})$$

describes all possible self-interactions of the reggeon fields A_\pm in the tree level approximation. In particular, the trilinear term gives the transition $A_\pm \rightarrow A_\mp A_\mp$ (suppressed by Gribov's signature conservation [Gri03]); the quadrilinear term includes the $1 \rightarrow 3$ reggeon transition and the BFKL kernel describing the scattering of two reggeons¹⁰. The six-linear term includes the $2 \rightarrow 4$ transition [BW95, BLW96] and the simplest BKP kernel [BFLV13]. These terms are important to describe the screening corrections due to pomeron loops [LR90].

To calculate loop corrections to the reggeon Lagrangian one should perform a semiclassical expansion, writing $v = \tilde{v} + \epsilon$ and computing perturbatively the functional integral in ϵ . For instance, one could in principle obtain the 2-loop gluon Regge trajectory (SEC. III.109) by expanding S_{eff} to order ϵ^4 and taking into account bilinear terms in A_\pm .

It is interesting to also explore the relation of Lipatov's EFT with other formalisms describing high-energy scattering. As noticed in [JMKMW97a], the effective action (III.32) is very similar to the color glass condensate action (SEC. (I.5.2)) if one identifies the reggeon currents $\partial_{\perp\sigma}^2 A_\pm$ with the static color charge density $\rho(\mathbf{x})\delta(x^\mp)$. The Wilson line term describing the

¹⁰For a derivation of the BFKL kernel in the effective action approach, see [Hen09b]

interaction of reggeons and gluons is very similar in both approaches¹¹. One is also tempted to identify the reggeon propagator with the functional $W[\rho]$ describing the statistical weight with which a given charge density (reggeon) configuration is present in the hadronic wave function. However, the physics of both terms turns out to be rather different [JMCMW97a]. Moreover, the dilute-dense asymmetry of the JIMWLK equation is not present in Lipatov's effective action, although certain approaches have been put forward to fix this problem (see, e.g. [Hat07]). Yet another formalism to describe high-energy scattering is Balitsky's high-energy operator product expansion [Bal96, Bal01]. It is difficult to identify the reggeon in these alternative formalisms. It is also to be checked whether they can reproduce the results of SEC. (III.1.2).

2 LOOP COMPUTATIONS AND LIPATOV'S ACTION

[CHMS12a]

Having introduced Lipatov's high-energy effective action, in the remainder of the chapter we will present a procedure to apply this action to perturbative computations beyond tree level of amplitudes in QMRK. It is not easy to reconcile the two pillars of the effective action, gauge invariance and the implicitly assumed locality in rapidity of interactions, when doing loop computations. In this section we present the main problems that arise and the strategies put forward to solve them.

2.1 Overcounting and Spurious Divergences

A striking feature of the action (III.32) is that new degrees of freedom are added to the *whole* QCD action. This is in stark contrast with the Wilsonian paradigm of integrating out heavy degrees of freedom described in SEC. I.1.2. Of course, the redundancy is due to a description which is local in rapidity: the whole action (III.32) should not be used to describe interactions between particles separated in rapidity by $\Delta y > \eta$, which can only be mediated through reggeon exchange according to high-energy factorization.

A further complication arising when going beyond tree level is the appearance of spurious rapidity divergences due to the nonlocal operators $\frac{1}{\partial_{\pm}}$ in the Wilson lines (III.29), which

¹¹In fact, Wilson lines appear naturally in high-energy scattering [Bal01]. Performing the path integral in A_{\pm} for the terms in S_{eff} responsible for quasielastic processes, one gets under certain approximations a two-dimensional σ -model describing the interaction of two Wilson lines [Lip97], first obtained by Verlinde and Verlinde under rather general assumptions [VV93].

in the Feynman rules in momentum space (APP. A) give rise to light-cone denominators $1/k^\pm$. This is not a problem at tree level because kinematics of outgoing particles is fixed by the mass-shell condition, but it is an issue for loop computations, where these poles lead to divergences in the integrations over longitudinal momenta.

2.2 Light-Cone Regularization and Pole Prescription

A convenient way of regularizing rapidity divergences in a gauge invariant way is inspired in the idea of tilting soft and collinear Wilson lines off the light-cone to avoid divergences due to the possible interactions with gluons with infinite rapidity [CS81, CS82, KR87].

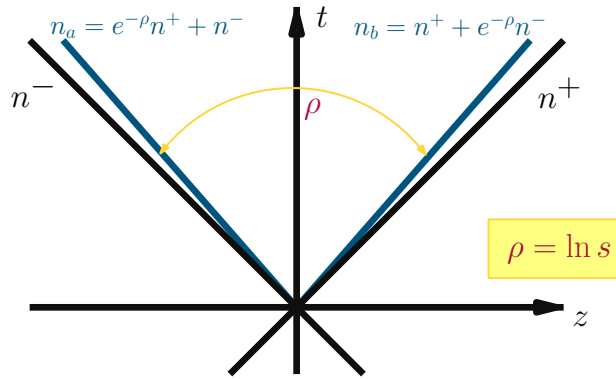


Figure III.4: Light-cone regularization.

We tilt the light-cone vectors to form a hyperbolic angle in Minkowski space ρ (FIG. III.4), which must be evaluated in the limit $\rho \rightarrow \infty$. As we will see this parameter is useful since it can be identified with $\ln s$ factors directly. The regularized light-cone vectors read

$$n^- \rightarrow n_a = e^{-\rho}n^+ + n^-, \quad n^+ \rightarrow n_b = n^+ + e^{-\rho}n^-. \quad (\text{III.36})$$

It is important also to adopt a pole prescription respecting symmetries as much as possible in order to simplify calculations. The induced vertices in APP. B obey Bose symmetry, i.e. symmetry under simultaneous exchange of color, polarization and momenta of the external gluons, as can be verified making use of the light-cone momentum conservation constraint ($\sum_{i=0}^n k_i^\pm = 0$ for an order g^n vertex), coming from (III.21), and the Jacobi identity (A.1). These symmetries are lost e.g., with a Cauchy principal value prescription $\frac{1}{[k]_{\text{PV}}} \equiv \frac{1}{2} \left(\frac{1}{k+i0} + \frac{1}{k-i0} \right)$, mainly because the eikonal identity does not simply hold but an additional term is generated [BNS91]

$$\frac{1}{[k_1^\pm]_{\text{PV}}[k_1^\pm + k_2^\pm]_{\text{PV}}} + \frac{1}{[k_1^\pm]_{\text{PV}}[k_1^\pm + k_2^\pm]_{\text{PV}}} = \frac{1}{[k_1^\pm]_{\text{PV}}[k_2^\pm]_{\text{PV}}} + \pi^2 \delta(k_1^\pm) \delta(k_2^\pm). \quad (\text{III.37})$$

III. Lipatov Effective Action Approach to High Energy QCD

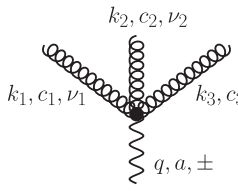
An alternative regularization respecting the symmetries of unregulated induced vertices was proposed in [Hen12]. It is based on replacing the unregulated operator $A_{\pm}(v)$ in (III.32) by

$$A_{\pm}^{\epsilon}[v] = \frac{1}{2} \left[\mathcal{P}_A \left(v_{\pm} \frac{1}{D_{\pm} - \epsilon} \partial_{\pm} \right) + \mathcal{P}_A \left(v_{\pm} \frac{1}{D_{\pm} + \epsilon} \partial_{\pm} \right) \right], \quad \epsilon \rightarrow 0. \quad (\text{III.38})$$

The projector \mathcal{P}_A is needed since the color structure of the induced vertices is defined in terms of only antisymmetric color structure, in terms of the $SU(N_c)$ structure constants f^{abc} . While for non-zero values of the operators $1/\partial_{\pm}$ this happens automatically, a pole prescription of the above kind leads to momentum space expressions which are proportional to symmetric color tensors multiplied by a delta-function in one of the light-cone momenta. We remove these subleading terms using a suitable projector, keeping in this way the same color structure as in the unregulated case. The projector \mathcal{P}_A acts then order by order in g on the $SU(N_c)$ color structure of the gluonic fields $v_{\pm}(x) = -it^a v^a(x)$,

$$\begin{aligned} \mathcal{P}_A \left(v_{\pm} \frac{1}{D_{\pm} - \epsilon} \partial_{\pm} \right) \equiv & -i \left(P_A^{(1)}(t^a) v_{\pm}^a - (-ig) v_{\pm}^{a_1} \frac{1}{\partial_{\pm} - \epsilon} v_{\pm}^{a_2} P_A^{(2)}(t^{a_1} t^{a_2}) \right. \\ & \left. + (-ig)^2 v_{\pm}^{a_1} \frac{1}{\partial_{\pm} - \epsilon} v_{\pm}^{a_2} \frac{1}{\partial_{\pm} - \epsilon} v_{\pm}^{a_3} P_A^{(3)}(t^{a_1} t^{a_2} t^{a_3}) - \dots \right), \end{aligned} \quad (\text{III.39})$$

where $P_A^{(n)}$ are the projectors of the color tensors with n adjoint indices on the maximal antisymmetric subsector of order n . The latter can be defined by an iterative procedure, outlined in [Hen12]. For the second order (RGG) vertex this prescription amounts to a principal value. Regarding the reggeon–3-gluon vertex, it is needed to replace the unregulated form appearing in APP. B by¹²



$$= -ig^2 \mathbf{q}^2 [f^{c_3 c_2 e} f^{c_1 e a} g_2^{\pm}(3, 2, 1) + f^{c_3 c_1 e} f^{c_2 e a} g_2^{\pm}(3, 2, 1)] (n^{\pm})_{\nu_1} (n^{\pm})_{\nu_2} (n^{\pm})_{\nu_3},$$

$$g_2^{\pm}(i, j, m) = \left[\frac{-1/3}{k_i^{\pm} - i0} \left(\frac{1}{k_m^{\pm} + i0} + \frac{1/2}{k_m^{\pm} - i0} \right) + \frac{-1/3}{k_i^{\pm} + i0} \left(\frac{1}{k_m^{\pm} - i0} + \frac{1/2}{k_m^{\pm} + i0} \right) \right]. \quad (\text{III.40})$$

¹²Let us recall that from now all in all the expressions where n^+ and n^- appear we should eventually perform the substitutions (III.36).

sequently confirmed in [BRvN98], clarifying an ambiguity due to a slightly deviating result presented in [KK96]. The original result was further verified by explicitly evaluating the high-energy limit of 2-loop partonic scattering amplitudes [dDG01]. While the explicit result for the 2-loop trajectory is by now firmly established, our calculation provides an important confirmation of its universality: unlike previous computations, the effective action defines the Regge trajectory of the gluon without making any particular reference to a particular QCD scattering process.

3.1 Subtraction and Renormalization

The procedure which allows the derivation of the gluon trajectory from the effective action has been originally discussed in [CHMS12a]. It consists of two steps

- determination of the propagator of the reggeized gluon to the desired order in α_s ;
- renormalization of the rapidity divergencies of the reggeized gluon propagator where the gluon Regge trajectory is identified as the coefficient of the ρ dependent term in the renormalization factor.

To obtain the reggeized gluon propagators to order α_s^2 it is needed to determine the one- and two-loop self-energies of the reggeized gluon. Following the subtraction procedure proposed in [HS12] (SEC. III.2.3) these self-energies can be obtained through

- determination of the self-energy of the reggeized gluon from the effective action, with the reggeized gluon treated as a background field;
- subtraction of all disconnected contributions containing internal reggeized gluon lines.

Using a symmetric pole prescription as given in SEC. III.2.2, all disconnected diagrams that possibly contribute to the one loop self-energy can be shown to vanish and no subtraction is necessary. The contributing diagrams are shown in FIG. III.6.

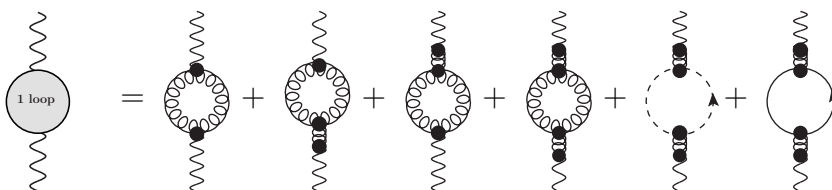


Figure III.6: *Diagrams contributing to the one-loop reggeized gluon self-energy.*

with $G(a)$ obtained from $\Gamma_R(\bar{\alpha}_s)$ using the principle of maximal transcendentality [KLOV04].

III. Lipatov Effective Action Approach to High Energy QCD

Keeping the $\mathcal{O}(\rho, \rho^2)$ terms, for $\rho \rightarrow \infty$, and using the notation

$$\bar{g}^2 = \frac{g^2 N_c \Gamma(1 - \epsilon)}{(4\pi)^{2+\epsilon}}, \quad (\text{III.48})$$

we have the following result¹⁴:

$$\begin{aligned} \text{1 loop} &= \Sigma^{(1)} \left(\rho; \epsilon, \frac{\mathbf{q}^2}{\mu^2} \right) \\ &= \frac{(-2i\mathbf{q}^2)\bar{g}^2\Gamma^2(1 + \epsilon)}{\Gamma(1 + 2\epsilon)} \left(\frac{\mathbf{q}^2}{\mu^2} \right)^\epsilon \left\{ \frac{i\pi - 2\rho}{\epsilon} - \frac{1}{(1 + 2\epsilon)\epsilon} \left[\frac{5 + 3\epsilon}{3 + 2\epsilon} - \frac{N_f}{N_c} \left(\frac{2 + 2\epsilon}{3 + 2\epsilon} \right) \right] \right\}. \end{aligned} \quad (\text{III.49})$$

To determine the 2-loop self-energy it is needed to subtract disconnected diagrams, whereas diagrams with multiple internal reggeized gluon can be shown to yield zero result, using the symmetric pole prescription. Schematically one has

$$\Sigma^{(2)} \left(\rho; \epsilon, \frac{\mathbf{q}^2}{\mu^2} \right) = \text{2 loop} = \text{2 loop} - \text{1 loop} - \text{1 loop}, \quad (\text{III.50})$$

where the black blob denotes the unsubtracted 2-loop reggeized gluon self-energy which is obtained through the direct application of the Feynman rules of the effective action, with the reggeized gluon itself treated as a background field. Its determination will be discussed in detail in the forth-coming section. The (bare) two-loop reggeized gluon propagators then reads

$$G \left(\rho; \epsilon, \mathbf{q}^2, \mu^2 \right) = \frac{i/2}{\mathbf{q}^2} \left\{ 1 + \frac{i/2}{\mathbf{q}^2} \Sigma \left(\rho; \epsilon, \frac{\mathbf{q}^2}{\mu^2} \right) + \left[\frac{i/2}{\mathbf{q}^2} \Sigma \left(\rho; \epsilon, \frac{\mathbf{q}^2}{\mu^2} \right) \right]^2 + \dots \right\}. \quad (\text{III.51})$$

with

$$\Sigma \left(\rho; \epsilon, \frac{\mathbf{q}^2}{\mu^2} \right) = \Sigma^{(1)} \left(\rho; \epsilon, \frac{\mathbf{q}^2}{\mu^2} \right) + \Sigma^{(2)} \left(\rho; \epsilon, \frac{\mathbf{q}^2}{\mu^2} \right) + \dots \quad (\text{III.52})$$

¹⁴In the original expression presented in [HS12] and reproduced in [CHMS12a] a finite result for the second and third diagrams has been erroneously included. It turns out that these diagrams are actually zero within our regularization. The correct expressions are presented here.

where the dots indicate higher order terms. As discussed in SEC. III.2.2 and as directly apparent from (III.49), the reggeized gluon self-energies are divergent in the limit $\rho \rightarrow \infty$. In [HS12, CHMS12b] it has been demonstrated by explicit calculations that these divergences cancel at one-loop level for both quark-quark and gluon-gluon scattering amplitudes against divergences in the couplings of the reggeized gluon to external particles (see also SEC. III.4). The entire one-loop amplitude is then found to be free of any high energy singularity in ρ . High energy factorization then suggests that such a cancelation holds not only at one-loop but to all loop orders. Starting from this assumption, it is possible to define a renormalized reggeized gluon propagator through

$$G^R(M^+, M^-; \epsilon, \mathbf{q}^2, \mu^2) = \frac{G(\rho; \epsilon, \mathbf{q}^2, \mu^2)}{Z^+ \left(\frac{M^+}{\sqrt{\mathbf{q}^2}}, \rho; \epsilon, \frac{\mathbf{q}^2}{\mu^2} \right) Z^- \left(\frac{M^-}{\sqrt{\mathbf{q}^2}}, \rho; \epsilon, \frac{\mathbf{q}^2}{\mu^2} \right)}, \quad (\text{III.53})$$

where the (wavefunction) renormalization factors need to cancel against corresponding renormalization factors associated with the vertex to which the reggeized gluon couples with ‘plus’ (Z^+) and ‘minus’ (Z^-) parametrization. In their most general form these renormalization factors are parametrized as

$$Z^\pm \left(\frac{M^\pm}{\sqrt{\mathbf{q}^2}}, \rho; \epsilon, \frac{\mathbf{q}^2}{\mu^2} \right) = \exp \left[\left(\frac{\rho}{2} - \ln \frac{M^\pm}{\sqrt{\mathbf{q}^2}} \right) \omega \left(\epsilon, \frac{\mathbf{q}^2}{\mu^2} \right) + f \left(\epsilon, \frac{\mathbf{q}^2}{\mu^2} \right) \right], \quad (\text{III.54})$$

with the coefficient of the ρ -divergent term given by the gluon Regge trajectory $\omega(\epsilon, \mathbf{q}^2)$. It is assumed to have the following perturbative expansion

$$\omega \left(\epsilon, \frac{\mathbf{q}^2}{\mu^2} \right) = \omega^{(1)} \left(\epsilon, \frac{\mathbf{q}^2}{\mu^2} \right) + \omega^{(2)} \left(\epsilon, \frac{\mathbf{q}^2}{\mu^2} \right) + \dots, \quad (\text{III.55})$$

and it is determined through the requirement that the renormalized reggeized gluon propagator is free at every loop order of any ρ divergence. At one loop we obtain from (III.49)

$$\omega^{(1)} \left(\epsilon, \frac{\mathbf{q}^2}{\mu^2} \right) = -\frac{2\bar{g}^2 \Gamma^2(1 + \epsilon)}{\Gamma(1 + 2\epsilon) \epsilon} \left(\frac{\mathbf{q}^2}{\mu^2} \right)^\epsilon. \quad (\text{III.56})$$

The function $f(\epsilon, \mathbf{q}^2)$ parametrizes finite contributions and is, in principle, arbitrary. While the symmetry of scattering amplitude requires $f^+ = f^- = f$, Regge theory suggests fixing it in such a way that terms which are not enhanced in ρ are entirely transferred from reggeized gluon propagators to the vertices to which the reggeized gluon couples. With the perturbative expansion

$$f\left(\epsilon, \frac{\mathbf{q}^2}{\mu^2}\right) = f^{(1)}\left(\epsilon, \frac{\mathbf{q}^2}{\mu^2}\right) + f^{(2)}\left(\epsilon, \frac{\mathbf{q}^2}{\mu^2}\right) \dots \quad (\text{III.57})$$

we obtain from (III.49)

$$f^{(1)}\left(\epsilon, \frac{\mathbf{q}^2}{\mu^2}\right) = \frac{\bar{g}^2 \Gamma^2(1+\epsilon)}{\Gamma(1+2\epsilon)} \left(\frac{\mathbf{q}^2}{\mu^2}\right)^\epsilon \frac{(-1)}{(1+2\epsilon)2\epsilon} \left[\frac{5+3\epsilon}{3+2\epsilon} - \frac{N_f}{N_c} \left(\frac{2+2\epsilon}{3+2\epsilon}\right) \right]. \quad (\text{III.58})$$

The renormalized reggeized gluon propagator is then at one loop accuracy given by

$$G^{\text{R}}(M^+, M^-; \epsilon, \mathbf{q}^2, \mu^2) = 1 + \omega^{(1)}\left(\epsilon, \frac{\mathbf{q}^2}{\mu^2}\right) \left(\log \frac{M^+ M^-}{\mathbf{q}^2} - \frac{i\pi}{2} \right) + \dots \quad (\text{III.59})$$

The scales M^+ and M^- are arbitrary; their role is analogous to the renormalization scale in UV renormalization and the factorization scale in collinear factorization. They are naturally chosen to coincide with the corresponding light-cone momenta of scattering particles to which the reggeized gluon couples. To determine the gluon Regge trajectory at two loops we require in addition the ρ enhanced terms of the two-loop reggeized gluon self-energy. From (III.59) we obtain the following relation

$$\begin{aligned} \omega^{(2)}\left(\epsilon, \frac{\mathbf{q}^2}{\mu^2}\right) &= \lim_{\rho \rightarrow \infty} \frac{1}{\rho} \left[\frac{\Sigma^{(2)}}{(-2i\mathbf{q}^2)} + \left(\frac{\Sigma^{(1)}}{(-2i\mathbf{q}^2)} \right)^2 - (\rho\omega^{(1)} + 2f^{(1)}) \frac{\Sigma^{(1)}}{(-2i\mathbf{q}^2)} \right. \\ &\quad \left. + \frac{\rho^2}{2} (\omega^{(1)})^2 + 2\rho f^{(1)} \omega^{(1)} \right] \\ &= \lim_{\rho \rightarrow \infty} \frac{1}{\rho} \left[\frac{\Sigma^{(2)}}{(-2i\mathbf{q}^2)} + \frac{\rho^2}{2} (\omega^{(1)})^2 + 2\rho f^{(1)} \omega^{(1)} \right] \end{aligned} \quad (\text{III.60})$$

where we omitted on the right hand side the dependences on ϵ and \mathbf{q}^2/μ^2 and expressed in the last line $\Sigma^{(1)}$ in terms of the functions $\omega^{(1)}$ and $f^{(1)}$. We stress that this is a non-trivial definition and that it is not clear a priori whether the right hand side even exists. Confirmation of this relation provides therefore an important non-trivial check on the validity of our formalism.

3.2 Computation of the Reggeon Self-Energy

The necessary diagrams for the determination of the unsubtracted reggeized gluon self-energy are shown in FIG. III.7. Diagrams (a₁)-(d₃), containing internal quark loops and leading to

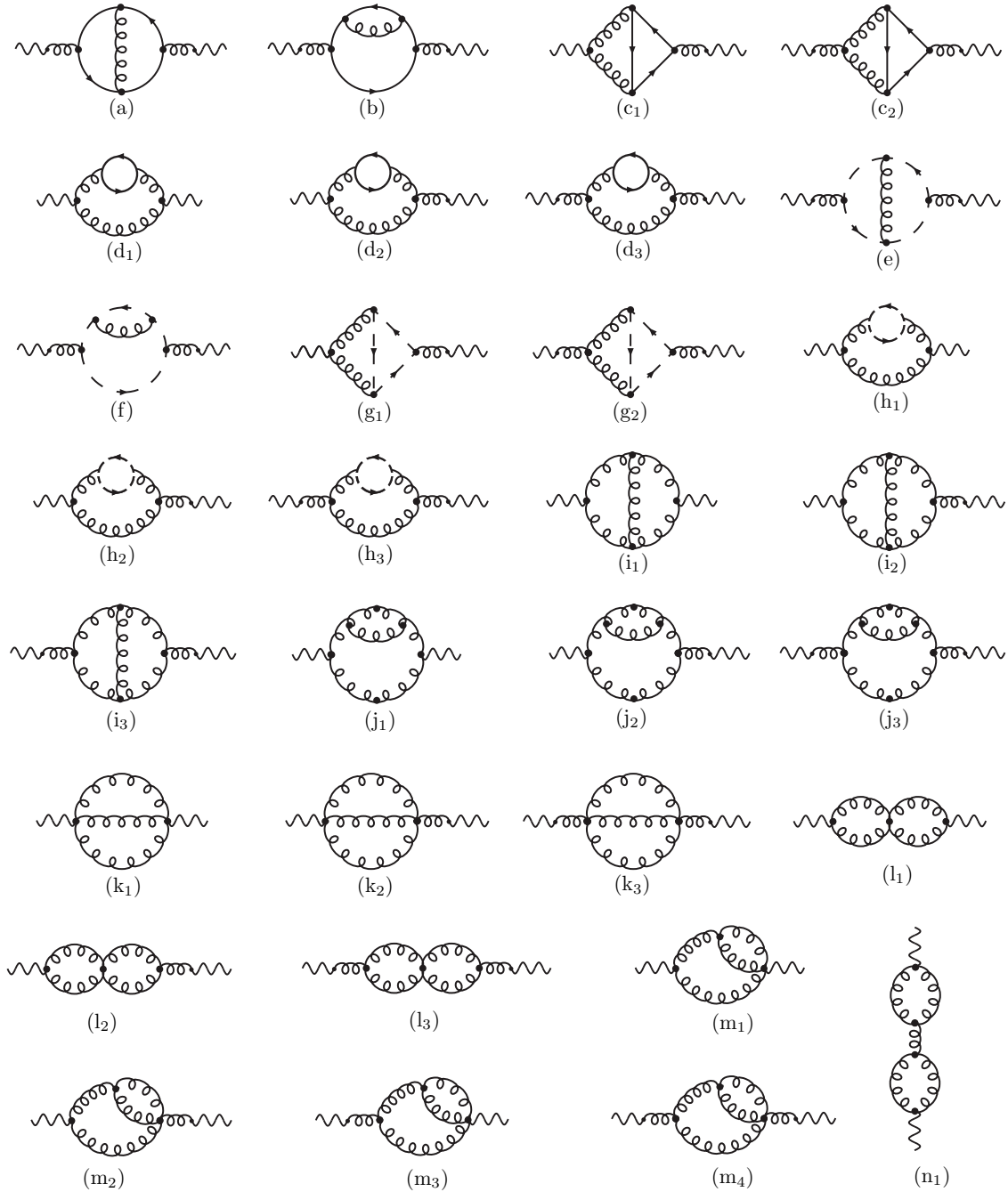


Figure III.7: Diagrams for the two-loop trajectory in the effective action formalism. Tadpole-like contributions are zero in dimensional regularization and are omitted.

III. Lipatov Effective Action Approach to High Energy QCD

an overall factor N_f , have been computed in [CHMS12c] and lead to the following result,

$$\begin{array}{c} \text{2-loop} \\ \text{quark-contr.} \end{array} = -\rho(-i2\mathbf{q}^2)\bar{g}^4 \frac{4N_f \Gamma^2(2+\epsilon)}{\epsilon N_c \Gamma(4+2\epsilon)} \cdot \frac{3\Gamma(1-2\epsilon)\Gamma(1+\epsilon)\Gamma(1+2\epsilon)}{\Gamma^2(1-\epsilon)\Gamma(1+3\epsilon)\epsilon} + \mathcal{O}(\rho^0). \quad (\text{III.61})$$

Actually, all the ρ -enhanced contribution (III.61) comes from diagram (d₂), as can be seen from the following scaling argument¹⁵.

The scaling argument The number of diagrams, which can be potentially enhanced by a factor ρ^k , $k \geq 1$, is largely reduced by scaling arguments: only those diagrams where both reggeized gluons couple to the internal gluon lines through induced reggeized gluon- n -gluon vertices with $n \geq 2$, have the potential to lead to an enhancement through a factor ρ . This is immediately clear for diagrams where both reggeized gluons couple through the reggeized gluon-1-gluon vertex¹⁶ to the internal QCD lines. Those diagrams constitute a simple projection of the 2-loop QCD polarization tensor onto the kinematics of reggeized gluons and no ρ -enhancement can be expected.

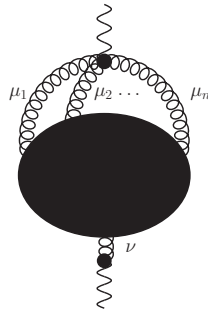


Figure III.8: *General non-enhanced diagram.*

To address the case where only one of the reggeized gluons couples through an induced reggeized gluon- n -gluon vertices with $n \geq 2$ vertex to the internal QCD particles, we consider the general diagram in FIG. III.8. The dependence on the light-cone vectors of the reggeon- n -gluon vertex in FIG. III.8 is, up to permutations, of the form $\frac{n_a^{\mu_1} n_a^{\mu_2} \dots n_a^{\mu_d}}{n_a \cdot k_1 n_a \cdot k_2 \dots n_a \cdot k_{n-1}}$. The denominators $n_a \cdot k_i$, $i = 1, \dots, n-1$ appear in the integrals that give rise to an amplitude

¹⁵Diagram (d₁) can be expressed in terms of the master integral \mathcal{B} in TAB. III.1. In the following we will offer only the derivation of the piece of the 2-loop trajectory not proportional to N_f . The quark loop piece follows much more easily along the same lines [CHMS12c].

¹⁶We follow the formalism of [ALKC05], where instead of obtaining the Feynman rules making perturbation theory around the classical value A_{\pm} of the gluon field v_{\pm} , a direct transition reggeon-gluon vertex was introduced (APP. B).

$A_{\mu_1\mu_2\dots\mu_n\nu}$. In a general diagram such as in FIG. III.8, the only vectors that are not integrated over in the amplitude are q , the momentum transfer, and n_a , which enters through the denominators of the induced vertex. The vector n_b only contracts with the four-vector index ν . The whole diagram can be therefore written as

$$n_a^{\mu_1} n_a^{\mu_2} \dots n_a^{\mu_n} A_{\mu_1\mu_2\dots\mu_n\nu}(n_a, q) n_b^\nu. \quad (\text{III.62})$$

As a consequence, the tensor structure of $\mathcal{M}_{\mu_1\mu_2\dots\mu_n\nu}(n_a, q)$ can only consist of combinations of the the four vector n_a^μ and the metric tensor $g_{\mu\nu}$, since the external reggeized gluons imply $q \cdot n_a = q \cdot n_b = 0$. The only scalar combinations that can appear are therefore \mathbf{q}^2 and n_a^2 . These factors must give the dimensions required by scale transformations. If s is the number of metric tensors in the numerator for a given term and l the number of n_a^μ numerators, then $n + 1 = 2s + l$ and the associated scalar function must scale as

$$\frac{1}{n_a^{n-1+l}} = \frac{1}{(n_a^2)^{d-s}}. \quad (\text{III.63})$$

Next we consider the contractions with the vertex currents. If n_b^ρ is contracted through a metric tensor then we have a factor

$$(n_a^2)^l n_a \cdot n_b (n_a^2)^{s-1} = (n_a^2)^{n-s} a \cdot b; \quad (\text{III.64})$$

if on the other hand n_b^ρ is directly contracted with one of the n_a 's, we obtain a factor

$$n_a \cdot n_b (n_a^2)^s (n_a^2)^{l-1} = (n_a^2)^{n-s} n_a \cdot n_b. \quad (\text{III.65})$$

In both cases the factors of n_a^2 cancel against the corresponding factors in the denominators and no enhancement can occur. Thus in our case, apart from diagram (d₁), only diagrams (h₁), (i₁), (j₁), (k₁), (l₁), (m₁) and (n₁) are potentially enhanced by (powers of) ρ .

A further class of diagrams that can be omitted are tadpole diagrams and diagrams with internal reggeized gluon loops. Tadpole diagrams, such as FIG. III.9 (a), have been verified to vanish in dimensional regularization. Possible loop diagrams with internal reggeized gluon lines, such as FIG. III.9 (b) vanish identically by symmetry if the pole prescription of SEC. III.2.2 is employed for the induced vertices.

Calculation of the enhanced diagrams Direct computation reveals that diagram (l₁) is identically zero. Using the notation $\xi = n_a^2 = n_b^2 = 4e^{-\rho}$, $\delta = n_a \cdot n_b \sim 2$, and the following

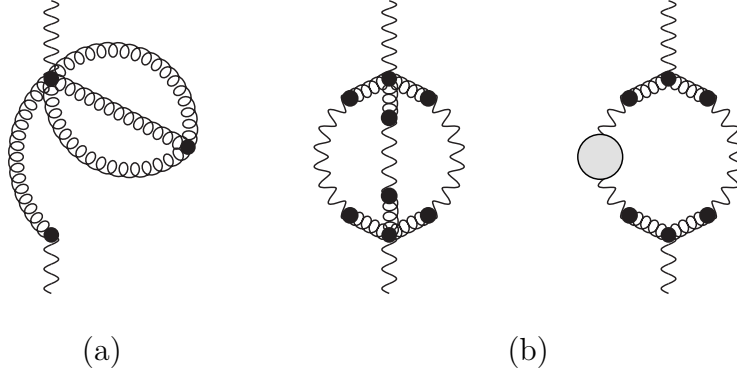


Figure III.9: (a) Typical tadpole contribution to the 2-loop self-energy; (b) Disconnected diagrams with internal reggeized gluon loops which would contribute to possible subtraction terms. Both contributions can be shown to vanish.

shorthand notation for the master integral

$$[\alpha_1, \alpha_2, \dots, \alpha_9] = (\mu^2)^{4-d} \iint \frac{d^d k}{(2\pi)^d} \frac{d^d l}{(2\pi)^d} \frac{1}{(-k^2 - i0)^{\alpha_1} [-(k-q)^2 - i0]^{\alpha_2} (-l^2 - i0)^{\alpha_3}} \cdot \frac{1}{[-(l-q)^2 - i0]^{\alpha_4} [-(k-l)^2 - i0]^{\alpha_5}} \cdot \frac{1}{(-n_a \cdot k)^{\alpha_6} (-n_b \cdot k)^{\alpha_7} (-n_a \cdot l)^{\alpha_8} (-n_b \cdot l)^{\alpha_9}}, \quad (\text{III.66})$$

with $n_a \cdot q = n_b \cdot q = 0$ and the eikonal factors taken with the pole prescription defined in SEC. III.2.2. Dropping all terms that cannot give terms enhanced as $\rho \rightarrow \infty$, we have the following contributions from each diagram:

$$\begin{aligned} [iA_{h_1}]_{\text{enh}} &= -\frac{3ig^4}{4(3+2\epsilon)S_{h_1}} \delta^2 \mathbf{q}^2 N_c^2 [1, 0, 0, 1, 1, 0, 0, 1, 1]; \quad S_{h_1} = 1. \\ [iA_{i_1}]_{\text{enh}} &= \frac{ig^4}{2S_{i_1}} (\mathbf{q}^2)^2 N_c^2 \left[\delta^2 \left\{ 2\mathbf{q}^2 [1, 1, 1, 1, 1, 1, 0, 0, 1] + [1, 1, 1, 1, 0, 1, 0, 0, 1] \right. \right. \\ &\quad \left. \left. - 4[1, 1, 1, 0, 1, 1, 0, 0, 1] \right\} + 8\xi [1, 1, 1, 1, 1, 1, -2, 0, 1] \right]; \quad S_{i_1} = 2. \\ [iA_{j_1}]_{\text{enh}} &= -\frac{3ig^4}{2S_{j_1}} \mathbf{q}^2 N_c^2 \delta^2 \frac{19+12\epsilon}{3+2\epsilon} [1, 0, 0, 1, 1, 0, 0, 1, 1]; \quad S_{j_1} = 2. \\ [iA_{k_1}]_{\text{enh}} &= \frac{3ig^4}{2S_{k_1}} (\mathbf{q}^2)^2 N_c^2 \delta^3 [1, 0, 0, 1, 1, 1, 1, 1, 1]; \quad S_{k_1} = 6. \\ [iA_{m_1}]_{\text{enh}} &= \frac{ig^4}{S_{m_1}} (\mathbf{q}^2)^2 N_c^2 \delta \left[-\frac{6\delta}{\mathbf{q}^2} [1, 0, 0, 1, 1, 0, 0, 1, 1] + 2[1, 1, 1, 0, 1, 1, 0, 0, 1] \right. \\ &\quad \left. + 2\xi [1, 1, 0, 1, 1, 1, 1, -1, 1] \right]; \quad S_{m_1} = 1. \\ [iA_{n_1}]_{\text{enh}} &= 0. \end{aligned} \quad (\text{III.67})$$

In some cases, we have used the FIRE implementation [Smi08] of the Laporta algorithm [Lap00] to reduce the number and complexity of master integrals through integration-by-parts identities [CT81]. We see that we can express the entire unsubtracted two-loop self-energy in terms of 7 master integrals $\mathcal{A} - \mathcal{G}$ with a certain coefficient associated with each master integral, see TAB. III.1.

master integral	coefficient
$\mathcal{A} \equiv [1, 1, 1, 1, 0, 1, 0, 0, 1]$	$c_{\mathcal{A}} = -\frac{\mathbf{q}^2}{2}$
$\mathcal{B} \equiv [1, 0, 0, 1, 1, 0, 0, 1, 1]$	$c_{\mathcal{B}} = \frac{66 + 42\epsilon}{3 + 2\epsilon}$
$\mathcal{C} \equiv [1, 1, 1, 1, 1, 1, 0, 0, 1]$	$c_{\mathcal{C}} = -(\mathbf{q}^2)^2$
$\mathcal{D} \equiv [1, 0, 0, 1, 1, 1, 1, 1, 1]$	$c_{\mathcal{D}} = -\mathbf{q}^2$
$\mathcal{E} \equiv [1, 1, 0, 1, 1, 1, 1, -1, 1]$	$c_{\mathcal{E}} = -2\xi\mathbf{q}^2$
$\mathcal{F} \equiv [1, 1, 1, 1, 1, 1, -2, 0, 1]$	$c_{\mathcal{F}} = -\xi\mathbf{q}^2$
$\mathcal{G} \equiv [1, 1, 1, 0, 1, 1, 0, 0, 1]$	$c_{\mathcal{G}} = 0$

Table III.1: *Coefficients of the master integrals. Each coefficient should be multiplied by the common overall factor $(-2i\mathbf{q}^2)g^4N_c^2$.*

The master integral \mathcal{A} can be shown to vanish by symmetry if the symmetric pole prescription is employed for the eikonal poles of the induced vertices. The ρ -enhanced pieces of the remaining master integrals are computed up to terms of order $\mathcal{O}(\epsilon)$ using the Mellin-Barnes technique, for a review see e.g. [Smi06]. To this end, we first derive multi-contour integral representations for the master integrals, where we refer for details to APP. C. As a second step we resolve the structure of singularities in ϵ , using the codes MB [Cza06] and MBresolve [SS09]. In this way we obtain a set of Mellin-Barnes integrals that can be safely expanded in ϵ at the level of the integrand.

Here we point out the following important observation: it is possible to simplify the expressions by expanding in ϵ , using the routine MBexpand, and capturing the leading behavior in ρ using MBasymptotics [Cza, Cza06]¹⁷. In principle, both procedures commute and the ordering in which they are applied is irrelevant, which we have verified to be the

¹⁷Eventually some of the remaining integrals can be further simplified using Barnes' lemmas implemented in barnesroutines [Kos], and performing straightforward changes of variables.

III. Lipatov Effective Action Approach to High Energy QCD

case. However, after applying these two procedures, unphysical divergences in the light-cone regulator appear (*e.g.* terms of order $\mathcal{O}(\rho^3)$) which would invalidate the general procedure formulated in SEC. III.3.1. It is therefore important to note that such terms are an artifact of the combination of our two regularizations, which leads to ambiguous terms of the form $e^{-k\rho\epsilon}$, $k \in \mathbb{Z}$. Indeed there exists a wide class of such examples in the literature, for instance massive integrals with a mass scale m . In the latter case, the limit $m \rightarrow 0$ cannot be taken in a sensible way after the integration has been carried out in dimensional regularization. Indeed, such an attempt would lead to spurious divergences. Instead, the massless result can be successfully recovered by expanding in the small parameter m *before* performing the expansion in ϵ and removing those terms of the form $m^{k\epsilon}$, $k \in \mathbb{Z}$. Since we remove pieces of the integrand, the limits do no longer commute and the ordering is important. In our present case, we stick to the following prescription: we first use the code `MBasymptotics` to expand in ρ ; then we delete the terms proportional to $e^{-k\rho\epsilon}$, $k \in \mathbb{Z}$, and eventually expand in ϵ .

Following this procedure we obtain for the master integrals the following result:¹⁸

$$\begin{aligned}
c_{\mathcal{B}} \cdot \mathcal{B} &= \frac{1}{(4\pi)^4} \left[\frac{11}{\epsilon^2} - \frac{1 + 66\Xi}{3\epsilon} + \frac{400 + 12\Xi + 396\Xi^2 - 33\pi^2}{18} \right] \rho, \\
c_{\mathcal{C}} \cdot \mathcal{C} &= \frac{1}{(4\pi)^4} \left(\left[-\frac{4}{\epsilon^3} - \frac{8(1-\Xi)}{\epsilon^2} - \frac{\pi^2 + 8(1-\Xi)^2}{\epsilon} - 2\pi^2(1-\Xi) \right. \right. \\
&\quad \left. \left. - \frac{16(1-\Xi)^3}{3} - \frac{50}{3}\zeta(3) \right] \rho + \left[\frac{2}{\epsilon^2} + \frac{4(1-\Xi)}{\epsilon} + \frac{1}{3}(12(1-\Xi)^2 - \pi^2) \right] \rho^2 \right), \\
c_{\mathcal{D}} \cdot \mathcal{D} &= \frac{1}{(4\pi)^4} \left[\frac{4}{\epsilon^3} + \frac{8(1-\Xi)}{\epsilon^2} + \frac{4(\pi^2 + 6(1-\Xi)^2)}{3\epsilon} + \frac{8\pi^2(1-\Xi)}{3} \right. \\
&\quad \left. + \frac{16(1-\Xi)^3}{3} + \frac{44\zeta(3)}{3} \right], \\
c_{\mathcal{E}} \cdot \mathcal{E} &= 0, \\
c_{\mathcal{F}} \cdot \mathcal{F} &= \frac{1}{(4\pi)^4} \left[-\frac{4}{\epsilon^2} + \frac{8\Xi}{\epsilon} + \frac{2\pi^2}{3} - 8(1 + \Xi^2) \right], \tag{III.68}
\end{aligned}$$

where we introduced the notation

$$\Xi = 1 - \gamma_E - \ln \frac{q^2}{4\pi\mu^2}. \tag{III.69}$$

Using these results, the (unsubtracted) contribution to the reggeon self-energy (with $N_f = 0$) is obtained as follows:

¹⁸We have not considered imaginary pieces in (III.68). Their contribution, computed at the end of this section, is shown in (III.70).

$$\begin{aligned}
 \text{2-loop gluon cont.} &= (-2i\mathbf{q}^2) \frac{g^4 N_c^2}{(4\pi)^4} \left(\left\{ \frac{2}{\epsilon^2} + \frac{4(1-\Xi)}{\epsilon} + 4(1-\Xi)^2 - \frac{\pi^2}{3} \right\} \rho^2 + \left\{ \frac{7}{\epsilon^2} - \frac{14\Xi}{\epsilon} - \frac{1-\pi^2}{3\epsilon} \right. \right. \\
 &\quad \left. \left. - 2\frac{\Xi(\pi^2-1)}{3} + 14(1+\Xi^2) + \frac{2}{9} - \frac{\pi^2}{2} + 2\zeta(3) - i\pi \left[\frac{1}{\epsilon^2} + 2\frac{\Xi-1}{\epsilon} + (\Xi-1)^2 \right] \right\} \rho. \right. \\
 &\hspace{15em} \text{(III.70)}
 \end{aligned}$$

Expanding (III.50) in ϵ , we find for the subtracted reggeized gluon self-energy with $N_f = 0$

$$\begin{aligned}
 \Sigma_{N_f=0}^{(2)} \left(\rho, \frac{\mathbf{q}^2}{\mu^2} \right) &= \text{2 loop} = \text{2 loop} - \text{1 loop} = -(-i2\mathbf{q}^2) \frac{g^4 N_c^2}{(4\pi)^4} \left\{ \left[\frac{2}{\epsilon^2} + \frac{4(1-\Xi)}{\epsilon} \right. \right. \\
 &\quad \left. \left. + 4(1-\Xi)^2 - \frac{\pi^2}{3} \right] \rho^2 + \left[\frac{1}{3\epsilon^2} + \frac{1}{9\epsilon} + \frac{\pi^2}{3\epsilon} - \frac{2\Xi}{3\epsilon} + \frac{\pi^2(11-12\Xi)}{18} \right. \right. \\
 &\quad \left. \left. + \frac{16}{27} - \frac{2}{9}\Xi + \frac{2}{3}\Xi^2 - \frac{1}{2}\zeta(3) \right] \rho \right\} + \mathcal{O}(\epsilon) + \mathcal{O}(\rho^0). \hspace{5em} \text{(III.71)}
 \end{aligned}$$

The next step is to confront our result for the 2-loop self-energy with the definition of the 2-loop gluon Regge trajectory (III.60). At first we realize that all divergent terms $\sim \rho$ cancel against each other since the terms quadratic in ρ in (III.71) cancel precisely the term $[\rho\omega^{(1)}]^2/2$ in (III.60), i.e.

$$(\omega^{(1)})^2 \frac{\rho^2}{2} + \frac{\Sigma_{\rho^2}^{(2)}}{(-2i\mathbf{q}^2)} = 0, \hspace{10em} \text{(III.72)}$$

if the first term is expanded up to $\mathcal{O}(\epsilon)$. Taking the function $f^{(1)}$ in the limit $N_f = 0$, the remaining terms then yield the 2-loop Regge gluon trajectory for zero flavors,

$$\omega^{(2)}(\mathbf{q}^2)|_{N_f=0} = \frac{(\omega^{(1)}(\mathbf{q}^2))^2}{4} \left[\frac{11}{3} + \left(\frac{\pi^2}{3} - \frac{67}{9} \right) \epsilon + \left(\frac{404}{27} - 2\zeta(3) \right) \epsilon^2 \right], \hspace{5em} \text{(III.73)}$$

which is in complete agreement with the results in the literature [FFK96a]. For the quark loop terms, one gets from (III.61) the- ρ enhanced terms of the subtracted 2-loop self-energy

$$\begin{aligned}
 \Sigma_{N_f}^{(2)} \left(\rho; \epsilon, \frac{\mathbf{q}^2}{\mu^2} \right) &= \frac{\rho(-2i\mathbf{q}^2)\bar{g}^4 4N_f}{\epsilon N_c} \frac{\Gamma^2(2+\epsilon)}{\Gamma(4+2\epsilon)} \left(\frac{\mathbf{q}^2}{\mu^2} \right)^{2\epsilon} \left(\frac{\Gamma^2(1+\epsilon)}{\Gamma(1+2\epsilon)} \frac{4}{\epsilon} \right. \\
 &\quad \left. - \frac{3\Gamma(1-2\epsilon)\Gamma(1+\epsilon)\Gamma(1+2\epsilon)}{\Gamma^2(1-\epsilon)\Gamma(1+3\epsilon)\epsilon} \right). \hspace{5em} \text{(III.74)}
 \end{aligned}$$

III. Lipatov Effective Action Approach to High Energy QCD

The whole result for the 2-loop gluon Regge trajectory with N_f flavors reads

$$\omega^{(2)}(\mathbf{q}^2) = \frac{(\omega^{(1)}(\mathbf{q}^2))^2}{4} \left[\frac{11}{3} - \frac{2N_f}{3N_c} + \left(\frac{\pi^2}{3} - \frac{67}{9} \right) \epsilon + \left(\frac{404}{27} - 2\zeta(3) \right) \epsilon^2 \right]. \quad (\text{III.75})$$

Imaginary Parts We want to check explicitly here that the expression of $\omega^{(2)}$ (and therefore of $\Sigma^{(2)}$) is real and imaginary parts cancel among the unsubtracted two-loop self-energy and the subtractions. Let us first consider the 1-loop self-energy¹⁹

$$\begin{aligned} \omega^{(1)} &\propto \int [dk] \frac{1}{(-k^2 - i0)(-(k-q)^2 - i0)(-n_a \cdot k)_{\text{PV}}(-n_b \cdot k)_{\text{PV}}} = \frac{1}{2}(C_{++} - C_{+-}); \\ C_{\pm\pm} &= \int [dk] \frac{1}{(-k^2 - i0)(-(k-q)^2 - i0)(-n_a \cdot k \pm i0)(-n_b \cdot k \pm i0)}, \quad n_a \cdot q = n_b \cdot q = 0. \end{aligned} \quad (\text{III.76})$$

We have used that $C_{++} = C_{--}$ and $C_{+-} = C_{-+}$, as it can be seen making the shift $k \rightarrow -k+q$ in the loop integral. Using standard techniques for Feynman integrals like those presented in APP. C, we have

$$C_{++} = \frac{i\rho}{(4\pi)^{2+\epsilon}} (\mathbf{q}^2)^{\epsilon-1} \frac{\Gamma(1-\epsilon)\Gamma^2(\epsilon)}{\Gamma(2\epsilon)} + \mathcal{O}(e^{-\rho}). \quad (\text{III.77})$$

Now one can extract the relevant piece of the result for C_{+-} from that of C_{++} without computing from scratch. To this end we rescale the light-cone vectors $n_{a,b} \rightarrow a, b = \frac{e^{\rho/2}}{2} n_{a,b}$, in such a way that $a^2 = b^2 = 1$ and $a \cdot b = \cosh \rho$. The rescaled integral, $\tilde{C}_{\pm\pm} = \frac{e^\rho}{4} C_{\pm\pm}$ can only depend on a and b through the combination $a \cdot b$. Making use of

$$\frac{1}{-a \cdot k + i0} = -\frac{1}{-(-a) \cdot k - i0}, \quad (\text{III.78})$$

we see that evaluating the integral with the $+i0$ pole prescription corresponds to evaluate the integral with the $-i0$ prescription making $a \rightarrow -a$. Due to the linearity of the scalar product this is equivalent to $\rho \rightarrow \rho - i\pi$ ²⁰. This accounts for the imaginary part in (III.49). An enhanced imaginary part appears in the subtraction, proportional to the 1-loop self-energy squared, since $(\rho - i\pi/2)^2 = \rho^2 - i\pi\rho + \mathcal{O}(\rho^0)$.

Expanding this enhanced imaginary contribution in ϵ , one can see that it exactly cancels in the expression for $\Sigma^{(2)}$ with the imaginary part appearing in master integral \mathcal{C} (Eq. (III.70)). This imaginary part is obtained exactly in the same way outlined before, performing the sub-

¹⁹Let us remind that our pole prescription coincides with the principal value for the RGG vertex.

²⁰In principle one has two possibilities $\rho \rightarrow \rho \pm i\pi$, since $\cosh(\rho \pm i\pi) = \cosh \rho$. The selection of $-i\pi$ is due to the initial imaginary part $+i0$ in the eikonal propagator.

stitution $\rho \rightarrow \rho - i\pi$ on the expression for the master integral computed with $-i0$ prescription in all propagators to obtain the other pieces of the principal value. It is also interesting to review the computation of diagram (k₁) in detail, since we have to use here the vertex (III.40) and we can check that the symmetry properties of our pole prescription respect hermiticity of the Lagrangian and do not give rise to spurious imaginary parts. This is done in APP. D.

4 FORWARD JET PRODUCTION [CHMS12b]

In this section we present the computation within Lipatov’s action framework of the vertex describing the production of a jet in a forward direction very close in the detector to one of the hadrons in hadron-hadron interactions at very high energies, in the next-to-leading approximation. This is done in the kinematic approximation where the jet is well separated in rapidity from other jets also produced in the scattering process. The convolution of this jet vertex with the NLL BFKL gluon Green’s function plays a very important role in the description of jet production at the LHC physics program [Sch07, MR09, MR09, DHJK09, CSSW10, CIM⁺12].

4.1 Real Corrections

High-Energy $gg \rightarrow gg$ Scattering in the Born Approximation Consider the gluon counterpart of the scattering process described in SEC. III.2.3. External gluons are on-shell: $p_a^2 = (p_a - q)^2 = p_b^2 = (p_b + q)^2 = 0$. In the high-energy limit the corresponding scattering amplitude factorizes into a reggeized gluon exchange in the t -channel and its couplings to the external particles, the impact factors. At tree level this is shown in FIG. III.10.

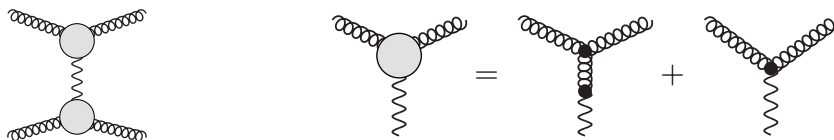


Figure III.10: Tree-level contribution to the gluon-gluon scattering amplitude in terms of effective vertices.

The polarization vectors must be physical, satisfying for the upper vertex $\varepsilon \cdot p_a = 0$ and $\varepsilon^* \cdot (p_a - q) = 0$. The last relation implies that $\varepsilon^* \cdot p_a = \varepsilon^* \cdot q$. Gauge invariance of the effective action enables us to choose *different* gauges for the upper and lower gluon-gluon-reggeized gluon couplings. We therefore impose the condition $\varepsilon(p_a) \cdot n^+ = \varepsilon^*(p_1) \cdot n^+ = 0$ for

III. Lipatov Effective Action Approach to High Energy QCD

the upper vertex and the condition $\varepsilon(p_b) \cdot n^- = \varepsilon^*(p_2) \cdot n^- = 0$ for the lower vertex, which implies that (I.5) applies, with p being the gluon momentum and $n = n^\pm$.

To define the impact factors we start from the general definitions (A.25) and (A.26). In the special case where all final state particles are produced either in the fragmentation region of particle a or particle b we rewrite, with $m = m_a + m_b$, the overall delta function (which exhibits overall momentum conservation) as follows²¹

$$(2\pi)^d \delta^d\left(p_a + p_b - \sum_{j=1}^m p_j\right) = \int \frac{d^d q}{(2\pi)^d} (2\pi)^{2d} \delta^d\left(p_a + q - \sum_{j=1}^{m_a} p_j\right) \times \delta^d\left(p_b - q - \sum_{l=1}^{m_b} p_l\right). \quad (\text{III.80})$$

The effective action naturally factorizes the amplitude $iA_{gr^* \rightarrow g_1}$ into two products of $iA_{gr^* \rightarrow g_1}$ times the square-root of the reggeized gluon propagator $i/2\mathbf{q}^2$. Squaring, averaging over color and polarization of the initial gluon and summing over color and polarization of the final state and reggeized gluon (at the level of the $gr^* \rightarrow g$ amplitudes), the $2 \rightarrow 2$ tree-level amplitude takes the following factorized form

$$\overline{|A_{g_a g_b \rightarrow g_1 g_2}|^2} = \frac{\overline{|A_{g_a r^* \rightarrow g_1}^{(0)}|^2}}{2\mathbf{q}^2 \sqrt{N_c^2 - 1}} \times \frac{\overline{|A_{g_b r^* \rightarrow g_2}^{(0)}|^2}}{2\mathbf{q}^2 \sqrt{N_c^2 - 1}}. \quad (\text{III.81})$$

The amplitude $iA_{gr^* \rightarrow g_1}$ itself receives at tree-level two contributions (FIG. III.10): one from the GGR vertex $(gf_{abc} \frac{\mathbf{q}_+^2}{p_a^+} (n^+)^{\mu_1} (n^+)^{\mu_2} \varepsilon_{\mu_1} \varepsilon_{\mu_2}^*)$ and the other from the projection of the 3-gluon vertex $(gf_{abc} [2g^{\mu_1 \mu_2} p_a^+ - (n^+)^{\mu_1} (p_a - q)^{\mu_2} - (n^+)^{\mu_2} (2q + p_a)^{\mu_1}] \varepsilon_{\mu_1} \varepsilon_{\mu_2}^*)$. We have, averaging over colors and polarizations of the initial gluon²²

$$\begin{aligned} \overline{|A_{gr^* \rightarrow g}|^2} &= \frac{N_c(N_c^2 - 1)}{2(N_c^2 - 1)} g^2 (2p_a^+)^2 g^{\mu\nu} g^{\mu'\nu'} \left[-g_{\mu\mu'} + \frac{(p_a)_\mu (n^+)_{\mu'} + (p_a)_{\mu'} (n^+)_{\mu}}{p_a^+} \right] \\ &\times \left[-g_{\nu\nu'} + \frac{(p_a)_\nu (n^+)_{\nu'} + (p_a)_{\nu'} (n^+)_{\nu}}{p_a^+} \right] = 4N_c g^2 (p_a^+)^2. \end{aligned} \quad (\text{III.82})$$

The phase space reads

²¹The generalization to the additional production of n particle clusters at central rapidities, with $m = m_a + m_b + \sum_i^n m_i$, reads

$$\begin{aligned} (2\pi)^d \delta^d\left(p_1 + p_2 - \sum_{j=1}^m p_j\right) &= \prod_{i=0}^n \int \frac{d^d k_i}{(2\pi)^d} (2\pi)^{(2+n)d} \delta^d\left(p_a + k_0 - \sum_{l_0=1}^{m_a} p_{l_0}\right) \times \\ &\delta^d\left(p_b - k_n - \sum_{l_n=1}^{m_b} p_{l_n}\right) \times (2\pi)^{nd} \delta^d\left(k_0 - k_1 - \sum_{l_1=1}^{m_1} p_{l_1}\right) \times \dots \delta^d\left(k_n - k_{n+1} - \sum_{l_n=1}^{m_n} p_{l_n}\right). \end{aligned} \quad (\text{III.79})$$

²²A multiplicative factor $(1 + \epsilon)$ appears if one computes the tree level amplitude in $4 + 2\epsilon$ dimensions.

$$\begin{aligned} \int d\Pi_2 &= \iint \frac{d^d p_1}{(2\pi)^{d-1}} \frac{d^d p_2}{(2\pi)^{d-1}} \delta(p_1^2) \delta(p_2^2) (2\pi)^d \delta^d(p_1 + p_2 - p_a - p_b) = \int \frac{d^d p_1}{(2\pi)^{2+2\epsilon}} \delta(p_1^2) \delta((p_a + p_b - p_1)^2) \\ &= \frac{1}{(2\pi)^{2+2\epsilon}} \int d^d k \delta((p_a + q)^2) \delta((p_b - q)^2) = \frac{1}{(2\pi)^{2+2\epsilon}} \frac{1}{2p_a^+ p_b^-} \int d^{2+2\epsilon} \mathbf{q}, \end{aligned} \quad (\text{III.83})$$

where we have performed a shift in the momentum variable and used that $(p_a + q)^2 = p_a^+ q^-$, $(p_b - q)^2 = -p_b^- q^+$ and $d^d q = \frac{1}{2} dq^+ dq^- d^{d-2} \mathbf{q}$. The flux factor appearing in (A.25) is $\Phi = \frac{1}{2s} = \frac{1}{2p_a^+ p_b^-}$, so that putting everything together we get

$$h_{a,\text{gluon}}^{(0)}(\mathbf{q}) = \frac{N_c}{\sqrt{N_c^2 - 1}} \frac{g^2}{\mathbf{q}^2} \frac{1}{(2\pi)^{1+\epsilon}} = \frac{2^{1+\epsilon} \tilde{\alpha}_s C_A}{\mu^{2\epsilon} \Gamma(1 - \epsilon) \sqrt{N_c^2 - 1}} \frac{1}{\mathbf{q}^2}. \quad (\text{III.84})$$

Real Corrections: Gluon Initiated Vertex We have two types of corrections at next-to-leading order. On one hand we have the 1-loop corrections to the GGR vertex; on the other, the production of an extra particle in the final state (real corrections). The real corrections to the Born-level process can be organized into three contributions to the five-point amplitude with central and quasielastic gluon production (FIG. III.11). In the same way as the effective action gives rise to divergences near the lightcone when computing virtual corrections, a cutoff in rapidity must be enforced in the longitudinal integrations that will appear in the phase space.

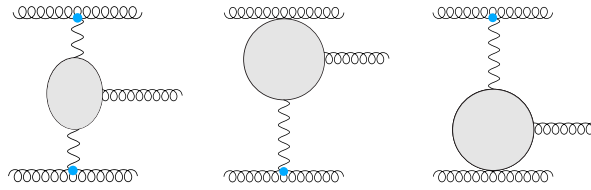


Figure III.11: Central (left) and quasi-elastic (middle and right) gluon production.

The central production amplitude yields the unintegrated real part of the forward leading order BFKL kernel (the Lipatov vertex) and is obtained from the sum of the following three effective diagrams:

$$\begin{aligned} \text{Diagram} &= \text{Diagram 1} + \text{Diagram 2} + \text{Diagram 3}. \end{aligned} \quad (\text{III.85})$$

The squared amplitude for (III.85), averaged over color of the incoming reggeons and summed over final state colors and helicities reads [HS12]

III. Lipatov Effective Action Approach to High Energy QCD

$$\overline{|A|^2}_{r^*r^* \rightarrow g} = \frac{16g^2 N_c (\mathbf{q} - \mathbf{k})^2 \mathbf{k}^2}{N_c^2 - 1 \mathbf{q}^2}. \quad (\text{III.86})$$

The contribution of central production to the exclusive differential cross section

$$d\sigma_{ab}^{(c)} = h_a^{(0)}(\mathbf{k}') h_b^{(0)}(\mathbf{k}) \mathcal{V}(\mathbf{k}, \mathbf{k}'; y_a, y_b) d^{2+2\epsilon} \mathbf{k}' d^{2+2\epsilon} \mathbf{k} dy, \quad (\text{III.87})$$

is written in terms of the regularized production vertex $\mathcal{V}(\mathbf{k}, \mathbf{k}'; y_a, y_b) \equiv V(\mathbf{k}, \mathbf{k}') \Theta(y_a - y) \Theta(y - y_b)$, which is given by [HS12]

$$\mathcal{V}(\mathbf{k}, \mathbf{k}') = \frac{N_c^2 - 1}{8(2\pi)^{3+2\epsilon} \mathbf{k}'^2 \mathbf{k}^2} \overline{|A|^2}_{r^*r^* \rightarrow g} = \frac{\tilde{\alpha}_s N_c}{\pi_\epsilon \pi (\mathbf{k} + \mathbf{k}')^2}; \quad \pi_\epsilon \equiv \pi^{1+\epsilon} \Gamma(1 - \epsilon) \mu^{2\epsilon}. \quad (\text{III.88})$$

On the other hand, the quasielastic contribution $g(p_a) r^*(k) \rightarrow g(p) g(q)$ (see the notation in FIG. III.12) is given by the sum of effective diagrams in FIG. III.13. The details of the computation of the diagrams are given in APP. D.

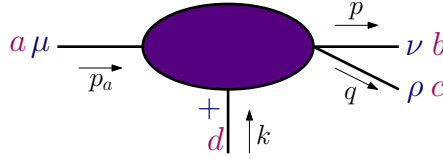


Figure III.12: Notation for external momenta and colour indices in the quasi-elastic contribution.

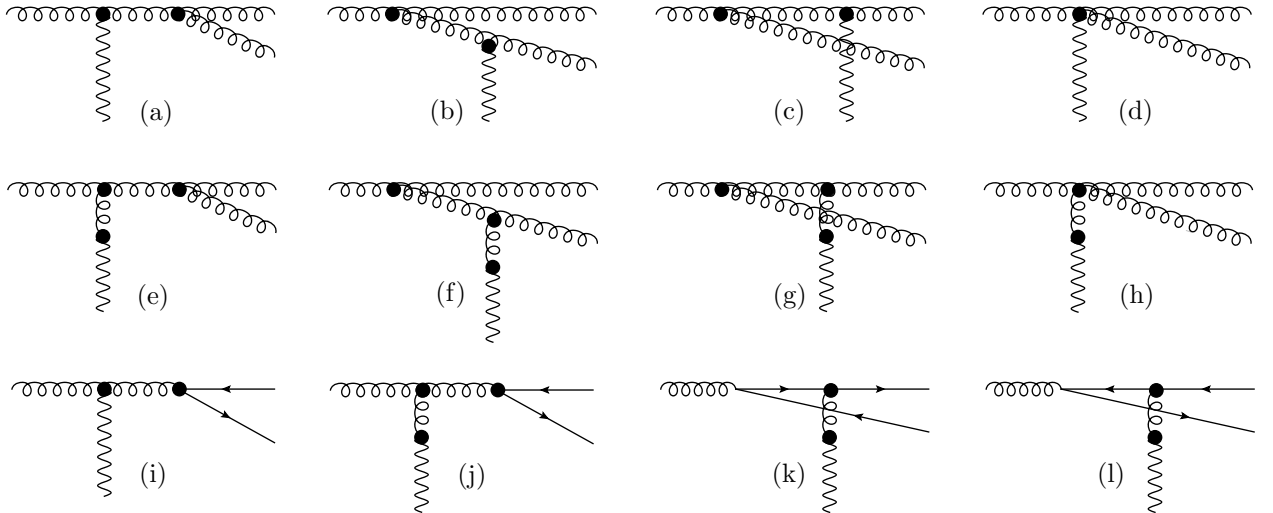


Figure III.13: Diagrams involved in the computation of the real corrections. In the case of a final $q\bar{q}$ state, the external quark has momentum p and the external antiquark momentum q .

Let us note that we have two different final states: gg and $q\bar{q}$. In the first case, we perform the sum over polarization vectors using (I.5). Then one gets, summing the amplitudes for

diagrams (e), (f) and (g), given in APP. D, squaring and averaging over initial colors and polarizations

$$\begin{aligned} \overline{|A^2|}_{gg \rightarrow ggg} &= \frac{8g^4 N_c^2}{stu} (p_a^+)^2 \frac{(1+\epsilon)[1-z(1-z)]^2}{z(1-z)} \mathbf{k}^2 (s-zt - (1-z)u) \\ &= -\frac{8g^4 N_c}{t} (p_a^+)^2 z(1+\epsilon) \mathcal{P}_{gg}(z) \mathbf{k}^2 \left[\frac{z^2(\mathbf{k}-\mathbf{q})^2 + (1-z)^2 \mathbf{q}^2 - z(1-z) \mathbf{q} \cdot (\mathbf{k}-\mathbf{q})}{\mathbf{q}^2(\mathbf{q}-z\mathbf{k})^2} \right]. \end{aligned} \quad (\text{III.89})$$

where $\mathcal{P}_{gg}(z) = N_c \frac{1+z^4+(1-z)^4}{z(1-z)}$ is the gluon-gluon Altarelli-Parisi function. In the same way, joining the contributions of diagrams (j), (k) and (l) we get for the $q\bar{q}$ final state

$$\begin{aligned} \overline{|A^2|}_{gg \rightarrow q\bar{q}} &= -\frac{2g^4}{sut} N_f (p_a^+)^2 \mathbf{k}^2 [1+\epsilon - 2z(1-z)] \left[\frac{s}{N_c} + N_c(zt + (1-z)u) \right] \\ &= \frac{8g^4}{ut} N_f N_c (p_a^+)^2 (1+\epsilon) \mathcal{P}_{qg}(z, \epsilon) \mathbf{k}^2 \left[\frac{C_F}{C_A} + z(1-z) \frac{\mathbf{q} \cdot (\mathbf{k}-\mathbf{q})}{(\mathbf{q}-z\mathbf{k})^2} \right], \end{aligned} \quad (\text{III.90})$$

with $\mathcal{P}_{qg}(z, \epsilon) = \frac{1}{2} \left[1 - \frac{2z(1-z)}{1+\epsilon} \right]$ the quark-gluon splitting function.

The only remaining ingredient is the phase space for the 3-particle final state. It reads

$$\int d\Pi_3 = \iiint \frac{d^d p}{(2\pi)^{d-1}} \frac{d^d q}{(2\pi)^{d-1}} \frac{d^d p_2}{(2\pi)^{d-1}} \delta(p^2) \delta(q^2) \delta(p_2^2) (2\pi)^d \delta^d(p_a + p_b - p - q - p_2). \quad (\text{III.91})$$

Using that the squared amplitude does not depend explicitly on the momenta of the final particles we can perform a shift in the integration momenta and use the momentum conservation Dirac delta to write

$$\int d\Pi_3 = \frac{1}{(2\pi)^{5+4\epsilon}} \iint d^d k d^d q \delta((p_a + k - q)^2) \delta(q^2) \delta((p_b - k)^2). \quad (\text{III.92})$$

Now we use the decomposition $d^d k = \frac{1}{2} dk^+ dk^- d^{d-2} \mathbf{k}$, we write $q^+ = zp_a^+$ and evaluate the Dirac deltas

$$\begin{aligned} \delta((p_b - k)^2) &= \frac{1}{p_b^-} \delta\left(k^+ - \frac{\mathbf{k}^2}{p_b^-}\right); & \delta(q^2) &= \frac{1}{zp_a^+} \delta\left(q^- - \frac{\mathbf{q}^2}{zp_a^+}\right); \\ \delta((p_a + k - q)^2) &= \frac{1}{p_a^+(1-z)} \delta\left[k^- - \left(\mathbf{k}^2 + \frac{\mathbf{q}^2}{z}\right)\right], \end{aligned} \quad (\text{III.93})$$

to write

$$\int d\Pi_3 = \frac{1}{4(2\pi)^{5+4\epsilon} p_a^+ p_b^-} \int d\mathbf{k} d\mathbf{q} \frac{dz}{z(1-z)}, \quad (\text{III.94})$$

so that the cross-section (for, e.g. the gluon-gluon final state) is

III. Lipatov Effective Action Approach to High Energy QCD

$$\sigma_{qg \rightarrow qgg} = \frac{1}{(2p_a^+ p_b^-)^2} \frac{1}{2(2\pi)^{5+4\epsilon}} \iint d\mathbf{k} d\mathbf{q} \frac{dz}{z(1-z)} \frac{1}{4(N_c^2 - 1)(\mathbf{k}^2)^2} |A^{(0)}|_{g_a r^* \rightarrow gg}^2 |A^{(0)}|_{q_b r^* \rightarrow qg}^2. \quad (\text{III.95})$$

Extracting the quasielastic correction for each of the final states is easier if we consider the process $qg \rightarrow \{qgg, qq\bar{q}\}$. We then define, following [BCV03]²³

$$d\sigma_{qg \rightarrow \text{fin}} = h_{\text{quark}}^{(0)}(\mathbf{k}) F_{\text{fin}}(\mathbf{k}, \mathbf{k}', z) h_{\text{gluon}}^{(0)}(\mathbf{k}') d\mathbf{k} d\mathbf{k}' dz \quad \left(z > z_{\text{cut}} \equiv e^{-y_b} \frac{\sqrt{\mathbf{q}^2}}{p_a^+} \right), \quad (\text{III.97})$$

where $h_{\text{quark}}^{(0)}$ and $h_{\text{gluon}}^{(0)}$ are given in (III.44) and (III.84) respectively. Using all the above information, we get

$$F_{ggg}(\mathbf{k}, \mathbf{k}', z) = \frac{1}{2} \frac{\alpha_s}{2\pi\pi_\epsilon} \mathcal{P}_{gg}(z) \left[\frac{z^2 \mathbf{k}'^2 + (1-z)^2 \mathbf{q}^2 - z(1-z) \mathbf{q} \cdot \mathbf{k}'}{\mathbf{q}^2 \Delta^2} \right], \quad (\text{III.98})$$

where $\Delta \equiv \mathbf{q} - z\mathbf{k}$, and

$$F_{gq\bar{q}}(\mathbf{k}, \mathbf{k}', z) = \frac{\alpha_s}{2\pi\pi_\epsilon} N_f \mathcal{P}_{qg}(z, \epsilon) \frac{1}{\mathbf{q}^2} \left[\frac{C_f}{C_a} + z(1-z) \frac{\mathbf{q} \cdot \Delta}{\Delta^2} \right]. \quad (\text{III.99})$$

The overall factor 1/2 for the gg final state stems from the indistinguishability of identical bosons in the final state. The results (III.98) and (III.99) are in complete agreement with those previously found in the literature [BCV02, BCV03].

Parameterizing the momentum fraction z in terms of the rapidity difference $\Delta y \equiv y_p - y_q$ of the final state gluons,

$$z = \frac{e^{\Delta y}}{(\mathbf{k}'^2/\mathbf{q}^2) + e^{\Delta y}}, \quad (\text{III.100})$$

it is straightforward to see that F_{ggg} reduces in the limits $\Delta y \rightarrow \pm\infty$ (including a corresponding Jacobian factor) to half the central production vertex (III.88). To regularize the resulting divergence of the rapidity integral we introduce a lower bound $|\Delta y| > -\eta_b$, where η_b is again taken in the limit $\eta_b \rightarrow -\infty$, and define $\mathcal{F}_{ggg}(\mathbf{k}, \mathbf{k}', z, \eta_b) = F_{ggg}(\mathbf{k}, \mathbf{k}', z) \Theta(|\Delta y| + \eta_b)$. According to our general procedure, we have to subtract the contribution from gluon production

²³One can also define one-loop impact factors through the formula [CHMS12b]

$$h_{\{gg, q\bar{q}\}}^{(1)}(\mathbf{k}) = \int dz d^{2+2\epsilon} \mathbf{k}' F_{\{ggg, gq\bar{q}\}}(\mathbf{k}, \mathbf{k}', z) h_{\text{gluon}}^{(0)}(\mathbf{k}'). \quad (\text{III.96})$$

at central rapidities to construct the complete differential cross section, schematically:

$$\text{Diagram 1} = \text{Diagram 2} - \text{Diagram 3} - \text{Diagram 4} \quad (\text{III.101})$$

This leads to the definition of the coefficient

$$\mathcal{G}_{ggg}^{(a)}(\mathbf{k}, \mathbf{k}', z, \eta_b) = \mathcal{F}_{ggg}(\mathbf{k}, \mathbf{k}', z, \eta_b) - \frac{1}{2} \left[\frac{1}{z} \mathcal{V}(\mathbf{k}, \mathbf{k}'; \mathbf{q}; \eta_a, \eta_b) + \frac{1}{1-z} \mathcal{V}(\mathbf{k}, \mathbf{q}; \mathbf{k}'; \eta_a, \eta_b) \right]. \quad (\text{III.102})$$

Finally, defining the cross-section for quasi-elastic production as

$$d\sigma_{ab}^{(qea)} = h_{a,\text{gluon}}^{(0)}(\mathbf{k}') \mathcal{G}_{ggg}^{(a)}(\mathbf{k}, \mathbf{k}', z, \eta_b) h_{b,\text{gluon}}^{(0)} dz d^{2+2\epsilon} \mathbf{k} d^{2+2\epsilon} \mathbf{k}', \quad (\text{III.103})$$

the sum of of central and quasi-elastic contributions,

$$d\sigma_{ab} = d\hat{\sigma}_{ab}^{(c)} + d\sigma_{ab}^{(qea)} + d\sigma_{ab}^{(qeb)}, \quad (\text{III.104})$$

turns out to be finite when integrated over the gluon rapidity, with a well-defined limit $\eta_{a,b} \rightarrow \pm\infty$. The computation of the forward jet vertex in the quark-initiated case is carried out exactly in the same way, see [HS12] for details.

4.2 One-Loop Gluon-Gluon-Reggeon Vertex

The one-loop corrections to this gluon-gluon-reggeized gluon vertex are shown in FIG. III.14. All diagrams are evaluated in the limit $\rho \rightarrow \infty$, while we only keep track of divergent ($\mathcal{O}(\rho)$)

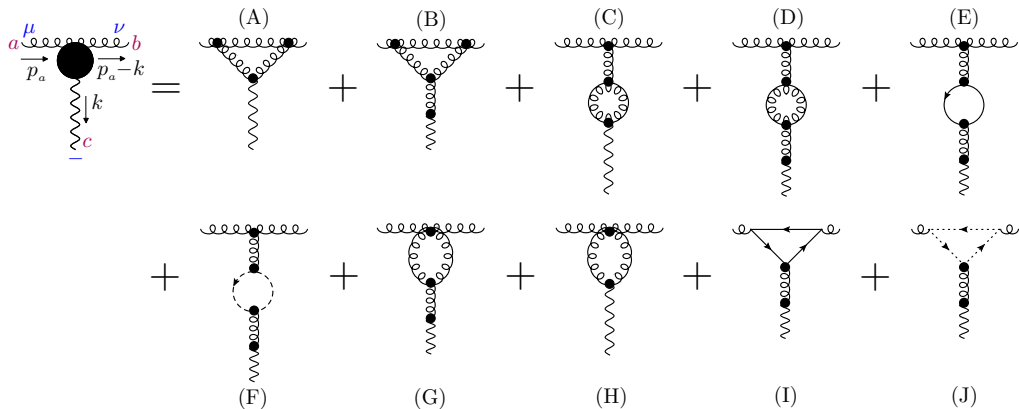


Figure III.14: One-loop virtual corrections to the gluon-initiated jet vertex.

III. Lipatov Effective Action Approach to High Energy QCD

and finite ($\mathcal{O}(\rho^0)$) terms; ϵ is on the other hand kept finite. Details about the calculation of individual diagrams can be found in APP. D. The final result for the 1-loop $gr^* \rightarrow g$ amplitude reads

$$\begin{aligned}
iA_{gr^* \rightarrow g_1}^{(1)} = & -\frac{g^3 \mu^{2\epsilon} p_a^+}{(4\pi)^{2+\epsilon}} f_{abc} \left(\frac{\mathbf{q}^2}{\mu^2}\right)^\epsilon \left\{ N_c \epsilon \cdot \epsilon^* \frac{\Gamma(1-\epsilon)\Gamma^2(\epsilon)}{\Gamma(2\epsilon)} \left[2 \ln \left(\frac{p_a^+}{|\mathbf{q}|}\right) + \rho + \psi(1) \right. \right. \\
& - 2\psi(\epsilon) + \psi(1-\epsilon) \left. \right] + 8[N_c(1+\epsilon) - N_f] \left[-\frac{1}{2} \epsilon \cdot \epsilon^* \frac{\Gamma^2(1+\epsilon)\Gamma(-\epsilon)}{\Gamma(4+2\epsilon)} \right. \\
& + \left. \frac{\epsilon \cdot q \epsilon^* \cdot q \Gamma(\epsilon)\Gamma(1-\epsilon)}{\mathbf{q}^2 \Gamma(4+2\epsilon)} (2\Gamma(1+\epsilon) + \Gamma(2+\epsilon)) \right] \\
& + 8[N_c(1+\epsilon) - N_f] \frac{\epsilon \cdot q \epsilon^* \cdot q}{\mathbf{q}^2} \frac{\Gamma(-\epsilon)\Gamma^2(1+\epsilon)}{(2+2\epsilon)\Gamma(2+2\epsilon)} + \epsilon \cdot \epsilon^* (4N_c - N_f) \frac{\Gamma(-\epsilon)\Gamma^2(1+\epsilon)}{\epsilon \Gamma(2+2\epsilon)} \\
& - \epsilon \cdot \epsilon^* (4N_c - N_f) \frac{1+2\epsilon}{\epsilon} \frac{\Gamma(-\epsilon)\Gamma^2(1+\epsilon)}{\Gamma(2+2\epsilon)} + 2N_c \epsilon \cdot \epsilon^* \frac{\Gamma(-\epsilon)\Gamma^2(1+\epsilon)}{\Gamma(2+2\epsilon)} \\
& \left. + 2\epsilon \cdot \epsilon^* [(1+\epsilon)N_c - N_f] \frac{\Gamma(-\epsilon)\Gamma^2(1+\epsilon)}{(3+2\epsilon)\Gamma(2+2\epsilon)} - 2\epsilon \cdot \epsilon^* [4N_c - N_f] \frac{\Gamma(-\epsilon)\Gamma^2(1+\epsilon)}{\Gamma(2+2\epsilon)} \right\}.
\end{aligned} \tag{III.105}$$

Our result contains two types of tensor structures involving the initial and final polarization tensors, namely, $\epsilon \cdot \epsilon^*$ and $\epsilon \cdot q \epsilon^* \cdot q / \mathbf{q}^2$. These are related to the helicity conserving and helicity violating terms [FFKP00]

$$\epsilon \cdot \epsilon^* = \delta_{\lambda_a, \lambda_1}; \quad \epsilon \cdot \epsilon^* + \frac{2}{\mathbf{q}^2} \epsilon \cdot q \epsilon^* \cdot q = -\delta_{\lambda_a, -\lambda_1}. \tag{III.106}$$

To avoid double counting we have to subtract (SEC III.2.3) all effective diagrams containing internal reggeized gluon propagators in the t -channel from the above result. With

$$\begin{aligned}
& \text{Diagram: A black circle labeled "1 loop" with a wavy line at the bottom and a horizontal line at the top.} \\
& = iA_{gr^* \rightarrow g_1}^{(1)},
\end{aligned} \tag{III.107}$$

the subtraction procedure results into the following coefficient

$$\begin{aligned}
\mathcal{C}_{gr^* \rightarrow g} \left(\frac{p_a^+}{\sqrt{\mathbf{q}^2}}, \rho; \epsilon \frac{\mathbf{q}^2}{\mu^2} \right) = & \text{Diagram: A grey circle labeled "1 loop" with a wavy line at the bottom and a horizontal line at the top.} \\
= & \text{Diagram: A black circle labeled "1 loop" with a wavy line at the bottom and a horizontal line at the top.} \\
- & \text{Diagram: A grey circle labeled "1 loop" with a wavy line at the bottom and a horizontal line at the top, with a vertical line connecting the top and bottom lines.}
\end{aligned} \tag{III.108}$$

The high energy limit of the gluon-gluon scattering amplitude at one-loop is then obtained as the following sum of diagrams

$$\text{Diagram} = \text{Diagram}_1 + \text{Diagram}_2 + \text{Diagram}_3 + \text{Diagram}_4 \quad (\text{III.109})$$

While each diagram on the right side is divergent in the limit $\rho \rightarrow \infty$, the divergence cancels in their sum, resulting into a finite one-loop amplitude, as explicitly checked in [HS12, CHMS12a]. We can therefore define renormalized gluon-gluon-reggeized gluon coupling coefficients,

$$\mathcal{C}_{gr^* \rightarrow g}^{\text{R}} \left(\frac{p_a^+}{M^+}; \epsilon, \frac{\mathbf{q}^2}{\mu^2} \right) = Z^+ \left(\frac{M^+}{\sqrt{\mathbf{q}^2}}, \rho; \epsilon, \frac{\mathbf{q}^2}{\mu^2} \right) \mathcal{C}_{gr^* \rightarrow g} \left(\frac{p_a^+}{\sqrt{\mathbf{q}^2}}, \rho; \epsilon, \frac{\mathbf{q}^2}{\mu^2} \right), \quad (\text{III.110})$$

$$\mathcal{C}_{gr^* \rightarrow g}^{\text{R}} \left(\frac{p_b^-}{M^-}; \epsilon, \frac{\mathbf{q}^2}{\mu^2} \right) = Z^- \left(\frac{M^-}{\sqrt{\mathbf{q}^2}}, \rho; \epsilon, \frac{\mathbf{q}^2}{\mu^2} \right) \mathcal{C}_{gr^* \rightarrow g} \left(\frac{p_b^-}{\sqrt{\mathbf{q}^2}}, \rho; \epsilon, \frac{\mathbf{q}^2}{\mu^2} \right), \quad (\text{III.111})$$

where the renormalization factors are those in (III.54), so that they cancel in the complete scattering amplitude. The renormalized GGR couplings allows then to extract the NLO corrections to the gluon impact factor. Extracting the Born contribution and decomposing into helicity conserving and non-conserving parts

$$\mathcal{C}_{gr^* \rightarrow g}^{\text{R}} \left(1; \epsilon, \frac{\mathbf{q}^2}{\mu^2} \right) = 2g f_{abc} \cdot \left[\Gamma_a^{(+)} \delta_{\lambda_a, \lambda_1} + \Gamma_a^{(-)} \delta_{\lambda_a, -\lambda_1} \right], \quad (\text{III.112})$$

where the helicity tensors are for finite ϵ defined through (III.106), we have

$$\begin{aligned} \Gamma_a^{(+)} &= -\frac{1}{2} \omega^{(1)} \left[-\psi(1) + 2\psi(2\epsilon) - \psi(1-\epsilon) + \frac{1}{4(1+2\epsilon)(3+2\epsilon)} + \frac{7}{4(1+2\epsilon)} - \frac{n_f}{N_c} \frac{1+\epsilon}{(1+2\epsilon)(3+2\epsilon)} \right] \\ &= \frac{\alpha_s N_c}{4\pi} \left(\frac{\mathbf{q}^2}{\mu^2} \right)^\epsilon \left[-\frac{1}{\epsilon^2} + \frac{\beta_0}{2\epsilon} - \frac{(67-\pi^2)N_c - 10N_f}{18} \right] + \mathcal{O}(\epsilon), \quad \beta_0 = \frac{11}{3}N_c - \frac{2}{3}N_f; \\ \Gamma_a^{(-)} &= -\frac{1}{2} \omega^{(1)} \left[\frac{\epsilon}{(1+\epsilon)(1+2\epsilon)(3+2\epsilon)} \left(1 + \epsilon - \frac{N_f}{N_c} \right) \right] = \frac{\alpha_s}{12\pi} (N_c - N_f) + \mathcal{O}(\epsilon). \end{aligned} \quad (\text{III.113})$$

which is in precise agreement with the literature²⁴ [FL93, FF92, Lip97, dDS98, FFKP00].

²⁴As noted in [dDS98], the original result [FL93] contains several misprints. The correct expression can be found e.g. in [Lip97, dDS98, FFKP00].

III. Lipatov Effective Action Approach to High Energy QCD

IV

Conclusions and Outlook

Current applications of high-energy QCD phenomenology range from the study of perturbative observables, such as cross-sections for forward jet or diffractive vector meson production, over transverse momentum dependent parton distribution functions in the low- x region, up to the study of phenomena in heavy ion collisions. Their common base is the factorization of QCD scattering amplitudes in the multi-Regge limit of parametrically large center of mass energies and small dispersion angles, combined with a resummation of large perturbative logarithmically enhanced corrections. While it is important to keep in mind that specific physical environments—which can be characterized e.g. by the presence of high parton densities or the appearance of large collinear and soft logarithms—require suitable modifications and extensions, the perturbative basis for the resummation of high energy logarithms is always given by the BFKL equation, based on the reggeization ansatz and bootstrap consistency. This is the main idea we wanted to emphasize in our extensive description of high-energy QCD in CH. I.

Despite the apparent simplicity of the QCD action, the computation of its S -matrix—at least to date—seems completely out of reach. This dynamical complexity is mostly due to the running of its coupling. On one hand, it renders many apparently simple phenomena, like the description of its simplest bound states, non-perturbative. On the other hand, the

IV. Conclusions and Outlook

breaking of the classical conformal invariance of the QCD Lagrangian also complicates a lot the perturbative structure of scattering amplitudes. This has led in the last years to consider $\mathcal{N} = 4$ Super Yang-Mills theory, a supersymmetric and conformal invariant relative of QCD, as a suitable toy model to learn important aspects of strong interactions. Indeed, most of the simplicity of the Regge limit seems to be linked to the similarity between QCD and $\mathcal{N} = 4$ SYM in this kinematic region. The purpose of CH. II is to analyze quantitatively this similarity for specific well-behaved observables.

The first proposed observable is the azimuthal decorrelation of Mueller-Navelet jets (SEC. II.2), conveniently expressed in terms of the ratios (II.30), which do not depend on the non-perturbative details of parton densities and are rather insensitive to collinear contamination, thus allowing for a sensible comparison of QCD and $\mathcal{N} = 4$ SYM predictions. The results (FIGS. II.8 and II.9) show that ratios of azimuthal correlations are strikingly similar in both theories, especially using a renormalization scheme like BLM that captures the bulk of conformal contributions (which are expected to be important for these observables exploring the $SL(2, \mathbb{C})$ symmetry of the transverse plane to the collision axis). This is not the case for other usually analyzed observables like the evolution in rapidity of the total dijet cross section or its moments in the azimuthal angle, which have a worse perturbative convergence. The important conclusion is that one can expect $\mathcal{N} = 4$ SYM computations to reproduce closely the QCD behavior in the multi-Regge limit for well-chosen observables. Another possible observables to which one can extend this comparative analysis are suitably defined energy-momentum tensor correlations [HM08], or the cross-section for $\gamma^* \gamma^*$ scattering, where photons can be simulated in $\mathcal{N} = 4$ SYM by R -currents belonging to its global $SU_R(4)$ symmetry [CHKM⁺06, BMS08, CCP10, BC10].

A second study on the relation of QCD and $\mathcal{N} = 4$ SYM in the Regge limit has been presented in SEC. II.3. Using a Monte Carlo method, we have been able to analyze the different contributions to the NLO BFKL Green's function for the scattering of two off-shell reggeized gluons in $\mathcal{N} = 4$ SYM. We have shown the better collinear behavior of $\mathcal{N} = 4$ SYM with respect to QCD (FIGS. II.10 and II.11): while the effect of the scalar and gluino sectors is minimal for conformal spins $n > 0$, it is very important for $n = 0$, making also the growth with energy of the forward amplitude to be much faster than for the purely gluonic contributions (FIG. II.13). This is related to a larger final state multiplicity, which is also the source of the larger azimuthal decorrelation for $\mathcal{N} = 4$ SYM dijets appearing in FIG. II.8. We have also seen (FIG. II.15) that scalars and gluinos do not appreciably affect the

diffusion pattern into the IR. It would be desirable to extend these results to the strong coupling regime, but the corresponding BFKL kernel is not known as of today.

In CH. III we have considered a rather different approach to the study of high-energy QCD, based on Lipatov's effective action [Lip95]. This is a remarkable construction which allows to extract the all-orders production vertices in quasi-multi-Regge kinematics just using gauge invariance and high-energy factorization. Unlike in the usual Wilsonian setup, heavy modes are not directly integrated out, but rather an explicit rapidity cutoff is used to determine the region where the effective action applies. Beyond tree level it is necessary to enforce such a cutoff in loop integrals. This is an ambiguous procedure which moreover breaks gauge invariance explicitly and heavily undermines the computational power of the effective action.

We have alternatively proposed a gauge invariant subtraction method based on the locality in rapidity of the effective action which by construction avoids any double counting. Spurious rapidity divergences have been also regularized in a way that respects gauge invariance, confirming that the dependence on the regulator vanishes in concrete examples as expected. This method allows to employ the standard techniques of computation of loop integrals, since Lorentz covariance is kept untouched during the calculation. In our approach, the reggeon field essentially enters as a background field, i.e. it does not propagate inside loops. We have put forward a renormalization interpretation of the perturbative corrections to the effective vertices, which can be seen as defining order by order the Lagrangian of the underlying reggeon field theory. This can be seen as a matching procedure [Geo93], which should be formalized in the future.

In general, the whole procedure proposed here should be considered as a first step in the direction of making an efficient and motivated use of Lipatov's action. Apart from the necessity of giving a more rigorous justification of some of our assumptions, it remains to be understood the connection of Lipatov's action with other formalisms like the color glass condensate or Balitsky's OPE (SEC. III.1.4). This can also help fix the range of applicability of these other effective theories; let us remind the reader that it is not clear that they can reproduce the perturbative results for amplitudes in QMRK.

We have been able to exactly reproduce several highly non-trivial results: the one-loop quark and gluon-initiated jet vertices and the two-loop gluon Regge trajectory. This shows the consistency of Lipatov's approach at loop level. Having checked the procedure by reproducing

IV. Conclusions and Outlook

known results in the literature, the effective action is now ready to ease the calculation of other phenomenologically important effective vertices whose result is not known, like the NLO Mueller-Tang impact factor [HM12], which is the only missing element for a complete NLO BFKL description of dijet events with a rapidity gap.



Conclusiones

Las aplicaciones de la fenomenología de QCD a altas energías engloban un amplio espectro: desde el estudio de observables perturbativos, como las secciones eficaces para chorros (*jets*) ampliamente separados en rapidez o la producción difractiva de mesones vectoriales, pasando por el análisis de las distribuciones partónicas con dependencia en el momento transversal a bajos valores de x , hasta el complicado estudio de fenómenos en colisiones de iones pesados. La base común de todas estas aplicaciones es la factorización de las amplitudes de dispersión que ocurre en QCD en el límite de Regge, caracterizado por energías de centro de masas asintóticamente grandes y ángulos de dispersión pequeños, combinada con una resumación perturbativa de correcciones logarítmicas dominantes. Si bien se debe tener en cuenta que ciertos entornos físicos específicos —que pueden venir caracterizados e.g. por la presencia de elevadas densidades partónicas o por la aparición de logaritmos colineales— requieren apropiadas modificaciones y extensiones de este marco general, la base perturbativa para la resumación de los logaritmos dominantes en energía viene siempre dada por la ecuación BFKL, basada en la propiedad de reggeización y consistente con *bootstrap*. Esta es la idea principal que queríamos enfatizar en nuestra discusión exhaustiva de QCD a altas energías en el CAP. I.

A pesar de la aparente simplicidad del Lagrangiano de QCD, el cálculo exacto de su matriz

V. Conclusiones

S parece —al menos a día de hoy— una labor imposible. Esta complejidad dinámica se debe en buena medida a la variación del acoplo con el grupo de renormalización. Por una parte, éste hace que numerosos fenómenos a priori sencillos, como la descripción de los estados ligados más simples, sea no perturbativa. Por otra parte, la ruptura de la invariancia conforme que posee clásicamente la acción de QCD también complica notablemente la estructura perturbativa de las amplitudes de dispersión. Esta observación ha llevado en los últimos años a considerar la teoría $\mathcal{N} = 4$ Super Yang-Mills, una versión supersimétrica e invariante conforme de QCD, como un apropiado modelo simplificado del que podemos extraer importantes lecciones sobre la física de las interacciones fuertes. De hecho, se cree que la simplicidad del límite de Regge se debe a la similitud que presentan QCD y $\mathcal{N} = 4$ SYM en esta región cinemática. El propósito del CAP. II es analizar cuantitativamente esta semejanza para observables concretos con un buen comportamiento perturbativo.

El primer observable que proponemos es la decorrelación azimutal de jets de Mueller-Navelet (SEC. II.2), convenientemente expresada en términos de los cocientes (II.30), que no dependen de los detalles no perturbativos de las distribuciones partónicas y son altamente insensibles a la contaminación colineal, permitiendo una comparación coherente de predicciones en QCD y $\mathcal{N} = 4$ SYM. Los resultados (FIGS. II.8 y II.9) muestran que los cocientes de correlaciones azimutales exhiben un comportamiento sorprendentemente similar en ambas teorías, especialmente cuando usamos un esquema de renormalización como BLM que captura el grueso de las contribuciones conformes (que se espera sean importantes para estos observables, que exploran la simetría $SL(2, \mathbb{C})$ del plano transversal al eje de colisión). Esto no ocurre para otros observables típicamente estudiados como la evolución en rapidez de la sección eficaz total de producción de dos chorros (*dijets*) o sus momentos en el ángulo azimutal, que tienen una peor convergencia perturbativa. La conclusión importante de este análisis es que cabe esperar que las predicciones de $\mathcal{N} = 4$ SYM reproduzcan prácticamente los cálculos de QCD para observables convenientemente escogidos en el límite de Regge. Otros posibles observables a los que se puede extender este análisis comparativo son ciertas correlaciones del tensor de energía-momento [HM08], o la sección eficaz para dispersión $\gamma^* \gamma^*$, donde los fotones pueden ser simulados en $\mathcal{N} = 4$ SYM mediante corrientes asociadas a su simetría global $SU_R(4)$ [CHKM⁺06, BMS08, CCP10, BC11].

En la SEC. II.3 hemos presentado un segundo estudio sobre la relación entre QCD y $\mathcal{N} = 4$ SYM en el límite de Regge. Utilizando un método de Monte Carlo, hemos sido capaces de analizar las diferentes contribuciones a la función de Green de BFKL,

que describe la dispersión de dos reggeones fuera de la capa de masas, a orden NLO en $\mathcal{N} = 4$ SYM. Hemos mostrado el mejor comportamiento colineal de $\mathcal{N} = 4$ SYM con respecto a QCD (FIGS. II.10 y II.11): mientras que el efecto de los escalares y gluínos es mínimo para espines conformes $n > 0$, éste sí que resulta muy importante para $n = 0$, haciendo que la función de Green crezca mucho más deprisa en rapidez que al considerar únicamente contribuciones gluónicas (FIG. II.13). Esto se refleja en una mayor multiplicidad en el estado final, que es también el origen de las mayores decorrelaciones azimutales entre dijets que se obtienen en $\mathcal{N} = 4$ SYM (FIG. II.8). También hemos podido comprobar (FIG. II.15) que los escalares y gluínos no afectan de modo apreciable el patrón de difusión hacia el infrarrojo. Sería muy interesante extender estos resultados al régimen de acoplo fuerte, pero no conocemos actualmente la ecuación BFKL en este régimen.

En el CAP. III hemos considerado un enfoque muy diferente para estudiar QCD a altas energías, basado en la acción efectiva de Lipatov [Lip95]. Esta formulación es muy interesante, ya que permite obtener los vértices efectivos en la cinemática de quasi-multi-Regge a todos los órdenes usando únicamente invariancia gauge y la factorización a altas energías. En contraste con la habitual imagen de Wilson, los modos pesados no son directamente integrados, sino que existe un límite explícito de rapidez que determina la región en la que la acción efectiva (III.32) es válida. Más allá del nivel árbol es necesario introducir este límite en las integrales a varios lazos. Este procedimiento es ambiguo y rompe manifiestamente la invariancia gauge, además de complicar enormemente los cálculos.

Alternativamente, proponemos un método de sustracción que mantiene la invariancia gauge en los estadios intermedios del cálculo, basado en la localidad en rapidez de la acción, y que por construcción evita cualquier doble contaje. En nuestro enfoque, el campo del reggeón aparece como un campo no dinámico, que no se propaga en el interior de los lazos. Hemos ofrecido una interpretación en el contexto del grupo de renormalización de las correcciones perturbativas a los vértices efectivos; se puede considerar que de este modo se define orden a orden el Lagrangiano de la teoría de campos reggeizados subyacente. Dicho procedimiento puede verse como un ejemplo de *matching* [Geo93], que debe ser mejor entendido en un futuro.

En general, nuestra propuesta debe ser considerada como un primer paso para conseguir una aplicación eficiente y motivada del uso de la acción de Lipatov. Aparte de la necesidad de formalizar de forma rigurosa nuestro enfoque, otro problema importante es intentar

V. Conclusiones

entender la conexión de la acción de Lipatov con otros formalismos como el *color glass condensate* o la expansión en producto de operadores de Balitsky (SEC. III.1.4). Entender esta conexión puede ayudar también a determinar el rango de validez de estas otras teorías efectivas; recordemos que no está en absoluto claro que sean capaces de reproducir los resultados perturbativos para amplitudes en cinemática de quasi-multi-Regge.

En cualquier caso, hemos sido capaces de reproducir de forma exacta varios resultados altamente no triviales: los vértices de jet producidos por quarks y gluones a un lazo, y la trayectoria de Regge del gluón a dos lazos. Esto muestra la consistencia de la acción efectiva para correcciones virtuales. Habiendo comprobado que nuestro procedimiento reproduce importantes resultados conocidos en la literatura, la acción efectiva está ahora lista para calcular otros vértices efectivos con importancia fenomenológica, como el factor de impacto para jets de Mueller-Tang con precisión NLO [HM12], que es el único elemento que falta para una descripción completa a orden NLO de la producción difractiva de dijets en el marco de BFKL.

Part III

Appendices



Miscellaneous Formulæ

SU(3) Matrices, Color Algebra and Color Projectors

The generators \hat{T}^a of the color group $SU(N_c)$ obey the commutation relations

$$[\hat{T}^a, \hat{T}^b] = i f^{abc} \hat{T}^c, \quad f_{abe} f_{ecd} + f_{cbe} f_{aed} + f_{dce} f_{ace} = 0, \quad (\text{A.1})$$

where f^{abc} are the fully antisymmetric group structure constants. Generators in the adjoint representation are usually denoted by T^a , so that $(T^a)_{bc} = -i f^{abc}$. In the fundamental representation generators are denoted t^a and have the following properties

$$\text{Tr } t^a = 0, \quad t^a = t^{a\dagger}, \quad \text{Tr } (t^a t^b) = T_R \delta^{ab}, \quad T_R = \frac{1}{2}. \quad (\text{A.2})$$

Together with the identity matrix they create a complete set of $N_c \times N_c$ matrices. The completeness condition, sometimes called Fierz identity, can be written as¹

$$t_{ij}^a t_{kl}^a = \frac{1}{2} \left[\delta_{il} \delta_{jk} - \frac{1}{N_c} \delta_{ij} \delta_{kl} \right]. \quad (\text{A.4})$$

¹A $N_c \times N_c$ matrix can be expressed as $M = n^0 \mathbb{1} + n^a t^a$. The coefficients n^0 and n^a are found taking traces: $\text{Tr } M = n^0 N_c$; $\text{Tr } (M t^b) = n^a \frac{1}{2} \delta^{ab}$, hence $M = \frac{1}{N_c} \text{Tr } M \mathbb{1} + 2 \text{Tr } (M t^a) t^a$. For the case $M_k^i = \delta_{(j)}^i \delta_k^{(l)}$ (fixed j and l) one finds the Fierz identity. A graphical representation of this relation is

A. Miscellaneous Formulæ

From (A.4) one can obtain the following results

$$t^a t^a = C_F \mathbb{1} \quad (t_{ij}^a t_{jk}^a = C_F \delta_{ik}); \quad t^a t^b t^a = \left(C_F - \frac{C_A}{2}\right) t^b; \quad t^a t^b t^c t^a = \frac{1}{4} \delta^{bc} \mathbb{1} + \left(C_F - \frac{C_A}{2}\right) t^b t^c, \quad (\text{A.5})$$

with C_F and C_A the values of the Casimir in the fundamental and adjoint representations:

$$C_F = \frac{N_c^2 - 1}{2N_c}, \quad C_A = N_c \quad (\text{Tr}(T^a T^b) = f^{acd} f^{bcd} = C_A \delta^{ab}). \quad (\text{A.6})$$

One can also introduce the completely symmetric symbols d_{abc} ² through the relation

$$\{t^a, t^b\} = \frac{1}{N_c} \delta^{ab} \mathbb{1} + d^{abc} t^c. \quad (\text{A.7})$$

They satisfy the following identities

$$d_{abb} = 0, \quad d_{acd} d_{bcd} = \frac{N_c^2 - 4}{N_c} \delta_{ab}, \quad f_{abe} d_{ecd} + f_{cbe} d_{aed} + f_{dbe} d_{ace} = 0, \quad (\text{A.8})$$

and the trace of three t matrices can be expressed in terms of them as

$$\text{Tr}(t^a t^b t^c) = \frac{1}{4} (d^{abc} + i f^{abc}). \quad (\text{A.9})$$

Further useful relations can be found in [Dok97, IFL10]. Its derivation can be simplified a lot by the use of diagrammatic techniques introduced by Cvitanović [Cvi76, Cvi08]. Implementation of these relations and many more in FeynCalc [MBD91] is very useful.

We now illustrate the use of these techniques to obtain the projection operators that allow us to extract the contribution of an irreducible representation from the Clebsch-Gordan series for the product of two irreducible representations. Consider a $2 \rightarrow 2$ process with amplitude $\Gamma_{l_2' l_1'}^{l_1 l_2} \equiv \langle L_1' l_1' L_2' l_2' | \Gamma | L_1 l_1 L_2 l_2 \rangle$ (we explicit color indices, while omitting spin and flavor ones), where $|L_i l_i\rangle$, $l_i = 1, 2, \dots, n_{L_i}$ is the basis of the irreducible representation L_i

$$\begin{array}{c} j \longrightarrow i \\ l \longleftarrow k \end{array} = \frac{1}{N_c} \underbrace{\begin{array}{c} j \longrightarrow \downarrow \\ l \longleftarrow \uparrow \end{array}}_{\mathcal{P}_1} + 2 \underbrace{\begin{array}{c} j \searrow \quad \swarrow i \\ \quad \circ \circ \circ \circ \circ \circ \circ \circ \\ l \nearrow \quad \nwarrow k \end{array}}_{\mathcal{P}_8}. \quad (\text{A.3})$$

²For SU(2) one has $f^{abc} = \epsilon^{abc}$ and $d^{abc} = 0$. In the case of interest, SU(3), things are more complicated. The non-vanishing structure constants (up to trivial permutations) are $f_{123} = 1, f_{458} = f_{678} = \frac{\sqrt{3}}{2}, f_{147} = f_{165} = f_{246} = f_{345} = f_{376} = f_{257} = \frac{1}{2}$, and the non-zero d_{abc} , $d_{118} = d_{228} = d_{338} = -d_{888} = \frac{1}{\sqrt{3}}, d_{146} = d_{157} = d_{256} = d_{344} = d_{355} = -d_{247} = -d_{366} = -d_{377} = \frac{1}{2}, d_{448} = d_{558} = d_{668} = d_{778} = -\frac{1}{2\sqrt{3}}$.

to which the incoming parton i belongs, n_{L_i} being its dimension. The representations of interest for us will be $L_i = \mathbf{3}, \bar{\mathbf{3}}, \mathbf{8}$, corresponding respectively to quarks, antiquarks and gluons.

In the study of addition of angular momenta, basis vectors for the composite system can be formed from the tensor products of eigenstates of each of the components: $|j_1 m_1 j_2 m_2\rangle = |j_1 m_1\rangle \otimes |j_2 m_2\rangle$. On the other hand, another basis of states for the composite system is given by its eigenstates $|j m\rangle$ (eigenstates of $\mathbf{J}^2 = (\mathbf{J}_1 + \mathbf{J}_2)^2$ and $\mathbf{J}_z = \mathbf{J}_{z1} + \mathbf{J}_{z2}$), which can be expressed in terms of the former tensor products through the Clebsch-Gordan coefficients. In our case, considering color rather than spin, we have the same situation:

$$|Ll\rangle = \sum_{l_1, l_2} \langle L_1 l_1 L_2 l_2 | Ll \rangle |L_1 l_1\rangle |L_2 l_2\rangle. \quad (\text{A.10})$$

The most general form of the operator Γ in the new basis of eigenstates reads $\Gamma = \sum_{L, L'} \sum_{l, l'}^{n_L, n_{L'}} \Gamma_{L' l' L l} |L' l'\rangle \langle L l|$, but, since color is conserved, Γ commutes with all SU(3) generators and then according to Schur's lemma it is proportional to the identity in color indices within each irreducible basis, i.e. $\Gamma_{L' l' L l} = \Gamma_L \delta_{L' L} \delta_{l' l}$, so that we get

$$\Gamma = \sum_L \Gamma_L \sum_l |Ll\rangle \langle Ll| = \sum_L \Gamma_L \mathcal{P}_L, \quad \mathcal{P}_L \equiv \sum_l |Ll\rangle \langle Ll|. \quad (\text{A.11})$$

\mathcal{P}_L is the projector on the representation \mathbf{L} . Defining $\langle l'_1 l'_2 | \mathcal{P} | l_1 l_2 \rangle \equiv \mathcal{P}_{l'_2 l'_1}^{l_1 l_2}$, we have

$$\mathcal{P}_{L' l'_2 l'_1}^{m_1 m_2} \Gamma_{L l_2 l_1}^{l_1 l_2} = \sum_L \Gamma_L \mathcal{P}_{L' l'_2 l'_1}^{m_2 m_1} \mathcal{P}_L^{l_1 l_2} = \Gamma_{L'} \underbrace{\mathcal{P}_{L' m_2 m_1}^{m_1 m_2}}_{=\text{Tr } \mathcal{P}_{L'} = n_{L'}}, \quad (\text{A.12})$$

that determines the coefficients Γ_L in (A.11): $\Gamma_L = \frac{\text{Tr } \mathcal{P}_L \Gamma}{\text{Tr } \mathcal{P}_L}$. One cannot choose to normalize the projectors with unit trace if the identity (I.108) is to be satisfied.

We begin with the $\mathbf{3} \times \bar{\mathbf{3}} = \mathbf{1} + \mathbf{8}$ case. Here we can readily read the projectors from (A.3): considering i of M_k^i as the color index of a quark and k as the color index of an antiquark, the interpretation of the diagram in (A.3) is clear: it is the decomposition of N_c^2 color states of a $q\bar{q}$ system into the color singlet and octet parts: $\psi^i \bar{\chi}_k = \frac{1}{N_c} \delta_k^i (\bar{\chi} \psi) + R_k^i$, $R_i^i = 0^3$. In (A.3) we have already defined the singlet and octet projectors, conveniently normalized.

Now we turn to the important $\mathbf{8} \times \mathbf{8}$, which we also use in the present work. Four color

³Such a decomposition is analogous to the decomposition of a product of vector representations into traceless symmetric, antisymmetric, and trace parts for orthogonal groups. Under a SU(N_c) transformation both parts R_k^i and δ_k^i do not mix among them.

A. Miscellaneous Formulæ

indices of $SU(3)$ can be contracted in the following ways: $\delta_{aa'}\delta_{bb'}$; $\delta_{ab}\delta_{a'b'}$; $\delta_{ab'}\delta_{a'b}$; $d_{aa'c}d_{bb'c}$; $d_{abc}d_{a'b'c}$; $d_{ab'c}d_{a'bc}$; $f_{aa'c}f_{bb'c}$; $f_{abc}f_{a'b'c}$ and $f_{ab'c}f_{a'bc}$. Not all of these combinations are independent [LRS92]. One can readily identify among them the simplest projectors, corresponding to the singlet and octet,

$$\begin{aligned} \mathcal{P}_1 &= \frac{1}{N_c^2 - 1} \left(\text{diagram: two wavy lines connected by a vertical line} \right) \left(= \frac{1}{N_c^2 - 1} \delta^{ab} \delta_{b'a'} \right); & \mathcal{P}_{8_s} &= \frac{N_c}{N_c^2 - 4} \left(\text{diagram: two wavy lines connected by a vertical line with a dot} \right) \left(= \frac{N_c}{N_c^2 - 4} d^{abc} d_{b'a'c} \right); \\ \mathcal{P}_{8_a} &= \frac{1}{N_c} \left(\text{diagram: two wavy lines connected by a vertical line with a dot} \right) \left(= \frac{1}{N_c} i f^{abc} i f_{cb'a'} = \frac{1}{N_c} T_c^{ab} T_{b'a'}^c \right). \end{aligned} \quad (\text{A.13})$$

Indeed, the index c in f_{abc} (represented by a dot) and d_{abc} (represented by a star) transforms in the adjoint, and while f_{abc} is completely antisymmetric, d_{abc} is completely symmetric. By direct calculation one can check that the projector identities (I.108) are satisfied. To obtain the remaining projectors one begins with the identity in color space and splits it in different contributions [DM06]. We draw the pictorial identity

$$\mathbb{1}_{b'a'}^{ab} = \delta_{a'}^a \delta_{b'}^b = \left(\text{diagram: two wavy lines connected by a vertical line} \right) = 4 \left(\text{diagram: two wavy lines connected by a loop} \right) \quad (\text{A.14})$$

where a, b (a', b') are color indices of incoming (outgoing) gluons. We have used that

$$\left(\text{diagram: two wavy lines connected by a loop} \right) = \text{Tr} (t^a t^{a'}) = \frac{1}{2} \delta_{aa'}. \quad (\text{A.15})$$

Applying the Fierz identity (A.3) to two of the intermediate quark (antiquark) lines in this expression one can recover terms equal to the projectors (A.13). By interchanging quark and antiquark lines we can also construct four tensors with a given symmetry with respect to quark and, separately, antiquark color indices:

$$\mathbb{1} = \Pi_+^+ + \Pi_-^+ + \Pi_+^- + \Pi_-^-; \quad \Pi_d^u = \frac{1}{4} \left(\begin{array}{c} \left(\text{diagram: two wavy lines connected by a vertical line} \right) + u d \left(\text{diagram: two wavy lines connected by a vertical line with a dot} \right) \\ \underbrace{\hspace{10em}}_{\equiv \mathbb{1}} \quad \underbrace{\hspace{10em}}_{\equiv \mathbb{X} (= \delta_{b'}^a \delta_b^{a'})} \end{array} \right) + u \left(\text{diagram: two wavy lines connected by a loop with a dot} \right) + d \left(\text{diagram: two wavy lines connected by a loop} \right), \quad (\text{A.16})$$

where $u, d = \pm$ label the symmetry with respect to the two ‘internal’ quarks and antiquarks, respectively. For example, Π_+^+ is symmetric under interchanging quarks and antiquarks, and Π_-^+ is symmetric with respect to quarks and antisymmetric with respect to antiquarks. Exchanging gluons $a \leftrightarrow b$ we have $\mathbb{1} \leftrightarrow \mathbb{X}$ and $\mathbb{W}_+ \leftrightarrow \mathbb{W}_-$, so that Π_+^+ and Π_-^- are symmetric with respect to exchanging gluon indices a and b , while Π_-^+ and Π_+^- are antisymmetric.

Introducing the notation⁴ $(A \cdot B)_{b'a'}^{ab} = A_{b'a'}^{cd} B_{cd}^{ab}$ (sum over c, d understood), one has now

$$\mathbb{W}_\pm \cdot \mathcal{P}_1 = -\frac{1}{4N_c} \mathcal{P}_1, \quad \mathbb{W}_\pm \cdot \mathcal{P}_{\mathbf{8}_a} = 0, \quad \mathbb{W}_\pm \cdot \mathcal{P}_{\mathbf{8}_s} = -\frac{1}{2N_c} \mathcal{P}_{\mathbf{8}_s}. \quad (\text{A.17})$$

These relations help us construct the remaining irreducible representations. To this end we subtract from the tensors Π_d^y (A.16) their projections onto the singlet and two octets (A.17), and derive the four higher projectors [DM06]:

$$\begin{aligned} \mathcal{P}_{27} &= \Pi_+^+ - \frac{N_c - 2}{2N_c} \mathcal{P}_{\mathbf{8}_s} - \frac{N_c - 1}{2N_c} \mathcal{P}_1 = \frac{1}{4}(\mathbb{1} + \mathbb{X}) - \frac{N_c - 2}{2N_c} \mathcal{P}_{\mathbf{8}_s} - \frac{N_c - 1}{2N_c} \mathcal{P}_1 + (\mathbb{W}_+ + \mathbb{W}_-); \\ \mathcal{P}_{10} &= \Pi_-^+ - \frac{1}{2} \mathcal{P}_{\mathbf{8}_a}, \quad \mathcal{P}_{\overline{10}} = \Pi_+^- - \frac{1}{2} \mathcal{P}_{\mathbf{8}_a} \implies \mathcal{P}_{10} + \mathcal{P}_{\overline{10}} = \frac{1}{2}(\mathbb{1} - \mathbb{X}) - \mathcal{P}_{\mathbf{8}_a}; \\ \mathcal{P}_0 &= \Pi_-^- - \frac{N_c + 2}{2N_c} \mathcal{P}_{\mathbf{8}_s} - \frac{N_c + 1}{2N_c} \mathcal{P}_1 = \frac{1}{4}(\mathbb{1} + \mathbb{X}) - \frac{N_c + 2}{2N_c} \mathcal{P}_{\mathbf{8}_s} - \frac{N_c + 1}{2N_c} \mathcal{P}_1 - (\mathbb{W}_+ + \mathbb{W}_-). \end{aligned} \quad (\text{A.18})$$

The projector \mathcal{P}_0 is relevant for $N_c > 3$, in which case a new representation with dimension $n_{N_c > 3} = \frac{(N_c + 1)N_c^2(N_c - 3)}{4}$ appears. Making use of (A.17) and the relations

$$16\mathbb{W}_\pm \cdot \mathbb{W}_{\pm(\mp)} = \mathbb{1}(\mathbb{X}) - \frac{N_c^2 - 1}{N_c^2} \mathcal{P}_1 - \frac{N_c^2 - 4}{N_c^2} \mathcal{P}_{\mathbf{8}_s} - (+)\mathcal{P}_{\mathbf{8}_a}, \quad (\text{A.19})$$

one can verify that the operators (A.18) are indeed projectors ($\mathcal{P}_\alpha \cdot \mathcal{P}_\beta = \mathcal{P}_\alpha \delta_{\alpha\beta}$)⁵.

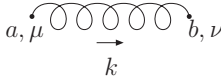
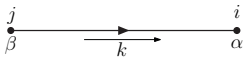
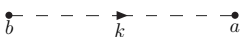
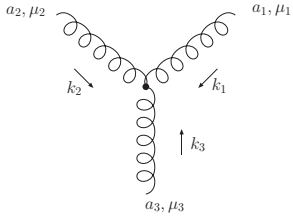
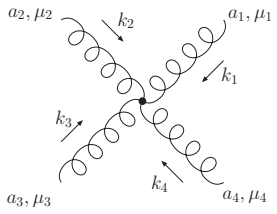
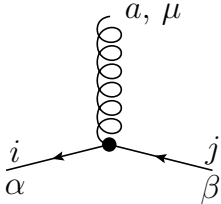
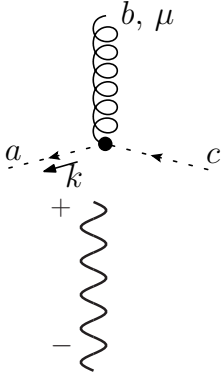

⁴In bra-ket notation $\langle a'b'|AB|ab\rangle = \langle a'b'|A|cd\rangle\langle cd|B|ab\rangle$.

⁵For completeness we list here all relevant normalized projectors for $N_c = 3$ [Mek85, Cvi08].

$$\begin{aligned} qq : \mathbf{3} \times \mathbf{3} &= \overline{\mathbf{3}} + \mathbf{6} & \langle i'j'|\mathcal{P}_{\overline{\mathbf{3}}(\mathbf{3})}|ij\rangle &= \frac{1}{2}(\delta_{i'j'}\delta_{ij} - \delta_{i'j}\delta_{j'i}) \\ [\overline{q}\overline{q} : \mathbf{3} \times \mathbf{3} &= \mathbf{3} + \overline{\mathbf{6}}]; & \langle i'j'|\mathcal{P}_{\overline{\mathbf{6}}(\mathbf{6})}|ij\rangle &= \frac{1}{2}(\delta_{i'j'}\delta_{ij} + \delta_{i'j}\delta_{j'i}); \\ q\overline{q} : \mathbf{3} \times \overline{\mathbf{3}} &= \mathbf{1} + \mathbf{8}; & \langle i'j'|\mathcal{P}_1|ij\rangle &= \frac{1}{3}\delta_{i'j'}\delta_{ij}, \quad \langle i'j'|\mathcal{P}_8|ij\rangle = \delta_{i'j'}\delta_{ij} - \frac{1}{3}\delta_{i'j}\delta_{j'i} = 2t_{ij}^a t_{i'j'}^a; \\ qq : \mathbf{3} \times \mathbf{8} &= \mathbf{3} + \mathbf{6} + \mathbf{15} & \langle i'a'|\mathcal{P}_{\overline{\mathbf{3}}(\overline{\mathbf{3}})}|ia\rangle &= \frac{3}{4}(t^a t^a)_{i'i}, \quad \langle i'a'|\mathcal{P}_{\overline{\mathbf{6}}(\overline{\mathbf{6}})}|ia\rangle = \frac{1}{2}\delta_{i'i}\delta_{a'a} - (t^a t^a)_{i'i} \\ [\overline{q}\overline{q} : \mathbf{3} \times \mathbf{8} &= \overline{\mathbf{3}} + \overline{\mathbf{6}} + \overline{\mathbf{15}}]; & -\frac{1}{2}(t^a t^a)_{i'i}, & \langle i'a'|\mathcal{P}_{\mathbf{15}(\overline{\mathbf{15}})}|ia\rangle = \frac{1}{2}\delta_{i'i}\delta_{a'a} + (t^a t^a)_{i'i} - \frac{1}{4}(t^a t^a)_{i'i}; \\ gg : \mathbf{8} \times \mathbf{8} &= \mathbf{1} + \mathbf{8}_{\text{sym}} & \langle a'b'|\mathcal{P}_1|ab\rangle &= \frac{1}{8}\delta_{ab}\delta_{a'b'}, \quad \langle a'b'|\mathcal{P}_{\mathbf{8}_s}|ab\rangle = \frac{3}{5}d_{abe}d_{a'b'e}, \quad \langle a'b'|\mathcal{P}_{\mathbf{8}_a}|ab\rangle = \frac{1}{3}f_{abe}f_{a'b'e}, \\ &+ \mathbf{8}_{\text{ant}} + \mathbf{10} + \overline{\mathbf{10}} + \mathbf{27}; & \langle a'b'|\mathcal{P}_{\overline{\mathbf{10}}(\overline{\mathbf{10}})}|ab\rangle &= \frac{1}{4}\left(\delta_{aa'}\delta_{bb'} - \delta_{ab'}\delta_{ba'} - \frac{2}{3}f_{abe}f_{a'b'e}\right) (\pm) \frac{i}{4}(d_{a'ae}f_{b'be} + d_{b'be}f_{a'ae}), \\ & & \langle a'b'|\mathcal{P}_{27}|ab\rangle &= \frac{1}{2}\left(\delta_{aa'}\delta_{bb'} + \delta_{ab'}\delta_{ba'} - \frac{1}{4}\delta_{ab}\delta_{a'b'} - \frac{6}{5}d_{abe}d_{a'b'e}\right). \end{aligned} \quad (\text{A.20})$$

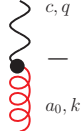
Feynman Rules for QCD and the High-Energy Effective Action

We compile in this section the Feynman rules for QCD [PS95] and the lowest order (unregularized) couplings in Lipatov's effective action [ALKC05]⁶. Reggeons are denoted by wavy lines

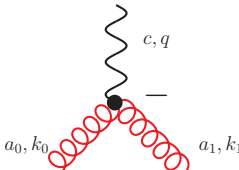
	$\frac{-ig_{\mu\nu}}{k^2 + i0}$	gluon propagator
	$i\delta^{ij} \frac{(\not{k} + m)_{\alpha\beta}}{k^2 - m^2 + i0}$	quark propagator
	$\frac{-i\delta^{ab}}{k^2 + i0}$	ghost propagator
	$-gf_{a_1 a_2 a_3} [g^{\mu_2 \mu_3} (k_2 - k_3)^{\mu_1} + g^{\mu_3 \mu_1} (k_3 - k_1)^{\mu_2} + g^{\mu_1 \mu_2} (k_1 - k_2)^{\mu_3}]$	3-gluon vertex
	$-ig^2 [f_{a_1 a_2 b} f_{a_3 a_4 b} (g^{\mu_1 \mu_3} g^{\mu_2 \mu_4} - g^{\mu_1 \mu_4} g^{\mu_2 \mu_3}) + f_{a_1 a_3 b} f_{a_2 a_4 b} (g^{\mu_1 \mu_2} g^{\mu_3 \mu_4} - g^{\mu_1 \mu_4} g^{\mu_2 \mu_3}) + f_{a_1 a_4 b} f_{a_2 a_3 b} (g^{\mu_1 \mu_2} g^{\mu_3 \mu_4} - g^{\mu_1 \mu_3} g^{\mu_2 \mu_4})]$	4-gluon vertex
	$ig(t^a)_{ij} (\gamma^\mu)_{\alpha\beta}$	qqg vertex
	$gf^{abc} k^\mu$	gGG vertex
	$\frac{1}{(-2i\mathbf{q}^2)}$	reggeon propagator

(A.21)

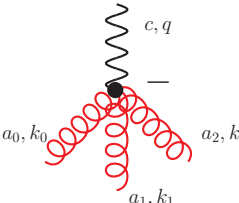
⁶In [ALKC05] there is a mismatch in the conventions used for the QCD and induced pieces of Lipatov's action. We stick to the conventions in [Hen09b]. The procedure to extract the Feynman rules from a general Lagrangian is reviewed in [CL82]. Feynman rules in $\mathcal{N} = 4$ SYM theory are derived in great detail in [Gro12]. Feynman gauge is used for the gluon propagator.



$$\Delta_{a_0 c}^{\nu_0 -} = -i\mathbf{q}^2 \delta^{a_0 c} (n^-)^{\nu_0} [k_0^- = 0] \quad Rg \text{ transition}$$



$$\Delta_{a_0 a_1 c}^{\nu_0 \nu_1 -} = g\mathbf{q}^2 f^{a_0 a_1 c} \frac{1}{k_0^-} (n^-)^{\nu_0} (n^-)^{\nu_1} [k_0^- + k_1^-] = 0 \quad Rgg \text{ vertex}$$



$$\Delta_{a_0 a_1 a_2 c}^{\nu_0 \nu_1 \nu_2 -} = ig^2 \mathbf{q}^2 \left(\frac{f^{a_2 a_1 a} f^{a_0 a c}}{k_2^- k_0^-} + \frac{f^{a_2 a_0 a} f^{a_1 a c}}{k_2^- k_1^-} \right) \times (n^-)^{\nu_0} (n^-)^{\nu_1} (n^-)^{\nu_2} [k_0^- + k_1^- + k_2^-] = 0 \quad Rggg \text{ vertex}$$

(A.22)

S-Matrix Elements, Cross Sections and the Optical Theorem

The S -matrix is the linear operator transforming the initial state $|i\rangle$ of a scattering process into the final state $|f\rangle$, $S|i\rangle = |f\rangle$. *In* $|i\rangle$ and *out* $|f\rangle$ states are defined at times $-\infty$ and $+\infty$ respectively, represent free particles and form complete sets of states [Wei95, Dun12]. The S -matrix is given by the unitary time evolution operator U :

$$S \equiv U(-\infty, +\infty) = \mathbb{1} + \sum_{n=1}^{\infty} \frac{i^n}{n!} \int d^4 x_1 \cdots d^4 x_n \mathcal{T}(H'_{\text{int}}(x_1) \cdots H'_{\text{int}}(x_n)), \quad (\text{A.23})$$

where H'_{int} is the interaction Hamiltonian (in interaction picture) and \mathcal{T} denotes the time-ordered product. From S -matrix elements we define the scattering amplitude $A(i \rightarrow f)$,

$$S_{if} \equiv \langle f|S|i\rangle \equiv \delta_{if} + iT_{if} = \delta_{if} + i(2\pi)^4 \delta^4(p_f - p_i) A(i \rightarrow f), \quad (\text{A.24})$$

in terms of which the differential cross section for a $1 + 2 \rightarrow n$ particles process reads

$$d\sigma = \frac{1}{\Phi} |A(i \rightarrow f_n)|^2 d\Pi_n, \quad \sigma_{\text{tot}} = \frac{1}{\Phi} \sum_n \int d\Pi_n |A(i \rightarrow f_n)|^2. \quad (\text{A.25})$$

with the phase space for n particles in the final state being

$$d\Pi_n = \prod_{j=1}^n \frac{d^4 p'_j}{(2\pi)^3} \delta(p_j'^2 - m_j^2) (2\pi)^4 \delta^4 \left(p_1 + p_2 - \sum_{j=1}^n p'_j \right) = \prod_{j=1}^n \frac{d^3 \mathbf{p}'_j}{(2\pi)^3 2E'_j} (2\pi)^4 \delta^4 \left(p_1 + p_2 - \sum_{j=1}^n p'_j \right), \quad (\text{A.26})$$

A. Miscellaneous Formulæ

and the incident flux being given by

$$\Phi = 2E_1 2E_2 |\mathbf{v}_1 - \mathbf{v}_2| = 2\lambda^{1/2}(s, m_1^2, m_2^2), \quad \Phi \stackrel{s \rightarrow \infty}{\simeq} 2s. \quad (\text{A.27})$$

E_i and $\mathbf{v}_i = \mathbf{p}_i/E_i$, $i = 1, 2$, are the energies and velocities of colliding particles in the LAB system⁷. Unitarity of the S -matrix, $SS^\dagger = S^\dagger S = \mathbb{1}$, follows from conservation of probability:

$$\sum_k \text{Prob}(i \rightarrow k) = \sum_k |\langle k|S|i\rangle|^2 = \sum_k \langle i|S^\dagger|k\rangle \langle k|S|i\rangle = \langle i|S^\dagger S|i\rangle = 1 \implies S^\dagger S = 1. \quad (\text{A.28})$$

In terms of the transition matrix T_{if} defined in (A.24) ($S = \mathbb{1} + iT$), this reads⁸

$$i\langle f|T^\dagger - T|i\rangle = \sum_{\{n\}} \langle f|T^\dagger|n\rangle \langle n|T|i\rangle \implies 2\Im m T_{if} = \sum_{\{n\}} T_{fn}^* T_{in}. \quad (\text{A.29})$$

Extracting from T the 4-momentum conservation δs , we have in terms of amplitudes

$$2\Im m A(i \rightarrow f) = \sum_n \int d\Pi_n A^*(f \rightarrow n) A(i \rightarrow n). \quad (\text{A.30})$$

(A.30) tells us that, in order to compute the imaginary part of the scattering amplitude of some process at the n -th perturbative order, we just need to compute the amplitudes up to the $(n - 1)$ -th order. While it is not possible to deal in full generality with the set (A.30) of nonlinear coupled integral equations, some important results can be derived from them. The easiest one is the special case $|i\rangle = |f\rangle$ (in the sense also that individual momenta of particles remain the same after the collision). For a $2 \rightarrow 2$ process, this is the case of forward elastic scattering ($t = 0$). In this case one gets from (A.30), using (A.25) and (A.27)

$$2\Im m A_{\text{el}(t=0)} = \sum_n \int d\Pi_n |A(i \rightarrow n)|^2 \implies \sigma_{\text{tot}} = \frac{2}{\Phi} \Im m A_{\text{el}(t=0)} \underset{s \rightarrow \infty}{\simeq} \frac{1}{s} \Im m A_{\text{el}(t=0)}. \quad (\text{A.31})$$

(A.31) is called the optical theorem⁹. Its importance is difficult to overemphasize. It states that the total cross section (the cross section for $1 + 2 \rightarrow \text{anything}$) is given by only one S -matrix element.

⁷The second equality in (A.27), expressing Φ in terms of Källén's λ (B.9), is only valid for systems boosted in the beam direction with respect to the LAB one, so the flux is not totally Lorentz invariant.

⁸In (A.29), $\sum_{\{n\}}$ contains integration over all continuous variables and sum over all discrete quantum numbers. For a system of n spinless particles this is given by $\sum_{\{n\}} = \sum_n \int \prod_{j=1}^n \frac{d^3 \mathbf{q}_j}{(2\pi)^3 2E_j}$.

⁹There is a deep analogy between optical diffraction and high energy scattering, see [BP02].

B

Kinematics of Scattering Processes

Mandelstam Variables

Consider a generic scattering process of the form

$$1 + 2 \rightarrow 3 + 4 + \cdots + N. \quad (\text{B.1})$$

Conservation of 4-momentum, $p_1 + p_2 = \sum_{j=3}^N p_j$ gives 4 constraints. N further kinematical constraints come from mass-shell conditions $p_i^2 = m_i^2, i = 1, \dots, N$. Finally, the arbitrariness in fixing a 4-dimensional reference frame (which could be rotated or boosted) supplies 6 more constraints. All in all, from the a priori $4N$ variables describing process (B.1) —the components of the 4-momenta—, the number of independent Lorentz-invariant variables for the reaction is $4N - 4 - N - 6 = 3N - 10$. In practice, one of these variables, say the center-of-mass energy of the colliding particles, is fixed when preparing the initial state. In particular, for $N = 2$, we have two independent variables, usually taken among the Mandelstam invariants

$$s = (p_1 + p_2)^2 = (p_3 + p_4)^2, \quad t = (p_1 - p_3)^2 = (p_2 - p_4)^2, \quad u = (p_1 - p_4)^2 = (p_2 - p_3)^2. \quad (\text{B.2})$$

B. Kinematics of Scattering Processes

The Mandelstam variables satisfy the identity $s + t + u = \sum_{i=1}^4 m_i^2$. In general, we take s and t as independent variables.¹ In the reaction (B.1), s is the square of the total c.m. energy and t is the squared momentum transfer. We refer to (B.1), or its time-reversed, as to the s -channel process. Analogously, t -channel (u -channel) means that t (u , respectively), is the square of the total c.m. energy. The t -channel and u -channel reactions are then

$$1 + \bar{3} \rightarrow \bar{2} + 4, \quad (t\text{-channel}), \quad 1 + \bar{4} \rightarrow \bar{2} + 3, \quad (u\text{-channel}), \quad (\text{B.3})$$

together with their time reversed processes. Here $\bar{3}$, for instance, means that the momentum of particle 3 as been reversed and all additive quantum numbers have changed sign, that is $\bar{3}$ is the antiparticle of 3 with opposed momentum.

Elastic Scattering in the Center-of-Mass System

Consider the s -channel reaction (B.1) in the center-of-mass (CM) system where $\mathbf{p}_1 + \mathbf{p}_2 = 0$ (FIGURE B.1). Assuming particles 1 and 2 to travel along z axis, we have

$$\begin{aligned} p_1 &= (E_1, \mathbf{p}) = (E_1, 0, 0, p_z); & p_2 &= (E_2, -\mathbf{p}) = (E_2, 0, 0, -p_z); \\ p_3 &= (E_3, \mathbf{p}') = (E_3, \mathbf{p}_\perp, p'_z); & p_4 &= (E_4, -\mathbf{p}') = (E_4, -\mathbf{p}_\perp, -p'_z). \end{aligned} \quad (\text{B.4})$$

Only two of the variables appearing in (B.4) are independent. We choose them to be the

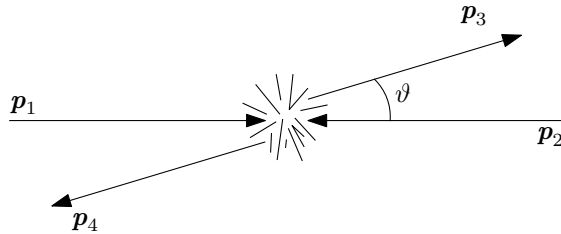


Figure B.1: $2 \rightarrow 2$ scattering in the center-of-mass system.

CM momentum $|\mathbf{p}| = p_z$ and the scattering angle ϑ , defined by

$$p'_z = |\mathbf{p}'| \cos \vartheta; \quad |\mathbf{p}_\perp| = |\mathbf{p}'| \sin \vartheta. \quad (\text{B.5})$$

Energies are given in terms of s by

¹In some cases it may be convenient to use a different pair of variables. For instance, if we look at backward scattering, s and u are a more practical choice, since the backward direction corresponds to $u = 0$ for equal-mass particles, whereas the forward direction corresponds to $t = 0$ (B.14).

$$E_{1,2} = \frac{1}{2\sqrt{s}}(s \pm m_1^2 \mp m_2^2), \quad E_{3,4} = \frac{1}{2\sqrt{s}}(s \pm m_3^2 \mp m_4^2). \quad (\text{B.6})$$

Using the mass-shell conditions, one also gets the relations

$$\mathbf{p}^2 = p_z^2 = E_1^2 - m_1^2 = \frac{1}{4s}[s - (m_1 + m_2)^2][s - (m_1 - m_2)^2] = \frac{1}{4s}\lambda(s, m_1^2, m_2^2), \quad (\text{B.7})$$

$$\mathbf{p}'^2 = \mathbf{p}'_\perp{}^2 + p_z^2 = E_3^2 - m_3^2 = \frac{1}{4s}[s - (m_3 + m_4)^2][s - (m_3 - m_4)^2] = \frac{1}{4s}\lambda(s, m_3^2, m_4^2), \quad (\text{B.8})$$

where the Källén function is given by

$$\lambda(x, y, z) = x^2 + y^2 + z^2 - 2xy - 2yz - 2xz. \quad (\text{B.9})$$

In the high-energy limit ($s \rightarrow \infty$) masses can be neglected and one has

$$E_1, E_2, E_3, E_4 \underset{s \rightarrow \infty}{\simeq} \frac{\sqrt{s}}{2}; \quad |\mathbf{p}|, |\mathbf{p}'| \underset{s \rightarrow \infty}{\simeq} \frac{\sqrt{s}}{2}. \quad (\text{B.10})$$

Relations between the CM variables $|\mathbf{p}|, \vartheta$ and the Mandelstam invariants s, t can be obtained from the previous expressions

$$t = (p_1 - p_3)^2 = m_1^2 + m_3^2 - 2E_1E_3 + 2|\mathbf{p}||\mathbf{p}'| \cos \vartheta, \quad (\text{B.11})$$

$$\cos \vartheta = \frac{s^2 + s(2t - \sum_i m_i^2) + (m_1^2 - m_2^2)(m_3^2 - m_4^2)}{\lambda^{1/2}(s, m_1^2, m_2^2)\lambda^{1/2}(s, m_3^2, m_4^2)} \quad (\text{B.12})$$

and are much simpler in the case of equal masses $m_1 = m_2 = m_3 = m_4 \equiv m$:

$$|\mathbf{p}| = \frac{1}{2}\sqrt{s - 4m^2}, \quad \cos \vartheta = 1 + \frac{2t}{s - 4m^2}. \quad (\text{B.13})$$

Inverting, we get Mandelstam variables in terms of CM momentum and scattering angle

$$s = 4(\mathbf{p}^2 + m^2), \quad t = -2\mathbf{p}^2(1 + \cos \vartheta), \quad u = -2\mathbf{p}^2(1 - \cos \vartheta). \quad (\text{B.14})$$

For massless particles or in the limit when masses can be neglected ($s \rightarrow \infty$)

$$\cos \vartheta = 1 + \frac{2t}{s}, \quad t \simeq -\mathbf{p}_\perp^2. \quad (\text{B.15})$$

B. Kinematics of Scattering Processes

The kinematical limits $p \geq 0$ and $-1 \leq \cos \vartheta \leq 1$ translate, using (B.14), in the physical region of the s -channel in the Mandelstam plane

$$s \geq 4m^2, \quad t \leq 0, \quad u \leq 0. \quad (\text{B.16})$$

Similar reasoning [BP02] gives the physical domain of the t and u -channels

$$t \geq 4m^2, \quad s \leq 0, \quad u \leq 0 \quad (t\text{-channel}), \quad u \geq 4m^2, \quad s \leq 0, \quad t \leq 0 \quad (u\text{-channel}). \quad (\text{B.17})$$

So the physical domains of the s , t and u channels are different and non-overlapping (FIG. B.2). Nevertheless, crossing symmetry of the S -matrix tells us that s, t, u -channel processes are described by the same amplitude (or appropriate combinations of the same amplitudes).

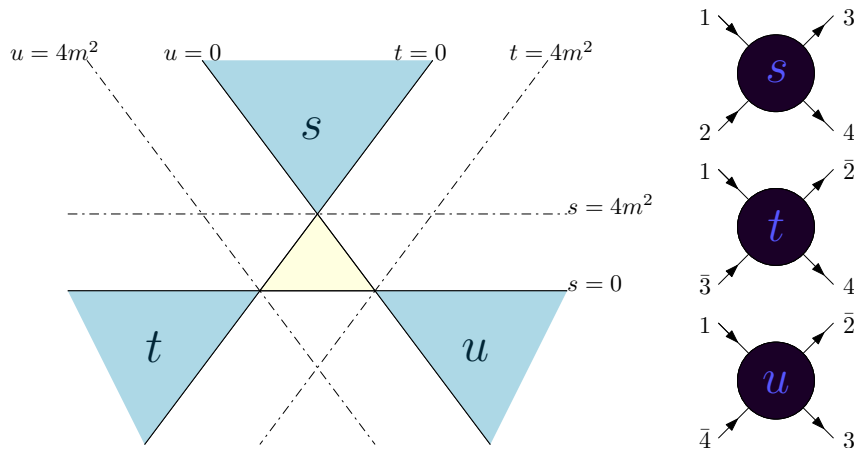


Figure B.2: *The Mandelstam plot showing the physical regions of the s, t and u channels (in blue).*

Light-Cone Components, Sudakov Parametrization and Rapidity

Light-cone (LC) components of a 4-vector A^μ are defined as

$$A^\pm = A_\mp = A^0 \pm A^3. \quad (\text{B.18})$$

In these components we write $A^\mu = (A^+, A^-, \mathbf{A}_\perp)$, and scalar products are given by

$$A \cdot B = A^0 B^0 - \mathbf{A} \cdot \mathbf{B} = \frac{1}{2} [A^+ B^- + A^- B^+] - \mathbf{A}_\perp \cdot \mathbf{B}_\perp, \quad A^2 = A^+ A^- - \mathbf{A}_\perp^2, \quad (\text{B.19})$$

i.e. we have a metric with non-null entries $2g_{+-} = 2g_{-+} = -g_{xx} = -g_{yy} = 1$. Now we take a basis of light-cone vectors $n^- = (\Lambda, 0, 0, \Lambda)$ (in LC components $(2\Lambda, 0, 0, 0)$) and $n^+ =$

$(\Lambda^{-1}, 0, 0, -\Lambda^{-1})$ (in LC components $(0, 2\Lambda^{-1}, 0, 0)$), which have the usual² normalization $n^+ \cdot n^- = 2$. The Sudakov decomposition of an arbitrary 4-vector A^μ is

$$A^\mu = \alpha(n^-)^\mu + \beta(n^+)^\mu + A_\perp^\mu = \frac{1}{2} \left[\underbrace{(A \cdot n^+)}_{\Lambda^{-1}A^+} (n^-)^\mu + \underbrace{(A \cdot n^-)}_{\Lambda A^-} (n^+)^\mu \right] + A_\perp^\mu = (2\alpha\Lambda, 2\beta\Lambda^{-1}, \mathbf{A}_\perp). \quad (\text{B.20})$$

One has then in terms of Sudakov components

$$A^2 = A^+ A^- - \mathbf{A}_\perp^2 = 4\alpha\beta - \mathbf{A}_\perp^2. \quad (\text{B.21})$$

In the following we take $\Lambda = 1$ so that

$$A^\mu = A^+ \frac{(n^-)^\mu}{2} + A^- \frac{(n^+)^\mu}{2} + A_\perp^\mu. \quad (\text{B.22})$$

The non-transverse part of the metric can be expressed in terms of the Sudakov vectors:

$$g^{\mu\nu} = g_\perp^{\mu\nu} + \frac{1}{2} [(n^-)^\mu (n^+)^\nu + (n^+)^\mu (n^-)^\nu], \quad (\text{B.23})$$

where $g_\perp^{\mu\nu}$ projects on the plane perpendicular to n^- and n^+

$$g_\perp^{\mu\nu} A_\mu = A^\nu - \frac{1}{2} (A \cdot n^-) (n^+)^\nu - \frac{1}{2} (A \cdot n^+) (n^-)^\nu = A_\perp^\nu. \quad (\text{B.24})$$

In terms of its LC components, rapidity is defined for a particle of momentum p as

$$y = \frac{1}{2} \ln \frac{p^+}{p^-}; \quad \tanh y = \frac{p_z}{E} \equiv \frac{p^3}{p^0}. \quad (\text{B.25})$$

Defining the transverse mass $m_\perp = \sqrt{m^2 + p_\perp^2}$, so that the mass-shell condition reads $E^2 = p_z^2 + m_\perp^2$, we have

$$p_z = m_\perp \sinh y; \quad E = m_\perp \cosh y. \quad (\text{B.26})$$

In this way we have the following parametrization for p

$$p = (m_\perp e^y, m_\perp e^{-y}; \mathbf{p}_\perp), \quad \mathbf{p}_\perp = (p_\perp \cos \phi, p_\perp \sin \phi) \quad (\text{B.27})$$

being ϕ the azimuthal angle between the vector \mathbf{p}_\perp and an arbitrary vector in the transverse plane. For massless particles, (B.5) and (B.25) give $\tanh y = \cos \vartheta$, from which one gets the

²Note, however, that there is a factor 2 difference with the conventions of [BP02], for instance. The following properties of Sudakov vectors are evident: $(n^+)^2 = (n^-)^2 = 0$, $(n^+ \cdot A_\perp) = (n^- \cdot A_\perp) = 0$, $(n^-)^- = (n^+)^+ = 0$.

B. Kinematics of Scattering Processes

definition of pseudorapidity η

$$\eta = y(m = 0) = \frac{1}{2} \ln \frac{1 + \cos \vartheta}{1 - \cos \vartheta} = -\ln \tan \frac{\vartheta}{2}, \quad (\text{B.28})$$

that is, rather than y , the variable used in high-energy experiments, since its determination requires just tracking the particle direction. When $p_{\perp} \gg m$ both definitions coincide. However, one should keep in mind that it is y , and not η , that has the great property of transforming additively under boosts in the beam direction and gives the correct measure for phase space

$$\frac{d^3\mathbf{p}}{2E(2\pi)^3} = \frac{dy d^2\mathbf{p}_{\perp}}{4\pi (2\pi)^2}. \quad (\text{B.29})$$

Multi-Regge Kinematics

Now we move to parton scattering in which $n + 2$ partons are produced (FIGURE B.3). 4-momenta of incoming and outgoing partons are assumed to fulfill $p_A^2 = p_B^2 = k_i^2 = 0$, $i = 0, \dots, n + 1$ ³. According to parametrization (B.27) we have, in CM system,

$$p_A = (\sqrt{s}, 0; \mathbf{0}); \quad p_B = (0, \sqrt{s}; \mathbf{0}); \quad k_i = (k_{i\perp} e^{y_i}, k_{i\perp} e^{-y_i}; \mathbf{k}_{i\perp}), \quad i = 0, \dots, n + 1. \quad (\text{B.30})$$

Momentum conservation gives for each of the light-cone components

$$\mathbf{0} = \sum_{i=0}^{n+1} \mathbf{k}_{i\perp}, \quad \sqrt{s} = \sum_{i=0}^{n+1} k_{i\perp} e^{y_i} = \sum_{i=0}^{n+1} k_{i\perp} e^{-y_i}. \quad (\text{B.31})$$

Using (B.31), generalized Mandelstam invariants can be written as⁴

$$s = 2p_A \cdot p_B = \sum_{i,j=0}^{n+1} k_{i\perp} k_{j\perp} e^{y_i - y_j}, \quad (\text{B.32})$$

$$s_{ij} = 2k_i \cdot k_j = 2k_{i\perp} k_{j\perp} [\cosh(y_i - y_j) - \cos(\phi_i - \phi_j)] \quad (\text{B.33})$$

It is convenient to introduce for the present analysis a Sudakov parametrization taking as Sudakov vectors p_A and p_B , which satisfy a different normalization ($p_A \cdot p_B = \frac{s}{2}$):

$$A^{\mu} = \alpha p_A^{\mu} + \beta p_B^{\mu} + A_{\perp}^{\mu}. \quad (\text{B.34})$$

³The following analysis can be easily generalized to the case of slightly off-shell incoming and outgoing momenta, see for instance the discussion in [IFL10].

⁴Note that Mandelstam invariants only depend on rapidity differences, which are boost-invariant.

In this case, formulas (B.21), (B.22) and (B.23) should be substituted by⁵

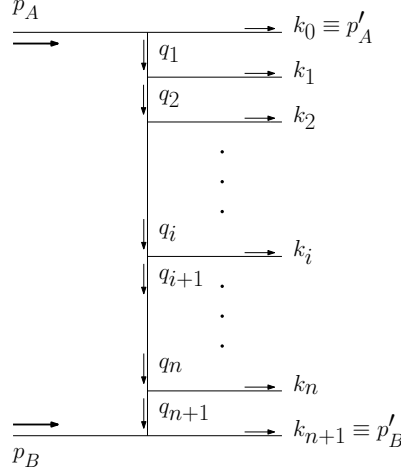


Figure B.3: Notation for $2 \rightarrow n + 2$ scattering processes.

$$A^2 = s\alpha\beta - \mathbf{A}_\perp^2; \quad A = \frac{1}{\sqrt{s}} [A^+ p_A + A^- p_B] + A_\perp; \quad g^{\mu\nu} = g_\perp^{\mu\nu} + \frac{2}{s} [p_A^\mu p_B^\nu + p_B^\mu p_A^\nu]. \quad (\text{B.35})$$

s -channel and t -channel momenta in FIGURE B.3 are then parametrized as

$$k_i = \alpha_i p_A + \beta_i p_B + k_{i\perp}, \quad i = 0, \dots, n+1; \quad q_i = \bar{\alpha}_i p_A + \bar{\beta}_i p_B + q_{i\perp}, \quad i = 1, \dots, n+1. \quad (\text{B.36})$$

We define multi-Regge kinematics (MRK) as the kinematic region where the outgoing partons are strongly ordered in rapidity and have comparable transverse momentum, of size k_\perp ,

$$y_0 \gg y_1 \gg \dots \gg y_{n+1}; \quad k_{i\perp} \simeq k_\perp. \quad (\text{B.37})$$

From (B.30) and (B.36), one can see that (B.37) is equivalent to a strong ordering for the Sudakov components of the outgoing partons⁶

$$1 \gtrsim \alpha_0 \gg \alpha_1 \gg \dots \gg \alpha_{n+1} \gtrsim (k_\perp/s)^2; \quad (k_\perp/s)^2 \lesssim \beta_0 \ll \beta_1 \ll \dots \ll \beta_{n+1} \lesssim 1. \quad (\text{B.38})$$

In the MRK regime (B.37), (B.32) can be approximated by

$$s \simeq k_{0\perp} k_{n+1\perp} e^{y_0 - y_{n+1}}, \quad s_{ij} \simeq k_{i\perp} k_{j\perp} e^{|y_i - y_j|}, \quad (\text{B.39})$$

giving us an equivalent characterization of the multi-Regge regime:

⁵For an arbitrary normalization of Sudakov vectors (B.23) is to be substituted by $g^{\mu\nu} = g_\perp^{\mu\nu} + \frac{p_A^\mu p_B^\nu + p_B^\mu p_A^\nu}{p_A \cdot p_B}$.

⁶Relations $\alpha_0 \lesssim 1, \alpha_{n+1} \gtrsim (k_\perp/s)^2$, and the analogous equations for β_0 and β_{n+1} , follow from (B.31) in MRK: $\sqrt{s} \simeq k_\perp e^{y_0} \simeq k_\perp e^{-y_{n+1}}$.

B. Kinematics of Scattering Processes

$$s \gg s_{ij} \gg \mathbf{k}_{i\perp}^2, \quad \prod_{i=0}^n s_i \simeq s \prod_{i=1}^n \mathbf{k}_{i\perp}^2, \quad (\text{B.40})$$

where we have defined $s_i \equiv s_{i,i+1}$. This can be also seen using (B.30) and (B.35)

$$s_i = s(\beta_{i-1} + \beta_i)(\alpha_{i-1} + \alpha_i) - (\mathbf{k}_{i-1,\perp} + \mathbf{k}_{i\perp})^2 \simeq s\beta_i\alpha_{i-1} = \frac{\alpha_{i-1}}{\alpha_i} \mathbf{k}_{i\perp}^2 \gg \mathbf{k}_{i\perp}^2, \quad (\text{B.41})$$

Now consider the first t -channel momentum exchange, $q_1 = p_A - k_0$. We have

$$q_1 = (\sqrt{s}, 0; \mathbf{0}) - (k_{0\perp}e^{y_0}, k_{0\perp}e^{-y_0}; \mathbf{k}_{0\perp}) \simeq (k_{1\perp}e^{y_1}, -k_{0\perp}e^{-y_0}, -\mathbf{k}_{0\perp}). \quad (\text{B.42})$$

Squaring and retaining only the leading term ($y_1 \ll y_0$)

$$q_1^2 = -k_{0\perp}k_{1\perp}e^{y_1-y_0} - \mathbf{k}_{0\perp}^2 \simeq -\mathbf{k}_{0\perp}^2 = -\mathbf{q}_{1\perp}^2, \quad (\text{B.43})$$

i.e. only transverse degrees of freedom are relevant in the momentum transfer q_1 . This analysis can be now repeated for the second momentum exchanged in the t channel,

$$\begin{aligned} q_2 &= q_1 - k_1 \simeq (k_{2\perp}e^{y_2}, -k_{1\perp}e^{-y_1}, -\mathbf{k}_{0\perp} - \mathbf{k}_{1\perp}), \\ q_2^2 &= -k_{1\perp}k_{2\perp}e^{y_2-y_1} - (\mathbf{k}_{0\perp} + \mathbf{k}_{1\perp})^2 \simeq -(\mathbf{k}_{0\perp} + \mathbf{k}_{1\perp})^2 = -\mathbf{q}_{2\perp}^2. \end{aligned} \quad (\text{B.44})$$

Generalization to successive momenta in the t -channel is obvious: only transverse components are relevant to parametrize the propagators of partons exchanged in the t channel

$$t_i \equiv q_i^2 \simeq -\mathbf{q}_{i\perp}^2; \quad q_i \simeq \left(k_{i\perp}e^{y_i}, -k_{i-1,\perp}e^{-y_{i-1}}, -\sum_{j=0}^i \mathbf{k}_{j\perp} \right). \quad (\text{B.45})$$

Moreover, $\mathbf{q}_{i\perp}^2 \sim \mathbf{k}_{i\perp}^2$ ⁷, so that we can rephrase (B.40) as

$$s_i \gg -t_i, \quad (\text{B.46})$$

that is, multi-Regge kinematics is the direct generalization of the Regge or high-energy limit $s \gg -t$. To end up, we notice that (B.45) gives us yet another equivalent characterization of MRK, based on the strong ordering of Sudakov components of t -channel exchanges:

$$1 \gg \bar{\alpha}_1 \gg \bar{\alpha}_2 \gg \cdots \gg \bar{\alpha}_{n+1} \gg \frac{k_{1\perp}^2}{s}; \quad 1 \gg |\bar{\beta}_{n+1}| \gg \cdots \gg |\bar{\beta}_2| \gg |\bar{\beta}_1| \gg \frac{k_{1\perp}^2}{s}. \quad (\text{B.47})$$

⁷One can see this relation as obtained from averaging in the azimuthal angles ϕ_i in the expression $q_{i\perp}^2 = \sum_{j=0}^i k_{j\perp}^2$. To make things more rigorous, one should also enforce the constraint (B.31).



Feynman Integrals and Mellin-Barnes Representation

The Mellin Transform

The Mellin transform $\tilde{f}(\omega)$ of a function $f(s)$ is defined as

$$\tilde{f}(\omega) = \int_1^\infty d\left(\frac{s}{s_0}\right) \left(\frac{s}{s_0}\right)^{-\omega-1} f(s), \quad (\text{C.1})$$

where we introduce the scale s_0 for dimensional reasons. Notice the similarity with the usually more familiar Laplace transform. The inverse Mellin transform is

$$f(s) = \frac{1}{2\pi i} \int_C d\omega \left(\frac{s}{s_0}\right)^\omega \tilde{f}(\omega), \quad (\text{C.2})$$

where the integration contour C lies to the right of all singularities of $\tilde{f}(\omega)$ in the complex ω plane. A useful example for this work is

$$f(s) = s^\alpha \ln^p s, \quad \tilde{f}(\omega) = s_0^\alpha \frac{\Gamma(p+1)}{(\omega-\alpha)^{p+1}}. \quad (\text{C.3})$$

C. Feynman Integrals and Mellin-Barnes Representation

We see that the Mellin transform of a pure power of s gives rise to a simple pole, while if the power is accompanied by a logarithmic factor, a cut results in the Mellin transform.

The great property of Mellin transforms is the transformation of convolutions into products. Consider a convolution of n functions g_i , $1 \leq i \leq n$

$$f(s) = \prod_{i=1}^n \int_{\alpha_{i+1}}^1 \frac{d\alpha_i}{\alpha_i} g_i \left(\frac{\alpha_{i-1}}{\alpha_i} \right) s_0 \delta(\alpha_n s - s_0), \quad (\text{C.4})$$

with $\alpha_0 = 1$ and $\alpha_{n+1} = 0$. Doing the integration over s using that $\delta(\alpha_n s - s_0) = \frac{1}{s_0 \alpha_n} \delta\left(\frac{s}{s_0} - \frac{1}{\alpha_n}\right)$ and $\alpha_n < 1$ gives

$$\tilde{f}(\omega) = s_0 \int_1^\infty d\left(\frac{s}{s_0}\right) \left(\frac{s}{s_0}\right)^{-\omega-1} \prod_{i=1}^n \int_{\alpha_{i+1}}^1 \frac{d\alpha_i}{\alpha_i} g_i \left(\frac{\alpha_{i-1}}{\alpha_i} \right) \delta(\alpha_n s - s_0) = \prod_{i=1}^n \int_{\alpha_{i+1}}^1 \frac{d\alpha_i}{\alpha_i} g_i \left(\frac{\alpha_{i-1}}{\alpha_i} \right) \alpha_n^\omega. \quad (\text{C.5})$$

Now we change variables to $\rho_i = \frac{\alpha_i}{\alpha_{i-1}}$, so that $\alpha_n = \prod_{i=1}^n \rho_i$. The Jacobian matrix $\frac{\partial \rho_i}{\partial \alpha_j} = \delta_{ij} \frac{1}{\alpha_{i-1}} - \delta_{i-1,j} \frac{\alpha_i}{\alpha_{i-1}^2}$ is triangular and hence the determinant is given by the product of diagonal elements, $\prod_{i=1}^{n-1} \alpha_i^{-1}$. The final result for $\tilde{f}(\omega)$ is

$$\tilde{f}(\omega) = \prod_{i=1}^n \int_0^1 d\rho_i \rho_i^{\omega-1} g_i \left(\frac{1}{\rho_i} \right) = \prod_{i=1}^n \tilde{g}_i(\omega). \quad (\text{C.6})$$

Mellin-Barnes Representation and Evaluation of Master Integrals for the Two-Loop Gluon Trajectory

In this section we present in detail the derivation of Mellin-Barnes representations for the general two-loop master integral considered in this work with arbitrary powers of the propagators. The principal tool in this analysis is the Mellin-Barnes representation

$$\begin{aligned} \frac{1}{(X_1 + \dots + X_n)^\lambda} &= \frac{1}{\Gamma(\lambda)} \frac{1}{(2\pi i)^{n-1}} \int \dots \int_{-i\infty}^{+i\infty} dz_2 \dots dz_n \prod_{i=2}^n X_i^{z_i} X_1^{-\lambda - z_2 - \dots - z_n} \\ &\times \Gamma(\lambda + z_2 + \dots + z_n) \prod_{i=2}^n \Gamma(-z_i), \end{aligned} \quad (\text{C.7})$$

where the contours of integration are such that poles with a $\Gamma(\dots + z_i)$ dependence are to the left of the z_i contour and poles with a $\Gamma(\dots - z_i)$ dependence lie to the right of the z_i contour. Consider the integral ($a \cdot q = b \cdot q = 0$)

$$\mathfrak{S}_1 = \int [dk] \frac{1}{(-k^2 - i0)^C [-(k-q)^2 - i0]^D [-(k-l)^2 - i0]^E (-a \cdot k - i0)^{\mu_1} (-b \cdot k - i0)^{\mu_2}}. \quad (\text{C.8})$$

Using Schwinger parameters, we can write

$$\mathbb{S}_1 = \frac{i^{C+D+E+\mu_1+\mu_2}}{\Gamma(C)\Gamma(D)\Gamma(E)\Gamma(\mu_1)\Gamma(\mu_2)} \int_0^\infty \cdots \int_0^\infty d\alpha d\beta d\gamma d\tilde{\delta} d\tilde{\sigma} \alpha^{C-1} \beta^{D-1} \gamma^{E-1} \tilde{\delta}^{\mu_1-1} \tilde{\sigma}^{\mu_2-1} \int [dk] e^{i\mathcal{D}},$$

$$\mathcal{D} = \alpha k^2 + \beta(k-q)^2 + \gamma(k-l)^2 + \tilde{\delta} a \cdot k + \tilde{\sigma} b \cdot k = (\alpha + \beta + \gamma)k^2 + \beta q^2 + \gamma l^2 - 2k \cdot \left(\beta q + \gamma l - \left[\tilde{\delta} \frac{a}{2} + \tilde{\sigma} \frac{b}{2} \right] \right). \quad (\text{C.9})$$

Now, performing the usual shift in momentum and performing the changes of variable $\lambda = \alpha + \beta + \gamma$, $\xi = \frac{\beta}{\alpha+\beta}$, $\eta = \frac{\gamma}{\alpha+\beta+\gamma}$; $\tilde{\delta} = 2\lambda\delta$, $\tilde{\sigma} = 2\lambda\sigma$, and $x = 2(\delta + \sigma)$, $y = \frac{\delta}{\delta+\sigma}$, we arrive to

$$\mathbb{S}_1 = \frac{i^{C+D+E+\mu_1+\mu_2}}{\Gamma(C)\Gamma(D)\Gamma(E)\Gamma(\mu_1)\Gamma(\mu_2)} \int_0^\infty d\lambda \int_0^1 d\xi \int_0^1 d\eta \int_0^\infty dx \int_0^1 dy \lambda^{C+D+E+\mu_1+\mu_2-1} \xi^{D-1} (1-\xi)^{C-1} \eta^{E-1}$$

$$\times (1-\eta)^{C+D-1} x^{\mu_1+\mu_2-1} y^{\mu_1-1} (1-y)^{\mu_2-1} \int [dk] \exp [i\lambda(k^2 - (1-\eta)^2 \xi(1-\xi) \mathbf{q}^2 - \eta(1-\eta)(1-\xi)(-l^2)$$

$$- \eta(1-\eta)\xi[-(l-q)^2] - \eta x[y(-a \cdot l) + (1-y)(-b \cdot l) - x^2(\Psi y(1-y) + e^{-\rho})], \quad (\text{C.10})$$

where $\Psi \equiv \frac{1}{2}(a \cdot b - 4e^{-\rho})$ is equal to one up to exponentially suppressed corrections. Making the integrating over momentum and the parameter λ , and using (C.7), results in

$$\mathbb{S}_1 = \frac{i}{(4\pi)^{d/2} \Gamma(C)\Gamma(D)\Gamma(E)\Gamma(\mu_1)\Gamma(\mu_2)} \int_0^1 d\xi \int_0^1 d\eta \int_0^\infty dx \int_0^1 dy \xi^{D-1} (1-\xi)^{C-1} \eta^{E-1} (1-\eta)^{C+D-1}$$

$$\times x^{\mu_1+\mu_2-1} y^{\mu_1-1} (1-y)^{\mu_2-1} \Lambda,$$

$$\Lambda = \int \cdots \int_{-i\infty}^{+i\infty} \frac{dz_2}{2\pi i} \cdots \frac{dz_7}{2\pi i} \Gamma(-z_2) \cdots \Gamma(-z_7) \Gamma(z_2 + z_3 + z_4 + z_5 + z_6 + z_7 + C + D + E + \mu_1 + \mu_2 - d/2)$$

$$\times \frac{[(1-\eta)^2 \xi(1-\xi) \mathbf{q}^2]^{z_2} [\eta(1-\eta)(1-\xi)(-l^2)]^{z_3} [\eta(1-\eta)\xi(-(l-q)^2)]^{z_4} [\eta x y(-a \cdot l)]^{z_5} [\eta x(1-y)(-b \cdot l)]^{z_6}}{[x^2 y(1-y)]^{z_2+z_3+z_4+z_5+z_6+z_7+C+D+E+\mu_1+\mu_2-d/2} [x^2(e^{-\rho})]^{-z_7}}. \quad (\text{C.11})$$

The integrations over parameters can now be performed. In some cases integrals of the form

$$\int_0^1 dy y^{\alpha-1} (1-y)^{-\alpha-1} = \int_0^\infty dt t^{-\alpha-1} = 2\pi i \delta(\alpha) \quad (\text{C.12})$$

appear. The Dirac- δ in (C.12) arises as follows. We have to consider that the integral takes place inside a contour integral over a variable ω , as it is the case in our application. Then we break up the integration over t in two intervals $[0, a]$ and $[a, \infty)$. One can then move the contours (of the ω integral) such that both integrals are convergent and yield as a result

$$\int \frac{d\omega}{2\pi i} f(\omega) \int_0^\infty \frac{dt}{t} t^{\omega-\omega_0} = \int \frac{d\omega}{2\pi i} f(\omega) \int_0^a \frac{dt}{t} t^{\omega-\omega_0} + \int \frac{d\omega}{2\pi i} f(\omega) \int_a^\infty \frac{dt}{t} t^{\omega-\omega_0}$$

$$= - \int \frac{d\omega}{2\pi i} f(\omega) \Theta(\omega_0 - \text{Re}(\omega)) \frac{a^{\omega-\omega_0}}{\omega - \omega_0} + \int \frac{d\omega}{2\pi i} f(\omega) \Theta(\text{Re}(\omega) - \omega_0) \frac{a^{\omega-\omega_0}}{\omega - \omega_0}. \quad (\text{C.13})$$

Both expressions cancel each other up to the Θ -function, i.e. the fact that for the first integral the ω contour is to the left of the pole at ω_0 and for the second one it is to the right. We therefore move the pole of e.g. the first integral to the right of the pole, picking up a

C. Feynman Integrals and Mellin-Barnes Representation

factor $-2\pi i$ times the residue at ω_0 , and we are left with

$$\int \frac{d\omega}{2\pi i} f(\omega) \int_0^\infty \frac{dt}{t} t^{\omega-\omega_0} = f(\omega_0). \quad (\text{C.14})$$

The δ -functions allows for the reduction of contour integrals. Eventually, we arrive at

$$\begin{aligned} \mathfrak{S}_1 &= \frac{i}{(4\pi)^{d/2} \Gamma(C) \Gamma(D) \Gamma(E) \Gamma(\mu_1) \Gamma(\mu_2)} \int \dots \int \frac{dz_2 dz_3 dz_4 dz_5 dz_7}{2\pi i 2\pi i 2\pi i 2\pi i 2\pi i} \frac{\Gamma(-z_2) \Gamma(-z_3) \Gamma(-z_4) \Gamma(-z_5) \Gamma(-z_7)}{\Gamma(-2z_7)} \\ &\times \Gamma(2z_2 + 2z_3 + 2z_4 + z - 5 + 2C + 2D + 2E + \mu_1 + \mu_2 - d) \Gamma(-z_2 - z_3 - z_4 + z_7 - C - D - E + d/2) \\ &\times \Gamma(z_2 + z_3 + z_4 + z_5 - z_7 + C + D + E + \mu_1 - d/2) \Gamma(-z_2 - z_3 - z_4 - z_5 - z_7 - C - D - E - \mu_1 + d/2) \\ &\times \frac{\Gamma(-2z_2 - z_3 - z_4 - 2C - 2D - E - \mu_1 - \mu_2 + d) \Gamma(z_2 + z_3 + C) \Gamma(z_2 + z_4 + D)}{\Gamma(-C - D - E - \mu_1 - \mu_2 + d)} \Psi^{z_2+z_3+z_4-z_7+C+D+E-d/2} \\ &\times (\mathbf{q}^2)^{z_2} (-l^2)^{z_3} (-l-q)^2{}^{z_4} (-a \cdot l)^{z_5} (-b \cdot l)^{-2z_2-2z_3-2z_4-z_5-2C-2D-2E-\mu_1-\mu_2+d} (e^{-\rho})^{z_7}. \end{aligned} \quad (\text{C.15})$$

In a similar way, we can obtain the following MB representation

$$\begin{aligned} \mathfrak{S}_2 &= \int [dk] \frac{1}{(-k^2 - i0)^A [-(k-q)^2 - i0]^B (-\Psi a \cdot k - i0)^{\lambda_1} (-b \cdot k - i0)^{\lambda_2}} \quad (\Psi = \pm 1, a \cdot q = b \cdot q = 0) \\ &= \frac{i \Gamma(A+B+\frac{\lambda_1+\lambda_2}{2}-\frac{d}{2})}{2(4\pi)^{d/2} \Gamma(A) \Gamma(B) \Gamma(\lambda_1) \Gamma(\lambda_2)} \frac{\Gamma(\frac{d}{2}-A-\frac{\lambda_1+\lambda_2}{2}) \Gamma(\frac{d}{2}-B-\frac{\lambda_1+\lambda_2}{2})}{\Gamma(d-A-B-\lambda_1-\lambda_2) (\mathbf{q}^2)^{A+B+\frac{\lambda_1+\lambda_2}{2}-\frac{d}{2}} \Psi^{\frac{\lambda_1+\lambda_2}{2}}} \\ &\times \int \frac{dz}{2\pi i} \frac{\Gamma(-z)}{\Gamma(-2z)} \Gamma\left(z + \frac{\lambda_1 + \lambda_2}{2}\right) \Gamma\left(-z + \frac{\lambda_1 - \lambda_2}{2}\right) \Gamma\left(-z - \frac{\lambda_1 - \lambda_2}{2}\right) \left(\frac{e^{-\rho}}{\Psi}\right)^z. \end{aligned} \quad (\text{C.16})$$

Iterating the results (C.15) and (C.16), we get the MB representation for the general two-loop master integral

$$\begin{aligned} \mathfrak{S} &= \iint [dk][dl] \frac{1}{(-k^2 - i0)^A [-(k-q)^2 - i0]^B (-l^2 - i0)^C [-(l-q)^2 - i0]^D [-(k-l)^2 - i0]^E} \\ &\times \frac{1}{(-\sigma_1 a \cdot k - i0)^{\lambda_1} (-\sigma_2 b \cdot k - i0)^{\lambda_2} (-\tau_1 a \cdot l - i0)^{\mu_1} (-\tau_2 b \cdot l - i0)^{\mu_2}} \quad (\sigma_i = \pm 1, \tau_j = \pm 1, a \cdot q = b \cdot q = 0) \\ &= \frac{-1}{2(4\pi)^d \Gamma(C) \Gamma(D) \Gamma(E) \Gamma(\mu_1) \Gamma(\mu_2) (\mathbf{q}^2)^{A+B+C+D+E+\frac{\lambda_1+\lambda_2+\mu_1+\mu_2}{2}-d}} \\ &\times \int \dots \int \frac{dz_1}{2\pi i} \dots \frac{dz_6}{2\pi i} \frac{\Gamma(-z_1) \Gamma(-z_2) \Gamma(-z_3) \Gamma(-z_4) \Gamma(-z_5) \Gamma(-z_6)}{\Gamma(-2z_1) \Gamma(-2z_6)} \Gamma\left(z_1+z_2+z_3+z_4+C+D+E+\frac{\lambda_1+\lambda_2+\mu_1+\mu_2}{2}-\frac{d}{2}\right) \\ &\times \Gamma\left(-z_1-z_2-z_3-z_4-z_5-C-D-E+\frac{\lambda_1-\lambda_2-\mu_1-\mu_2}{2}+\frac{d}{2}\right) \Gamma\left(-z_1+z_2+z_3+z_4+z_5+C+D+E-\frac{\lambda_1-\lambda_2-\mu_1-\mu_2}{2}-\frac{d}{2}\right) \\ &\times \frac{\Gamma\left(-z_2-z_3-B-C-D-E-\frac{\lambda_1+\lambda_2+\mu_1+\mu_2}{2}+d\right) \Gamma\left(-z_2-z_4-A-C-D-E-\frac{\lambda_1+\lambda_2+\mu_1+\mu_2}{2}+d\right)}{\Gamma(-2z_2-z_3-z_4-A-B-2C-2D-2E-\lambda_1-\lambda_2-\mu_1-\mu_2+2d) \Gamma(2z_2+2z_3+2z_4+z_5+2C+2D+2E+\lambda_2+\mu_1+\mu_2-d)} \\ &\times \Gamma(2z_2+2z_3+2z_4+z_5+2C+2D+2E+\mu_1+\mu_2-d) \Gamma(-z_2-z_3-z_4+z_6-C-D-E+d/2) \Gamma\left(z_2+A+B+C+D+E+\frac{\lambda_1+\lambda_2+\mu_1+\mu_2}{2}-d\right) \\ &\times \Gamma(z_2+z_3+z_4+z_5-z_6+C+D+E+\mu_1-d/2) \Gamma(-z_2-z_3-z_4-z_5-z_6-C-D-E-\mu_1+d/2) \\ &\times \frac{\Gamma(-2z_2-z_3-z_4-2C-2D-E-\mu_1-\mu_2+d) \Gamma(z_2+z_3+C) \Gamma(z_2+z_4+D)}{\Gamma(-z_3+A) \Gamma(-z_4+B) \Gamma(-z_5+\lambda_1) \Gamma(-C-D-E-\mu_1-\mu_2+d)} (e^{-\rho})^{z_1+z_6} (\sigma_1 \sigma_2)^{-z_1-z_2-z_3-z_4-C-D-E-\frac{\lambda_1+\lambda_2+\mu_1+\mu_2}{2}+\frac{d}{2}} \\ &\times \sigma_1^{-z_5} \sigma_2^{2z_2+2z_3+2z_4+z_5+2C+2D+2E+\mu_1+\mu_2-d} (\tau_1 \tau_2)^{z_2+z_3+z_4-z_6+C+D+E-d/2}. \end{aligned} \quad (\text{C.17})$$

The inclusion of the parameters σ_i and τ_j in (C.17) is very useful when computing principal values.

D

Details of Some Computations

Cancellation of Imaginary Parts for Diagram (d₁), Fig. III.7

Defining the measure

$$\int d\Phi \equiv \int d^d k_1 \int d^d k_2 \int d^d k_3 \delta^{(d)}(q - k_1 - k_2 - k_3) \frac{1}{k_1^2 k_2^2 k_3^2} \quad (\text{D.1})$$

where k_i , $i = 1, 2, 3$ denote the momenta of the three t -channel propagators, diagram (d₁) reads up to overall factors

$$(k_1) = \int d\Phi [2g_2^+(3, 2, 1) + g_2^+(3, 1, 2)]g_2^-(3, 2, 1) = \int d\Phi [g_2^+(3, 2, 1) - g_2^+(1, 3, 2)]g_2^-(3, 2, 1), \quad (\text{D.2})$$

where we have used that $g_2(3, 2, 1) + g_2(3, 1, 2) = -g_2(1, 3, 2)$. g_2 can be written as

$$g(3, 2, 1) = -\frac{1}{3!} \left[\frac{2}{(k_1 - i0)(k_3 + i0)} + \frac{2}{(k_1 + i0)(k_3 - i0)} - \frac{1}{(k_1 - i0)(k_2 + i0)} - \frac{1}{(k_1 + i0)(k_2 - i0)} - \frac{1}{(k_3 - i0)(k_2 + i0)} - \frac{1}{(k_3 + i0)(k_2 - i0)} \right], \quad (\text{D.3})$$

D. Details of Some Computations

and therefore

$$g(3, 2, 1) - g(1, 3, 2) = -\frac{1}{2} \left[\frac{1}{(k_1 - i0)(k_3 + i0)} + \frac{1}{(k_1 + i0)(k_3 - i0)} - \frac{1}{(k_1 - i0)(k_2 + i0)} - \frac{1}{(k_1 + i0)(k_2 - i0)} \right]. \quad (\text{D.4})$$

We make now the following observation: the combinations of terms

$$\frac{1}{(n_a \cdot k_1 - i0)(n_a \cdot k_3 + i0)} \frac{1}{(n_b \cdot k_1 - i0)(n_b \cdot k_3 + i0)} \quad (\text{D.5})$$

lead, with $k_1 = k$, $k_2 = k - l$ and $k_3 = q - l$, to the master integral \mathcal{D} (TAB. III.1), for which the result is known. Combinations such as

$$\frac{1}{(n_a \cdot k_1 + i0)(n_a \cdot k_3 - i0)} \frac{1}{(n_b \cdot k_1 - i0)(n_b \cdot k_3 + i0)} \quad (\text{D.6})$$

can be treated with the $n_a \rightarrow -n_a$ trick explained in SEC. III.3.2. Note that the same is true if we exchange $k_3 \leftrightarrow k_2$ as we simply reparametrize momenta. Since integral \mathcal{D} is proportional to ρ , making $\rho \rightarrow \rho - i\pi$ we do not get any enhanced imaginary parts. We are therefore left with terms of the form

$$\int d\Phi \left[\frac{1}{(n_a \cdot k_1 - i0)(n_a \cdot k_3 + i0)} + \frac{1}{(n_a \cdot k_1 + i0)(n_a \cdot k_3 - i0)} \right] \times \left[\frac{1}{(n_b \cdot k_1 + i0)(n_b \cdot k_2 - i0)} + \frac{1}{(n_b \cdot k_1 - i0)(n_b \cdot k_2 - i0)} \right]. \quad (\text{D.7})$$

To demonstrate that such diagrams have no enhanced imaginary part, we note that

$$\begin{aligned} \frac{1}{(n_b \cdot k_1 - i0)(n_b \cdot k_2 + i0)} &= -\frac{1}{(n_b \cdot k_1 - i0)(n_b \cdot k_1 + n_b \cdot k_3 - i0)} \\ &= -\frac{1}{(n_b \cdot k_1 - i0)(n_b \cdot k_3 - i0)} - \frac{1}{(n_b \cdot k_3 - i0)(n_b \cdot k_2 + i0)} \end{aligned} \quad (\text{D.8})$$

and

$$\begin{aligned} &\frac{1}{(n_b \cdot k_1 - i0)(n_b \cdot k_2 + i0)} \\ &= \frac{1}{2} \left[\frac{1}{(n_b \cdot k_1 - i0)(n_b \cdot k_2 + i0)} - \frac{1}{(n_b \cdot k_1 - i0)(n_b \cdot k_3 - i0)} - \frac{1}{(n_b \cdot k_3 - i0)(n_b \cdot k_2 + i0)} \right]. \end{aligned} \quad (\text{D.9})$$

Since the first line of (D.7) is symmetric under $k_3 \leftrightarrow k_1$, the first and the last terms in (D.9) cancel and we are left with

$$\begin{aligned}
& - \int d\Phi \left[\frac{1}{(n_a \cdot k_1 - i0)(n_a \cdot k_3 + i0)} + \frac{1}{(n_a \cdot k_1 + i0)(n_a \cdot k_3 - i0)} \right] \\
& \left[\frac{1}{(n_b \cdot k_1 - i0)(n_b \cdot k_3 - i0)} + \frac{1}{(n_b \cdot k_1 + i0)(n_b \cdot k_3 + i0)} \right]. \tag{D.10}
\end{aligned}$$

Now

$$\frac{1}{(n_b \cdot k_1 \mp i0)(n_b \cdot k_3 \mp i0)} = \frac{1}{(n_b \cdot k_1 \pm i0)(n_b \cdot k_3 \mp i0)} \pm 2i\pi\delta(n_b \cdot k_1) \frac{1}{(n_b \cdot k_3 \mp i0)}, \tag{D.11}$$

and

$$\begin{aligned}
& \frac{1}{(n_b \cdot k_1 + i0)(n_b \cdot k_3 + i0)} + \frac{1}{(n_b \cdot k_1 - i0)(n_b \cdot k_3 - i0)} \\
& = \frac{1}{(n_b \cdot k_1 - i0)(n_b \cdot k_3 + i0)} + \frac{1}{(n_b \cdot k_1 + i0)(n_b \cdot k_3 - i0)} - 4\pi^2\delta(n_b \cdot k_1)\delta(n_b \cdot k_3). \tag{D.12}
\end{aligned}$$

Inserting (D.12) into (D.10) we find again terms which can (up to $n_a \rightarrow -n_a$ etc.) be written as the master integral \mathcal{D} . We therefore only need to address the term

$$\int d\Phi \left[\frac{1}{(n_a \cdot k_1 - i0)(n_a \cdot k_3 + i0)} + \frac{1}{(n_a \cdot k_1 + i0)(n_a \cdot k_3 - i0)} \right] 4\pi^2\delta(n_b \cdot k_1)\delta(n_b \cdot k_3). \tag{D.13}$$

Using that $n_b \cdot k = k^- + k^+e^{-\rho}$ we have, up to overall numerical factors and omitting the Jacobian factor $\sim 1/(1 + e^\rho)$,

$$\int \prod_{i=1}^3 dk_i^+ d^{d-2}\mathbf{k}_i \frac{1}{(k_i^+)^2 e^{-\rho} - \mathbf{k}_i^2} \left[\frac{1}{(k_1^+ - i0)(k_3^+ + i0)} + \frac{1}{k_1^+ + i0)(k_3^+ - i0)} \right] \delta\left(\sum_{j=1}^3 k_j^+\right) \delta^{(d-2)}\left(\sum_{j=1}^3 \mathbf{k}_j\right). \tag{D.14}$$

With the help of (D.9), and after relabeling momenta (e.g. $k_1 \rightarrow k_2$) for the last term we end up with the second term of the above expression and find altogether

$$\begin{aligned}
& \int \prod_{i=1}^3 dk_i^+ d^{d-2}\mathbf{k}_i \frac{1}{(k_i^+)^2 e^{-\rho} - \mathbf{k}_i^2} \left[- \frac{1}{(k_1 - i0)(k_2 - i0)} + \frac{1}{k_1^+ + i0)(k_3^+ - i0)} \right] \delta\left(\sum_{j=1}^3 k_j^+\right) \delta^{(d-2)}\left(\sum_{j=1}^3 \mathbf{k}_j\right) \\
& = \int \prod_{i=1}^3 dk_i^+ d^{d-2}\mathbf{k}_i \frac{1}{(k_i^+)^2 e^{-\rho} - \mathbf{k}_i^2} \left[- 2i\pi\delta(k_1^+) \frac{1}{(k_3^+ - i0)} \right] \delta\left(\sum_{j=1}^3 k_j^+\right) \delta^{(d-2)}\left(\sum_{j=1}^3 \mathbf{k}_j\right), \tag{D.15}
\end{aligned}$$

where we relabeled again the momenta for the first term. Evaluating the delta functions in

D. Details of Some Computations

the plus momenta we obtain $k_1^+ = 0$ and $k_2^+ = -k_3^+$ and

$$-2i\pi \int dk_3^+ \prod_{i=1}^3 d^{d-2} \mathbf{k}_i \frac{1}{-\mathbf{k}_1^2} \frac{1}{(k_3^+)^2 e^{-\rho} - \mathbf{k}_2^2} \frac{1}{(k_3^+)^2 e^{-\rho} - \mathbf{k}_3^2} \left[\frac{1}{[k_3^+]_{\text{PV}}} + i\pi \delta(k_3^+) \right] \delta^{d-2} \left(\sum_{j=1}^3 \mathbf{k}_j \right). \quad (\text{D.16})$$

The integral over the first term is now convergent at infinity and antisymmetric under $k_3^+ \rightarrow -k_3^+$ and therefore vanishes. The second term is trivially evaluated. We conclude that diagram (k_1) has no enhanced imaginary parts.

Details on the Virtual Corrections to the Gluon-Induced Forward Jet Vertex

We refer for the notation to FIG. III.14. Tadpole contributions vanish in dimensional regularization. The contribution for each of these diagrams can be written in terms of master integrals labeled with the following notation: M, S, P, and Q denote, respectively, the existence of a propagator of the form k^+ ($\rightarrow n_b \cdot k$), k^2 , $(k - p_a)^2$ or $(k - q)^2$. The number at the end (0, 1, 2, or 3) indicates how many tensor indices are present in the numerator (e.g. 2 stands for a factor $k^\mu k^\nu$). $\xi = n_a^2 = n_b^2 = 4e^{-\rho}$ are chosen to indicate the squares of the new light-cone vectors. For diagrams (E), (F), (I) and (J) in Fig. III.14 the contribution with reversed arrows is included. Diagrams (G) and (H) turn out to vanish completely. The symmetry factors for the diagrams, which are included, are equal to one apart from diagrams (C) and (D), for which it is two. In more detail, these are all the contributing expressions:

$$\begin{aligned} iA_{(A)} &= -\frac{ig^3}{2} \mathbf{q}^2 f_{abc} N_c \int \frac{d^d k}{(2\pi)^d} \frac{(k^+ - 2p_a^+)^2 \varepsilon \cdot \varepsilon^* + 4\xi \varepsilon \cdot k \varepsilon^* \cdot (k - q)}{k^+ k^2 (k - p_a)^2 (k - q)^2} \\ &= -\frac{ig^3}{2} \mathbf{q}^2 f_{abc} N_c \{ 16e^{-\rho} \varepsilon_\mu \varepsilon_\nu^* [\text{MSPQ2}] - 16e^{-\rho} \varepsilon^* \cdot q \varepsilon_\mu [\text{MSPQ1}] - 4p_a^+ \varepsilon \cdot \varepsilon^* [\text{SPQ0}] \\ &\quad + 4(p_a^+)^2 \varepsilon \cdot \varepsilon^* [\text{MSPQ0}] + (n^+)_{\mu} \varepsilon \cdot \varepsilon^* [\text{SPQ1}] \}; \\ iA_{(B)} &= -\frac{ig^3}{2} f_{abc} N_c \int \frac{d^d k}{(2\pi)^d} \frac{1}{k^2 (k - p_a)^2 (k - q)^2} [4p_a^+ \{ \varepsilon \cdot \varepsilon^* ((k - p_a)^2 - \mathbf{q}^2) \\ &\quad + 4(\varepsilon \cdot k \varepsilon^* \cdot q - \varepsilon \cdot q \varepsilon^* \cdot k) \} + k^+ \{ 7\mathbf{q}^2 \varepsilon \cdot \varepsilon^* + (18 + 16\varepsilon) \varepsilon \cdot k \varepsilon^* \cdot (k - q) + 16\varepsilon \cdot q \varepsilon^* \cdot q \}] \\ &= -\frac{ig^3}{2} f_{abc} N_c \{ (18 + 16\varepsilon) (n^+)_{\mu} \varepsilon_\nu \varepsilon_\rho^* [\text{SPQ3}] - (18 + 16\varepsilon) (n^+)_{\mu} \varepsilon_\nu \varepsilon^* \cdot q [\text{SPQ2}] \\ &\quad + [(n^+)_{\mu} (16\varepsilon \cdot q \varepsilon^* \cdot q + 7\mathbf{q}^2 \varepsilon \cdot \varepsilon^*) - 16p_a^+ (\varepsilon \cdot q \varepsilon_\mu^* - \varepsilon^* \cdot q \varepsilon_\mu)] [\text{SPQ1}] \\ &\quad - 4p_a^+ \mathbf{q}^2 \varepsilon \cdot \varepsilon^* [\text{SPQ0}] + 4p_a^+ \varepsilon \cdot \varepsilon^* [\text{SQ0}] \}; \\ iA_{(C)} &= -\frac{ig^3}{2} f_{abc} N_c \int \frac{d^d k}{(2\pi)^d} \frac{1}{k^+ k^2 (k - q)^2} [4\xi (\varepsilon \cdot k \varepsilon^* \cdot q - \varepsilon \cdot q \varepsilon^* \cdot k) \\ &\quad + \varepsilon \cdot \varepsilon^* (4k^+ p_a^+ + \xi (2(k - p_a)^2 - \mathbf{q}^2))] \\ &= -\frac{ig^3}{2} f_{abc} N_c \{ -16e^{-\rho} (\varepsilon \cdot \varepsilon^* p_{a\mu} + \varepsilon \cdot q \varepsilon_\mu^* - \varepsilon^* \cdot q \varepsilon_\mu) [\text{MSQ1}] \\ &\quad - 4e^{-\rho} \mathbf{q}^2 \varepsilon \cdot \varepsilon^* [\text{MSQ0}] + 4p_a^+ \varepsilon \cdot \varepsilon^* [\text{SQ0}] \}; \end{aligned}$$

$$\begin{aligned}
iA_{(D)} &= \frac{ig^3}{2\mathbf{q}^2} f_{abc} N_c \int \frac{d^d k}{(2\pi)^d} \frac{1}{k^2(k-q)^2} [-8p_a^+ \mathbf{q}^2 \varepsilon \cdot \varepsilon^* + (5+4\epsilon)k^+ \{\varepsilon \cdot \varepsilon^*(\mathbf{q}^2 \\
&\quad - 2(k-p_a)^2) + 4\varepsilon \cdot q \varepsilon^* \cdot k - 4\varepsilon \cdot k \varepsilon^* \cdot q\}] \\
&= \frac{ig^3}{2\mathbf{q}^2} f_{abc} N_c \{(20+16\epsilon)(n^+)_{\mu} (\varepsilon \cdot q \varepsilon_{\nu}^* - \varepsilon^* \cdot q \varepsilon_{\nu} + \varepsilon \cdot \varepsilon^* p_{a\nu}) [\text{SQ2}] \\
&\quad + (5+4\epsilon)\mathbf{q}^2 \varepsilon \cdot \varepsilon^*(n^+)_{\mu} [\text{SQ1}] - 8p_a^+ \mathbf{q}^2 \varepsilon \cdot \varepsilon^* [\text{SQ0}]\}; \\
iA_{(E)} &= \frac{2ig^3}{\mathbf{q}^2} f_{abc} N_f \int \frac{d^d k}{(2\pi)^d} \frac{1}{k^2(k-q)^2} [p_a^+ \mathbf{q}^2 \varepsilon \cdot \varepsilon^* + k^+ [\varepsilon \cdot \varepsilon^*(2(k-p_a)^2 - \mathbf{q}^2) \\
&\quad + 4(\varepsilon \cdot k \varepsilon^* \cdot q - \varepsilon \cdot q \varepsilon^* \cdot k)]] \\
&= -\frac{2ig^3}{\mathbf{q}^2} f_{abc} N_f \{4(n^+)_{\mu} (\varepsilon \cdot q \varepsilon_{\nu}^* - \varepsilon^* \cdot q \varepsilon_{\nu} + \varepsilon \cdot \varepsilon^* p_{a\nu}) [\text{SQ2}] \\
&\quad + \varepsilon \cdot \varepsilon^* \mathbf{q}^2 (n^+)_{\mu} [\text{SQ1}] - p_a^+ \mathbf{q}^2 \varepsilon \cdot \varepsilon^* [\text{SQ0}]\}; \\
iA_{(F)} &= \frac{ig^3}{2\mathbf{q}^2} f_{abc} N_c \int \frac{d^d k}{(2\pi)^d} \frac{k^+}{k^2(k-q)^2} [\varepsilon \cdot \varepsilon^*(2(k-p_a)^2 - \mathbf{q}^2) + 4(\varepsilon \cdot k \varepsilon^* \cdot q - \varepsilon \cdot q \varepsilon^* \cdot k)] \\
&= -\frac{ig^3}{2\mathbf{q}^2} f_{abc} N_c \{4(n^+)_{\mu} (\varepsilon \cdot \varepsilon^* p_{a\nu} + \varepsilon \cdot q \varepsilon_{\nu}^* - \varepsilon^* \cdot q \varepsilon_{\nu}) [\text{SQ2}] \\
&\quad + \mathbf{q}^2 \varepsilon \cdot \varepsilon^*(n^+)_{\mu} [\text{SQ1}]\}; \\
iA_{(I)} &= ig^3 f_{abc} N_f \int \frac{d^d k}{(2\pi)^d} \frac{1}{k^2(k-p_a)^2(k-q)^2} [p_a^+ (-\mathbf{q}^2 \varepsilon \cdot \varepsilon^* \\
&\quad + 2(\varepsilon \cdot k \varepsilon^* \cdot q - \varepsilon \cdot q \varepsilon^* \cdot k)) + k^+ (\varepsilon \cdot \varepsilon^*(\mathbf{q}^2 - 2(k-p_a)^2) \\
&\quad + 8\varepsilon \cdot k \varepsilon^* \cdot (k-q) + 2\varepsilon \cdot q \varepsilon^* \cdot q)] \\
&= ig^3 f_{abc} N_f \{8(n^+)_{\mu} \varepsilon_{\nu} \varepsilon_{\rho}^* [\text{SPQ3}] - 8\varepsilon^* \cdot q (n^+)_{\mu} \varepsilon_{\nu} [\text{SPQ2}] \\
&\quad + [(\mathbf{q}^2 \varepsilon \cdot \varepsilon^* + 2\varepsilon \cdot q \varepsilon^* \cdot q)(n^+)_{\mu} + 2p_a^+ \varepsilon^* \cdot q \varepsilon_{\mu} - 2p_a^+ \varepsilon \cdot q \varepsilon_{\mu}^*] [\text{SPQ1}] - \mathbf{q}^2 p_a^+ \varepsilon \cdot \varepsilon^* [\text{SPQ0}]\}; \\
iA_{(J)} &= ig^3 f_{abc} N_c \int \frac{d^d k}{(2\pi)^d} \frac{k^+}{k^2(k-p_a)^2(k-q)^2} \varepsilon \cdot k \varepsilon^* \cdot (k-q) \\
&= ig^3 f_{abc} N_c (n^+)_{\mu} \{\varepsilon_{\nu} \varepsilon_{\rho}^* [\text{SPQ3}] - \varepsilon^* \cdot q \varepsilon_{\nu} [\text{SPQ2}]\}.
\end{aligned}$$

Those integrals which are not suppressed in the $\rho \rightarrow \infty$ limit are:

$$\begin{aligned}
[\text{SQ0}] &= \frac{i}{(4\pi)^{2+\epsilon}} (\mathbf{q}^2)^{\epsilon} \frac{\Gamma(-\epsilon)\Gamma^2(1+\epsilon)}{\Gamma(2+2\epsilon)}; \quad [\text{SQ2}] = (g^{\mu\nu} \mathbf{q}^2 + q^{\mu} q^{\nu} (4+2\epsilon)) \frac{1}{4(3+2\epsilon)} [\text{SQ0}]; \\
[\text{SPQ0}] &= \frac{1+2\epsilon}{\epsilon \mathbf{q}^2} [\text{SQ0}]; \quad [\text{SPQ1}] = \left(q^{\mu} + \frac{1}{\epsilon} p_a^{\mu} \right) [\text{SQ0}]; \\
[\text{SPQ2}] &= \left\{ \frac{1}{2+2\epsilon} \left[\frac{1}{2} g^{\mu\nu} + \left(\frac{q^{\mu} p_a^{\nu} + p_a^{\mu} q^{\nu}}{\mathbf{q}^2} \right) + \frac{2 p_a^{\mu} p_a^{\nu}}{\epsilon \mathbf{q}^2} \right] + \frac{1}{\mathbf{q}^2} q^{\mu} q^{\nu} \right\} [\text{SQ0}]; \\
[\text{SPQ3}] &= \frac{1}{\epsilon(1+\epsilon)(3+2\epsilon)} \left\{ \frac{1}{\mathbf{q}^2} \left[p_a^{\mu} p_a^{\nu} p_a^{\rho} + \epsilon q^{\mu} p^{\nu} p^{\rho} + \frac{1}{2} \epsilon (1+\epsilon) q^{\mu} q^{\nu} p^{\rho} \right. \right. \\
&\quad \left. \left. - \frac{1}{6} (1-\epsilon)(2+\epsilon)^2 q^{\mu} q^{\nu} q^{\rho} \right] + \frac{\epsilon}{4} [p^{\mu} g^{\nu\rho} + (1+\epsilon) q^{\mu} g^{\nu\rho}] \right. \\
&\quad \left. + \text{cyclic permutations of } \mu, \nu \text{ and } \rho \right\} [\text{SQ0}];
\end{aligned}$$

D. Details of Some Computations

$$[\text{MSQ1}] = \frac{b^\mu}{\xi} [\text{SQ0}] + \frac{1}{2} q^\mu \left\{ \frac{-i}{(4\pi)^{2+\epsilon}} \frac{\Gamma^2\left(\frac{1}{2} + \epsilon\right) \Gamma\left(\frac{1}{2} - \epsilon\right) \Gamma\left(\frac{1}{2}\right)}{\Gamma(1 + 2\epsilon)(\mathbf{q}^2)^{\frac{1}{2} - \epsilon} \xi^{\frac{1}{2}}} \right\};$$

$$[\text{MSPQ0}] = -\frac{i}{(4\pi)^{2+\epsilon}} \frac{(\mathbf{q}^2)^{\epsilon-1} \Gamma(1 - \epsilon) \Gamma^2(\epsilon)}{p_a^+ \Gamma(2\epsilon)} \left(\ln \left[\frac{p_a^+}{|\mathbf{q}|} \right] + \frac{\rho}{2} + \frac{\psi(1) - 2\psi(\epsilon) + \psi(1 - \epsilon)}{2} \right).$$

Details on the Real Correction to Gluon-Induced Forward Jet Vertex

We refer for the notation to FIGS. III.12, III.13. We use the following choice of polarization vectors: $\varepsilon_a \cdot p_a = \varepsilon_b \cdot p = \varepsilon_c \cdot q = \varepsilon_a \cdot n^+ = \varepsilon_b \cdot n^+ = \varepsilon_c \cdot n^+ = 0$; together with the Sudakov decomposition

$$p_a = p_a^+ \frac{n^-}{2}, \quad p_b = p_b^- \frac{n^+}{2}, \quad p = (p_a^+ - q^+) \frac{n^-}{2} + p^- \frac{n^+}{2} + k_\perp - q_\perp,$$

$$k = k^- \frac{n^+}{2} + k_\perp, \quad q = q^+ \frac{n^-}{2} + (k^- - p^-) \frac{n^+}{2} + q_\perp.$$
(D.17)

The kinematic constraint $k^+ = 0$ makes it possible the parametrization $q^+ = zp_a^+$, $p_a^+ = (1 - z)p_a^+$. We will use the notation $(v_\perp)^2 = -\mathbf{v}^2$. With our choice of polarization vectors, diagrams (a), (b), (c), (d) and (i) are automatically zero. Diagram (h) turns out to vanish as well. One should also recall that the on-shell constraints imply $p_a^2 = p^2 = q^2 = 0$. Therefore

$$p^2 = 0 \rightarrow p^- = \frac{(\mathbf{k} - \mathbf{q})^2}{(1 - z)p_a^+}; \quad q^2 = 0 \rightarrow k^- = \frac{z(\mathbf{k} - \mathbf{q})^2 + (1 - z)\mathbf{q}^2}{z(1 - z)p_a^+} = \frac{(\mathbf{q} - z\mathbf{k})^2 + z(1 - z)\mathbf{k}^2}{z(1 - z)p_a^+}.$$
(D.18)

We can introduce the Mandelstam invariants $s = (p_a + k)^2 = (p + q)^2$, $t = (p_a - p)^2 = (q - k)^2$, $u = (p_a - q)^2 = (p - k)^2$. Then all possible scalar products are

$$p_a \cdot p = -\frac{t}{2}; \quad p_a \cdot q = -\frac{u}{2} = \frac{s + t + \mathbf{k}^2}{2}; \quad p_a \cdot k = \frac{s + \mathbf{k}^2}{2}; \quad p \cdot q = \frac{s}{2}; \quad k \cdot q = -\frac{t + \mathbf{k}^2}{2}; \quad k \cdot p = -\frac{u + \mathbf{k}^2}{2} = \frac{s + t}{2};$$

$$\mathbf{k} \cdot \mathbf{q} = \frac{1}{2}(zs + t + (1 + z)\mathbf{k}^2), \quad \mathbf{q}^2 = -zu = z(s + t + \mathbf{k}^2); \quad s = \frac{(\mathbf{q} - z\mathbf{k})^2}{z(1 - z)}, \quad t = -\frac{(\mathbf{k} - \mathbf{q})^2}{1 - z}.$$
(D.19)

The amplitudes for the non-vanishing diagrams can be finally written in the following form

$$iA_{(e)} = \varepsilon_{a\mu} \varepsilon_{b\nu}^* \varepsilon_{c\rho}^* 2ig^2 \frac{f_{ade} f_{bce}}{s} p_a^+ \left\{ g^{\nu\rho} [k^\mu (1 - 2z) - p^\mu + q^\mu] + g^{\mu\nu} (2p^\rho + q^\rho) - g^{\mu\rho} (2q^\nu + p^\nu) \right\};$$

$$iA_{(f)} = \varepsilon_{a\mu} \varepsilon_{b\nu}^* \varepsilon_{c\rho}^* (-ig^2) \frac{f_{abe} f_{cde}}{t} p_a^+ \left\{ -4z(g^{\nu\rho} p^\mu + g^{\mu\rho} p_a^\nu) + g^{\mu\nu} [k^\rho (2 - z) + p^\rho (2 + z) + p_a^\rho (-2 + 3z)] \right\};$$

$$iA_{(g)} = \varepsilon_{a\mu} \varepsilon_{b\nu}^* \varepsilon_{c\rho}^* (-ig^2) \frac{f_{ace} f_{bde}}{u} p_a^+ \left\{ -4(1 - z)[g^{\mu\nu} p_a^\rho + g^{\nu\rho} q^\mu] + g^{\mu\rho} [k^\nu (1 + z) + p_a^\nu (1 - 3z) + q^\nu (3 - z)] \right\};$$

$$iA_{(j)} = -\frac{2g^2 f_{acd} t^c}{s} \varepsilon_{a\mu} [k^\mu (n^+)^\sigma - p_a^+ g^{\mu\sigma}] \bar{u}(p) \gamma_\sigma v(q);$$

$$iA_{(k)} = -\frac{ig^2 t^d t^a}{u} \varepsilon_{a\mu} \bar{u}(p) \not{n}^+ (\not{p}_a - \not{q}) \gamma^\mu v(q);$$

$$iA_{(l)} = \frac{ig^2 t^a t^d}{t} \varepsilon_{a\mu} \bar{u}(p) \gamma^\mu (\not{p}_a - \not{p}) \not{n}^+ v(q).$$
(D.20)

References

- [ABSW75] H. D. I. ABARBANEL, J. B. BRONZAN, R. L. SUGAR AND A. R. WHITE, *Reggeon Field Theory: Formulation and Use*. Phys. Rep. **21**, 119 (1975).
- [AC75] T. APPELQUIST AND J. CARAZZONE, *Infrared Singularities and Massive Fields*. Phys. Rev. **D11**, 2856 (1975).
- [ACMS11] M. ANGIONI, G. CHACHAMIS, J. D. MADRIGAL AND A. SABIO VERA, *Dijet Production at Large Rapidity Separation in $\mathcal{N} = 4$ SYM*. Phys. Rev. Lett. **107**, 191601 (2011).
- [AFS62] D. AMATI, S. FUBINI AND A. STANGHELLINI, *Asymptotic Properties of Scattering and Multiple Production*. Phys. Lett. **1**, 29 (1962).
- [AGM⁺00] O. AHARONY, S. S. GUBSER, J. M. MALDACENA, H. OOGURI AND Y. OZ, *Large N Field Theories, String Theory and Gravity*. Phys. Rep. **323**, 183 (2000).
- [AGOTY01] C. ANASTASIOU, E. W. N. GLOVER, C. OLEARI AND M. E. TEJEDA-YEOMANS, *Two-Loop QCD Corrections to Massless Quark Gluon Scattering*. Nucl. Phys. **B605**, 486 (2001).
- [AGS96] B. ANDERSSON, G. GUSTAFSON AND J. SAMUELSSON, *The Linked Dipole Chain Model for DIS*. Nucl. Phys. **B467**, 443 (1996).
- [AGVM12] L. ÁLVAREZ-GAUMÉ AND M. Á. VÁZQUEZ-MOZO, *An Invitation to Quantum Field Theory*. Springer-Verlag, Berlin (2012).
- [AHBC⁺11] N. ARKANI-HAMED, J. L. BOURJAILY, F. CACHAZO, S. CARON-HUOT AND J. TRNKA, *The All-Loop Integrand for Scattering Amplitudes in Planar $\mathcal{N} = 4$ SYM*. JHEP **01**, 041 (2011).
- [AHCC10] N. ARKANI-HAMED, F. CACHAZO AND C. CHEUNG, *The Grassmannian Origin of Dual Superconformal Invariance*. JHEP **1003**, 036 (2010).
- [AHCK10] N. ARKANI-HAMED, F. CACHAZO, C. CHEUNG AND J. KAPLAN, *A Duality for the S -Matrix*. JHEP **1003**, 020 (2010).
- [AHCK10] N. ARKANI-HAMED, F. CACHAZO AND J. KAPLAN, *What Is the Simplest Quantum Field Theory?*. JHEP **09**, 016 (2010).
- [AKMS94] A. J. ASKEW, J. KWIECIŃSKI, A. D. MARTIN AND P. J. SUTTON, *Properties of the BFKL Equation and Structure Function Predictions for DESY HERA*. Phys. Rev. **D49**, 4402 (1994).
- [AKT70] E. ABERS, R. A. KELLER AND V. L. TEPLITZ, *Reggeization of the Spinor in Yang-Mills Theory*. Phys. Rev. **D2**, 1757 (1970).
- [Ald08] L. F. ALDAY, *Lectures on Scattering Amplitudes via AdS/CFT* (2008), <http://www.arxiv.org/abs/0804.0951v1>.
- [ALKC05] E. N. ANTONOV, L. N. LIPATOV, E. A. KURAEV AND I. O. CHEREDNIKOV, *Feynman Rules for Effective Regge Action*. Nucl. Phys. **B721**, 111 (2005).
- [And72] P. W. ANDERSON, *More Is Different. Broken Symmetry and the Hierarchical Structure of Science*. Science **177**, 393 (1972).
- [AP77] G. ALTARELLI AND G. PARISI, *Asymptotic Freedom in Parton Language*. Nucl. Phys. **B126**, 298 (1977).
- [AR08] L. F. ALDAY AND R. ROIBAN, *Scattering Amplitudes, Wilson Loops and the String/Gauge Theory Correspondence*. Phys. Rep. **468**, 153 (2008).
- [AS03] J. R. ANDERSEN AND A. SABIO VERA, *Solving the BFKL Equation in the Next-to-Leading Approximation*. Phys. Lett. **B567**, 116 (2003).

- [AS04a] J. R. ANDERSEN AND A. SABIO VERA, *The Gluon Green's Function in $\mathcal{N} = 4$ Supersymmetric Yang-Mills Theory*. Nucl. Phys. **B699**, 90 (2004).
- [AS04b] J. R. ANDERSEN AND A. SABIO VERA, *The Gluon Green's Function in the BFKL Approach at Next-to-Leading Logarithmic Accuracy*. Nucl. Phys. **B679**, 345 (2004).
- [B⁺12] N. BEISERT ET AL., *Review of AdS/CFT Integrability: An Overview*. Lett. Math. Phys. **99**, 3 (2012).
- [Bal96] IA. IA. BALITSKY, *Operator Expansion for High-Energy Scattering*. Nucl. Phys. **B463**, 99 (1996).
- [Bal01] IA. IA. BALITSKY, *High-Energy QCD and Wilson Lines*. In M. SHIFMAN (Ed.) *At the Frontiers of Particle Physics: Handbook of QCD II*, World Scientific, Singapore (2001).
- [Ban08] T. BANKS, *Modern Quantum Field Theory. A Concise Introduction*. Cambridge University Press, Cambridge (2008).
- [Bar80a] J. BARTELS, *High-Energy Behavior in a Non-Abelian Gauge Theory. II. First Corrections to $T_{n \rightarrow m}$ Beyond the Leading ln s Approximation*. Nucl. Phys. **B175**, 365 (1980).
- [Bar80b] J. BARTELS, *High Energy Behaviour of Nonabelian Gauge Theories*. Acta Phys. Pol. **B11**, 281 (1980).
- [Bar93] J. BARTELS, *A Note on the Infrared Cutoff Dependence of the BFKL Pomeron*. J. Phys. **G19**, 1611 (1993).
- [BC10] IA. IA. BALITSKY AND G. CHIRILLI, *High-Energy Amplitudes in $\mathcal{N} = 4$ SYM in the Next-to-Leading Order*. Phys. Lett. **B687**, 204 (2010).
- [BC11] IA. IA. BALITSKY AND G. A. CHIRILLI, *Photon Impact Factor in the Next-to-Leading Order*. Phys. Rev. **D83**, 031502 (2011).
- [BCDF02] M. BENEKE, A. P. CHAPOVSKY, M. DIEHL AND T. FELDMANN, *Soft-Collinear Effective Theory and Heavy-to-Light Currents Beyond Leading Power*. Nucl. Phys. **B643**, 431 (2002).
- [BCFW05] R. BRITTO, F. CACHAZO, B. FENG AND E. WITTEN, *Direct Proof of Tree-Level Recursion Relation in Yang-Mills Theory*. Phys. Rev. Lett. **94**, 181602 (2005).
- [BCGK02] J. BARTELS, D. COLFERAI, S. GIESEKE AND A. KYRIELEIS, *NLO Corrections to the Photon Impact Factor: Combining Real and Virtual Corrections*. Phys. Rev. **D66**, 094017 (2002).
- [BCV02] J. BARTELS, D. COLFERAI AND G. P. VACCA, *The NLO Jet Vertex for Mueller-Navelet and Forward Jets: the Quark Part*. Eur. Phys. J. **C24**, 83 (2002).
- [BCV03] J. BARTELS, D. COLFERAI AND G. P. VACCA, *The NLO Jet Vertex for Mueller-Navelet and Forward Jets: the Gluon Part*. Eur. Phys. J. **C29**, 235 (2003).
- [BDDK94] Z. BERN, L. J. DIXON, D. C. DUNBAR AND D. A. KOSOWER, *One-Loop n-Point Gauge Theory Amplitudes, Unitarity and Collinear Limits*. Nucl. Phys. **B425**, 217 (1994).
- [BdG12] S. J. BRODSKY AND L. DI GIUSTINO, *Setting the Renormalization Scale in QCD: The Principle of Maximum Conformality*. Phys. Rev. **D86**, 085026 (2012).
- [BDK04] Z. BERN, L. J. DIXON AND D. A. KOSOWER, *$\mathcal{N} = 4$ Super-Yang-Mills Theory, QCD and Collider Physics*. C. R. Phys. **5**, 955 (2004).
- [BdRL96] J. BARTELS, A. DE ROECK AND H. LOTTER, *The $\gamma^* \gamma^*$ Total Cross Section and the BFKL Pomeron at e^+e^- Colliders*. Phys. Lett. **B389**, 742 (1996).
- [BDS05] Z. BERN, L. J. DIXON AND V. A. SMIRNOV, *Iteration of Planar Amplitudes in Maximally Supersymmetric Yang-Mills Theory at Three Loops and Beyond*. Phys. Rev. **D72**, 085001 (2005).
- [BES07] N. BEISERT, B. EDEN AND M. STAUDACHER, *Transcendentality and Crossing*. J. Stat. Mech. **0701**, 021 (2007).
- [Bet31] H. BETHE, *On the Theory of Metals. I. Eigenvalues and Eigenfunctions for the Linear Atomic Chain*. Z. Phys. **71**, 205 (1931).
- [BF94] R. D. BALL AND S. FORTE, *Double Asymptotic Scaling at HERA*. Phys. Lett. **B335**, 77 (1994).

- [BFF03] J. BARTELS, V. S. FADIN AND R. FIORE, *The Bootstrap Conditions for the Gluon Reggeization*. Nucl. Phys. **B672**, 329 (2003).
- [BFK⁺99] S. J. BRODSKY, V. S. FADIN, V. T. KIM, L. N. LIPATOV AND G. B. PIVOVAROV, *The QCD Pomeron with Optimal Renormalization*. JETP Lett. **70**, 155 (1999), [Pis'ma ZhETF **70**, 161 (1999)].
- [BFK⁺02] S. J. BRODSKY, V. S. FADIN, V. T. KIM, L. N. LIPATOV AND G. B. PIVOVAROV, *High-Energy QCD Asymptotic Behavior of Photon-Photon Collisions*. JETP Lett. **76**, 249 (2002).
- [BFLV13] J. BARTELS, V. S. FADIN, L. N. LIPATOV AND G. P. VACCA, *NLO Corrections to the Kernel of the BKP-Equations*. Nucl. Phys. **B867**, 827 (2013).
- [BFPS01] C. W. BAUER, S. FLEMING, D. PIRJOL AND I. W. STEWART, *An Effective Field Theory for Collinear and Soft Gluons: Heavy to Light Decays*. Phys. Rev. **D63**, 114020 (2001).
- [BG72] C. G. BOLLINI AND J. J. GIAMBIAGI, *Lowest Order "Divergent" Graphs in ν -Dimensional Space*. Phys. Lett. **B40**, 566 (1972).
- [BG88] F. A. BERENDS AND W. T. GIELE, *Recursive Calculations for Processes with n Gluons*. Nucl. Phys. **B306**, 759 (1988).
- [BGK02] J. BARTELS, S. GIESEKE AND A. KYRIELEIS, *The Process $\gamma^*(L) + q \rightarrow (q\bar{q}g) + q$: Real Corrections to the Virtual Photon Impact Factor*. Phys. Rev. **D65**, 014006 (2002).
- [Bin06] P. BINÉTRUY, *Supersymmetry: Theory, Experiment and Cosmology*. Oxford University Press, Oxford (2006).
- [Bjo69] J. D. BJORKEN, *Asymptotic Sum Rules at Infinite Momentum*. Phys. Rev. **179**, 1547 (1969).
- [BK04] J. BARTELS AND A. KYRIELEIS, *NLO Corrections to the γ^* Impact Factor: First Numerical Results for the Real Corrections to $\gamma^*(L)$* . Phys. Rev. **D70**, 114003 (2004).
- [BKM03] V. M. BRAUN, G. P. KORCHEMSKY AND D. MÜLLER, *The Uses of Conformal Symmetry in QCD*. Prog. Part. Nucl. Phys. **51**, 311 (2003).
- [BKVZ09] L. V. BORK, D. I. KAZAKOV, G. S. VARTANOV AND A. V. ZHIHOEDOV, *Infrared Safe Observables in $\mathcal{N} = 4$ Super Yang-Mills Theory*. Phys. Lett. **B681**, 296 (2009).
- [BL78] IA. IA. BALITSKY AND L. N. LIPATOV, *The Pomeron Singularity in Quantum Chromodynamics*. Sov. J. Nucl. Phys. **28**, 822 (1978).
- [BL79] IA. IA. BALITSKY AND L. N. LIPATOV, *Calculation of Meson Meson Interaction Cross-Section in Quantum Chromodynamics*. JETP Lett. **30**, 355 (1979).
- [BL95] S. J. BRODSKY AND H. J. LU, *Commensurate Scale Relations in Quantum Chromodynamics*. Phys. Rev. **D51**, 3652 (1995).
- [BLM83] S. J. BRODSKY, G. P. LEPAGE AND P. B. MACKENZIE, *On the Elimination of Scale Ambiguities in Perturbative Quantum Chromodynamics*. Phys. Rev. **D28**, 228 (1983).
- [BLN83] L. BRINK, O. LINDGREN AND B. E. W. NILSSON, *The Ultraviolet Finiteness of the $\mathcal{N} = 4$ Yang-Mills Theory*. Phys. Lett. **B123**, 323 (1983).
- [BLS09] J. BARTELS, L. N. LIPATOV AND A. SABIO VERA, *BFKL Pomeron, Reggeized Gluons and Bern-Dixon-Smirnov Amplitudes*. Phys. Rev. **D80**, 045002 (2009).
- [BLV96] J. BARTELS, H. LOTTER AND M. VOGT, *A Numerical Estimate of the Small- k_T Region in the BFKL Pomeron*. Phys. Lett. **B373**, 215 (1996).
- [BLV00] J. BARTELS, L. N. LIPATOV AND G. P. VACCA, *A New Odderon Solution in Perturbative QCD*. Phys. Lett. **B477**, 178 (2000).
- [BLW96] J. BARTELS, L. N. LIPATOV AND M. WÜSTHOFF, *Conformal Invariance of the Transition Vertex $2 \rightarrow 4$ Gluons*. Nucl. Phys. **B464**, 298 (1996).
- [BM07] C. P. BURGESS AND G. D. MOORE, *The Standard Model: A Primer*. Cambridge University Press, Cambridge (2007).
- [BMS08] J. BARTELS, A.-M. MISCHLER AND M. SALVADORE, *Four Point Function of R -Currents in $\mathcal{N} = 4$ SYM in the Regge Limit at Weak Coupling*. Phys. Rev. **D78**, 016004 (2008).

- [BNS91] A. BASSETTO, G. NARDELLI AND R. SOLDATI, *Yang-Mills Theories in Algebraic Non-Covariant Gauges*. World Scientific, Singapore (1991).
- [Bou07] R. BOUSSO, *TASI Lectures on the Cosmological Constant* (2007), <http://arxiv.org/abs/hep-th/0708.4231v2>.
- [BP69] J. D. BJORKEN AND E. A. PASCHOS, *Inelastic Electron-Proton and γ -Proton Scattering and the Structure of the Nucleon*. Phys. Rev. **185**, 1975 (1969).
- [BP02] V. BARONE AND E. PREDAZZI, *High-Energy Particle Diffraction*. Cambridge University Press, Cambridge (2002).
- [BPST07] R. C. BROWER, J. POLCHINSKI, M. J. STRASSLER AND C. I. TAN, *The Pomeron and Gauge-String Duality*. JHEP **12**, 005 (2007).
- [Bra00] M. A. BRAUN, *Structure Function of the Nucleus in the Perturbative QCD with $N_c \rightarrow \infty$ (BFKL Pomeron Fan Diagrams)*. Eur. Phys. J. **C16**, 337 (2000).
- [BRvN98] J. BLÜMLEIN, V. RAVINDRAN AND W. L. VAN NEERVEN, *Gluon Regge Trajectory in $\mathcal{O}(\alpha_s^2)$* . Phys. Rev. **D58**, 091502 (1998).
- [BRY97] Z. BERN, J. S. ROZOWSKY AND B. YAN, *Two-Loop Four-Gluon Amplitudes in $\mathcal{N} = 4$ Super-Yang-Mills*. Phys. Lett. **B401**, 273 (1997).
- [BSS77] L. BRINK, J. SCHERK AND J. H. SCHWARZ, *Supersymmetric Yang-Mills Theories*. Nucl. Phys. **B121**, 77 (1977).
- [BW95] J. BARTELS AND M. WÜSTHOFF, *The Triple Regge Limit of Diffractive Dissociation in Deep Inelastic Scattering*. Z. Phys. **C66**, 157 (1995).
- [Cal70] C. G. CALLAN, *Broken Scale Invariance in Scalar Field Theory*. Phys. Rev. **D2**, 1541 (1970).
- [Cao91] T. Y. CAO, *The Reggeization Program 1962-1982: Attempts at Reconciling Quantum Field Theory with S-Matrix Theory*. Arch. Hist. Exact Sci. **41**, 239 (1991).
- [Cao97] T. Y. CAO, *Conceptual Developments of 20th Century Field Theories*. Cambridge University Press, Cambridge (1997).
- [Cao10] T. Y. CAO, *From Current Algebra to Quantum Chromodynamics. A Case for Structural Realism*. Cambridge University Press, Cambridge (2010).
- [Car18] F. CARLSON, *Sur une Classe de Séries de Taylor*. Ph.D. thesis, Uppsala University (1918).
- [Car01] T. CARLI, *Physics at Small x* (2001), www.lp01.infn.it/talks/carli.pdf.
- [Cas74] W. E. CASWELL, *Asymptotic Behavior of Non-Abelian Gauge Theories to Two-Loop Order*. Phys. Rev. Lett. **33**, 244 (1974).
- [CC98] G. CAMICI AND M. CIAFALONI, *Energy Scale(s) and Next-to-Leading BFKL Equation*. Phys. Lett. **B430**, 349 (1998).
- [CC99] M. CIAFALONI AND D. COLFERAI, *The BFKL Equation at Next-to-Leading Level and Beyond*. Phys. Lett. **B452**, 372 (1999).
- [CCCd12] A. CAPPELLI, E. CASTELLANI, F. COLOMO AND P. DI VECCHIA (Eds.) *The Birth of String Theory*. Cambridge University Press, Cambridge (2012).
- [CCH90] S. CATANI, M. CIAFALONI AND F. HAUTMANN, *Gluon Contributions to Small x Heavy Flavour Production*. Phys. Lett. **B242**, 97 (1990).
- [CCH91] S. CATANI, M. CIAFALONI AND F. HAUTMANN, *High-Energy Factorization and Small x Heavy Flavor Production*. Nucl. Phys. **B366**, 135 (1991).
- [CCM⁺13] F. CAPORALE, G. CHACHAMIS, J. D. MADRIGAL, B. MURDACA AND A. SABIO VERA, *A Study of the Diffusion Pattern in $\mathcal{N} = 4$ SYM at High Energies* (2013), [Accepted for publication in Phys. Lett. B], [arXiv:1305.1474\[hep-th\]](https://arxiv.org/abs/1305.1474).
- [CCP07] L. CORNALBA, M. S. COSTA AND J. PENEDONES, *Eikonal Approximation in AdS/CFT: Resumming the Gravitational Loop Expansion*. JHEP **0709**, 037 (2007).
- [CCP10] L. CORNALBA, M. S. COSTA AND J. PENEDONES, *Deep Inelastic Scattering in Conformal QCD*. JHEP **1003**, 133 (2010).

- [CCS99] M. CIAFALONI, D. COLFERAI AND G. P. SALAM, *Renormalization Group Improved Small- x Equation*. Phys. Rev. **D60**, 114036 (1999).
- [CCSS03] M. CIAFALONI, D. COLFERAI, G. P. SALAM AND A. M. STAŚTO, *Renormalisation Group Improved Small- x Green's Function*. Phys. Rev. **D68**, 114003 (2003).
- [CDLO81] H. CHENG, J. A. DICKINSON, C. Y. LO AND K. OLAUSSEN, *Diagrammatic Derivation of the Eikonal Formula for High-Energy Scattering in Yang-Mills Theory*. Phys. Rev. **D23**, 534 (1981).
- [CdR12] S. CATANI, D. DE FLORIAN AND G. RODRIGO, *Space-Like (versus Time-Like) Collinear Limits in QCD: Is Factorization Violated?*. JHEP **1207**, 026 (2012).
- [CDSS11] G. CHACHAMIS, M. DEÁK, A. SABIO VERA AND P. STEPHENS, *A Comparative Study of Small x Monte Carlos With and Without QCD Coherence Effects*. Nucl. Phys. **B849**, 28 (2011).
- [CFR10] F. CAOLA, S. FORTE AND J. ROJO, *Deviations from NLO QCD Evolution in Inclusive HERA Data*. Phys. Lett. **B686**, 127 (2010).
- [CG69] C. G. CALLAN AND D. J. GROSS, *High-Energy Electroproduction and the Constitution of the Electric Current*. Phys. Rev. Lett. **22**, 156 (1969).
- [CG73] S. COLEMAN AND D. J. GROSS, *Price of Asymptotic Freedom*. Phys. Rev. Lett. **31**, 851 (1973).
- [CG79a] W. CELMASTER AND R. J. GONSALVES, *QCD Perturbation Expansions in a Coupling Constant Renormalized by Momentum Space Subtraction*. Phys. Rev. Lett. **42**, 1435 (1979).
- [CG79b] W. CELMASTER AND R. J. GONSALVES, *Renormalization-Prescription Dependence of the Quantum-Chromodynamic Coupling Constant*. Phys. Rev. **D20**, 1420 (1979).
- [CGP12] M. S. COSTA, V. GONCALVES AND J. PENEDONES, *Conformal Regge Theory*. JHEP **2012**, 091 (2012).
- [Cha06] G. CHACHAMIS, *Higher Order QCD Corrections in Small x Physics*. Ph.D. thesis, Hamburg University (2006).
- [Che61] G. F. CHEW, *S-Matrix Theory of Strong Interactions*. Benjamin, New York (1961).
- [CHKM⁺06] S. CARON-HUOT, P. KOVTUN, G. D. MOORE, A. STARINETS AND L. G. YAFFE, *Photon and Dilepton Production in Supersymmetric Yang-Mills Plasma*. JHEP **0612**, 015 (2006).
- [CHMS12a] G. CHACHAMIS, M. HENTSCHINSKI, J. D. MADRIGAL AND A. SABIO VERA, *Forward Jet Production and Quantum Corrections to the Gluon Regge Trajectory from Lipatov's High Energy Effective Action*. [To appear in Phys. Part. Nucl.] (2012), [arXiv:1211.2050](https://arxiv.org/abs/1211.2050)[hep-ph].
- [CHMS12b] G. CHACHAMIS, M. HENTSCHINSKI, J. D. MADRIGAL AND A. SABIO VERA, *NLO Corrections to the Gluon Induced Forward Jet Vertex from the High Energy Effective Action*. Phys. Rev. **D87**, 076009 (2012).
- [CHMS12c] G. CHACHAMIS, M. HENTSCHINSKI, J. D. MADRIGAL AND A. SABIO VERA, *Quark Contribution to the Gluon Regge Trajectory at NLO from the High Energy Effective Action*. Nucl. Phys. **B861**, 133 (2012).
- [CHMS13] G. CHACHAMIS, M. HENTSCHINSKI, J. D. MADRIGAL AND A. SABIO VERA, *NLO Gluon Regge Trajectory in the Lipatov Action Approach: The Gluon Piece* (2013), [arXiv:1305.xxxx](https://arxiv.org/abs/1305.xxxx)[hep-ph].
- [Chý04] J. CHÝLA, *Quarks, Partons and Quantum Chromodynamics* (2004), <http://www-hep.fzu.cz/~chyla/lectures/text.pdf>.
- [CIM⁺12] F. CAPORALE, D. Y. IVANOV, B. MURDACA, A. PAPA AND A. PERRI, *The Next-to-Leading Order Jet Vertex for Mueller-Navelet and Forward Jets Revisited*. JHEP **1202**, 101 (2012).
- [CL77] H. CHENG AND C. Y. LO, *High-Energy Amplitudes of Yang-Mills Theory in Arbitrary Perturbative Orders*. Phys. Rev. **D15**, 2959 (1977).
- [CL82] T.-P. CHENG AND L.-F. LI, *Gauge Theory of Elementary Particle Physics*. Clarendon Press, Oxford (1982).

- [CL86] W. E. CASWELL AND G. P. LEPAGE, *Effective Lagrangians for Bound State Problems in QED, QCD, and Other Field Theories*. Phys. Lett. **B167**, 437 (1986).
- [CM60] G. F. CHEW AND S. MANDELSTAM, *Theory of Low-Energy Pion-Pion Interaction*. Phys. Rev. **119**, 467 (1960).
- [CMSS13] F. CAPORALE, B. MURDACA, A. SABIO VERA AND C. SALAS, *Scale Choice and Collinear Contributions to Mueller-Navelet Jets at LHC Energies* (2013), [arXiv:1305.4620 \[hep-ph\]](https://arxiv.org/abs/1305.4620).
- [Col77] P. D. B. COLLINS, *An Introduction to Regge Theory and High-Energy Physics*. Cambridge University Press, Cambridge (1977).
- [Col11] J. C. COLLINS, *Foundations of Perturbative QCD*. Cambridge University Press, Cambridge (2011).
- [CS] G. CHACHAMIS AND A. SABIO VERA, *BFKL MC C++ Code*.
- [CS81] J. C. COLLINS AND D. E. SOPER, *Back-to-Back Jets in QCD*. Nucl. Phys. **B193**, 381 (1981).
- [CS82] J. C. COLLINS AND D. E. SOPER, *Parton Distribution and Decay Functions*. Nucl. Phys. **B194**, 445 (1982).
- [CS12a] G. CHACHAMIS AND A. SABIO VERA, *The Colour Octet Representation of the Non-Forward BFKL Green Function*. Phys. Lett. **B709**, 301 (2012).
- [CS12b] G. CHACHAMIS AND A. SABIO VERA, *The NLO $\mathcal{N} = 4$ SUSY BFKL Green Function in the Adjoint Representation*. Phys. Lett. **B717**, 458 (2012).
- [CSDL91] A. M. COOPER-SARKAR, R. C. E. DEVENISH AND M. LANCASTER, *Measurement of $F_L(x, Q^2)$ at Low- x and Extraction of the Gluon Distribution*. In W. BUCHMÜLLER AND G. INGELMAN (Eds.) *Physics at HERA* (1991).
- [CSLM⁺11] J. CASALDERREY-SOLANA, H. LIU, D. MATEOS, K. RAJAGOPAL AND U. A. WIEDEMANN, *Gauge/String Duality, Hot QCD and Heavy Ion Collisions* (2011), <http://arxiv.org/abs/hep-th/1101.0618v1>.
- [CSS89] J. C. COLLINS, D. E. SOPER AND G. STERMAN, *Factorization of Hard Processes in QCD*. In A. H. MUELLER (Ed.) *Perturbative Quantum Chromodynamics*, World Scientific, Singapore (1989).
- [CSSW10] D. COLFERAI, F. SCHWENNSSEN, L. SZYMANOWSKI AND S. WALLON, *Mueller Navelet Jets at LHC — Complete Next-to-Leading BFKL Calculation*. JHEP **12**, 026 (2010).
- [CSW04] F. CACHAZO, P. SVRČEK AND E. WITTEN, *MHV Vertices and Tree Amplitudes in Gauge Theory*. JHEP **0409**, 006 (2004).
- [CT81] K. G. CHETYRKIN AND F. V. TKACHOV, *Integration by Parts: The Algorithm to Calculate β -Functions in 4 Loops*. Nucl. Phys. **B192**, 159 (1981).
- [Cus90] J. T. CUSHING, *Theory Construction and Selection in Modern Physics: The S-Matrix*. Cambridge University Press, Cambridge (1990).
- [Cut60] R. E. CUTKOSKY, *Singularities and Discontinuities of Feynman Amplitudes*. J. Math. Phys. (N.Y.) **1**, 429 (1960).
- [Cvi76] P. CVITANOVIĆ, *Group Theory for Feynman Diagrams in Non-Abelian Gauge Theories*. Phys. Rev. **D14**, 1536 (1976).
- [Cvi08] P. CVITANOVIĆ, *Group Theory. Birdtracks, Lie's, and Exceptional Groups*. Princeton University Press, Princeton (2008).
- [CW69] H. CHENG AND T. T. WU, *High-Energy Collision Processes in Quantum Electrodynamics. I*. Phys. Rev. **182**, 1852 (1969).
- [CW70a] H. CHENG AND T. T. WU, *Limit of Cross Sections at Infinite Energy*. Phys. Rev. Lett. **24**, 1456 (1970).
- [CW70b] H. CHENG AND T. T. WU, *Logarithmic Factors in the High-Energy Behavior of Quantum Electrodynamics*. Phys. Rev. **D1**, 2775 (1970).
- [Cza] M. CZAKON, *MBasymptotics.m*, <http://projects.hepforge.org/mbtools/>.

- [Cza06] M. CZAKON, *Automatized Analytic Continuation of Mellin-Barnes Integrals*. Comput. Phys. Commun. **175**, 559 (2006).
- [D0 96] D0 COLLABORATION [S. ABACHI ET AL.], *The Azimuthal Decorrelation of Jets Widely Separated in Rapidity*. Phys. Rev. Lett. **77**, 595 (1996).
- [D0 00] D0 COLLABORATION [B. ABBOTT ET AL.], *Probing BFKL Dynamics in the Dijet Cross Section at Large Rapidity Intervals in $p\bar{p}$ Collisions at $\sqrt{s} = 1800$ GeV and 630 GeV*. Phys. Rev. Lett. **84**, 5722 (2000).
- [DCS09] R. DEVENISH AND A. M. COOPER-SARKAR, *Deep Inelastic Scattering*. Oxford University Press, Oxford (2009).
- [dD95] V. DEL DUCA, *An Introduction to the Perturbative QCD Pomeron and to Jet Physics at Large Rapidities* (1995), <http://arxiv.org/abs/hep-ph/9503226v1>.
- [dD96a] V. DEL DUCA, *Quark-Antiquark Contribution to the Multigluon Amplitudes in the Helicity Formalism*. Phys. Rev. **D54**, 4474 (1996).
- [dD96b] V. DEL DUCA, *Real Next-to-Leading Corrections to the Multi-Gluon Amplitudes in the Helicity Formalism*. Phys. Rev. **D54**, 989 (1996).
- [dDG01] V. DEL DUCA AND E. W. N. GLOVER, *The High Energy Limit of QCD at Two Loops*. JHEP **0110**, 035 (2001).
- [DDLN02] A. DONNACHIE, H. G. DOSCH, P. V. LANDSHOFF AND O. NACHTMANN, *Pomeron Physics and QCD*. Cambridge University Press, Cambridge (2002).
- [dDS94a] V. DEL DUCA AND C. R. SCHMIDT, *Dijet Production at Large Rapidity Intervals*. Phys. Rev. **D49**, 4510 (1994).
- [dDS94b] V. DEL DUCA AND C. R. SCHMIDT, *Mini-Jet Corrections to Higgs Production*. Phys. Rev. **D49**, 4510 (1994).
- [dDS98] V. DEL DUCA AND C. R. SCHMIDT, *Virtual Next-to-Leading Corrections to the Impact Factors in the High-Energy Limit*. Phys. Rev. **D57**, 4069 (1998).
- [dDS99] V. DEL DUCA AND C. R. SCHMIDT, *Virtual Next-to-Leading Corrections to the Lipatov Vertex*. Phys. Rev. **D59**, 074004 (1999).
- [DDT80] YU. L. DOKSHITZER, D. I. DIAKONOV AND S. I. TROYAN, *Hard Processes in Quantum Chromodynamics*. Phys. Rep. **58**, 269 (1980).
- [Dev02] V. DEVANATHAN, *Angular Momentum Techniques in Quantum Mechanics*. Kluwer Academic Publishers, New York (2002).
- [DeW64] B. S. DEWITT, *Theory of Radiative Corrections for Non-Abelian Gauge Fields*. Phys. Rev. Lett. **12**, 742 (1964).
- [DeW67] B. S. DEWITT, *Quantum Theory of Gravity II. The Manifestly Covariant Theory*. Phys. Rev. **162**, 1195 (1967).
- [DH09] J. M. DRUMMOND AND J. M. HENN, *All Tree-level Amplitudes in $\mathcal{N} = 4$ SYM*. JHEP **0904**, 018 (2009).
- [DHJK09] M. DÉAK, F. HAUTMANN, H. JUNG AND K. KUTAK, *Forward Jet Production at the Large Hadron Collider*. JHEP **0909**, 121 (2009).
- [DHKS08] J. M. DRUMMOND, J. M. HENN, G. P. KORCHEMSKY AND E. SOKATCHEV, *Generalized Unitarity for $\mathcal{N} = 4$ Super-Amplitudes* (2008), <http://www.arxiv.org/abs/0808.0491v1>.
- [DHP09] J. M. DRUMMOND, J. M. HENN AND J. PLEFKA, *Yangian Symmetry of Scattering Amplitudes in $\mathcal{N} = 4$ Super Yang-Mills Theory*. JHEP **0905**, 046 (2009).
- [Dix96] L. J. DIXON, *Calculating Scattering Amplitudes Efficiently* (1996), <http://www.arxiv.org/abs/hep-ph/9601359v2>.
- [DKMT91] YU. L. DOKSHITZER, V. A. KHOZE, A. H. MUELLER AND S. I. TROYAN, *Basics of Perturbative QCD*. Editions Frontières, Gif-sur-Yvette (1991).
- [DKS08] G. DISSERTORI, I. G. KNOWLES AND M. SCHMELLING, *Quantum Chromodynamics. High Energy Experiments and Theory*. Clarendon Press, Oxford (2008).

- [DL92] A. DONNACHIE AND P. V. LANDSHOFF, *Total Cross Sections*. Phys. Lett. **B296**, 227 (1992).
- [DM06] YU. L. DOKSHITZER AND G. MARCHESINI, *Soft Gluons at Large Angles in Hadron Collisions*. JHEP **01**, 007 (2006).
- [Dok77] YU. L. DOKSHITZER, *Calculation of the Structure Functions for Deep Inelastic Scattering and e^+e^- Annihilation by Perturbation Theory in Quantum Chromodynamics*. Sov. Phys. JETP **46**, 641 (1977).
- [Dok97] YU. L. DOKSHITZER, *Perturbative QCD (and Beyond)*. In F. LENZ, H. GRIESSHAMMER AND D. STOLL (Eds.) *Lectures on QCD. Applications*, Springer, Berlin (1997).
- [Don95] J. F. DONOGHUE, *General Relativity as an Effective Field Theory: The Leading Quantum Corrections*. Phys. Rev. **D50**, 3874 (1995).
- [Don09] J. F. DONOGHUE, *When Effective Field Theories Fail*. PoS **EFT09**, 001 (2009).
- [dR12] A. DE ROECK, *Forward Physics at the LHC*. In T. BINOTH, C. BUTTAR, P. J. CLARK AND E. W. N. GLOVER (Eds.) *LHC Physics*, CRC Press, Boca Raton (2012).
- [dRGP⁺74] A. DE RÚJULA, S. L. GLASHOW, H. D. POLITZER, S. B. TREIMAN, F. WILCZEK AND A. ZEE, *Possible Non-Regge Behavior of Electroproduction Structure Functions*. Phys. Rev. **D10**, 1649 (1974).
- [Dun12] A. DUNCAN, *The Conceptual Framework of Quantum Field Theory*. Oxford University Press, Oxford (2012).
- [DW10] J. F. DONOGHUE AND D. WYLER, *On Regge Kinematics in SCET*. Phys. Rev. **D81**, 114023 (2010).
- [ELOP66] R. J. EDEN, P. V. LANDSHOFF, D. I. OLIVE AND J. C. POLKINGHORNE, *The Analytic S-Matrix*. Cambridge University Press, Cambridge (1966).
- [ES06] B. EDEN AND M. STAUDACHER, *Integrability and Transcendentality*. J. Stat. Mech. **0611**, 014 (2006).
- [ESW03] R. K. ELLIS, W. J. STIRLING AND B. R. WEBBER, *QCD and Collider Physics*. Cambridge University Press, Cambridge (2003).
- [Ewe03] C. EWERZ, *The Odderon in Quantum Chromodynamics* (2003), [arXiv:0306137\[hep-ph\]](https://arxiv.org/abs/0306137).
- [Fey70] R. P. FEYNMAN, *High Energy Collisions*. Gordon and Breach, New York (1970).
- [Fey85] R. P. FEYNMAN, *The Character of Physical Law*. The MIT Press, Cambridge (Mass.) (1985).
- [FF92] V. S. FADIN AND R. FIORE, *Quark Contribution to the Gluon-Gluon-Reggeon Vertex in QCD*. Phys. Lett. **B294**, 286 (1992).
- [FFFK98] V. S. FADIN, R. FIORE, A. FLACHI AND M. I. KOTSKY, *Quark-Antiquark Contribution to the BFKL Kernel*. Phys. Lett. **B422**, 287 (1998).
- [FFK95] V. S. FADIN, R. FIORE AND M. I. KOTSKY, *Gluon Reggeization in QCD in the Next to Leading Order*. Phys. Lett. **B359**, 181 (1995).
- [FFK96a] V. S. FADIN, R. FIORE AND M. I. KOTSKY, *Gluon Regge Trajectory in the Two-Loop Approximation*. Phys. Lett. **B387**, 539 (1996).
- [FFK96b] V. S. FADIN, R. FIORE AND M. I. KOTSKY, *Gribov's Theorem on Soft Emission and the Reggeon-Reggeon-Gluon Vertex at Small Transverse Momentum*. Phys. Lett. **B389**, 737 (1996).
- [FFKP00] V. S. FADIN, R. FIORE, M. I. KOTSKY AND A. PAPA, *The Quark Impact Factors*. Phys. Rev. **D61**, 094005 (2000).
- [FFKR06] V. S. FADIN, R. FIORE, M. G. KOZLOV AND A. V. REZNICHENKO, *Proof of the Multi-Regge Form of QCD Amplitudes with Gluon Exchanges in the NLA*. Phys. Lett. **B639**, 74 (2006).
- [FFQ94] V. S. FADIN, R. FIORE AND A. QUARTAROLO, *Radiative Corrections to Quark-Quark-Reggeon Vertex in QCD*. Phys. Rev. **D50**, 5893 (1994).
- [FFQ96] V. S. FADIN, R. FIORE AND A. QUARTAROLO, *Reggeization of the Quark-Quark Scattering Amplitude in QCD*. Phys. Rev. **D53**, 2729 (1996).

- [FGL70] G. V. FROLOV, V. N. GRIBOV AND L. N. LIPATOV, *On Regge Poles in Quantum Electrodynamics*. Phys. Lett. **B31**, 34 (1970).
- [FGL71] G. V. FROLOV, V. N. GRIBOV AND L. N. LIPATOV, *The Leading Singularity in the j Plane in Quantum Electrodynamics*. Sov. J. Nucl. Phys. **12**, 543 (1971).
- [FGML73] H. FRITZSCH, M. GELL-MANN AND H. LEUTWYLER, *Advantages of the Color Octet Picture*. Phys. Lett. **B47**, 365 (1973).
- [FILM02] E. FERREIRO, E. IANCU, A. LEONIDOV AND L. D. MCLERRAN, *Nonlinear Gluon Evolution in the Color Glass Condensate II*. Nucl. Phys. **A703**, 489 (2002).
- [FK95] L. D. FADDEEV AND G. P. KORCHEMSKY, *High-Energy QCD as a Completely Integrable Model*. Phys. Lett. **B342**, 311 (1995).
- [FKL75] V. S. FADIN, E. A. KURAEV AND L. N. LIPATOV, *On the Pomeron Singularity in Asymptotic Free Theories*. Phys. Lett. **B60**, 50 (1975).
- [FKL76] V. S. FADIN, E. A. KURAEV AND L. N. LIPATOV, *Multi-Reggeon Processes in the Yang-Mills Theory*. Sov. Phys. JETP **44**, 443N (1976).
- [FKL77] V. S. FADIN, E. A. KURAEV AND L. N. LIPATOV, *The Pomeron Singularities in Nonabelian Gauge Theories*. Sov. Phys. JETP **45**, 199 (1977).
- [FKL97] V. S. FADIN, M. I. KOTSKY AND L. N. LIPATOV, *One-Loop Correction to the BFKL Kernel from Two Gluon Production*. Phys. Lett. **B415**, 97 (1997).
- [FKLP02] V. S. FADIN, V. T. KIM, L. N. LIPATOV AND G. B. PIVOVAROV, *The BFKL Pomeron within Physical Renormalization Schemes and Scales* (2002), <http://arXiv.org/abs/hep-ph/0207296v3>.
- [FL89] V. S. FADIN AND L. N. LIPATOV, *Gluon Production in a Quasi-Multi-Regge Kinematics*. Sov. J. Nucl. Phys. **50**, 712 (1989).
- [FL93] V. S. FADIN AND L. N. LIPATOV, *Radiative Corrections to QCD Scattering Amplitudes in a Multi-Regge Kinematics*. Nucl. Phys. **B406**, 259 (1993).
- [FL96] V. S. FADIN AND L. N. LIPATOV, *Next-to-Leading Corrections to the BFKL Equation from Gluon and Quark Production*. Nucl. Phys. **B477**, 767 (1996).
- [FL98] V. S. FADIN AND L. N. LIPATOV, *BFKL Pomeron in the Next-to-Leading Approximation*. Phys. Lett. **B429**, 127 (1998).
- [FO01] J. M. FIGUEROA-O'FARRILL, *BUSSTEEP Lectures on Supersymmetry* (2001), <http://arXiv.org/abs/hep-th/9905111>.
- [Fos01] B. FOSTER, *Low- x Physics*. Phil. Trans. R. Soc. **A359**, 325 (2001).
- [FP63] L. F. FOLDY AND R. F. PEIERLS, *Isotopic Spin of Exchanged Systems*. Phys. Rev. **130**, 1585 (1963).
- [FP67] L. D. FADDEEV AND V. N. POPOV, *Feynman Diagrams for the Yang-Mills Field*. Phys. Lett. **B25**, 29 (1967).
- [FR97] J. R. FORSHAW AND D. A. ROSS, *Quantum Chromodynamics and the Pomeron*. Cambridge University Press, Cambridge (1997).
- [Fra63] S. C. FRAUTSCHI, *Regge Poles and S-Matrix Theory*. W.A. Benjamin, New York (1963).
- [Fri91] J. I. FRIEDMAN, *Deep Inelastic Scattering: Comparisons with the Quark Model*. Rev. Mod. Phys. **63**, 573 (1991), [See also the following contributions by H. W. KENDALL and R. E. TAYLOR].
- [Fro61] M. FROISSART, *Asymptotic Behavior and Subtractions in the Mandelstam Representation*. Phys. Rev. **123**, 1053 (1961).
- [FRS99] J. R. FORSHAW, D. A. ROSS AND A. SABIO VERA, *Rapidity Veto Effects in the NLO BFKL Equation*. Phys. Lett. **B455**, 273 (1999).
- [FRS01] J. R. FORSHAW, D. A. ROSS AND A. SABIO VERA, *Solving the BFKL Equation with Running Coupling*. Phys. Lett. **B498**, 149 (2001).

- [FS76] L. L. FRANKFURT AND V. E. SHERMAN, *Reggeization of the Vector Particles and the Vacuum Singularity in Renormalizable Yang-Mills Type Theories*. Sov. J. Nucl. Phys. **23**, 581 (1976).
- [FS10] Y. FRISHMAN AND J. SONNENSCHNEIN, *Non-Perturbative Field Theory: From Two-Dimensional Conformal Field Theory to QCD in Four Dimensions*. Cambridge University Press, Cambridge (2010).
- [FSW05] L. L. FRANKFURT, M. STRIKMAN AND C. WEISS, *Small- x Physics: From HERA to LHC and Beyond*. Annu. Rev. Nucl. Part. Sci. **55**, 403 (2005).
- [GBKMS94] K. GOLEC-BIERNAT, J. KWIECIŃSKI, A. D. MARTIN AND P. J. SUTTON, *Transverse Energy Flow at HERA*. Phys. Lett. **B337**, 367 (1994).
- [GBW99] K. J. GOLEC-BIERNAT AND M. WÜSTHOFF, *Saturation in Diffractive Deep Inelastic Scattering*. Phys. Rev. **D60**, 114023 (1999).
- [Gel11] F. GELIS, *Color Glass Condensate and Glasma*. Nucl. Phys. **A854**, 10 (2011).
- [Geo90] H. GEORGI, *An Effective Field Theory for Heavy Quarks at Low Energies*. Phys. Lett. **B240**, 447 (1990).
- [Geo93] H. GEORGI, *Effective Field Theory*. Ann. Rev. Nucl. Part. Sci. **43**, 209 (1993).
- [GIJMV10] F. GELIS, E. IANCU, J. JALILIAN-MARIAN AND R. VENUGOPALAN, *The Color Glass Condensate*. Ann. Rev. Nucl. Part. Sci. **60**, 463 (2010).
- [GKP98] S. S. GUBSER, I. R. KLEBANOV AND A. M. POLYAKOV, *Gauge Theory Correlators from Non-Critical String Theory*. Phys. Lett. **B428**, 105 (1998).
- [GL72] V. N. GRIBOV AND L. N. LIPATOV, *Deep Inelastic ep Scattering in Perturbation Theory*. Sov. J. Nucl. Phys. **15**, 430 (1972).
- [GLR83] L. V. GRIBOV, E. M. LEVIN AND M. G. RYSKIN, *Semihard Processes in QCD*. Phys. Rep. **100**, 1 (1983).
- [GLV07] F. GELIS, T. LAPPI AND R. VENUGOPALAN, *High Energy Scattering in Quantum Chromodynamics*. Int. J. Mod. Phys. **E16**, 2595 (2007).
- [GM64] M. GELL-MANN, *A Schematic Model of Baryons and Mesons*. Phys. Lett. **8**, 214 (1964).
- [GMG62] M. GELL-MANN AND M. L. GOLDBERGER, *Elementary Particles of Conventional Field Theory as Regge Poles*. Phys. Rev. Lett. **9**, 275 (1962).
- [GMGL⁺64a] M. GELL-MANN, M. L. GOLDBERGER, F. E. LOW, E. MARX AND F. ZACHARIASEN, *Elementary Particles of Conventional Field Theory as Regge Poles. II*. Phys. Rev. **133B**, 145 (1964).
- [GMGL⁺64b] M. GELL-MANN, M. L. GOLDBERGER, F. E. LOW, E. MARX AND F. ZACHARIASEN, *Elementary Particles of Conventional Field Theory as Regge Poles. III*. Phys. Rev. **133B**, 161 (1964).
- [GML54] M. GELL-MANN AND F. E. LOW, *Quantum Electrodynamics at Small Distances*. Phys. Rev. **95**, 1300 (1954).
- [Gol61] J. GOLDSTONE, *Field Theories with “Superconductor” Solutions*. Nuovo Cimento **19**, 154 (1961).
- [Got71] T. GOTO, *Relativistic Quantum Mechanics of One-Dimensional Mechanical Continuum and Subsidiary Condition of Dual Resonance Model*. Prog. Theor. Phys. **46**, 1560 (1971).
- [Gre64] O. W. GREENBERG, *Spin and Unitary Spin Independence in a Paraquark Model of Baryons and Mesons*. Phys. Rev. Lett. **13**, 598 (1964).
- [Gre11] J. GREENSITE, *An Introduction to the Confinement Problem*. Springer, Heidelberg (2011).
- [Gri61] V. N. GRIBOV, *Partial Waves with Complex Orbital Angular Momenta and the Asymptotic Behavior of the Scattering Amplitude*. Zh. Eksp. Teor. Fiz. **41**, 667 (1961), [Sov. Phys. JETP **14**, 478 (1962)].
- [Gri68] V. N. GRIBOV, *A Reggeon Diagram Technique*. Sov. Phys. JETP **26**, 414 (1968).

- [Gri00] V. N. GRIBOV, *Space-Time Description of the Hadron Interaction at High Energies* (2000), <http://arxiv.org/abs/hep-ph/0006158v1>.
- [Gri03] V. N. GRIBOV, *The Theory of Complex Angular Momenta*. Cambridge University Press, Cambridge (2003).
- [Gro98] D. J. GROSS, *Twenty Five Years of Asymptotic Freedom* (1998), <http://arXiv.org/abs/hep-th/9809060v1>.
- [Gro12] J. GROEGER, *Supersymmetric Wilson Loops in $\mathcal{N} = 4$ Super Yang-Mills-Theory*. Ph.D. thesis, Humboldt-Universität zu Berlin (2012).
- [GRS80] M. GRISARU, M. ROČEK AND W. SIEGEL, *Zero Value of the Three-Loop β -Function in $\mathcal{N} = 4$ Supersymmetric Yang-Mills Theory*. Phys. Rev. Lett. **45**, 1063 (1980).
- [Gru80] G. GRUNBERG, *Renormalization Group Improved QCD*. Phys. Lett. **B95**, 70 (1980), [Erratum-ibid. **B110**, 501 (1982)].
- [Gru84] G. GRUNBERG, *Renormalization Scheme-Invariant QCD and QED: The Method of Effective Charges*. Phys. Rev. **D29**, 2315 (1984).
- [GRV95] M. GLÜCK, E. REYA AND A. VOGT, *Dynamical Parton Distributions of the Proton and Small- x Physics*. Z. Phys. **C67**, 433 (1995).
- [GS79] M. T. GRISARU AND H. J. SCHNITZER, *Reggeization of Gauge Vector Mesons and Unified Theories*. Phys. Rev. **D20**, 784 (1979).
- [GSO77] F. GLIOZZI, J. SCHERK AND D. I. OLIVE, *Supersymmetry, Supergravity and the Dual Spinor Model*. Nucl. Phys. **B122**, 253 (1977).
- [GSS02] W. GREINER, S. SCHRAMM AND E. STEIN, *Quantum Chromodynamics*. Springer-Verlag, Berlin (2002).
- [GST73] M. T. GRISARU, H. J. SCHNITZER AND H. S. TSAO, *Reggeization of Elementary Particles in Renormalizable Gauge Theories: Vectors and Spinors*. Phys. Rev. **D8**, 4498 (1973).
- [GSVV10] A. B. GONCHAROV, M. SPRADLIN, C. VERGU AND A. VOLOVICH, *Classical Polylogarithms for Amplitudes and Wilson Loops*. Phys. Rev. Lett. **105**, 151605 (2010).
- [GSW87] M. B. GREEN, J. H. SCHWARZ AND E. WITTEN, *Superstring Theory (Vol. I, Introduction)*. Cambridge University Press, Cambridge (1987).
- [Gun10] C. J. E. GUNNESSON, *Symmetries of $\mathcal{N} = 4$ SYM and the Regge Limit of Gauge Theories*. Ph.D. thesis, Universidad Autónoma de Madrid (2010).
- [GW73] D. J. GROSS AND F. WILCZEK, *Ultraviolet Behavior of Non-Abelian Gauge Theories*. Phys. Rev. Lett. **30**, 1343 (1973).
- [H1 93] H1 COLLABORATION [I. ABT ET AL.], *Measurement of the Proton Structure Function $F_2(x, Q^2)$ in the Low x Region at HERA*. Nucl. Phys. **B407**, 515 (1993).
- [H1 95] H1 COLLABORATION [S. AID ET AL.], *Transverse Energy and Forward Jet Production in the Low Regime at HERA*. Phys. Lett. **B356**, 118 (1995).
- [H1 06] H1 COLLABORATION [A. AKTAS ET AL.], *Forward Jet Production in Deep Inelastic Scattering at HERA*. Eur. Phys. J. **C46**, 27 (2006).
- [H1 08] H1 COLLABORATION [P. D. AARON ET AL.], *Three- and Four- Jet Production at Low x at HERA*. Eur. Phys. J. **C54**, 389 (2008).
- [H1 10] H1 AND ZEUS COLLABORATIONS [F. D. AARON ET AL.], *Combined Measurement and QCD Analysis of the Inclusive $e^+ - p$ Scattering Cross Sections at HERA*. JHEP **1001**, 109 (2010).
- [Har10] S. A. HARTNOLL, *Lectures on Holographic Methods for Condensed Matter Physics* (2010), <http://arXiv.org/abs/hep-th/0903.3246v3>.
- [Hat07] Y. HATTA, *CGC Formalism with Two Sources*. Nucl. Phys. **A781**, 104 (2007).
- [HBL08] M. HENTSCHINSKI, J. BARTELS AND L. N. LIPATOV, *Longitudinal Loop Integrals in the Gauge Invariant Effective Action for High Energy QCD* (2008), [arXiv:0809.4146](http://arXiv.org/abs/0809.4146) [hep-ph].

- [Hei43] W. HEISENBERG, *Die 'Beobachtbaren Grössen' in der Theorie der Elementarteilchen*. Z. Phys. **120**, 513 (1943).
- [Hei52] W. HEISENBERG, *Mesonenerzeugung als Stosswellenproblem*. Z. Phys. **133**, 65 (1952).
- [Hen08] M. HENTSCHINSKI, *Unitarity Corrections from the High Energy QCD Effective Action*. Acta Phys. Pol. **B39**, 2567 (2008).
- [Hen09a] J. M. HENN, *Duality Between Wilson Loops and Gluon Amplitudes*. Fortschr. Phys. **57**, 729 (2009).
- [Hen09b] M. HENTSCHINSKI, *The High Energy Behavior of QCD: The Effective Action and the Triple-Pomeron Vertex*. Ph.D. thesis, Hamburg University (2009).
- [Hen12] M. HENTSCHINSKI, *Pole Prescription of Higher Order Induced Vertices in Lipatov's Effective Action*. Nucl. Phys. **B859**, 129 (2012).
- [HIM⁺06] Y. HATTA, E. IANCU, L. D. MCLERRAN, A. M. STAŚTO AND D. N. TRIANTAFYLLOPOULOS, *Effective Hamiltonian for QCD Evolution at High Energy*. Nucl. Phys. **A764**, 423 (2006).
- [HIM08] Y. HATTA, E. IANCU AND A. H. MUELLER, *Deep Inelastic Scattering at Strong Coupling from Gauge/String Duality. The Saturation Line*. JHEP **0801**, 026 (2008).
- [HKP98] Q. HO-KIM AND X.-Y. PHAM, *Elementary Particles and Their Interactions*. Springer-Verlag, Berlin (1998).
- [HM08] D. M. HOFMAN AND J. MALDACENA, *Conformal Collider Physics. Energy and Charge Correlations*. JHEP **0805**, 012 (2008).
- [HM12] M. HENTSCHINSKI AND B. MURDACA, *The Mueller-Tang Jet Impact Factor at NLO from the High Energy Effective Action*. AIP Conf. Proc. **1523**, 268 (2012).
- [Hol13] T. J. HOLLOWOOD, *Renormalization Group and Fixed Points in Quantum Field Theory*. Springer, Heidelberg (2013).
- [Hos74] A. HOSOYA, *Asymptotic Freedom and Finiteness of the Wave-Function Renormalization Constant*. Phys. Rev. **D10**, 3937 (1974).
- [HS12] M. HENTSCHINSKI AND A. SABIO VERA, *NLO Jet Vertex from Lipatov's QCD Effective Action*. Phys. Rev. **D85**, 056006 (2012).
- [HSS13] M. HENTSCHINSKI, A. SABIO VERA AND C. SALAS, *The Hard to Soft Pomeron Transition in Small x DIS Data Using Optimal Renormalization*. Phys. Rev. Lett. **110**, 041601 (2013).
- [Hua92] K. HUANG, *Quarks, Leptons and Gauge Fields*. World Scientific, Singapore (1992).
- [Hug81] R. J. HUGHES, *More Comments on Asymptotic Freedom*. Phys. Lett. **B186**, 376 (1981).
- [Ian08] E. IANCU, *Physics of the Color Glass Condensate*. Unpublished (2008), http://ipht.cea.fr/Docsphd/articles/t05/271/public/Iancu_HDR.pdf.
- [IFL10] B. L. IOFFE, V. S. FADIN AND L. N. LIPATOV, *Quantum Chromodynamics. Perturbative and Non-Perturbative Aspects*. Cambridge University Press, Cambridge (2010).
- [ILM01a] E. IANCU, A. LEONIDOV AND L. D. MCLERRAN, *Nonlinear Gluon Evolution in the Color Glass Condensate I*. Nucl. Phys. **A692**, 583 (2001).
- [ILM01b] E. IANCU, A. LEONIDOV AND L. D. MCLERRAN, *The Renormalization Group Equation for the Color Glass Condensate*. Phys. Lett. **B510**, 133 (2001).
- [IP06] D. YU. IVANOV AND A. PAPA, *Electroproduction of Two Light Vector Mesons in the Next-to-Leading Approximation*. Nucl. Phys. **B732**, 183 (2006).
- [IW77] A. C. IRVING AND R. P. WORDEN, *Regge Phenomenology*. Phys. Rep. **34**, 117 (1977).
- [Jar80] T. JAROSZEWICZ, *Infrared Divergences and Regge Behavior in QCD*. Acta Phys. Pol. **B11**, 965 (1980).
- [JMKMW97a] J. JALILIAN-MARIAN, A. KOVNER, L. D. MCLERRAN AND H. WEIGERT, *The BFKL Equation from the Wilson Renormalization Group*. Phys. Rev. **D55**, 5414 (1997).
- [JMKMW97b] J. JALILIAN-MARIAN, A. KOVNER, L. D. MCLERRAN AND H. WEIGERT, *The Intrinsic Glue Distribution at Very Small x* . Phys. Rev. **D55**, 5414 (1997).

- [JMKW98] J. JALILIAN-MARIAN, A. KOVNER AND H. WEIGERT, *The Wilson Renormalization Group for Low x Physics: Gluon Evolution at Finite Parton Density*. Phys. Rev. **D59**, 014015 (1998).
- [Jon74] D. R. T. JONES, *Two-Loop Diagrams in Yang-Mills Theories*. Nucl. Phys. **B75**, 531 (1974).
- [Jon77] D. T. R. JONES, *Charge Renormalization in a Supersymmetric Yang-Mills Theory*. Phys. Lett. **B72**, 199 (1977).
- [JP00] R. A. JANIK AND R. B. PESCHANSKI, *High-Energy Scattering and the AdS/CFT Correspondence*. Nucl. Phys. **B565**, 193 (2000).
- [JW59] M. JACOB AND G. C. WICK, *On the General Theory of Collisions for Particles with Spins*. Ann. Phys. (N.Y.) **7**, 404 (1959).
- [JW00] A. M. JAFFE AND E. WITTEN, *Quantum Yang-Mills Theory*. Clay Mathematics Institute Millenium Prize Problem (2000).
- [Käl52] G. KÄLLÉN, *On the Definition of the Renormalization Constants in Quantum Electrodynamics*. Helv. Phys. Acta **25**, 417 (1952).
- [Kep09] O. KEPKA, *QCD and Diffraction in the ATLAS Experiment at the LHC*. Ph.D. thesis, Charles University in Prague (2009).
- [Kin62] T. KINOSHITA, *Mass Singularities of Feynman Amplitudes*. J. Math. Phys. **3**, 650 (1962).
- [KK96] I. A. KORCHEMSKAYA AND G. P. KORCHEMSKY, *Evolution Equation for Gluon Regge Trajectory*. Phys. Lett. **B387**, 346 (1996).
- [KL00] A. V. KOTIKOV AND L. N. LIPATOV, *NLO Corrections to the BFKL Equation in QCD and in Supersymmetric Gauge Theories*. Nucl. Phys. **B582**, 19 (2000).
- [KL03] A. V. KOTIKOV AND L. N. LIPATOV, *DGLAP and BFKL Equations in the $\mathcal{N} = 4$ SUSY Gauge Theory*. Nucl. Phys. **B661**, 19 (2003).
- [KL07] A. V. KOTIKOV AND L. N. LIPATOV, *On the Highest Transcendentality in $\mathcal{N} = 4$ SUSY*. Nucl. Phys. **B769**, 217 (2007).
- [KL12] Y. V. KOVCHEGOV AND E. LEVIN, *Quantum Chromodynamics at High Energy*. Cambridge University Press, Cambridge (2012).
- [KL13] A. V. KOTIKOV AND L. N. LIPATOV, *Pomeron in the $\mathcal{N} = 4$ Supersymmetric Gauge Model at Strong Couplings* (2013), [arXiv:1301.0882\[hep-th\]](https://arxiv.org/abs/1301.0882).
- [KLM96] J. KWIECIŃSKI, C. A. M. LEWIS AND A. D. MARTIN, *Observable Jets from the BFKL Chain*. Phys. Rev. **D54**, 6664 (1996).
- [KLOV04] A. V. KOTIKOV, L. N. LIPATOV, A. I. ONISHCHENKO AND V. N. VELIZHANIN, *Three Loop Universal Anomalous Dimension of the Wilson Operators in $\mathcal{N} = 4$ SUSY Yang-Mills Model*. Phys. Lett. **B595**, 521 (2004).
- [KLR⁺07] A. V. KOTIKOV, L. N. LIPATOV, A. REJ, M. STAUDACHER AND V. N. VELIZHANIN, *Dressing and Wrapping*. J. Stat. Mech. **0710**, P10003 (2007).
- [KLR12] H. KOWALSKI, L. N. LIPATOV AND D. A. ROSS, *BFKL Evolution as a Communicator Between Small and Large Energy Scales* (2012), [arXiv:1205.6713\[hep-ph\]](https://arxiv.org/abs/1205.6713).
- [KLRW10] H. KOWALSKI, L. N. LIPATOV, D. A. ROSS AND G. WATT, *Using HERA Data to Determine the Infrared Behaviour of the BFKL Amplitude*. Eur. Phys. J. **C70**, 983 (2010).
- [KLS94] R. KIRSCHNER, L. N. LIPATOV AND L. SZYMANOWSKI, *Effective Action for Multi-Regge Processes in QCD*. Nucl. Phys. **B425**, 579 (1994).
- [KLS95] R. KIRSCHNER, L. N. LIPATOV AND L. SZYMANOWSKI, *Symmetry Properties of the Effective Action for High-Energy Scattering in QCD*. Phys. Rev. **D51**, 838 (1995).
- [Kor95] G. P. KORCHEMSKY, *Bethe Ansatz for QCD Pomeron*. Nucl. Phys. **B443**, 255 (1995).
- [Kor12] G. P. KORCHEMSKY, *Review of AdS/CFT Integrability, Chapter IV.4: Integrability in QCD and $\mathcal{N} < 4$ SYM*. Lett. Math. Phys. **99**, 425 (2012).
- [Kos] D. A. KOSOWER, *barnesroutines* <http://projects.hepforge.org/mtools/>.

- [Kov98] S. KOVACS, *$\mathcal{N} = 4$ Supersymmetric Yang-Mills Theory and the AdS/SCFT Correspondence*. Ph.D. thesis, Università Tor Vergata (1998).
- [Kov99] Y. V. KOVCHegov, *Small x F_2 Structure Function of a Nucleus Including Multiple Pomeron Exchanges*. Phys. Rev. **D60**, 034008 (1999).
- [Kov00] Y. V. KOVCHegov, *Unitarization of the BFKL Pomeron on a Nucleus*. Phys. Rev. **D61**, 074018 (2000).
- [Kov12] Y. V. KOVCHegov, *Running Coupling Evolution for Diffractive Dissociation and the NLO Odderon Intercept*. AIP Conf. Proc. **1523**, 335 (2012).
- [KP80] J. KWIECIŃSKI AND M. PRASZAŁOWICZ, *Three Gluon Integral Equation and Odd C Singlet Regge Singularities in QCD*. Phys. Lett. **B94**, 413 (1980).
- [KR87] G. P. KORCHEMSKY AND A. V. RADYUSHKIN, *Renormalization of the Wilson Loops Beyond the Leading Order*. Nucl. Phys. **B283**, 342 (1987).
- [LAK54] L. D. LANDAU, A. A. ABRIKOSOV AND I. M. KHALATNIKOV, *The Removal of Infinities in Quantum Electrodynamics*. Dokl. Akad. Nauk SSSR **95**, 497 (1954).
- [Lan60] L. D. LANDAU, *Fundamental Problems*. In M. FIERZ AND V. F. WEISSKOPF (Eds.) *Theoretical Physics in the Twentieth Century, a Memorial Volume to Wolfgang Pauli*, Interscience, New York (1960).
- [Lan96] M. LANCASTER, *Proton Structure at HERA: F_2 , QCD Fits and Beyond*. J. Phys. **G22**, 747 (1996).
- [Lap00] S. LAPORTA, *High-Precision Calculation of Multi-Loop Feynman Integrals by Difference Equations*. Int. J. Mod. Phys. **A15**, 5087 (2000).
- [Leh54] H. LEHMANN, *Über Eigenschaften von Ausbreitungsfunktionen und Renormierungskonstanten Quantisierter Felder*. Nuovo Cimento **11**, 342 (1954).
- [Lev95] E. LEVIN, *The Pomeron: Yesterday, Today and Tomorrow* (1995), <http://arXiv.org/abs/hep-ph/9503399v1>.
- [Lev97] A. LEVY, *Low- x Physics at HERA*. In F. LENZ, H. GRIESSHAMMER AND D. STOLL (Eds.) *Lectures on QCD*, Springer, Berlin (1997).
- [Lip75] L. N. LIPATOV, *The Parton Model and Perturbation Theory*. Sov. J. Nucl. Phys. **20**, 94 (1975).
- [Lip76] L. N. LIPATOV, *Reggeization of the Vector Meson and the Vacuum Singularity in Nonabelian Gauge Theories*. Sov. J. Nucl. Phys. **23**, 338 (1976).
- [Lip86] L. N. LIPATOV, *The Bare Pomeron in Quantum Chromodynamics*. Sov. Phys. JETP **63**, 904 (1986).
- [Lip91] L. N. LIPATOV, *High-Energy Scattering in QCD and in Quantum Gravity and Two-Dimensional Field Theories*. Nucl. Phys. **B365**, 614 (1991).
- [Lip93a] L. N. LIPATOV, *High Energy Asymptotics of Multi-Colour QCD and Two-Dimensional Conformal Field Theories*. Phys. Lett. **B309**, 394 (1993).
- [Lip93b] L. N. LIPATOV, *High-Energy Asymptotics of Multicolor QCD and Exactly Solvable Lattice Models* (1993), [arXiv:9311037 \[hep-th\]](https://arxiv.org/abs/9311037).
- [Lip94] L. N. LIPATOV, *Asymptotic Behavior of Multicolor QCD at High Energies in Connection with Exactly Solvable Spin Models*. JETP Lett. **59**, 596 (1994).
- [Lip95] L. N. LIPATOV, *Gauge Invariant Effective Action for High-Energy Processes in QCD*. Nucl. Phys. **B452**, 369 (1995).
- [Lip97] L. N. LIPATOV, *Small x Physics in Perturbative QCD*. Phys. Rep. **286**, 131 (1997).
- [LN64] T. D. LEE AND M. NAUENBERG, *Degenerate Systems and Mass Singularities*. Phys. Rev. **B133**, 1549 (1964).
- [LN87] P. V. LANDSHOFF AND O. NACHTMANN, *Vacuum Structure and Diffraction Scattering*. Z. Phys. **C35**, 405 (1987).
- [Low75] F. E. LOW, *Model of the Bare Pomeron*. Phys. Rev. **D12**, 163 (1975).

- [LP55] L. D. LANDAU AND I. YA. POMERANCHUK, *On Point Interactions in Quantum Electrodynamics*. Dokl. Akad. Nauk SSSR **102**, 489 (1955).
- [LP71] P. V. LANDSHOFF AND J. C. POLKINGHORNE, *The Dual Quark-Parton Model and High Energy Hadronic Processes*. Nucl. Phys. **B32**, 541 (1971).
- [LP11] E. LEADER AND E. PREDAZZI, *A Note on the Implications of Gauge Invariance in QCD* (2011), <http://arXiv.org/abs/hep-ph/1101.3425v1>.
- [LR90] E. M. LEVIN AND M. G. RYSKIN, *High-Energy Hadron Collisions in QCD*. Phys. Rep. **189**, 267 (1990).
- [LRS92] E. M. LEVIN, M. G. RYSKIN AND A. G. SHUVAEV, *Anomalous Dimension of the Twist Four Gluon Operator and Pomeron Cuts in Deep Inelastic Scattering*. Nucl. Phys. **B387**, 589 (1992).
- [LRSvN93] E. LAENEN, S. RIEMERSMA, J. SMITH AND W. VAN NEERVEN, *Complete $\mathcal{O}(\alpha_s)$ Corrections to Heavy Flavor Structure Functions in Electroproduction*. Nucl. Phys. **B392**, 162 (1993).
- [Mag05] M. MAGGIORE, *A Modern Introduction to Quantum Field Theory*. Oxford University Press, Oxford (2005).
- [Mal96] J. M. MALDACENA, *Black Holes in String Theory*. Ph.D. thesis, Princeton University (1996), <http://www.arxiv.org/abs/hep-th/9607235v2>.
- [Mal98] J. M. MALDACENA, *The Large N Limit of Superconformal Field Theories and Supergravity*. Adv. Theor. Math. Phys. **2**, 231 (1998).
- [Man58] S. MANDELSTAM, *Determination of the Pion-Nucleon Scattering Amplitude from Dispersion Relations and Unitarity. General Theory*. Phys. Rev. **112**, 1344 (1958).
- [Man65] S. MANDELSTAM, *Non-Regge Terms in the Vector-Spinor Theory*. Phys. Rev. **137B**, 949 (1965).
- [Man83] S. MANDELSTAM, *Light-Cone Superspace and the Ultraviolet Finiteness of the $\mathcal{N} = 4$ Model*. Nucl. Phys. **B213**, 149 (1983).
- [Man96] A. V. MANOHAR, *Effective Field Theories* (1996), <http://arxiv.org/abs/hep-ph/9606222>.
- [Man99] M. L. MANGANO, *Introduction to QCD*. In A. MASIERO, G. SENJANOVIĆ AND A. SMIRNOV (Eds.) *High Energy Physics and Cosmology (1998 Summer School, ICTP, Trieste)*, World Scientific, Singapore (1999).
- [Mar63] A. D. MARTIN, *Unitarity and High-Energy Behavior of Scattering Amplitudes*. Phys. Rev. **129**, 1432 (1963).
- [Mas76] A. L. MASON, *Factorization and Hence Reggeization in Yang-Mills Theories*. Nucl. Phys. **B117**, 493 (1976).
- [MBD91] R. MERTIG, M. BÖHM AND A. DENNER, *FEYNALC: Computer Algebraic Calculation of Feynman Amplitudes*. Comput. Phys. Commun. **64**, 345 (1991).
- [Mek85] M. MEKHFI, *Correlations in Color and Spin in Multiparton Processes*. Phys. Rev. **32**, 2380 (1985).
- [Min11] J. A. MINAHAN, *Spin Chains in $\mathcal{N} = 4$ Super Yang-Mills* (2011), <http://arxiv.org/abs/hep-th/1012.3983v3>.
- [MN87] A. H. MUELLER AND H. NAVELET, *An Inclusive Minijet Cross-Section and the Bare Pomeron in QCD*. Nucl. Phys. **B282**, 727 (1987).
- [Mos78] M. MOSHE, *Recent Developments in Reggeon Field Theory*. Phys. Rep. **37**, 255 (1978).
- [MP91] M. L. MANGANO AND S. J. PARKE, *Multiparton Amplitudes in Gauge Theories*. Phys. Rep. **200**, 301 (1991).
- [MP94] A. H. MUELLER AND B. PATEL, *Single and Double BFKL Pomeron Exchange and a Dipole Picture of High Energy Hard Processes*. Nucl. Phys. **B425**, 471 (1994).
- [MP03] S. MUNIER AND R. B. PESCHANSKI, *Geometric Scaling as Traveling Waves*. Phys. Rev. Lett. **91**, 232001 (2003).

- [MP04] S. MUNIER AND R. B. PESCHANSKI, *Traveling Wave Fronts and the Transition to Saturation*. Phys. Rev. **D69**, 034008 (2004).
- [MQ86] A. H. MUELLER AND J. QIU, *Gluon Recombination and Shadowing at Small Values of x* . Nucl. Phys. **B268**, 427 (1986).
- [MR09] C. MARQUET AND C. ROYON, *Azimuthal Decorrelation of Mueller-Navelet Jets at the Tevatron and the LHC*. Phys. Rev. **D79**, 034028 (2009).
- [MSTW09] A. D. MARTIN, W. J. STIRLING, R. S. THORNE AND G. WATT, *Parton Distributions at the LHC*. Eur. Phys. J. **C63**, 189 (2009).
- [MT92] A. H. MUELLER AND W.-K. TANG, *High Energy Parton-Parton Elastic Scattering in QCD*. Phys. Lett. **B284**, 123 (1992).
- [Mue90] A. H. MUELLER, *Parton Distributions at Very Small x -Values*. Nucl. Phys. B, Proc. Suppl. **18C**, 125 (1990).
- [Mue91] A. H. MUELLER, *Jets at LEP and HERA*. J. Phys. **G17**, 1443 (1991).
- [Mue94] A. H. MUELLER, *Soft Gluons in the Infinite-Momentum Wave Function and the BFKL Pomeron*. Nucl. Phys. **B415**, 373 (1994).
- [Mut10] T. MUTA, *Foundations of Quantum Chromodynamics*. World Scientific, Singapore (2010).
- [MV94] L. D. McLERRAN AND R. VENUGOPALAN, *Computing Quark and Gluon Distribution Functions for Very Large Nuclei*. Phys. Rev. **D49**, 2233 (1994).
- [MW76] B. M. MCCOY AND T. T. WU, *Theory of Fermion Exchange in Massive Quantum Electrodynamics at High Energy. I*. Phys. Rev. **D13**, 369 (1976), see also the subsequent papers in this volume by the same authors.
- [MWA⁺92] G. MARCHESINI, B. R. WEBBER, G. ABBIENDI, I. G. KNOWLES, M. H. SEYMOUR AND L. STANCO, *HERWIG 5.1 — a Monte Carlo Event Generator for Simulating Hadron Emission Reactions with Interfering Gluons*. Comput. Phys. Commun. **67**, 465 (1992).
- [N⁺08] P. M. NADOLSKY ET AL., *Implications of CTEQ Global Analysis for Collider Observables*. Phys. Rev. **D78**, 013004 (2008).
- [Nag10] Y. NAGASHIMA, *Elementary Particle Physics I. Quantum Field Theory and Particles*. Wiley-VCH, Weinheim (2010).
- [Nai88] V. P. NAIR, *A Current Algebra for Some Gauge Theory Amplitudes*. Phys. Lett. **B214**, 215 (1988).
- [Nam69] Y. NAMBU, *Quark Model and the Factorization of the Veneziano Amplitude*. In R. CHAUD (Ed.) *Proceedings of International Conference on Symmetries and Quark Models*, Wayne State Univ., Gordon and Breach, New York (1969).
- [Nas07] H. NASTASE, *Introduction to AdS-CFT* (2007), <http://www.arxiv.org/abs/0712.0689v2>.
- [Neu05] M. NEUBERT, *Effective Field Theory and Heavy Quark Physics (TASI 2004 Lectures)* (2005), [arXiv:hep-ph/0512222](http://arxiv.org/abs/hep-ph/0512222).
- [Nie70] H. B. NIELSEN, *An Almost Physical Interpretation of the Integrand of the n -Point Veneziano Model*. Submitted to the 15th International Conference on High Energy Physics, Kiev (1970).
- [Nie81] N. K. NIELSEN, *Asymptotic Freedom as a Spin Effect*. Am. J. Phys. **49**, 1171 (1981).
- [N JL61a] Y. NAMBU AND G. JONA-LASINIO, *A Dynamical Model of Elementary Particles Based on an Analogy with Superconductivity I*. Phys. Rev. **122**, 345 (1961).
- [N JL61b] Y. NAMBU AND G. JONA-LASINIO, *A Dynamical Model of Elementary Particles Based on an Analogy with Superconductivity II*. Phys. Rev. **124**, 246 (1961).
- [Nus75] S. NUSSINOV, *Colored-Quark Version of Some Hadronic Puzzles*. Phys. Rev. Lett. **34**, 1286 (1975).
- [NZZ94] N. N. NIKOLAEV, B. G. ZAKHAROV AND V. R. ZOLLER, *The Spectrum and Solutions of the Generalized BFKL Equation for Total Cross Section*. Phys. Lett. **B328**, 486 (1994).
- [OLBC10] F. W. J. OLVER, D. W. LOZIER, R. F. BOISVERT AND C. W. CLARK (Eds.) *NIST Handbook of Mathematical Functions*. Cambridge University Press, Cambridge (2010).

- [OP56] L. B. OKUN AND I. YA. POMERANCHUK, *The Conservation of Isotopic Spin and the Cross Section of the Interaction of High-Energy π -Mesons and Nucleons with Nucleons*. Sov. Phys. JETP **3**, 306 (1956).
- [OS97] L. H. ORR AND W. J. STIRLING, *Dijet Production at Hadron Hadron Colliders in the BFKL Approach*. Phys. Rev. **D56**, 5875 (1997).
- [Pan68] W. PANOFSKY, *Low Electrodynamics Elastic and Inelastic Electron (and Muon) Scattering*. In J. PRENTKI AND J. STEINBERGER (Eds.) *Proceedings of the 14th International Conference on High Energy Physics, Vienna* (1968).
- [Pap11] E. PAPANANTONIOPOULOS (Ed.) *From Gravity to Thermal Gauge Theories: The AdS/CFT Correspondence*. Springer, Heidelberg (2011).
- [Par10] PARTICLE DATA GROUP [K. NAKAMURA ET AL.], *Review of Particle Physics* (2010), <http://pdg.lbl.gov>.
- [Pic98] A. PICH, *Effective Field Theory* (1998), <http://arxiv.org/abs/hep-ph/9806303v1>.
- [Pok00] S. POKORSKI, *Gauge Field Theories*. Cambridge University Press, Cambridge (2000).
- [Pol73] H. D. POLITZER, *Reliable Perturbative Results for Strong Interactions?*. Phys. Rev. Lett. **30**, 1346 (1973).
- [Pol84] J. POLCHINSKI, *Renormalization and Effective Lagrangians*. Nucl. Phys. **B231**, 269 (1984).
- [Pol87] A. M. POLYAKOV, *Gauge Fields and Strings*. Harwood Academic Publishers, Chur (1987).
- [Pol92] J. POLCHINSKI, *Effective Field Theory and the Fermi Surface* (1992), [arXiv:hep-th/9210046](http://arxiv.org/abs/hep-th/9210046).
- [Pom56] I. YA. POMERANCHUK, *The Conservation of Isotopic Spin and the Scattering of Antinucleons by Nucleons*. Sov. Phys. JETP **3**, 306 (1956).
- [PP77] E. POGGIO AND H. PENDLETON, *Vanishing of Charge Renormalization and Anomalies in a Supersymmetric Gauge Theory*. Phys. Lett. **B72**, 200 (1977).
- [PS95] M. E. PESKIN AND D. V. SCHRÖDER, *An Introduction to Quantum Field Theory*. Perseus Books, Reading (Mass.) (1995).
- [PS02] J. POLCHINSKI AND M. J. STRASSLER, *Hard Scattering and Gauge-String Duality*. Phys. Rev. Lett. **88**, 031601 (2002).
- [PS03] J. POLCHINSKI AND M. J. STRASSLER, *Deep Inelastic Scattering and Gauge/String Duality*. JHEP **0305**, 012 (2003).
- [PT80] P. PASCUAL AND R. TARRACH, *Slavnov-Taylor Identities in Weinberg's Renormalization Scheme*. Nucl. Phys. **B174**, 123 (1980), [Erratum-ibid. **B181**, 546 (1981)].
- [PT86] S. J. PARKE AND T. R. TAYLOR, *An Amplitude for n Gluon Scattering*. Phys. Rev. Lett. **56**, 2459 (1986).
- [Reg59] T. REGGE, *Introduction to Complex Orbital Momenta*. Nuovo Cimento **14**, 951 (1959).
- [Rob90] R. G. ROBERTS, *The Structure of the Proton*. Cambridge University Press, Cambridge (1990).
- [Ros98] D. A. ROSS, *The Effect of Higher Order Corrections to the BFKL Equation on the Perturbative Pomeron*. Phys. Lett. **B431**, 161 (1998).
- [Sab05] A. SABIO VERA, *An All-Poles Approximation to Collinear Resummation in the Regge Limit of Perturbative QCD*. Nucl. Phys. **B722**, 65 (2005).
- [Sab06] A. SABIO VERA, *The Effect of NLO Conformal Spins in Azimuthal Angle Decorrelation of Jet Pairs*. Nucl. Phys. **B746**, 1 (2006).
- [Sal98] G. P. SALAM, *A Resummation of Large Sub-leading Corrections at Small x* . JHEP **07**, 019 (1998).
- [Sal99] G. P. SALAM, *An Introduction to Leading and Next-to-Leading BFKL*. Acta Phys. Pol. **B30**, 3679 (1999).
- [Säm09] C. SÄMANN, *Introduction to Supersymmetry* (2009), <http://www.christiansaemann.de/supersymmetry.html>.

- [Sch97] C. R. SCHMIDT, *A Monte Carlo Solution to the BFKL Equation*. Phys. Rev. Lett. **78**, 4531 (1997).
- [Sch99] C. R. SCHMIDT, *Rapidity-Separation Dependence and the Large Next-to-Leading Corrections to the BFKL Equation*. Phys. Rev. **D60**, 074003 (1999).
- [Sch07] F. SCHWENNSEN, *Phenomenology of Jet Physics in the BFKL Formalism at NLO*. Ph.D. thesis, University of Hamburg (2007), <http://arxiv.org/abs/hep-ph/0703198>.
- [Sch09] F. SCHWENNSEN, *BFKL Catch Up!*. In M. DEILE, D. D'ENTERRIA AND A. DE ROECK (Eds.) *Elastic and Diffractive Scattering. Proceedings, 13th International Conference, Blois Workshop* (2009), [arXiv:1002.3527](https://arxiv.org/abs/1002.3527) [hep-ph].
- [SGBK01] A. M. STAŚTO, K. J. GOLEC-BIERNAT AND J. KWIECIŃSKI, *Geometric Scaling for the Total γ^*p Cross-Section in the Low x Region*. Phys. Rev. Lett. **86**, 596 (2001).
- [Shi01] M. SHIFMAN, *Historical Curiosity: How Asymptotic Freedom of the Yang-Mills Theory Could Have Been Discovered Three Times Before Gross, Wilczek and Politzer, but Was Not*. In M. SHIFMAN (Ed.) *Handbook of QCD (Vol. I)*, World Scientific, Singapore (2001).
- [Sho07] A. SHOMER, *A Pedagogical Explanation for the Non-Renormalizability of Gravity* (2007), <http://arxiv.org/abs/hep-th/0709.3555v2>.
- [Sla72] A. A. SLAVNOV, *Ward Identities in Gauge Theories*. Theor. Math. Phys. **19**, 99 (1972).
- [Smi06] V. A. SMIRNOV, *Feynman Integral Calculus*. Springer-Verlag, Berlin (2006).
- [Smi08] A. V. SMIRNOV, *Algorithm FIRE - Feynman Integral REduction*. JHEP **10**, 107 (2008).
- [Soh85] M. F. SOHNIUS, *Introducing Supersymmetry*. Phys. Rep. **128**, 39 (1985).
- [Som49] A. SOMMERFELD, *Partial Differential Equations of Mathematical Physics*. Academic Press, New York (1949).
- [Sre07] M. SREDNICKI, *Quantum Field Theory*. Cambridge University Press, Cambridge (2007).
- [SS07] A. SABIO VERA AND F. SCHWENNSEN, *The Azimuthal Decorrelation of Jets Widely Separated in Rapidity as a Test of the BFKL Kernel*. Nucl. Phys. **B776**, 170 (2007).
- [SS09] A. V. SMIRNOV AND V. A. SMIRNOV, *On the Resolution of Singularities of Multiple Mellin-Barnes Integrals*. Eur. Phys. J. **C62**, 445 (2009).
- [Ste60] O. STEINMANN, *Über den Zusammenhang Zwischen den Wightmanfunktionen und den Retardierten Kommutatoren*. Helv. Phys. Acta **33**, 257 (1960).
- [Ste81a] P. M. STEVENSON, *Optimized Perturbation Theory*. Phys. Rev. **D23**, 2916 (1981).
- [Ste81b] P. M. STEVENSON, *Resolution of the Renormalisation-Scheme Ambiguity in Perturbative QCD*. Phys. Lett. **B100**, 61 (1981).
- [Ste08] G. STERMAN, *Some Basic Ideas of Perturbative QCD*. Acta Phys. Pol. **B39**, 2151 (2008).
- [Sti94] W. J. STIRLING, *Production of Jet Pairs at Large Relative Rapidity in Hadron Hadron Collisions as a Probe of the Perturbative Pomeron*. Nucl. Phys. **B423**, 56 (1994).
- [Str07] R. F. STREATER, *Lost Causes In and Beyond Physics*. Springer-Verlag, Berlin (2007).
- [Sus70] L. SUSSKIND, *Dual-Symmetric Theory of Hadrons. I.* Nuovo Cimento **69A**, 457 (1970).
- [SW81] M. F. SOHNIUS AND P. C. WEST, *Conformal Invariance in $\mathcal{N} = 4$ Supersymmetric Yang-Mills Theory*. Phys. Lett. **B100**, 245 (1981).
- [Sym70] K. SYMANZIK, *Small Distance Behaviour in Field Theory and Power Counting*. Commun. Math. Phys. **18**, 227 (1970).
- [Sym71] K. SYMANZIK, *Small-Distance Behaviour Analysis and Wilson Expansions*. Commun. Math. Phys. **23**, 49 (1971).
- [Szy94] L. SZYMANOWSKI, *The Effective Action for QCD at High Energies*. [arXiv: 9411114v1](https://arxiv.org/abs/9411114) [hep-th] (1994).
- [Tay71] J. C. TAYLOR, *Ward Identities and the Yang-Mills Field*. Nucl. Phys. **B33**, 436 (1971).

- [tH72] G. 'T HOOFT, *Remarks after Symanzik's Presentation*. In C. P. KORTHALS-ALTES (Ed.) *Renormalization of Yang-Mills and Applications to Particle Physics (Proceedings of the Marseille Conference)* (1972).
- [tH73a] G. 'T HOOFT, *Dimensional Regularization and the Renormalization Group*. Nucl. Phys. **B61**, 455 (1973).
- [tH73b] G. 'T HOOFT, *A Planar Diagram Theory for Strong Interactions*. Nucl. Phys. **B72**, 461 (1973).
- [tH98] G. 'T HOOFT, *When Was Asymptotic Freedom Discovered? or the Rehabilitation of Quantum Field Theory* (1998), <http://arXiv.org/abs/hep-th/9808154v2>.
- [Tho99] R. S. THORNE, *NLO BFKL Equation, Running Coupling and Renormalization Scales*. Phys. Rev. **D60**, 054031 (1999).
- [tHV72] G. 'T HOOFT AND M. VELTMAN, *Renormalization and Regularization of Gauge Fields*. Nucl. Phys. **B44**, 189 (1972).
- [TJZW85] S. B. TREIMAN, R. JACKIW, B. ZUMINO AND E. WITTEN, *Current Algebra and Anomalies*. Princeton University Press, Princeton (1985).
- [Tri05] D. N. TRIANTAFYLLOPOULOS, *Pomeron Loops in High Energy QCD*. Acta Phys. Pol. **B36**, 3593 (2005).
- [TVZ80] O. V. TARASOV, A. A. VLADIMIROV AND A. YU. ZHARKOV, *The Gell-Mann-Low Function of QCD in the Three-Loop Approximation*. Phys. Lett. **B93**, 429 (1980).
- [Tyb76] L. TYBURSKI, *Reggeization of the Fermion-Fermion Scattering Amplitude in Non-Abelian Gauge Theories*. Phys. Rev. **D13**, 1107 (1976).
- [Ura07] A. M. URANGA, *Introduction to String Theory* (2007), <http://gesalerico.ft.uam.es/paginaspersonales/angeluranga/firstpage.html>.
- [Ven68] G. VENEZIANO, *Construction of a Crossing-Symmetric, Regge-Behaved Amplitude for Linearly Rising Trajectories*. Nuovo Cimento **A57**, 190 (1968).
- [vRVL97] T. VAN RITBERGEN, J. A. M. VERMASEREN AND S. A. LARIN, *The Four-Loop β -Function in Quantum Chromodynamics*. Phys. Lett. **B400**, 379 (1997).
- [VT80] A. A. VLADIMIROV AND O. V. TARASOV, *Vanishing of the Three-Loop Charge Renormalization Function in a Supersymmetric Gauge Theory*. Phys. Lett. **B96**, 94 (1980).
- [VV93] H. VERLINDE AND E. VERLINDE, *QCD at High Energies and Two-Dimensional Field Theory* (1993), [arXiv:hep-th/9302104](http://arXiv.org/abs/hep-th/9302104).
- [Wat18] G. N. WATSON, *The Diffraction of Electric Waves by the Earth*. Proc. R. Soc. London, Ser. A **95**, 83 (1918).
- [WBM13] X. WU, S. J. BRODSKY AND M. MOJAZA, *The Renormalization Scale-Setting Problem in QCD* (2013), [arXiv:1302.0599](http://arXiv.org/abs/1302.0599)[hep-ph].
- [Wei73] S. WEINBERG, *Non-Abelian Gauge Theories of the Strong Interactions*. Phys. Rev. Lett. **31**, 494 (1973).
- [Wei79a] S. WEINBERG, *Baryon and Lepton Nonconserving Processes*. Phys. Rev. Lett. **43**, 1566 (1979).
- [Wei79b] S. WEINBERG, *Phenomenological Lagrangians*. Physica **A96**, 327 (1979).
- [Wei89] S. WEINBERG, *The Cosmological Constant Problem*. Rev. Mod. Phys. **61**, 1 (1989).
- [Wei95] S. WEINBERG, *The Quantum Theory of Fields (Vol. I. Foundations)*. Cambridge University Press, Cambridge (1995).
- [Wei09] S. WEINBERG, *Living with Infinities* (2009), <http://arxiv.org/abs/hep-th/0903.0568v1>.
- [Whi76] A. R. WHITE, *The Analytical Foundations of Regge Theory*. In R. BALIAN AND D. IAGOLNITZER (Eds.) *Les Houches Lectures on Structural Analysis of Collision Amplitudes*, North-Holland, Amsterdam (1976).
- [Wil69] K. G. WILSON, *Non-Lagrangian Models of Current Algebra*. Phys. Rev. **179**, 1499 (1969).

- [Wil71a] K. G. WILSON, *Renormalization Group and Critical Phenomena. I. Renormalization Group and the Kadanoff Scaling Picture*. Phys. Rev. **B4**, 3174 (1971).
- [Wil71b] K. G. WILSON, *Renormalization Group and Critical Phenomena. II. Phase-Space Cell Analysis of Critical Behavior*. Phys. Rev. **B4**, 3184 (1971).
- [Wil79] K. G. WILSON, *Problems in Physics with Many Scales of Length*. Sci. Am. **241**, 140 (1979).
- [Wit76] E. WITTEN, *Heavy Quark Contributions to Deep Inelastic Scattering*. Nucl. Phys. **B104**, 445 (1976).
- [Wit98] E. WITTEN, *Anti-de Sitter Space, Thermal Phase Transition, and Confinement in Gauge Theories*. Adv. Theor. Math. Phys. **2**, 505 (1998).
- [Wit04] E. WITTEN, *Perturbative Gauge Theory as a String Theory in Twistor Space*. Commun. Math. Phys. **252**, 189 (2004).
- [YM54] C. N. YANG AND R. L. MILLS, *Conservation of Isotopic Spin and Isotopic Gauge Invariance*. Phys. Rev. **96**, 191 (1954).
- [Ynd06] F. J. YNDURÁIN, *The Theory of Quark and Gluon Interactions*. Springer-Verlag, Berlin (2006).
- [Zee10] A. ZEE, *Quantum Field Theory in a Nutshell*. Princeton University Press, Princeton (2010).
- [ZEU96] ZEUS COLLABORATION [M. DERRICK ET AL.], *Measurement of the Proton Structure Function F_2 at Low x and Low Q^2 at HERA*. Z. Phys. **C69**, 607 (1996).
- [ZEU99] ZEUS COLLABORATION [J. BREITWEG ET AL.], *Forward Jet Production in Deep Inelastic Scattering at HERA*. Eur. Phys. J. **C6**, 239 (1999).
- [ZEU06] ZEUS COLLABORATION [S. CHEKANOV ET AL.], *Forward Jet Production in Deep Inelastic ep Scattering and Low- x Parton Dynamics at HERA*. Phys. Lett. **B632**, 239 (2006).
- [Zwe64] G. ZWEIG, *An $SU(3)$ Model for Strong Interaction Symmetry and Its Breaking: I and II*. Preprints CERN-TH 401 and 412 (1964).